



Design and Synthesis of Bi-functional, 1,2,4,5-Tetraoxane-based Molecular Wires and their Application in Microbial Fuel Cells

Thesis submitted in accordance with the requirements of the University of Liverpool for the
degree of Doctor of Philosophy

by

Katy King Wah Zhou

September 2013

Declaration

This thesis is the result of my own work. The material contained in this thesis has not been presented, nor is currently being presented, either wholly or in part for any other degree or qualification.

Katy King Wah Zhou

This research was carried out in the Department of Chemistry, University of Liverpool.

Acknowledgements

I would like to thank my supervisors Dr. Ian O'Neil and Prof. David Schiffrin for the fantastic opportunity to do this PhD and their continuous encouragement, support and advice. I also express my gratitude to the European Commission for funding the BacWire project. Special thanks must also go to Prof. Andrew Evans and Prof. Rick Cosstick for their invaluable advice after reviewing my written reports and conducting my first and second year vivas. I would also like to thank Moira Cowan for inspiring me to study Chemistry at degree level.

I am particularly grateful to Dr. Irfan Sulaman, Dr. James Chadwick and Dr. Matthew McConville for teaching me essential laboratory skills, providing feedback on my written work/presentations and for always being available to give support and advice to help me become a better chemist. I must also thank the technical staff (Moya, Jean, George and Tony) in the Chemistry Department for data collection of all compounds detailed in Chapter 5 and the staff in Chemistry Stores (Phil, Keith and James) and the Chemistry Finance Office (John, Ann and Anne) for dealing with my chemical orders.

This PhD has allowed me to travel overseas for the first time, to meet new people and experience different cultures. I would like to thank everyone who has contributed to the BacWire project and for their hospitality when I visited Alicante, Bern, Madrid and Mar del Plata for our BacWire progress meetings.

Thanks to Katie Alexander for being an amazing friend and my friends and colleagues in Chemistry, in particular, Carly Brooke, Lee Taylor and Chris Thomas for their support, advice and shared knowledge. Thanks to Dr. Nick Greeves and Dr. James Gaynor for letting me demonstrate in first year workshops and giving me a break from the lab!

I would like to thank my wonderful family: my brother Tony, for his assistance with my frequent computer problems ("Have you tried turning it off and on again?!"), my sister Jenny, for helping me stay sane with our food/retail therapy days (any excuse to stuff our faces and buy nice things!), my ever loving boyfriend Irfan, for his support and encouragement - you have been my rock! The final word goes to my parents for their love, guidance and support.

I dedicate this thesis to my Nan, who sadly passed away in April 2013.

Abstract

Chapter 1 begins with a general introduction to the main aspects of this work: Firstly, a species of electrogenic bacteria, *Geobacter sulfurreducens* is introduced. Their ability to take part in extracellular electron transfer, the mechanisms by which this happens, and their involvement in electricity generation and bioremediation when applied in microbial fuel cells is discussed; Secondly, microbial fuel cells (MFCs) as an alternative method of electricity generation to fossil fuels, their methods of operation and their potential for use in the treatment of wastewater is briefly reviewed; Finally, antimalarial drugs (including their semi-synthetic and synthetic analogues) and their mechanisms of action are presented. The possibility of exploiting them as a template for bi-functional molecular wires that are capable of tethering bacteria to carbon and/or gold electrode surfaces is discussed in detail.

Chapter 2 outlines our efforts towards novel analogues of synthetic antimalarials, dispiro-1,2,4-trioxolanes, for use as bi-functional molecular wires. These are shown to be capable of immobilising heme on carbon and gold surfaces *via* appropriate functional groups.

Chapter 3 discusses our efforts towards novel analogues of synthetic antimalarials, dispiro-1,2,4,5-tetraoxanes for use as bi-functional molecular wires. The syntheses of many novel precursors; namely functionalised adamantanone derivatives and their corresponding tetraoxanes are presented. Synthetic routes towards bi-functional tetraoxane molecular wires have been extensively optimised and the incorporation of functional groups that are compatible with carbon/gold surfaces has been attempted.

Chapter 4 briefly introduces the design and synthesis of β -turn mimetics and the synthesis of chiral enamine *N*-oxides.

Chapter 5 details the experimental procedures.

Publications

I. A. O'Neil, M. McConville, K. Zhou, C. Brooke, C. Robertson, N. Berry, The synthesis of chiral enamine *N*-oxides, *ChemComm*, **2013**, *accepted*.

C. Zuliani, M. McConville, K. Zhou, I. A. O'Neil, D. J. Schiffrin, Electrochemical mediation of heme for the activation of the peroxide bridge in dispiro-1,2,4-trioxolanes, **2013**, *manuscript in preparation*.

M. McConville, D. F. Bradley, K. Zhou, D. J. Schiffrin, I. A. O'Neil, Selective trioxolane based bifunctional molecular linkers for covalent heme surface functionalisation, *ChemComm*, **2014**, 50 (2), 186-188.

Abbreviations

aq.	Aqueous
Boc	<i>tert</i> -butoxycarbonyl
°C	Degrees Celsius
<i>ca.</i>	<i>circa.</i>
CAN	Ceric ammonium nitrate
CDCl ₃	Deuterated chloroform
CHCl ₃	Chloroform
CH ₃ CN	Acetonitrile
CI	Chemical ionisation
DCM	Dichloromethane
DHP	1,1-Dihydroperoxide
EDC.HCl	1-ethyl-3-(3-dimethylaminopropyl)carbodiimide hydrochloride
EDG	Electron-donating group
eq.	Molar equivalents
ESI	Electrospray ionisation
Et ₂ O	Diethyl ether
EtOAc	Ethyl acetate
EtOH	Ethanol
EWG	Electron-withdrawing group
FAD	Flavin adenine dinucleotide
FeBr ₂	Iron (II) bromide
FeCl ₃	Iron (III) chloride
FTIR	Fourier transform infrared spectroscopy
g	Grams
H ₂ O ₂	Hydrogen peroxide
HBr	Hydrobromic acid
HCl	Hydrochloric acid
HOBt	<i>N</i> -Hydroxybenzotriazole hydrate

H ₂ SO ₄	Sulfuric acid
hr(s)	Hour(s)
HRMS	High resolution mass spectrometry
Hz	Hertz
I ₂	Iodine
IR	Infra-red
K ₂ CO ₃	Potassium carbonate
LDA	Lithium diisopropylamine
LRMS	Low resolution mass spectrometry
<i>m</i>	meta
M	Molar
<i>m</i> -CPBA	<i>meta</i> -Chloroperbenzoic acid
mg	Milligrams
MeOH	Methanol
MgSO ₄	Magnesium sulfate
MHz	Megahertz
min(s)	Minute(s)
ml	Millilitres
mol	Mole(s)
mmol	Millimole(s)
MMV	Medicines for Malaria Venture
m.p	Melting point
N ₂	Nitrogen
NAD	Nicotinamide adenine dinucleotide
NaHCO ₃	Sodium hydrogen carbonate
NaOH	Sodium hydroxide
Na ₂ SO ₄	Sodium sulfate
NEt ₃	Triethylamine
<i>n</i> -Hex	<i>n</i> -Hexane

NMM	4-Methyl morpholine
NMR	Nuclear magnetic resonance
<i>o</i>	ortho
o/n	Overnight
<i>p</i>	para
PMA	Phosphomolybdic acid hydrate
ppm	Parts per million
Re ₂ O ₇	Rhenium (VII) oxide
rt	Room temperature
STM	Scanning tunnelling microscopy
STS	Scanning tunnelling spectroscopy
TBAI	Tetrabutylammonium iodide
TEMPO	(2,2,6,6-tetramethylpiperidin-1-yl)oxyl
TFA	Trifluoroacetic acid
TFAA	Trifluoroacetic anhydride
TfOH	Triflic acid
THF	Tetrahydrofuran
TLC	Thin layer chromatography
TMP	2,2,6,6-Tetramethylpiperidyl
TMS	Trimethylsilyl
<i>p</i> -TSA	<i>p</i> -Toluenesulfonic acid monohydrate
Vs.	Versus
WHO	World Health Organisation
w/v	Weight by volume

Table of Contents

	Page
Declaration	i
Acknowledgements	ii
Abstract	iii
Publications	iv
Abbreviations	v-vii
Table of Contents	viii-xiv
 Chapter 1: Introduction to <i>Geobacter</i>, microbial fuel cells and malaria	 1
1.1. Energy production and fossil fuels	2
1.1.1. Global warming	2-3
1.1.2. The future of non-renewable energy	3
1.1.3. Renewable energy	3-4
1.2. Electrogenic bacteria: <i>Geobacter sulfurreducens</i>	4
1.2.1. Introduction to <i>Geobacter</i>	4
1.2.2. Bacterial Respiration	4-6
1.2.3. Electrogenic properties of <i>Geobacter sulfurreducens</i>	6-7
1.2.4. Mechanisms of electron transfer	8-12
1.3. Fluorescent properties of <i>c</i> -type cytochromes in <i>Geobacter sulfurreducens</i>	13
1.4. Role of <i>Geobacter</i> and MFCs in bioremediation	13
1.4.1. Removal of uranium from contaminated groundwater	13-14
1.4.2. <i>Geobacter sulfurreducens</i> in MFCs	14
1.5. Microbial fuel cells (MFCs)	14-15
1.5.1. Introduction to MFCs	15
1.5.2. MFC set-up and operational conditions	16
1.5.3. Mediator and mediator-less MFCs	17
	viii

1.5.4. Wastewater treatment	17-18
1.6. Introduction to malaria	18
1.6.1. The malaria parasite life cycle	19
1.6.2. Hemoglobin digestion	20
1.7. Antimalarial drugs	20
1.7.1. Conventional treatment: <i>Cinchona</i> alkaloids	20-21
1.7.2. Artemisinin and analogues	21-22
1.8. How artemisinins work	22
1.8.1. Artemisinins as prodrugs	22
1.8.2. Activation by “free” Fe^{2+}	23
1.8.3. Activation by heme- Fe^{2+}	24-25
1.8.4. Fixed-dose artemisinin combination therapy	25-26
1.9. Drawbacks of artemisinin-based therapy	26
1.9.1. Extraction of artemisinin from <i>Artemisia annua</i>	26
1.9.2. Continuous flow synthesis of artemisinin	26-27
1.10. Toward synthetic peroxide-containing antimalarial drugs	27
1.10.1. Synthetic alternatives to artemisinin	27-28
1.11. Main concept behind research and aims of this work	28
1.12. Bibliography	29-32
Chapter 2: Synthetic antimalarials – Dispiro-1,2,4-trioxolanes	33
2.1. Introduction to 1,2,4-trioxolanes	34
2.1.1. Discovery of secondary ozonides as antimalarials	34
2.1.2. Chemical and metabolic stability	34-35
2.2. Proposed mechanism of action of 1,2,4-trioxolanes	35
2.2.1. Iron-mediated degradation	35-36
2.3. Synthesis of substituted 1,2,4-trioxolanes	37

2.3.1. The Griesbaum Co-ozonolysis	37-39
2.3.2. Diastereoselectivity and scope of the Griesbaum Co-ozonolysis	39-40
2.4. Mechanism of action of 1,2,4-trioxoanes	40
2.4.1. 1,2,4-Trioxolanes in iron-mediated degradation studies	41
2.4.2. 1,2,4-Trioxolanes in heme alkylation	41-42
2.5. Functional group transformations by post-ozonolysis reactions of 1,2,4-trioxolanes	42-43
2.6. Ozonide drug development	46
2.6.1. First generation ozonides	43
2.6.2. Second generation ozonides	44-45
2.6.3. Metabolites of OZ277	45
2.7. Results and discussion	46
2.7.1. Synthesis of <i>O</i> -methyl oximes	46
2.7.2. Optimisation of conditions for the synthesis of 1,2,4-trioxolanes	47
2.7.3. 1,2,4-Trioxolanes for heme alkylation experiments	48-49
2.7.4. 1,2,4-Trioxolanes with functionality on the adamantane moiety	49
2.7.5. 1,2,4-Trioxolane molecular wires synthesised within the O'Neil group	50-54
2.8. Bibliography	55-56
Chapter 3: Synthetic antimalarials – Dispiro-1,2,4,5-tetraoxanes	57
3.1. Introduction to 1,2,4,5-tetraoxanes	58
3.1.1. Stability and reactivity of synthetic endoperoxides: 1,2,4,5-tetraoxanes Vs. 1,2,4-trioxolanes	58-60
3.1.2. Mechanistic studies of RKA182 using TEMPO	61-63
3.1.3. Second generation analogues of RKA182	63-64
3.2. Molecular wire design	64-65
3.3. Methods of binding to carbon and gold surfaces	65

3.3.1. Binding to a carbon surface	65-66
3.3.2. Binding to a gold surface	67-68
3.4. Toward bi-functional 1,2,4,5-tetraoxane molecular wires	68
3.4.1. Introduction to 1,1-dihydroperoxides	68
3.4.2. Methods of synthesising 1,1-dihydroperoxides	68-69
3.4.3. Stability of and side products from 1,1-dihydroperoxides	69-71
3.4.4. Methods of synthesising 1,2,4,5-tetraoxanes	71-73
3.5. Results and discussion	73
3.5.1 Synthesis of 1,1-dihydroperoxides:	
Optimisation of 1,1-dihydroperoxide synthesis	73-75
3.5.2. Problems caused by the unstable nature of 1,1-dihydroperoxides	75-76
3.6. Synthesis of 1,2,4,5-tetraoxanes: Initial work on the synthesis of unfunctionalised tetraoxanes	76
3.6.1. Tetraoxane synthesis using different samples of Re_2O_7	77
3.6.2. Attempted synthesis of a tetraoxane for use as a control in heme alkylation experiments	77-79
3.7. Tetraoxane synthesis using camphor and norcamphor	79-81
3.8. Synthesis of cyclohexyl-functionalised tetraoxanes for heme alkylation experiments	81
3.9. Initial work on the synthesis of adamantyl-functionalised tetraoxanes	82-83
3.10. Initial attempts at synthesising functionalised adamantanes and adamantanones	83
3.10.1. $\text{S}_{\text{N}}1$ reactions using water as a catalyst	84
3.10.2. Attempted heck-type coupling reactions with 1-bromoadamantane	84
3.10.3. Attempted arylation of 5-hydroxy-2-adamantanone using Amberlite TM resin	85-86
3.11. Friedel Crafts arylations of 1-bromoadamantane and 5-bromo-2-adamantanone	86

3.11.1. Friedel Crafts arylation of 1-bromoadamantane	86-87
3.11.2. Attempted synthesis of 5-bromo-2-adamantanone	87-88
3.11.3. Friedel Crafts arylation of 5-bromo-2-adamantanone	88-89
3.11.4. Testing the scope of the Friedel Crafts arylation of 5-bromo-2-adamantanone	90-91
3.11.5. Solvent screen for Friedel Crafts reaction using a solid aryl substrate	91-92
3.11.6. Attempted silyl protection of aniline before Friedel Crafts arylation	92
3.12. Synthesis of 5-(4-bromophenyl)adamantan-2-one starting from 5-hydroxy-2-adamantanone	92-93
3.12.1. Testing the scope of the adamantyl arylation using triflic acid	93-94
3.13. Synthesis of novel adamantyl-functionalised tetraoxanes	94-95
3.14. Experiments to determine if concentration of dihydroperoxide affected tetraoxane yields	96
3.15. PMA-catalysed tetraoxane formation	96-97
3.15.1. Solvent screening for PMA-catalysed tetraoxane formation	98
3.16. Further transformations on adamantyl-functionalised tetraoxanes – organolithium chemistry	99
3.16.1. Experiments to determine stability of tetraoxane in the presence of <i>n</i> BuLi	100
3.16.2. Lithium-bromine exchange experiments involving electrophiles	100-101
3.16.3. Experiments using <i>i</i> PrMgCl in place of <i>n</i> BuLi	102
3.16.4. Experiment using a “TurboGrignard”: <i>i</i> PrMgCl.LiCl	102-103
3.16.5. Experiment using a “TurboGrignard”: TMPMgCl.LiCl	103
3.17. Attempted electrophilic amination on bromophenyl-functionalised tetraoxane	104
3.18. Attempted aminations using Pd chemistry	105-106
3.19. Attempted amination using Cu ₂ O catalyst	106
3.20. Attempted Suzuki cross coupling reaction	106

3.21. Attempted Sonogashira cross coupling reactions	107
3.22. Attempted lithium-bromine exchange on 5-(4-bromophenyl)spiro[adamantane-2,2'-[1,3]dioxolane]	108
3.23. Synthesis of tetraoxanes with meta-substituted aromatic rings	109-110
3.23.1. Tetraoxane formation using adamantanones bearing <i>meta</i> -substituted aromatic rings	110-111
3.23.2. Ester hydrolysis and subsequent amide coupling to incorporate a NH ₂ group	111-112
3.23.3. Attempted amide coupling to incorporate a thiol group	112
3.23.4. Solvent screening for amide coupling on tetraoxane	112-114
3.24. Synthesis of adamantanones functionalised with thiophene and thiophene derivatives	114
3.24.1. Attempted synthesis of adamantanone functionalised with thiophene	114
3.24.2. Attempted synthesis of adamantanone functionalised with ethyl 2-thiophenecarboxylate	115
3.25. Conclusions and further work	116
3.26. Bibliography	117-120

Chapter 4: Synthesis of β-turn mimetics and chiral enamine <i>N</i>-oxides	121
4.1. Introduction to amino acids and proteins	122
4.1.1. Primary structure of proteins	122
4.1.2. Secondary structure of proteins: α -helix and β -sheet	122-123
4.2. Introduction to β -turns	124
4.3. Introduction to protein β -turn mimetics	125
4.3.1. Design of peptidomimetics	125-126
4.3.2. β -Turn mimetic classification	127-128
4.4. Proposed route to β -turn mimetics based on a fused morpholine skeleton	128-130
4.5. Introduction to chiral enamine <i>N</i> -oxides	130-132

4.6.	Results and discussion	132
4.6.1.	Route to β -turn mimetics using a modified Ugi/Polonovski reaction	132-135
4.6.2.	Synthesis of β -turn mimetics using a reverse-Cope cyclisation	135-138
4.6.3.	Synthesis of chiral enamine <i>N</i> -oxides	138-139
4.7.	Conclusions and further work	140
4.8.	Bibliography	141-142
Chapter 5:	Experimental details	143
5.1.	General information	144
5.1.1.	Purification of chemicals	144
5.1.2.	Purification of solvents	144
5.1.3.	Titration of <i>n</i> BuLi	144
5.1.4.	Purification of <i>m</i> -CPBA	144
5.1.5.	Preparation of glassware	145
5.1.6.	Other apparatus	145
5.1.7.	Chromatography	145
5.1.8.	Characterisation of compounds	145
5.2.	Individual experimental procedures	146-197
5.3.	Bibliography	198

Chapter 1

Introduction to *Geobacter*, microbial fuel cells and malaria

1.1. Energy production and fossil fuels

1.1.1. Global warming

For years, scientists argued over the evidence and governments refused to accept that global warming was happening. There is no longer any doubt that our use of fossil fuels to meet our energy needs is changing the climate. Since the industrial revolution, the burning of fossil fuels; coal, oil and gas – has massively increased to power factories, heat homes and drive cars. Burning fossil fuels releases carbon dioxide – the main man-made greenhouse gas. It exacerbates environmental damage by contributing to the greenhouse effect (**Figure 1**). Carbon dioxide creates an artificial greenhouse effect, thickening the natural canopy of gases in the atmosphere, causing more heat to become trapped. As a result, the global temperature increases, throwing the world's climate out of its natural balance.

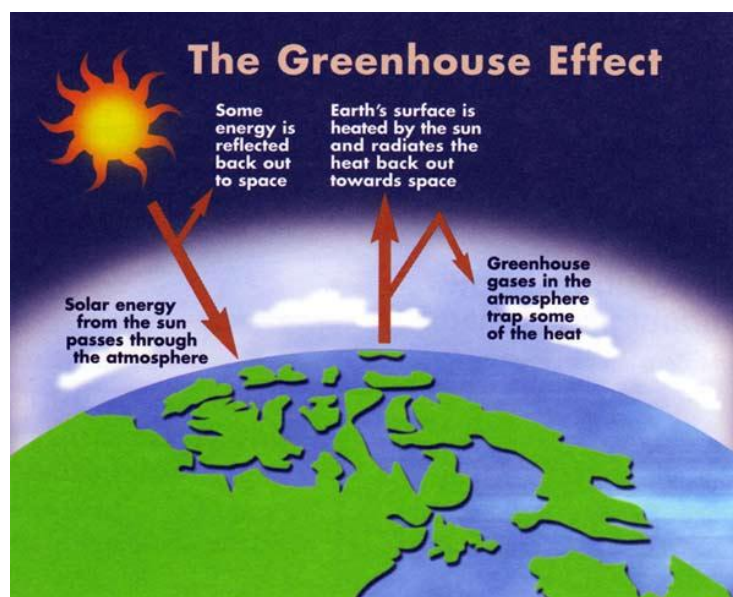


Figure 1: The Greenhouse Effect.¹

Electricity production currently accounts for 35% of total global fossil fuel use and around 41% of total energy-related carbon dioxide emissions. Coal is the most important energy source, producing 41% of the world's electricity in 2008 but is also the most carbon-intensive fuel and the single largest source of greenhouse gas emissions.^{2, 3} Our current rate of fossil fuel consumption is environmentally unsustainable because fossil fuels are finite natural resources and they are depleting rapidly.

It has been predicted that demand for fuel will exceed supply within the next ten to twenty years.⁴ Globally, energy use accounts for almost two thirds of greenhouse gas emissions, and these emissions are rising. Without urgent action to quit this fossil fuel addiction, the world is heading for dangerous levels of warming, well above the 1.5°C danger threshold.⁵

1.1.2. The future of non-renewable energy

It is predicted that fossil fuels will dominate the future energy picture at least through to 2035. While renewable energy is expected to increase its share of electric generation, it is thought to remain a small portion of total generation over the next 25 years. Even if tax incentives for renewable technologies were to be extended, energy from renewable resources would still account for less than a 20% share of generation in 2035.⁶ Supplies of cheap, conventional oil and gas are declining while demands continue to rocket in emerging economies such as China and India. It is clear that our current reliance on fossil fuels cannot continue.

1.1.3. Renewable Energy

By switching to renewable energy, a viable alternative to fossil fuels, the natural environment can be protected, the need for energy can be fulfilled and the consequences of global warming can be avoided. The Energy Report 2011 by the WWF outlines how the world's energy needs could be provided by 100% renewable energy by 2050, cleanly, renewably and economically.³ They envisage that this goal could be achieved with a “do more with less” approach by, for example, using energy efficient materials in building construction, developing more efficient forms of transport, changing lifestyles, using electricity generated by wind, solar and hydropower. However, sustainability for this very much depends on international co-operation and collaboration on an unprecedented level.

While it is well known that energy can be obtained from the sun, the Earth, water and wind, it has recently been found that with a microbial fuel cell (MFC), electricity can be generated from wastewater. The MFC converts organic material to electricity using bacteria, leaving behind clean drinking water in the process. This is an exciting prospect for people in countries where adequate sanitation and the means to afford it are lacking. Wastewater treatment plants also require a lot of power to treat water so a significant amount of money and resources would be saved if the wastewater itself could be used as a fuel. The form of renewable energy that will be the main focus in this work will be MFCs and the next section discusses the type of bacteria that are capable of generating electricity.

1.2. Electrogenic bacteria: *Geobacter sulfurreducens*

1.2.1. Introduction to *Geobacter*

Life evolved on the planet without an oxygen atmosphere and anaerobes evolved during this time using various methods to support metabolism without oxygen to drive respiration.⁴ The most fascinating bacteria are those that are able to transfer electrons outside the cell to an electron acceptor. Such bacteria are called exoelectrogens and the *Geobacter* genus is the main focus in this work. Like many bacteria, the *Geobacteraceae* family feed on and decompose organic material. *Geobacter* microbes were first discovered in 1987 under the Potomac River, downstream from Washington D.C. where there is no oxygen and plenty of iron. They have the unexpected ability of moving electrons into metal, which means that under the right conditions, *Geobacter* can simultaneously process waste and generate electricity.^{7, 8} In their natural environment, *Geobacter* grow on mineral surfaces where they can use solid metal oxides as the terminal electron acceptor for anaerobic respiration.

1.2.2. Bacterial respiration

In a MFC, the bacteria oxidise organic matter, such as acetate to CO₂, producing electrons that travel through a series of respiratory enzymes in the cell and make energy for the cell in the form of ATP. The electrons are then released to a terminal electron acceptor, which becomes reduced. Examples of terminal electron acceptors include oxygen, nitrate and sulfate, which can all readily diffuse into the cell to accept electrons and form products that can easily diffuse out of the cell.

To improve the efficiency of MFCs, it is vital to understand how and why microorganisms exchange electrons with electrodes in a fuel cell. It is important to have some notion of metabolism to understand why external electron transfer is essential for the bacteria and how the exchange with the electrode is occurring. Bacteria can process lipids, proteins and carbohydrates to supply themselves with carbon and energy. All of these organic substrates act as electron donors for a complex system of redox reactions that result in the production of an energy carrier molecule (ATP). They can be converted through glycolysis into the acetyl unit of acetyl-CoA, which is fed into the citric acid cycle (**Figure 2**).

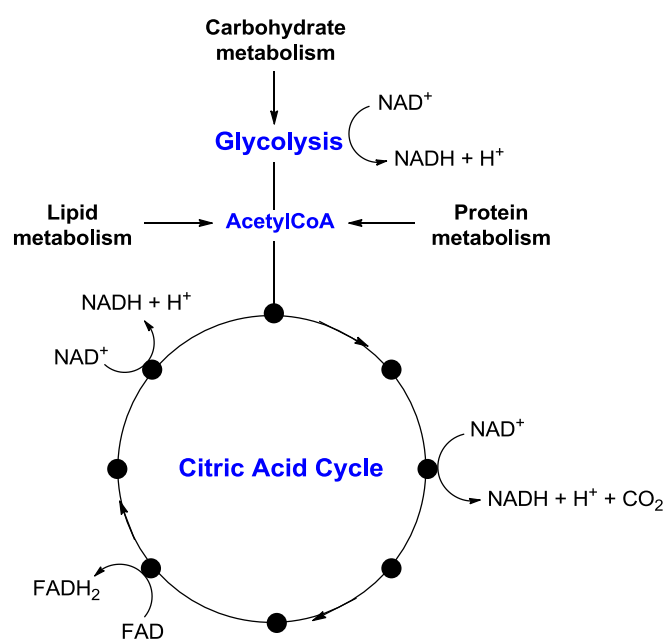


Figure 2: Citric acid cycle.⁹

This is where oxidation reactions are coupled to the reduction of NAD^+ and FAD to their electron carrier forms, NADH and FADH_2 (**Figures 3 and 4**). These electron carriers then transfer electrons from the cytoplasm, where the citric acid cycle occurs, to the cell membrane. Before being transmitted to a terminal electron acceptor e.g. oxygen, electrons are transferred through different mediators, some of them pumping protons out of the cell as they are reduced. The energy of this proton gradient is used by the cell to phosphorylate ADP to produce ATP. The process in which ATP is produced by the reduction of an inorganic terminal electron acceptor is called respiration.

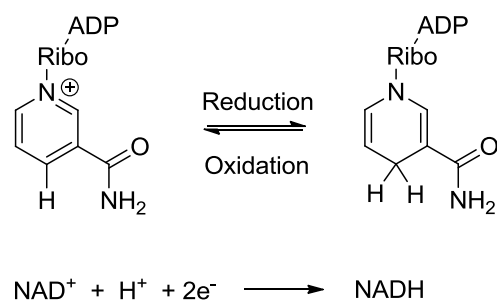


Figure 3: The redox reactions of NAD.

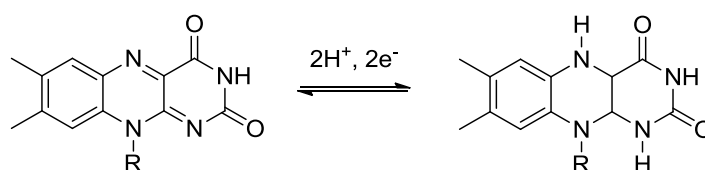


Figure 4: Reduction of FAD to FADH₂.

1.2.3. Electrogenic properties of *Geobacter sulfurreducens*

Although *Geobacter* conserve energy for growth by using metal oxides for anaerobic respiration, it has been shown that they can also exchange the electrons produced with a polarized electrode.¹⁰ This is extremely fascinating, especially as electrodes, per se, are not part of the natural environment. *Geobacter sulfurreducens* are also known to produce the highest current densities of any microorganism available in pure culture.¹¹ They can form multi-microbe thick, persistent biofilms not observed when respiring insoluble oxidants, in which microbes residing more than 20-cell lengths (20µm) away utilise the anode as their terminal electron acceptor.¹² The combination of robust direct electron transfer and high cell surface density (microbes across the entire biofilm generating electrons, which are collected by the underlying anode) enables *Geobacter* biofilms to achieve higher anodic current densities than any other species. However, in most cases, electrical outputs of MFCs are currently too low for most perceived practical applications and for them to be considered a viable alternative energy source. This is because electrodes employed in electrochemical applications are made from materials such as platinum or carbon. They are not natural electron acceptors for these bacteria which have very specific requirements regarding the crystal structure of the electron acceptor in order to establish an efficient electrical communication.

Most efforts for further optimisation have focused on modifying fuel cell architecture or electrode materials in an attempt to increase electrical current. To date, there has been little investigation into the properties of *Geobacter sulfurreducens* with the assumption that their current-production capacity was fixed. However, there was a breakthrough in 2012 when Lovley *et al.*¹¹ showed for the first time that there is a direct correlation between biofilm conductivity and current production. This was attributed not only to reduced resistance to electron flow through the biofilm but also to a lower activation energy barrier for electron transfer between the biofilm and the anode.

It has been suggested that some microorganisms have evolved effective strategies for extracellular electron exchange with insoluble minerals.¹³ There is, however, a significant difference between insoluble minerals and electrodes. Electrodes provide a surface with long-term electron-accepting or electron-donating capacity, whereas the ability of individual insoluble materials to accept or donate electrons is eventually depleted. This means that the relationship between cells and electrodes, and cells and minerals is significantly different and this is apparent with *Geobacter* species. Bond and Lovley¹⁴ showed that *Geobacter sulfurreducens* can grow on graphite electrodes and efficiently transfer electrons from the oxidation of acetate. The recovery of acetate as electrical current was found to be quantitative but the mechanism by which this transfer took place was not fully understood.

Before putting the idea of using bacteria in MFCs into practice, it is essential to decipher the exact mechanism by which the bacteria transfer electrons to the electrode. The rate is currently too slow so the power generated as a result is very small. One possible explanation for this, as proposed by Rittmann⁷, is that physical contact with the electrode surface is limiting electron transfer. Even though the bacteria are on the surface of the anode, only a tiny part of each cell actually touches the metal, and this may be hindering electron movement. Another possible factor is the voltage on the electrode; it needs to be high enough to make the bacteria give up their electrons.

1.2.4. Mechanisms of electron transfer

There are three most commonly considered mechanisms for electron transfer between bacteria and extracellular electron acceptors and each of these is discussed in the next section:

- 1) Electron “hopping” resulting from direct contact between redox-active proteins on the outer surface of the bacterial cells and the electron acceptor.
- 2) Electron transfer *via* soluble electron shuttling molecules (redox mediators).
- 3) The conduction of electrons along pili (natural nanowires).

1) Short-range direct electron transfer *via* redox-active proteins; *c*-type cytochromes

Geobacter sulfurreducens is the only microorganism capable of producing high current densities with direct electron transfer to electrodes in which the mechanisms for this electron transfer have been investigated.¹⁵ One possible electron transfer path between a microbe and an electrode is direct electron transfer (electron “hopping”) where the active centre of the bacterial membrane is connected directly to the electrode. In this case, the electron transfer rate can be very low due to insulation of the active site of the enzyme in the protein environment and isolation of the enzyme from the electrode surface by its relative burial into the bacterial membrane. However, in the case of exoelectrogens e.g. *Geobacter*, the redox enzymes involved in electron transfer are located on the outer surface of the bacterial membrane and oriented so that the active site is facing towards to the electrode.⁹

c-Type cytochromes are ubiquitous redox proteins whose principal biological function is electron transfer in cellular respiration, where single or di-heme cytochromes shuttle electrons between larger electron transfer proteins. *c*-Type cytochromes play vital roles in mediating electron transfer reactions associated with respiration in nearly all living organisms. *Geobacter sulfurreducens* have a wide diversity of *c*-type cytochromes exposed on the outer surface of the cell (**Figure 5**).¹³ Although their amino acid sequences differ greatly, all *c*-type cytochromes possess at least one heme that is covalently bound through amino acid side-chains of the proteins to position and orientate the heme moiety to facilitate efficient reactions.¹⁶ *Geobacter sulfurreducens* cells possess an abundance of multi-heme *c*-type cytochromes on their outer membrane, in extracellular polymeric structures and along pili. One example of such a cytochrome is OmcS, which has a molecular mass of approximately 50kDa and is predicted to contain six heme centres.¹⁷

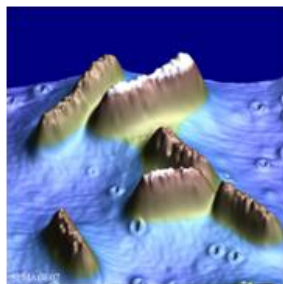


Figure 5: AFM image of *c*-type cytochromes in *Geobacter sulfurreducens* by Dr. Abraham Esteve-Núñez, University of Alcalá de Henares.

2) Electron transfer via soluble electron shuttling molecules (redox mediators)

Electron shuttles are chemical compounds that stimulate the biodegradation of contaminants by facilitating the transfer of electrons to/from bacteria.¹⁸ These compounds assist in microbial energy metabolism primarily as intracellular electron carriers e.g. NAD that transfers electrons mainly from the citrate cycle to the respiratory electron-transport chain. In general, shuttles facilitate electron transfer between microbes, from electron-donating substances to microbes and/or from microbes to electron-accepting substances.¹⁹ Mediated electron transfer usually proceeds at much faster rates. It relies on the addition of naturally occurring redox active species, stable in two redox states, which are able to quickly diffuse in and out of the enzymatic channels, hence effectively shuttling electrons to the electrode surface.⁹ However, reliance on soluble additives in the anolyte would not be compatible for the purpose of wastewater treatment. It is important to realise that added mediators, whether or not they are immobilised, are not essential for electron transfer between bacteria and an electrode.

A diversity of microorganisms e.g. *Pseudomonas* and *Shewanella*, have the ability to produce electron shuttles to promote electron transfer to electrodes.²⁰ Previous studies have shown that some microorganisms produce shuttles that promote electron transfer between cells and insoluble Fe(III) oxides. Oxidised shuttle molecules are reduced at the outer cell surface and the reduced shuttle molecules donate electrons to the electrode. Electrons can hop directly from *c*-type cytochromes to an electrode but this was shown to be possible only when anodes were artificially poised at positive potentials significantly higher than those of typical MFCs, and the rates of electron transfer were much faster in the presence of a shuttle molecule such as flavin.¹³

The maximum current densities produced by microorganisms that rely on electron shuttling to transfer electrons to electrodes are much lower than those for microorganisms that are capable of long-range electron transport through thick, conductive biofilms. This is because the major limiting factor for electron shuttling is that it relies on diffusion, which is slow. The energy investment to produce shuttles is also considerable and this can render the shuttling process thermodynamically inefficient or less favourable than direct transfer as used by *Geobacter* species.¹³ Systems that rely on the addition of artificial electron shuttles have proven to lack long-term stability and their toxicity to humans greatly limits applications.

3) Long-range electron transport via conductive pili



Figure 6: *Geobacter* cell with natural microbial nanowires known as pili. (Size of cell: 1 μ m.)

Geobacter sulfurreducens have natural microbial nanowires known as pili (**Figure 6**) on their outer surface, which are made of fibrous protein structures.⁹ Microbial nanowires are defined as protein filaments produced by microorganisms that are capable of performing long-range electron transport *in vivo* under physiologically relevant conditions.²¹ They are 3-5nm in width, making them 20,000 times finer than a human hair and up to 10-20 μ m in length.^{13, 15, 22} They offer the possibility of greatly enhancing microbe-electrode interactions and play an important role in electronic interactions of microorganisms with inorganic electron acceptors in their environment, as well as interspecies electron exchange. Pili have been shown to have electronic conductivities in the region of 5mScm⁻¹. This is comparable to nanostructured films of organic polymers e.g. polyacetylene and polyaniline.^{21, 23} In other words, electron conduction along the length of the pili is through conjugated π orbitals of pilin constituents, presumably aromatic amino acids.¹⁵

Pili are capable of long-range (μm to cm) electron transport *via* a metallic-like conductivity, which has not previously been observed in a biological material.^{13, 23} Type IV pili in *Geobacter sulfurreducens* are the only filaments that have been shown to be required for extracellular electron transport to extracellular electron acceptors or for conduction of electrons through biofilms.²¹

Electron hopping involving cytochromes or metallic-like conduction through pili – which mechanism occurs?

There is much debate between the groups of Lovley and Tender over which electron transfer mechanism actually occurs. The results presented by each of them are currently inconclusive. In 2012, Lovley *et al.*²⁴ showed multiple lines of evidence that were consistent with long-range electron transport through the biofilms of *Geobacter sulfurreducens* *via* networks of pili that possess metallic-like conductivity. The reported results refute the cytochrome hypothesis discussed above and provide additional data which suggest that electron transfer is *via* a metallic-like conductivity. The results^{21, 24} that supported electron transfer *via* a metallic-like conductivity (i.e. through pili) were:

1. The highest conductivity for pili was obtained at pH 2, a pH at which *c*-type cytochromes are denatured.
2. The conductivity of biofilms was found to be 5mScm^{-1} , which is consistent with the conductivity of pili, whereas the conductivity due to *c*-type cytochromes alone was 2000 times lower at $2.65\mu\text{Scm}^{-1}$.
3. Cells at a substantial distance ($>50\mu\text{m}$) from the anode surface remained metabolically active and contributed significantly to current production.
4. The most abundant cytochromes are localised in the periplasm or in membranes so not all hemes are available to participate in extracellular electron exchange.
5. Known outer-surface cytochromes are multi-heme so the number of cytochromes available for electron exchange is much lower than the number of hemes measured.
6. The only cytochrome known to be associated with pili is OmcS and deletion of OmcS caused an increase in biofilm conductivity and current density, not the decrease expected if OmcS was important in conferring conductivity required for long-range electron transport. The simplest explanation for these observations is that pili deliver electrons to OmcS, which transfers them to Fe(III) .²⁵

7. The average spacing between OmcS molecules was *ca.* 30nm and spacing between OmcS clusters were 100-200nm and these values far exceed the distances of <2nm required for electron hopping. The density of the cytochromes is therefore too low and spaced too far apart for electron hopping to take place.
8. OmcZ is the only outer-surface *c*-type cytochrome known to be necessary for current production. OmcZ was found to be specifically localised at the anode-biofilm interface, which suggests that it cannot be responsible for conduction of electrons through the bulk of the biofilm.
9. Finally, biofilms were treated with acetyl methionine, which binds to *c*-type cytochromes, making them non-functional. This did not negatively impact on conductivity in pili networks.

The above evidence suggests that *c*-type cytochromes do not contribute to long-range electron transport and the mechanism by which it happens is *via* a metallic-like conductivity. The mechanisms by which OmcZ contributes to electron exchange with electrodes need to be further evaluated.

In contrast to Lovley's proposals, Tender *et al.*¹² proposed that biofilm anode respiration is ultimately controlled by extracellular electron transfer among cytochromes and the following is a summary of the points that support their proposal:

1. They found that there was a linear increase in current with the number of *c*-type cytochromes in a *Geobacter* biofilm anode during biofilm growth.
2. The hypothesis of metallic-like conduction by pili does not provide explanations for the finite thickness of biofilms.
3. The biofilm anode grows in thickness until either the pH value near the anode surface becomes sufficiently low that it inhibits cytochrome function of the innermost cells (and thus limiting the ability of all cells in the biofilm to transfer electrons to the anode), or until the local concentration of oxidised cytochromes experienced by the outermost cells becomes too low to support additional growth.

1.3. Fluorescent properties of *c*-type cytochromes in *Geobacter sulfurreducens*

In 2008, Lovley *et al.*²⁶ reported a novel fluorescence technique for monitoring the redox status of *c*-type cytochromes in *Geobacter sulfurreducens*. This was developed to evaluate the capacity of these cytochromes to store electrons during periods in which an external electron acceptor was not available. When cytochromes were in a reduced state and excited at a wavelength of 350nm, they fluoresced with maxima at 402 and 437nm. Oxidation of the cytochromes resulted in a loss of fluorescence.

1.4. Role of *Geobacter* and MFCs in bioremediation

Microorganisms can aid environmental restoration by oxidising, binding or immobilising contaminants. There is significant interest in bioremediation because it promises to be simpler, cheaper and more environmentally friendly than non-biological options where contaminants are merely dug up and transported elsewhere.²⁷ As well as their electrogenic properties, *Geobacter* are also of interest because of their role in environment restoration. They are well known for their biodegradation capacities of pollutants such as aromatic hydrocarbons, nitroaromatic explosives and even uranium. For example, *Geobacter* species can destroy petroleum contaminants in polluted groundwater by oxidizing these compounds to harmless carbon dioxide.

1.4.1. Removal of uranium from contaminated groundwater

The addition of an organic electron donor such as acetate to groundwater contaminated with uranium can stimulate the growth of *Geobacter* species, which obtain most of their energy from the oxidation of the acetate with the reduction of Fe^{3+} oxides that are abundant in most subsurface environments. As U^{6+} -containing groundwater enters the zone of acetate addition, the *Geobacter* species also transfer electrons to the soluble U^{6+} reducing it to the highly insoluble U^{4+} .^{27, 28} This method solves the problem of further migration of the uranium, which is beneficial but the drawback is that it remains in the subsurface. However, if an electrode served as the electron donor, the U^{4+} that is produced can precipitate on the electrode surface instead.

Gregory and Lovley²⁹ showed that under anaerobic conditions, 87% of the uranium that had been removed from the contaminated groundwater was recovered from the electrode surface after it was pulled from the sediments. U^{4+} was not observed in the solution after 600hrs when the system was maintained under anaerobic conditions. However, if exposed to oxygen, the uranium would be expected to rapidly dissolve. There is a possibility of using this system to remove uranium from contaminated groundwater by concentrating it on the electrode and removing the electrode from the system. The uranium could then be concentrated in an external solution, and the electrode re-used. This method would only be feasible if performed under fully anaerobic conditions as intrusion of oxygen into the system would cause re-dissolution of the uranium, which would be problematic as it could potentially create a spike in chemical concentration.^{4, 29}

1.4.2 *Geobacter sulfurreducens* in MFCs

The fact that both biodegradation and electrogenic activities are present in *Geobacter sulfurreducens* makes them the most suitable microorganism for use in MFCs. The low electrical output from MFCs needs to be increased before they can be developed further for large scale commercial purposes. In an attempt to increase electrical output from MFCs, an efficient means of attachment of the bacteria to the electrode is required in the form of a molecular wire. As *Geobacter sulfurreducens* have accessible heme centres on their outer membranes, the O'Neil group decided to base the molecular wire design on synthetic antimalarial drugs because they are capable of alkylating the porphyrin ring in heme. This will be discussed further after an introduction to microbial fuel cells.

1.5. Microbial Fuel Cells (MFCs)

Microbial fuel cells (MFCs) are an emerging technology which directly converts chemical energy stored in organic matter to electricity. Driven by the increasing concern over the energy-climate calamity and environmental pollution, MFCs have been developed rapidly over the past decade.³⁰ MFCs make it possible to directly utilise bio-electricity from organic waste with a higher energy transforming efficiency than other traditional technologies. The wide application of MFCs will significantly reduce the energy dependence on fossil fuels as well as the problems of climate change and environmental pollution.

Currently, MFCs are in the process of making the challenging step from laboratory to practical application. However, it has been argued that a 10-fold increase in the efficiencies (compared to current laboratory reactors) is necessary for MFCs to be feasible commercial processes.¹⁹

1.5.1. Introduction to MFCs

The first evidence of electricity generation by bacteria in MFCs was reported by Potter in 1912.³¹ However, there was little interest in this field until a short revival almost half a century later. The main drawbacks at the time were low current generating capacity, a need for artificial electron mediators and successful development of other alternative technologies such as photovoltaic technology so early MFCs were not considered promising.

The greatest environmental challenge is to develop a new energy platform that is capable of simultaneously solving energy production and CO₂ releases. It is well known that microorganisms can produce fuels such as ethanol, methane and hydrogen from organic matter. It is less well known that microorganisms can also convert organic matter into electricity in devices known as microbial fuel cells.²⁸

MFC technology currently represents the newest renewable approach for generating electricity.⁴ In brief, this is a method of electricity generation from biomass using electrogenic bacteria without the need for combustion. MFCs consist of an anode that accepts electrons from microorganisms and a cathode that transfers electrons to an electron acceptor. This flow of electrons between the electrodes provides current that can be harvested to power electronic devices.²² Interest in MFCs is increasing as they offer the possibility of harvesting electricity from organic waste and they could also fill a niche that is significantly different from the better known abiotic hydrogen- and methanol-driven fuel cells. These abiotic cells involve the use of fuels that are highly explosive and/or toxic and also require expensive catalysts to promote oxidation of the electron donors, whereas naturally occurring microorganisms can catalyse the oxidation of the fuels (organic waste) in MFCs.²⁸

1.5.2. MFC set-up and operational conditions

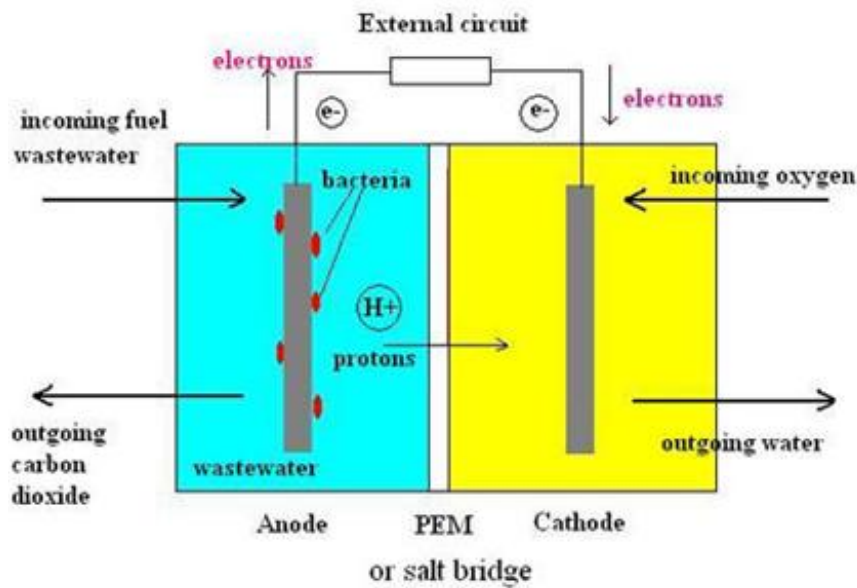


Figure 7: Diagram explaining how a MFC functions.³²

The MFC is a bio-electrochemical system in which bacteria are used to convert organic matter into electricity (**Figure 7**). Typically, a MFC comprises an anaerobic anode, an aerobic cathode, the proton-exchange membrane (PEM) or salt bridge, and the external circuit. The anode holds the bacteria and organic matter in an anaerobic environment. The cathode holds a conductive saltwater solution. As part of the digestive process (oxidation), the bacteria create protons and electrons. The electrons are pulled out of the solution onto the anode and are conducted through an external circuit to arrive at the cathode. The protons travel through the PEM or salt bridge to meet with the electrons at the cathode. The PEM or salt bridge separates the anode and the cathode but protons are able to move through to connect them. The salt bridge is a mesh of proteins that allows the protons to move from the anode to the cathode but keeps the solutions in the anode and cathode separate. Driven by the potential difference between the cathode and the anode, the protons and electrons combine with oxygen to create water in the cathode chamber.

It is now known that some bacteria can transfer electrons exogenously (i.e. outside the cell) to a terminal electron acceptor such as a metal oxide and it is these bacteria that can be used to produce power in a MFC. Bacterial attachment to and the formation of a biofilm on the anode surface are essential for the efficient biological transfer of electrons in a MFC.³³

1.5.3. Mediator and mediator-less MFCs

In a mediator MFC, the bacteria are electrochemically inactive. They digest organic matter and create electrons but have no mechanism to rid themselves of these electrons so a mediator is required. The mediator is an inorganic substance, such as thionine, methyl viologen, potassium ferricyanide or methylene blue, which crosses the membrane of the bacteria and frees the electrons. The mediator then carries the electrons away from the bacteria and deposits them onto the electrode. One disadvantage to the mediator MFC is that many of the mediators used are toxic in nature.³⁴

In a mediator-less MFC, the bacteria are electrochemically active and they themselves can carry the electrons they create through digestion of organic matter to the electrode. There are several factors that are limiting steps for electricity generation, such as fuel oxidation at the anode electron transfer from microorganism to the anode, proton transfer through the membrane to the cathode and oxygen reduction at the cathode.³⁴

However, as mediator-less MFCs are a recent development, this process is not yet completely understood.^{4, 32} Mediator-less MFCs are considered to be more suitable for practical MFCs as sustainable processes since mediators are generally costly.¹⁹

1.5.4. Wastewater Treatment

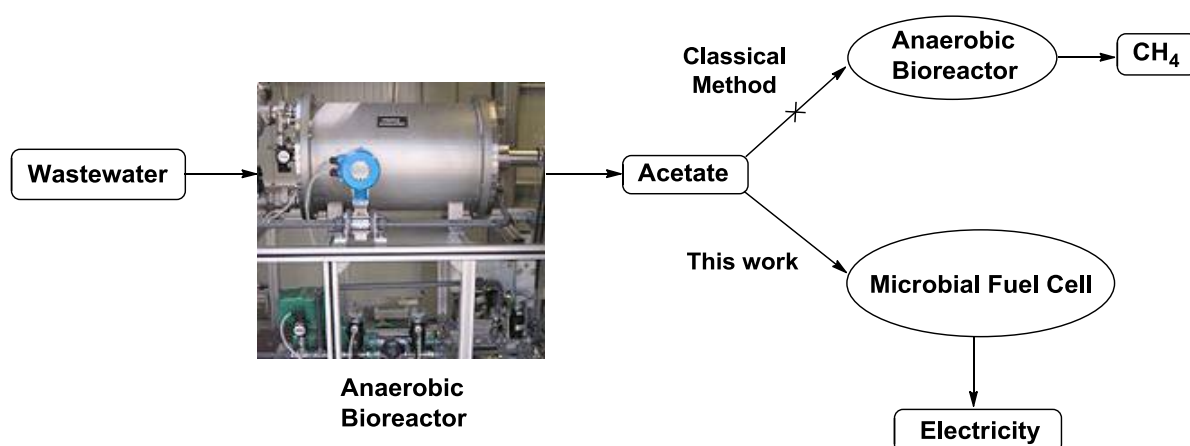


Figure 8: Application of MFC technology in wastewater treatment.

Wastewaters are classically processed under anaerobic conditions in order to transform organic matter into acetate and short chain organic acids. As shown in **Figure 8**, the acetate is further converted to methane. Although this could be used as an energy source in the wastewater treatment plant, it also constitutes a potent greenhouse effect gas whose energy absorbed per molecule is 25 times higher than CO₂. The ultimate aim of this research is to replace this methanogenic stage with an advanced MFC that is able to convert acetate into electricity rapidly by means of a highly inter-connected electrogenic biofilm.

The next section gives an introduction to malaria and discusses how synthetic antimalarial drugs can form the basis of our bi-functional molecular wires and their application in microbial fuel cells.

1.6. Introduction to malaria

According to the World Malaria Report 2011, there were about 216 million cases of malaria and an estimated 655,000 deaths in 2010. Malaria mortality rates have fallen by more than 25% globally since 2000 and by 33% in the WHO African Region. Most deaths occur among children under the age of 5 in Africa where a child dies every minute from malaria.

Malaria is the most important insect-transmitted disease. It is caused by parasites of the *Plasmodium* genus³⁵ and four of these species can cause malaria in humans: *Plasmodium falciparum*, *Plasmodium vivax*, *Plasmodium malariae* and *Plasmodium ovale*. *Plasmodium falciparum* and *Plasmodium vivax* are the most common and *Plasmodium falciparum* is the most deadly, hence a lot of effort has been focused towards designing antimalarial drugs that treat *falciparum* malaria.

Malaria is transmitted exclusively through the bites of infected mosquitoes from the *Anopheles* genus, called “malaria vectors”, which bite mainly between dusk and dawn.^{35, 36} Symptoms of infection include high fever, shaking, chills, severe anaemia, coma and if left untreated, death.³⁷ *P. falciparum* infections are the most prevalent and cause the majority of malaria-related mortality in non-immune individuals.³⁵

1.6.1. The malaria parasite life cycle

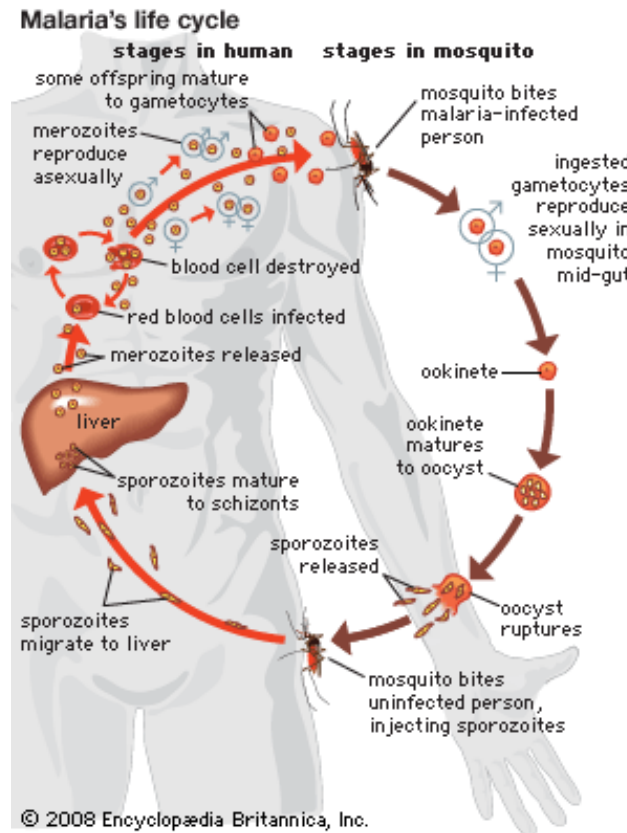
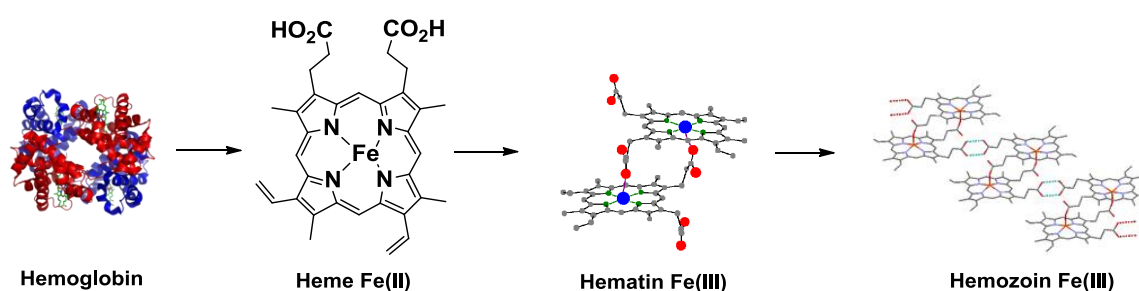


Figure 9: Life cycle of the malaria parasite.³⁸

The *Plasmodium* parasite spends its life cycle partly in humans and partly in mosquitoes (**Figure 9**). When an infected female *Anopheles* mosquito bites a human host to take a blood meal to nourish her eggs, it passes cells called sporozoites into the human's bloodstream. These sporozoites travel to the liver where they undergo asexual reproduction to form trophozoites, which then mature to produce schizonts. Their nuclei split to form thousands of new cells called merozoites. When the liver cells rupture, the merozoites enter the bloodstream and infect red blood cells which grow and divide to produce more merozoites, eventually causing the red blood cells to rupture. Some of these newly released merozoites go on to infect other red blood cells and some develop into sex cells known as male and female gametocytes. These gametocytes lie dormant in humans until another mosquito bites the infected human, ingesting the gametocytes. In the mosquito's stomach, the gametocytes mature and male and female gametocytes undergo sexual reproduction to form a zygote. The zygote multiplies to form sporozoites, which travel to the mosquito's salivary glands. The cycle begins again when this mosquito bites another human.

1.6.2. Hemoglobin digestion

During the blood stage of the malaria cycle where trophozoites form schizonts, *Plasmodium falciparum* uses hemoglobin in the human host as a food source to provide itself with amino acids to build its own proteins.³⁹ During the digestion process, a lot of free heme (Fe(II)) is released from hemoglobin and this is toxic to malaria parasites.⁴⁰ The free heme is autoxidised to hematin(Fe(III)),⁴¹ which is a dimer formed by covalent bonding between the carboxylic acid groups and iron. These dimers interact through hydrogen bonds to form crystals of a non-toxic, Fe(III) polymer called hemozoin or ‘malaria pigment’ (**Scheme 1**).



Scheme 1: Detoxification of hemoglobin to hemozoin.

1.7. Antimalarial drugs

1.7.1. Conventional treatment: *Cinchona* alkaloids

The only two antimalarial classes of medicines used to treat severe malaria come from plants: *cinchona* alkaloids and artemisinin.⁴² In the 16th century, the therapeutic action of the bark of the *cinchona* tree was discovered by natives of Peru.

Quinine (**Figure 10**), the alkaloid from *cinchona* bark was first isolated in 1834 by French chemist, Pelletier and this became the frontline treatment for malaria until the 1930s when synthetic antimalarials were developed.⁴³ Approximately 300–500 tons of quinine are commercially produced each year by extraction of the bark from *cinchona* species that are widely cultivated. About 40% of the quinine goes towards the production of pharmaceuticals, while the remaining 60% is used by the food industry as the bitter principle of soft drinks such as tonic water.⁴⁴

From the 1940s to 1990s, chloroquine (**Figure 10**) was the main treatment for malaria worldwide.⁴⁵ However, by the 1970s, it was reported that chloroquine was no longer effective in South East Asia, Africa and South America as *Plasmodium falciparum* had become resistant. This level of resistance escalated rapidly within the next ten years so there has been increased demand for unrelated classes of antimalarials to reduce the burden of malaria.

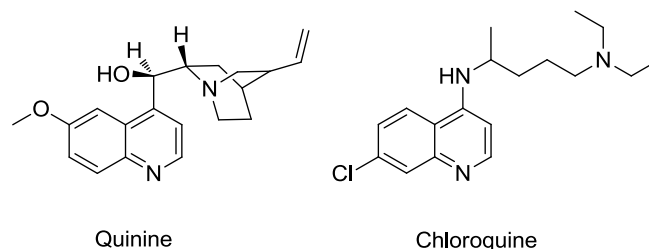


Figure 10: Quinoline-based antimalarials.

1.7.2. Artemisinin and analogues

The discovery of artemisinin and its derivatives is a milestone in the history of antimalarial drug research since the discovery of quinine. After a brief introduction on the chemistry and pharmacological aspects of artemisinin, we will focus this section of the review on the radical chemistry and alkylation properties of artemisinin and synthetic peroxides. It is clear that good knowledge of the mechanism of action of artemisinin allowed the rational design of new synthetic antimalarial drugs.

Artemisinin, a sesquiterpene lactone, was first isolated in 1971 from the Chinese herb, *artemisia annua*.⁴³ It was given the name *qinghaosu*, meaning “blue-green plant extract” but the name artemisinin is now commonly used. *Artemisia annua* has been used for many centuries in traditional Chinese medicine as a treatment for fever and malaria. Artemisinin is a “new entity” with a structure and mode of action that are unrelated to those of any other antimalarial because it differs from the classical quinoline-based drugs, quinine and chloroquine. This means that the chances of cross-resistance are unlikely and this is important due to the reported high resistance of parasites towards quinoline-based antimalarials.⁴⁶ Artemisinin has been used successfully in several thousand malaria patients in China, including those with chloroquine-sensitive and chloroquine-resistant strains of *Plasmodium falciparum*. Artemisinin is currently the most effective treatment against multi-drug resistant *Plasmodium* species.

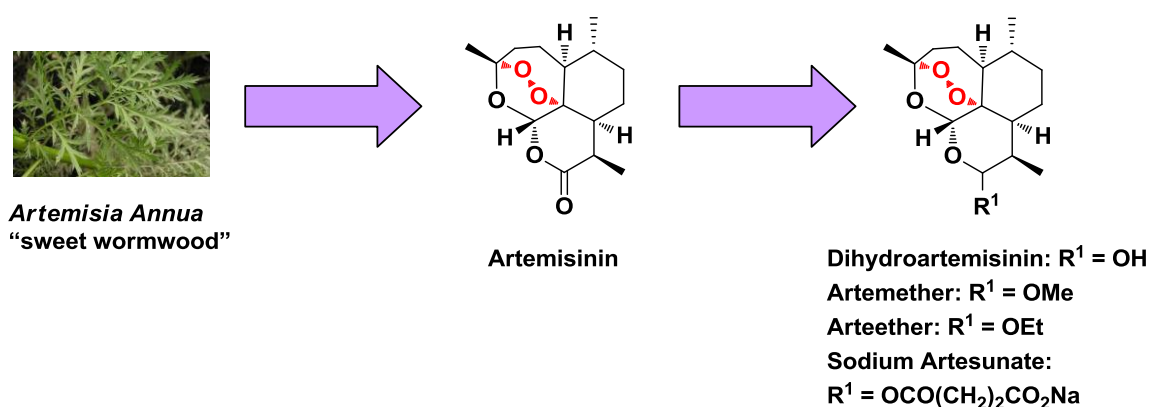


Figure 11: Artemisinin and its semi-synthetic analogues.

A series of semi-synthetic first generation analogues (**Figure 11**) have been made e.g. a water soluble derivative, sodium artesunate was prepared to treat advanced cases of malaria by intravenous injection. The other analogues listed can all be readily prepared from dihydroartemisinin (DHA), which in turn is prepared from borohydride reduction of the ring lactone of artemisinin. However, as a drug class, artemisinins suffer from chemical (semi-synthetic availability, purity, cost and hydrolytic instability of the lactone function), biopharmaceutical (poor bioavailability due to poor solubility in both oil and water and limiting pharmacokinetics) and treatment (non-compliance with long treatment regimes and recrudescence) issues that limit their therapeutic potential.⁴⁷

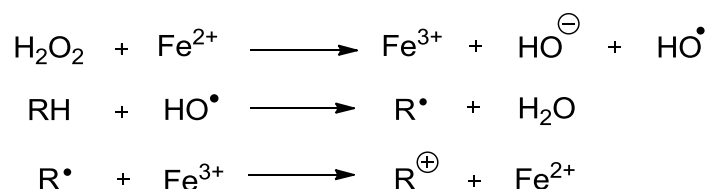
1.8. How artemisinins work

1.8.1. Artemisinins as prodrugs

It is considered that artemisinins, per se, are not antimalarial but instead act as 'prodrugs', which require the generation of antimalarial-active intermediates after encountering ferrous iron.⁴² In the context of artemisinin activation, ferrous iron is found in the food vacuole of the parasite, where digestion of hemoglobin takes place and free iron is detoxified by deposition in hemozoin.

1.8.2. Activation by “free” Fe²⁺

The Fenton reaction (**Scheme 2**), which involves reductive cleavage of peroxides by ferrous iron to generate alkoxy radicals then carbon-centred radicals, and finally neutral products, is well understood. This had been examined in detail before the advent of the artemisinins.⁴²



Scheme 2: The Fenton reaction.^{48, 49}

Cleavage of the peroxide bond generates two alkoxy radicals, O1 and O2. These rapidly rearrange *via* either hydrogen abstraction or β -scission to form the more stable C-centred radicals (**Figure 12**). These alkyl radicals are able to interact with vital parasite proteins such as heme, DNA or membranes that ultimately result in parasite death.⁵⁰

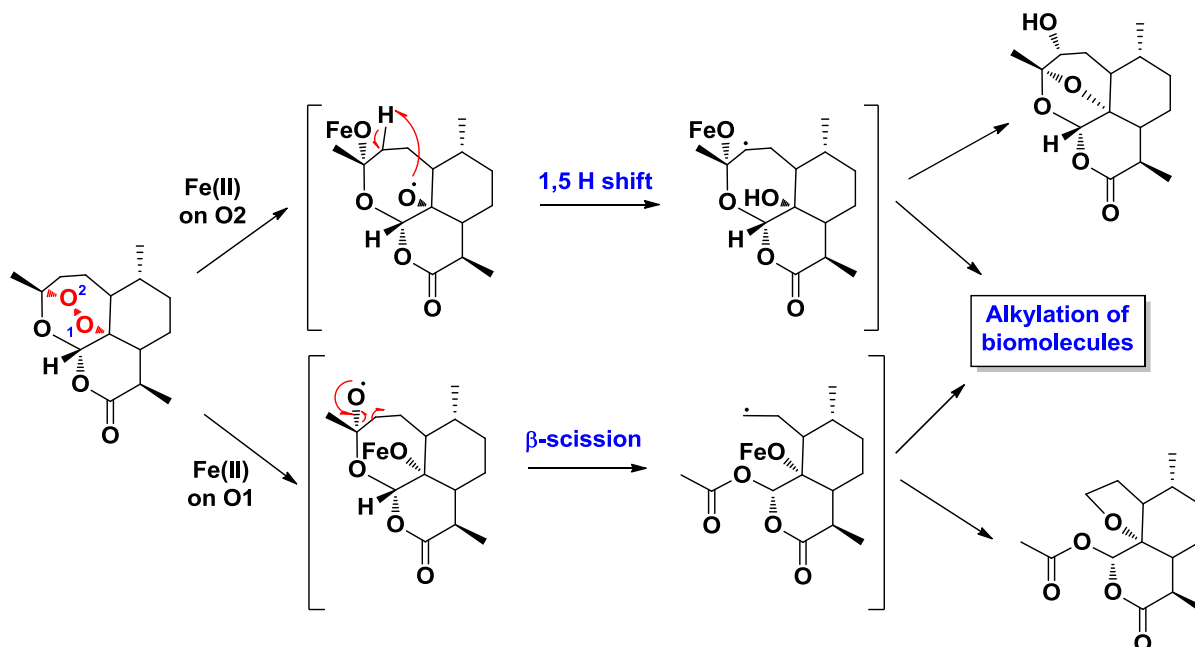


Figure 12: Mechanism of action of artemisinin to form C-centred radicals that can either alkylate biomolecules or self quench to give antimalarial-inactive products.^{42, 50, 51}

1.8.3. Activation by heme-Fe²⁺

During the early trophozoite stage in the malaria cycle, the parasite catabolises hemoglobin as a source of amino acids in its digestive vacuole to release heme.⁵² Virtually all of the heme is converted into hemozoin and very little is degraded by other pathways.⁵³ Of the total iron present in *Plasmodium falciparum* trophozoites, approximately 92% is located within the food vacuole and 88% of this is in the form of hemozoin. It was established that heme has to be in the ferrous state in order to react with artemisinin.

In 2001, the first covalent heme-artemisinin adduct produced from the alkylation of heme by artemisinin was fully characterised by Robert *et al.*⁵⁴ In 2002, they found that this reaction gave an 85% yield of heme derivatives alkylated at the α -, β - and δ -*meso* positions by a C-centred radical derived from artemisinin.³⁹

Work by Posner *et al.*⁵⁵ in 1994 showed that a C-centred radical was important for antimalarial activity by synthesising and testing the *in vitro* antimalarial activity of mono-methylated analogues of dihydroartemisinin (**Figure 13 and Table 1**). This work first highlighted the value of mechanistic understanding at the molecular level for the rational design of potent antimalarial trioxanes and illustrated how one small stereochemical change (diastereomer a Vs. diastereomer b) can be used as a molecular on-off switch for antimalarial activity.⁵⁵

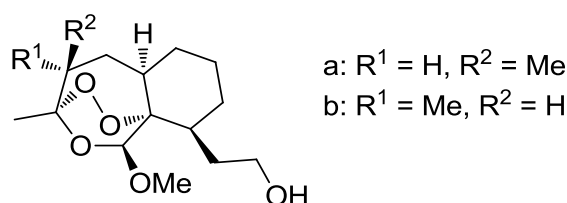


Figure 13: Mono-methylated trioxanes derived from dihydroartemisinin.

Compound	W-2 Indochina clone (IC ₅₀ (ng/ml))	D-6 African clone (IC ₅₀ (ng/ml))
a	4.5	3.5
b	>500	>500
artemisinin	8	8

Table 1: *In vitro* antimalarial activity of trioxanes a and b compared to artemisinin.

IC₅₀ is a measure of the effectiveness of a compound in inhibiting biological or biochemical function. It is a quantitative measure that indicates how much of a particular drug is needed to inhibit a given biological process by half. In other words, it is the half maximal (50%) inhibitory concentration (IC) of a substance; the smaller the IC₅₀ value, the more potent the drug. It is most commonly used as a measure of antagonist drug potency in pharmacological research.

1.8.4. Fixed-dose Artemisinin Combination Therapy (fACT)

Combining artemisinin with another slowly eliminated drug in a tablet is known as fixed-dose artemisinin combination therapy (fACT) e.g. Coartem[®] (artemether/lumefantrine) developed by Novartis represents 75% of the ACT market today.³⁷ ACTs are now generally accepted as the best treatments for uncomplicated falciparum malaria as they are rapidly and reliably effective, with efficacies exceeding 95%.⁵⁶

The rationale for fACTs is that the short-acting (3 day regimen) but highly potent artemisinin derivative delivers a rapid reduction in parasite biomass, with the remaining parasites being removed by the less active but more slowly eliminated partner drug that is structurally unrelated to artemisinin.⁵⁶ Distinct modes of action of artemisinin derivatives and partner drugs should, in theory, enable the combination to kill parasites that manifest decreased sensitivity to one agent alone and thus avoid or delay emergence of resistance.

fACTs are more complicated to produce and can be up to 20 times more expensive than monotherapy, which make them unaffordable in vulnerable populations. fACTs could make a major contribution to global malaria control but only a minority of people who need these drugs actually receive them because cost and access remain formidable obstacles.⁵⁶

More than 3 million people have been successfully treated using fACTs, which is a tremendous achievement. There are, however, 28 countries that still allow artemisinin monotherapy (despite the WHO advising against this) so resistance to fACTs was bound to occur. The first signs of emerging resistance to fACT were reported in 2009 in South East Asia where the parasite clearance time (PCT) was increased almost two-fold.³⁷

Current fACT regimens contain between 2.5-4mg/kg of the artemisinin derivative and are given daily for three days. They are easy to use and well tolerated with no adverse effects. The following fACTs are recommended by the WHO:

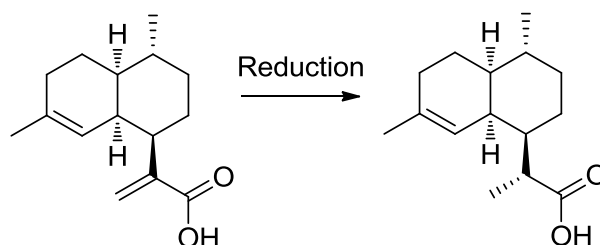
1. Artemether plus lumefantrine (currently the only internationally licensed ACT. Available in Asia and Africa.⁵⁷)
2. Artesunate plus amodiaquine (cures 70-90% of patients depending on geographic location.⁴²)
3. Artesunate plus mefloquine (consistently cures >95% of patients whereas mefloquine alone only worked for 50-60% of cases⁴², mainstay of antimalarial drug policy in South East Asia but too expensive for the African market.⁵⁷)
4. Artesunate plus sulfadoxine/pyrimethamine (used in some Asian countries but ineffective where sulfadoxine/pyrimethamine has failed as a replacement for chloroquine.⁵⁷)

1.9 Drawbacks of artemisinin-based therapy

1.9.1 Extraction of artemisinin from *Artemisia annua*

The drawback of using semi-synthetic analogues of artemisinin is that their production relies on extraction from *Artemisia annua* and in some countries, it is cultivated solely for this purpose but the yield obtained from extraction is only 0.1 - 0.8%. Reliance on cultivated *Artemisia annua* restricts supply of the drug and elevates costs for the patients who need it. Total syntheses of artemisinin have been achieved; one example is the route by Avery *et al.*⁵⁸ but it is too laborious (>10 steps) to be considered a viable alternative to extraction for supplying a highly cost sensitive market.

1.9.2. Continuous flow synthesis of artemisinin



Scheme 3: Reduction of artemisinic acid to dihydroartemisinic acid (DHA).

In 2012, Lévesque and Seeberger⁵⁹ proposed a continuous flow synthesis of artemisinin. They found that artemisinic acid, a much less complex molecular precursor can also be extracted from *Artemisia annua* in higher yields or it can be produced in engineered yeast. This makes artemisinic acid an ideal starting point for synthetically produced artemisinin. After purification, this method yielded 39% of artemisinin from DHA (**Scheme 3**), which is approximately 200g produced by the reactor per day. They estimated that 1500 of their reactors would be enough to meet the 225 million (number of cases of malaria as estimated by the WHO in 2009) doses of malaria medication needed per year.

However, the issues of reliance on natural products, cost and poor biopharmaceutical properties still remain and have resulted in complex administration regimens or recrudescence. To overcome these limitations, medicinal chemists have developed synthetic peroxides that have varying degrees of antimalarial activity.

1.10. Toward synthetic peroxide-containing antimalarial drugs

The need for affordable and readily available antimalarial therapies has spurred research into alternate methods for their manufacture and also the search for totally synthetic molecules that confer antimalarial activity analogous to artemisinin.

1.10.1. Synthetic alternatives to artemisinin

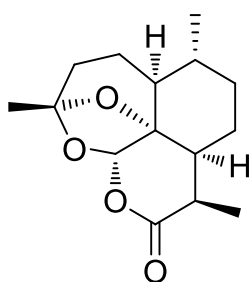


Figure 14: Structure of deoxyartemisinin.

The essential part of artemisinin is the peroxide bond in the 1,2,4-trioxane system and reduction of this peroxide bridge produces an analogue, deoxyartemisinin (**Figure 14**), which is devoid of antimalarial activity. Therefore, the reactivity of this peroxide function within the parasite is the crucial feature for superior pharmacological activity. The high cost of artemisinin extraction has driven the development of synthetic antimalarials that incorporate the key peroxide pharmacophore. Simpler structures containing this bridge e.g. 1,2,4-trioxolanes and 1,2,4,5-tetraoxanes, are far more accessible and in excess of 1000 new endoperoxides belonging to several classes have now been prepared.⁴⁶ These have provided alternative therapeutic possibilities and given medicinal chemists insight to their mode of action.

1.11. Main concept behind research and aims of this work

The aim of this work is to exploit the ability of synthetic antimalarials (1,2,4-trioxolanes and 1,2,4,5-tetraoxanes) to alkylate heme and apply them in MFCs. They could potentially act as a bi-functional molecular wire by alkylating heme on the outer membrane of *Geobacter sulfurreducens* and simultaneously tethering them to a carbon or gold electrode surface *via* an aryl diazonium or sulfur-based group respectively. This has involved the design and synthesis of novel, spiroadamantane peroxide antimalarials, which have appropriate functionality on the adamantane moiety. Chapter 2 discusses the mechanism of action of 1,2,4-trioxolane antimalarials and our efforts towards dispiro-1,2,4-trioxolane molecular wires that are capable of immobilising heme on carbon and gold surfaces. Chapter 3 discusses our efforts towards bi-functional, dispiro-1,2,4,5-tetraoxane molecular wires, including the syntheses of many novel precursors; namely functionalised adamantanone derivatives. Chapter 4 briefly introduces the synthesis of β -turn mimetics and chiral enamine *N*-oxides.

1.12. Bibliography

1. Clouds and Climate Change.
<http://www.realscience.org.uk/science-discussion-climate-change-clouds.html>.
2. Toth, F. L., *Energy for Development: Resources, Technology, Environment*. Dordrecht : Springer Netherlands: **2012**; Vol. 54.
3. The Energy Report **2011**.
http://www.wwf.org.uk/what_we_do/tackling_climate_change/climate_factsheets_and_reports/?4565/The-Energy-Report---100-renewable-energy-by-2050.
4. Logan, B. E., *Microbial Fuel Cells*. Wiley-Interscience: **2008**.
5. Renewable Energy.
http://www.wwf.org.uk/what_we_do/tackling_climate_change/renewable_energy/.
6. **2012** Energy Outlook: Fossil Fuels Leading the Future.
<http://www.instituteeforenergyresearch.org/2012/06/29/2012-energy-outlook-fossil-fuel-energy-leads-the-future/>.
7. Waste Not.
http://science.nasa.gov/science-news/science-at-nasa/2004/18may_wastenot/.
8. Lovley, D. R. *Geobacter* Project. <http://www.geobacter.org/>.
9. Schaetzle, O.; Barriere, F.; Baronian, K., Bacteria and yeasts as catalysts in microbial fuel cells: electron transfer from micro-organisms to electrodes for green electricity. *Energy & Environmental Science* **2008**, *1* (6), 607-620.
10. Busalmen, J. P.; Esteve-Nunez, A.; Berna, A.; Feliu, J. M., C-type cytochromes wire electricity-producing bacteria to electrodes. *Angew. Chem.-Int. Edit.* **2008**, *47* (26), 4874-4877.
11. Malvankar, N. S.; Tuominen, M. T.; Lovley, D. R., Biofilm conductivity is a decisive variable for high-current-density *Geobacter sulfurreducens* microbial fuel cells. *Energy & Environmental Science* **2012**, *5* (2), 5790-5797.
12. Bond, D. R.; Strycharz-Glaven, S. M.; Tender, L. M.; Torres, C. I., On Electron Transport through *Geobacter* Biofilms. *ChemSusChem* **2012**, *5* (6), 1099-1105.
13. Lovley, D. R., Electromicrobiology. *Annual Review of Microbiology* **2012**, *66*, 391-409.
14. Bond, D. R.; Lovley, D. R., Electricity production by *Geobacter sulfurreducens* attached to electrodes. *Appl. Environ. Microbiol.* **2003**, *69* (3), 1548-1555.
15. Lovley, D. R., Live wires: direct extracellular electron exchange for bioenergy and the bioremediation of energy-related contamination. *Energy & Environmental Science* **2011**, *4* (12), 4896-4906.
16. Shi, L.; Squier, T. C.; Zachara, J. M.; Fredrickson, J. K., Respiration of metal (hydr)oxides by *Shewanella* and *Geobacter*: a key role for multihaem c-type cytochromes. *Mol. Microbiol.* **2007**, *65* (1), 12-20.
17. Mehta, T.; Coppi, M. V.; Childers, S. E.; Lovley, D. R., Outer membrane c-type cytochromes required for Fe(III) and Mn(IV) oxide reduction in *Geobacter sulfurreducens*. *Appl. Environ. Microbiol.* **2005**, *71* (12), 8634-8641.
18. Electron Shuttles. http://toxics.usgs.gov/definitions/electron_shuttles.html.

19. Watanabe, K.; Manefield, M.; Lee, M.; Kouzuma, A., Electron shuttles in biotechnology. *Curr. Opin. Biotechnol.* **2009**, *20* (6), 633-641.
20. Rabaey, K.; Rodriguez, J.; Blackall, L. L.; Keller, J.; Gross, P.; Batstone, D.; Verstraete, W.; Nealon, K. H., Microbial ecology meets electrochemistry: electricity-driven and driving communities. *Isme J.* **2007**, *1* (1), 9-18.
21. Malvankar, N. S.; Lovley, D. R., Microbial Nanowires: A New Paradigm for Biological Electron Transfer and Bioelectronics. *ChemSusChem* **2012**, *5* (6), 1039-1046.
22. New Microbe Strain Makes More Electricity, Faster.
<http://www.sciencedaily.com/releases/2009/07/090729210821.htm>.
23. Malvankar, N. S.; Vargas, M.; Nevin, K. P.; Franks, A. E.; Leang, C.; Kim, B. C.; Inoue, K.; Mester, T.; Covalla, S. F.; Johnson, J. P.; Rotello, V. M.; Tuominen, M. T.; Lovley, D. R., Tunable metallic-like conductivity in microbial nanowire networks. *Nat. Nanotechnol.* **2011**, *6* (9), 573-579.
24. Malvankar, N. S.; Tuominen, M. T.; Lovley, D. R., Lack of cytochrome involvement in long-range electron transport through conductive biofilms and nanowires of *Geobacter sulfurreducens*. *Energy & Environmental Science* **2012**, *5*, 8651-8659.
25. Leang, C.; Qian, X. L.; Mester, T.; Lovley, D. R., Alignment of the c-Type Cytochrome OmcS along Pili of *Geobacter sulfurreducens*. *Appl. Environ. Microbiol.* **2010**, *76* (12), 4080-4084.
26. Esteve-Nunez, A.; Sosnik, J.; Visconti, P.; Lovley, D. R., Fluorescent properties of c-type cytochromes reveal their potential role as an extracytoplasmic electron sink in *Geobacter sulfurreducens*. *Environmental Microbiology* **2008**, *10* (2), 497-505.
27. Lovley, D. R., Cleaning up with genomics: Applying molecular biology to bioremediation. *Nat. Rev. Microbiol.* **2003**, *1* (1), 35-44.
28. Lovley, D. R., Bug juice: harvesting electricity with microorganisms. *Nat. Rev. Microbiol.* **2006**, *4* (7), 497-508.
29. Gregory, K. B.; Lovley, D. R., Remediation and recovery of uranium from contaminated subsurface environments with electrodes. *Environ. Sci. Technol.* **2005**, *39* (22), 8943-8947.
30. Yang, Y. G.; Sun, G. P.; Xu, M. Y., Microbial fuel cells come of age. *J. Chem. Technol. Biotechnol.* **2011**, *86* (5), 625-632.
31. Potter, M. C., Electrical effects accompanying the decomposition of organic compounds. *Proceedings of the Royal Society* **1912**, *84* (Part B), 260-276.
32. Waste Not, Want Not: Use the Microbial Fuel Cell to Create Electricity from Waste.
http://www.sciencebuddies.org/science-fair-projects/project_ideas/Energy_p026.shtml#background.
33. Ashley E. Franks, N. M., Kelly P. Nevin, Bacterial Biofilms: The Powerhouse of a Microbial Fuel Cell. *Biofuels* **2010**, *1* (4), 589-604.
34. Ghangrekar, M. M.; Shinde, V. B., Wastewater treatment in microbial fuel cell and electricity generation: a sustainable approach. In *12th International sustainable development research conference*, Hong Kong, **2006**.
35. Collins, F. H.; Paskewitz, S. M., Malaria - current and future prospects for control. *Annu. Rev. Entomol.* **1995**, *40*, 195-219.

36. WHO Malaria Fact Sheet.
<http://www.who.int/mediacentre/factsheets/fs094/en/index.html>.
37. Wells, T. N. When is Enough Enough? The Need for a Robust Pipeline of High-Quality Antimalarials.
<http://www.discoverymedicine.com/Timothy-N-Wells/2010/05/01/when-is-enough-enough-the-need-for-a-robust-pipeline-of-high-quality-antimalarials/>.
38. Britannica Online Encyclopedia.
<http://www.britannica.com/EBchecked/media/120605/Life-cycle-of-a-malaria-parasite>.
39. Robert, A.; Coppel, Y.; Meunier, B., Alkylation of heme by the antimalarial drug artemisinin. *Chem. Commun.* **2002**, (5), 414-415.
40. Orjih, A. U.; Banyal, H. S.; Chevli, R.; Fitch, C. D., Hemin lyses malaria parasites. *Science* **1981**, 214 (4521), 667-669.
41. Pagola, S.; Stephens, P. W.; Bohle, D. S.; Kosar, A. D.; Madsen, S. K., The structure of malaria pigment beta-haematin. *Nature* **2000**, 404 (6775), 307-310.
42. Krishna, S.; Uhlemann, A. C.; Haynes, R. K., Artemisinins: mechanisms of action and potential for resistance. *Drug Resist. Update* **2004**, 7 (4-5), 233-244.
43. Klayman, D. L., Qinghaosu (artemisinin) - an antimalarial drug from China. *Science* **1985**, 228 (4703), 1049-1055.
44. Kaufman, T. S.; Ruveda, E. A., The quest for quinine: Those who won the battles and those who won the war. *Angew. Chem.-Int. Edit.* **2005**, 44 (6), 854-885.
45. Leah Mwai, E. O., Abdi Abdirahman, Steven M. Kiara, Steve Ward, Gilbert Kokwaro, Philip Sasi, Kevin Marsh, Steffen Borrmann, Margaret Mackinnon, Alexis Nzila, Chloroquine resistance before and after its withdrawal in Kenya. *Malaria Journal* **2009**, 8 (106).
46. Meshnick, S. R.; Jefford, C. W.; Posner, G. H.; Avery, M. A.; Peters, W., Second-generation antimalarial endoperoxides. *Parasitol. Today* **1996**, 12 (2), 79-82.
47. Vennerstrom, J. L.; Arbe-Barnes, S.; Brun, R.; Charman, S. A.; Chiu, F. C. K.; Chollet, J.; Dong, Y. X.; Dorn, A.; Hunziker, D.; Matile, H.; McIntosh, K.; Padmanilayam, M.; Tomas, J. S.; Scheurer, C.; Scorneaux, B.; Tang, Y. Q.; Urwyler, H.; Wittlin, S.; Charman, W. N., Identification of an antimalarial synthetic trioxolane drug development candidate. *Nature* **2004**, 430 (7002), 900-904.
48. Wardman, P.; Candeias, L. P., Fenton chemistry: An introduction. *Radiat. Res.* **1996**, 145 (5), 523-531.
49. Barbusinski, K., Fenton reaction - controversy concerning the chemistry. *Ecological Chemistry and Engineering S* **2009**, 16 (3), 347-358.
50. Creek, D. J.; Chiu, F. C. K.; Pranker, R. J.; Charman, S. A.; Charman, W. N., Kinetics of iron-mediated artemisinin degradation: Effect of solvent composition and iron salt. *J. Pharm. Sci.* **2005**, 94 (8), 1820-1829.
51. Fugi, M. A.; Wittlin, S.; Dong, Y. X.; Vennerstrom, J. L., Probing the Antimalarial Mechanism of Artemisinin and OZ277 (Arterolane) with Nonperoxidic Isosteres and Nitroxyl Radicals. *Antimicrob. Agents Chemother.* **2010**, 54 (3), 1042-1046.
52. Sullivan, D. J., Theories on malarial pigment formation and quinoline action. *Int. J. Parasit.* **2002**, 32 (13), 1645-1653.

53. Egan, T. J.; Combrinck, J. M.; Egan, J.; Hearne, G. R.; Marques, H. M.; Ntenti, S.; Sewell, B. T.; Smith, P. J.; Taylor, D.; van Schalkwyk, D. A.; Walden, J. C., Fate of haem iron in the malaria parasite *Plasmodium falciparum*. *Biochem. J.* **2002**, 365, 343-347.
54. Robert, A.; Cazelles, J.; Meunier, B., Characterization of the alkylation product of heme by the antimalarial drug artemisinin. *Angew. Chem.-Int. Edit.* **2001**, 40 (10), 1954-1957.
55. Posner, G. H.; Oh, C. H.; Wang, D. S.; Gerena, L.; Milhous, W. K.; Meshnick, S. R.; Asawamahasadka, W., Mechanism-based design, synthesis and in vitro antimalarial testing of new 4-methylated trioxanes structurally related to artemisinin - the importance of a carbon-centred radical for antimalarial activity. *J. Med. Chem.* **1994**, 37 (9), 1256-1258.
56. Nosten, F.; White, N. J., Artemisinin-based combination treatment of falciparum malaria. *Am. J. Trop. Med. Hyg.* **2007**, 77 (6), 181-192.
57. Greenwood, B. M.; Bojang, K.; Whitty, C. J. M.; Targett, G. A. T., Malaria. *Lancet* **2005**, 365 (9469), 1487-1498.
58. Avery, M. A.; Jenningswhite, C.; Chong, W. K. M., The total synthesis of (+)-artemisinin and (+)-9-desmethyartemisinin. *Tetrahedron Lett.* **1987**, 28 (40), 4629-4632.
59. Levesque, F.; Seeberger, P. H., Continuous-Flow Synthesis of the Anti-Malaria Drug Artemisinin. *Angew. Chem.-Int. Edit.* **2012**, 51 (7), 1706-1709.

Chapter 2

Synthetic antimalarials - Dispiro-1,2,4-trioxolanes

This chapter contains a separate numbering system for all schemes, tables, figures and references.

2.1. Introduction to 1,2,4-trioxolanes

2.1.1. Discovery of secondary ozonides as antimalarials

There has been increased demand for synthetic cyclic peroxides because they have the potential to replace traditional antimalarial remedies. Ozonides are both reactive and unstable so they would not be an obvious first choice for a promising antimalarial drug candidate. However, Vennerstrom *et al.* showed that substituted ozonides (1,2,4-trioxolanes) are not only chemically stable, but also have potent antimalarial activity.¹ The drug discovery process relied on multi-dimensional lead optimisation made possible by a rapid and recurrent combination of antimalarial, physicochemical, metabolism, pharmacokinetic and toxicity data to guide the medicinal chemistry and create a lead prototype. 1,2,4-Trioxolanes exhibit structural simplicity and are synthetically more accessible and have superior antimalarial activity to artemisinin.

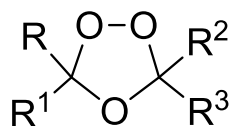


Figure 1: General structure of tetra-substituted trioxolanes.

2.2.1 Chemical and metabolic stability

Ozonides are formed from the ozonolysis of olefins, which rearrange to secondary ozonides or 1,2,4-trioxolanes. The stability of tetra-substituted trioxolanes may be due, in part to the lack of α -hydrogen atoms, which prevents heterolytic peroxide fragmentation reactions driven by formation of stable carbonyl-containing products.² Tetra-substituted trioxolanes have the general structure shown in **Figure 1** where the R groups represent combinations of ring systems, acyclic systems and functional groups that provide steric hindrance about the trioxolane ring, to provide both chemical and metabolic stability.¹

Tetra-substituted trioxolanes which possess a spiroadamantane ring are sterically hindered on one side of the trioxolane unit. This serves to protect the ring from premature chemical and metabolic decomposition *in situ*. The other side may incorporate a spirocyclohexyl ring, preferably functionalised at the 4'-position. This arrangement allows for an energetically favourable approach of Fe(II) to a relatively sterically unhindered peroxide oxygen atom to give exclusive β -scission of the spiroadamantane ring. Interestingly, closely related analogues where the peroxide bridge is too exposed or sterically inaccessible to an Fe(II) species are completely antimalarial-inactive (**Figure 2**).

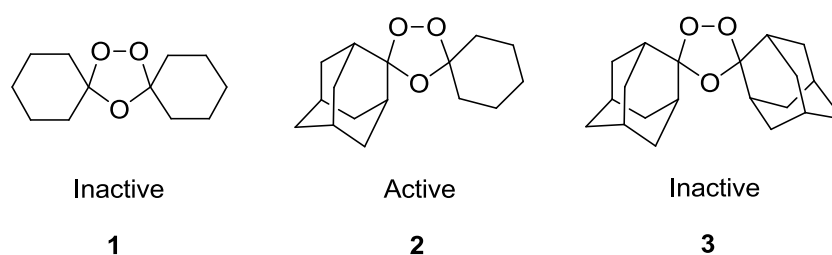


Figure 2: Active and inactive structurally-related trioxolanes.

2.2. Proposed mechanism of action of 1,2,4-trioxolanes

2.2.1. Iron-mediated degradation

Treating the active trioxolane with ferrous acetate as a model for heme indicates that the peroxide bond fragments to give an *O*-centred radical, followed by β -scission to give the secondary *C*-centred radical. This was subsequently trapped by TEMPO to form the corresponding aminoxy acid. No products were obtained from the β -scission of the spirocyclohexanone, supporting the hypothesis that attack of the Fe(II) species occurs on the less-hindered peroxide oxygen (**Figure 3**).

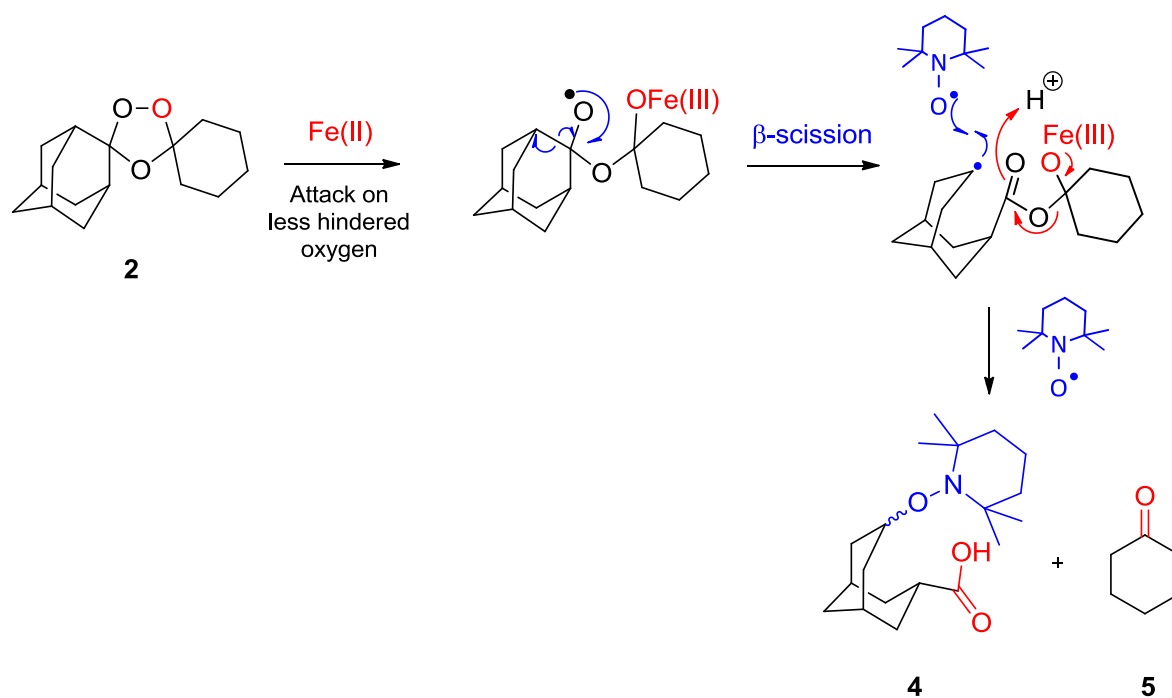


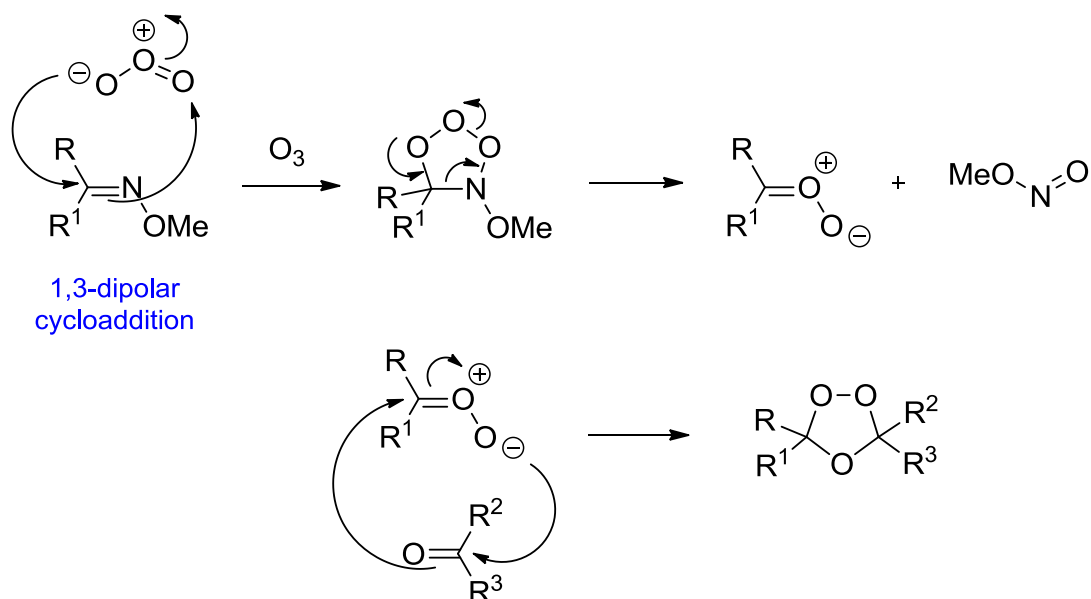
Figure 3: Iron-mediated degradation of trioxolane to form a C-centred radical and subsequent trapping with TEMPO.^{1,3}

It can be seen that analogues resembling the hindered and inactive di-adamantyl trioxolane **3** (**Figure 2**) are prevented from binding to Fe(II) or heme for steric reasons, which accounts for their inactivity. Studies by Creek *et al.*³ suggested that polarity can also play a major part in the biological activity of these compounds. They found that trioxolanes with a heteroatom incorporated in the cyclohexyl ring or a polar substituent at the 4'-position rendered the trioxolane chemically more reactive towards iron. As a result, these trioxolanes tended to degrade much faster than their non-polar counterparts. They also used **Fe(III)** in their work to determine whether or not it mediated any degradation of the trioxolanes but after 24hrs, no degradation had occurred. This indicated that reactions of the trioxolanes proceed *via* **Fe(II)**-mediated reduction of the peroxide bond and this result is consistent with iron-mediated degradations reported for artemisinin. However, it has been found that artemisinins are generally less efficient than trioxolanes at alkylating heme *in vitro* and are similarly poor at intercepting radical spin traps such as TEMPO.⁴

2.3. Synthesis of substituted 1,2,4-trioxolanes

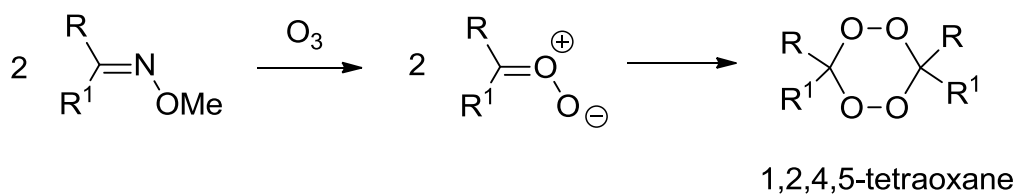
2.3.1. The Griesbaum Co-ozonolysis

In 1995, Griesbaum *et al.*⁵ reported a new type of cross-ozonolysis reaction where an *O*-alkyl ketone oxime was ozonised in the presence of activated carbonyl compounds (**Scheme 1**). They later also found that this method could also be applied efficiently to a number of unactivated ketones such as cyclohexanone.



Scheme 1: The Griesbaum Co-ozonolysis.

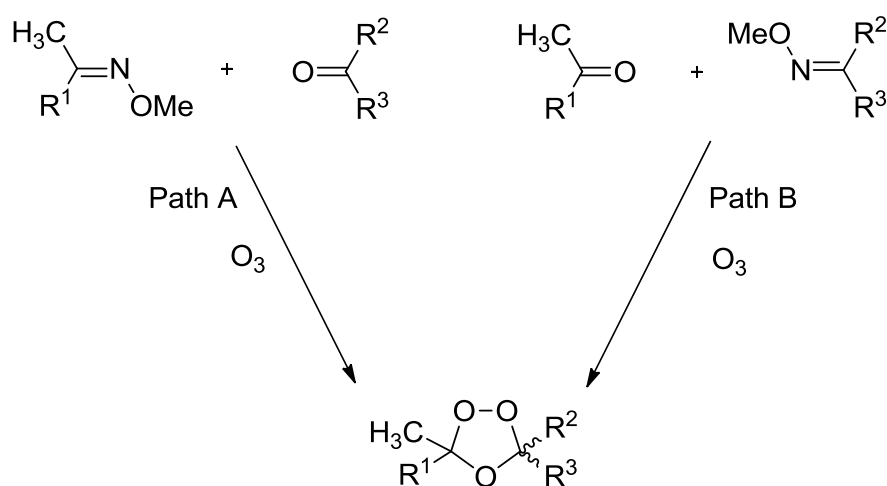
If no carbonyl compound is added in the second step, the carbonyl oxide can dimerise to form a 1,2,4,5-tetraoxane (**Scheme 2**). Tetraoxanes will be discussed in detail in Chapter 3.



Scheme 2: Dimerisation of carbonyl oxide.

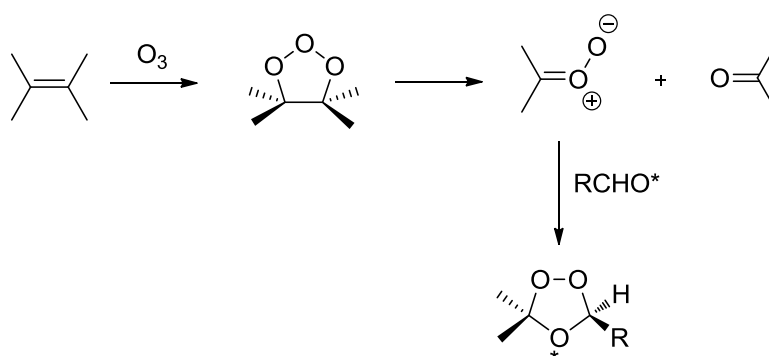
The Griesbaum co-ozonolysis provided for the first time, a widely applicable synthesis of both symmetrical and unsymmetrical tetra-substituted ozonides that are otherwise generally inaccessible by ozonolysis of a parent alkene or cross-ozonolysis of an alkene or enol ether in the presence of carbonyl compounds in solution.⁶ Another useful feature is that it avoids the need to synthesise parent tetra-substituted olefins or enol ethers and instead requires only the straightforward synthesis of oxime ethers. There is a lot of flexibility with this reaction, as a large number of ketones and oxime ether precursors are commercially available. If the yields for the co-ozonolysis are low, they can be improved dramatically simply by “reversing” the *O*-methyloxime and ketone.^{7, 8} This novel procedure provides a uniquely convenient method to synthesise spiro- and dispiro- trioxolanes that can be purified by crystallisation or flash chromatography.

In 1997, Griesbaum *et al.*⁸ carried out the ozonolyses of *O*-alkylated ketoximes in the presence of carbonyl groups. They showed a two-way approach, routes A and B (**Scheme 3**), which allowed optimisation of ozonide yields by the judicious selection of a pair of substrates containing the more reactive carbonyl compound. They did not manage to isolate methyl nitrite as a by-product due to its low boiling point of -12°C.



Scheme 3: Pathways for Griesbaum co-ozonolysis.

The detailed mechanism for the Griesbaum co-ozonolysis has not been well defined but the reaction outcome is consistent with the general pathway of the Criegee⁹ mechanism for ozonolysis of olefins, especially involving the key carbonyl oxide intermediate. In 1998, Geletneky and Berger¹⁰ showed that when a primary ozonide reacts with a ¹⁷O-labelled aldehyde, the Criegee model incorporates the ¹⁷O label in the ether linkage of the secondary ozonide only (**Scheme 4**). This was found to be the case for styrene and ethylenecyclohexane from which simple and clear ¹⁷O-NMR spectra could be obtained as they offered no stereochemical complications of *cis* and *trans* isomerism of the resulting ozonide.

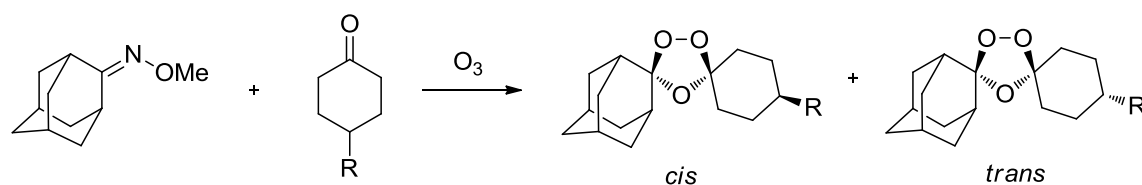


Scheme 4: Criegee mechanism for ozonolysis of olefins using a ¹⁷O (O*)-labelled aldehyde.

2.3.2. Diastereoselectivity and scope of the Griesbaum co-ozonolysis

Vennerstrom *et al.*⁶ have synthesised a number of trioxolane analogues *via* the Griesbaum co-ozonolysis. They investigated trioxolanes formed from reactions between *O*-methyl 2-adamantanone oxime and 4-substituted cyclohexanones. It was found that the majority of trioxolane isomers possessed *cis* configurations, suggesting a preferred axial attack of the carbonyl oxide on the cyclohexanone dipolarophiles.

Trioxolanes were labelled *cis* or *trans* indicating the position of the cyclohexyl-R group with respect to the axial peroxide bond (*cis* indicates that the R group is in the equatorial position whereas *trans* indicates the R group is in the axial position). The general result was that large cyclohexyl-R groups (Group I) gave almost exclusively the *cis* diastereoisomer with estimated *cis/trans* ratios of 20:1. 4'-Substituted cyclohexanones with functional groups linked by a single methylene (Group II) gave *cis/trans* ratios of 5:1. Ester and amide groups (Group III) provided *cis/trans* ratios ranging from 2.5:1 to 5:1 (**Figure 4**).



Group I (cis:trans 20:1)	R=C(CH ₃) ₃ , C ₆ H ₅ , <i>p</i> -C ₆ H ₄ OAc
Group II (cis:trans 5:1)	R=CH ₂ OAc, CH ₂ CO ₂ Et, CH ₂ SO ₂ C ₆ H ₅
Group III (cis:trans 2.5:1-5:1)	R=CO ₂ Et, COOCH ₂ C(CH ₃) ₃ , CON(CH ₂ CH ₃) ₂

Figure 4: Diastereoselectivity of the Griesbaum co-ozonolysis.

These results were attributed to preferred attack of the carbonyl oxide on the axial side of the cyclohexanone when the cyclohexyl-R* group increased in size (**Figure 5**).

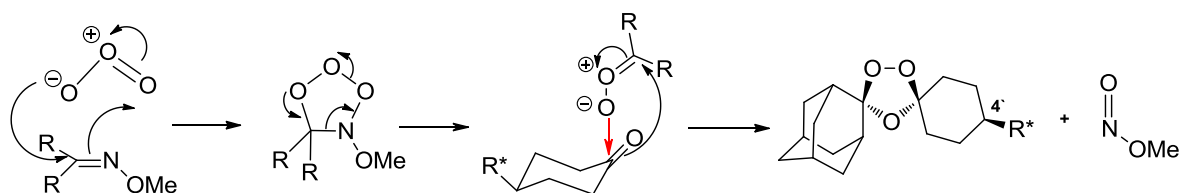


Figure 5: The stereochemistry of the resulting trioxolane is determined by the nature and size of the cyclohexyl-R* substituent at the 4'-position.

2.4. Mechanism of action of 1,2,4-trioxolanes

In the same way as artemisinin, synthetic peroxides generate highly reactive C-centred radicals. There are however, some subtle differences; artemisinin generates both a primary and a secondary carbon radical, whereas dispiro-cyclic trioxolanes produce only a secondary C-centred radical formed *via* the primary oxy radical. Once formed, it is proposed that these radicals react further by alkylating a nearby substrate.

2.4.1. 1,2,4-Trioxolanes in iron-mediated degradation studies

As for artemisinin, it was found that Fe(II)-mediated reactivity also applied to trioxolanes. Within the study carried out by Creek *et al.*³, in which the iron-mediated degradation kinetics of trioxolanes were investigated, some extraordinary reaction rates were observed. Some rate constants varied by as much as 1000-fold and they did not directly correlate with *in vitro* antimalarial activity. It is clear that not all trioxolanes that reacted with FeSO₄ were active antimalarials. However, the ones that did not react with FeSO₄ had no appreciable antimalarial activity. These results suggested that iron-mediated reactivity is a necessary, but insufficient, prerequisite for antimalarial activity. This implied that other molecular properties play important roles in the biological mechanism of action and experiments involving heme were required for confirmation of this hypothesis.

2.4.2. 1,2,4-Trioxolanes in heme alkylation

In 2008, Creek *et al.*⁴ investigated the Fe(II)-heme mediated reactivity of a series of trioxolanes. They compared structurally similar trioxolanes with a wide range of antimalarial activities to determine whether or not the reaction with heme showed any correlation with antimalarial potency. They found that all of the trioxolanes used in the study reacted with the Fe(II) centre of heme (**Figure 6**) and that these reactions occurred much faster than when inorganic Fe(II) salts were used, taking minutes rather than hours to reach completion. The extent of heme alkylation also correlated closely with *in vitro* antimalarial activity of the trioxolanes used in this investigation. This suggested that heme alkylation may be related to the mechanism of action for trioxolane antimalarials. However, the conditions used in this study reflect an extremely simplified system compared to the reaction with biological heme within the malaria parasite. Further research was required to correlate bio-mimetic studies with the actual environment of parasite-infected red blood cells.

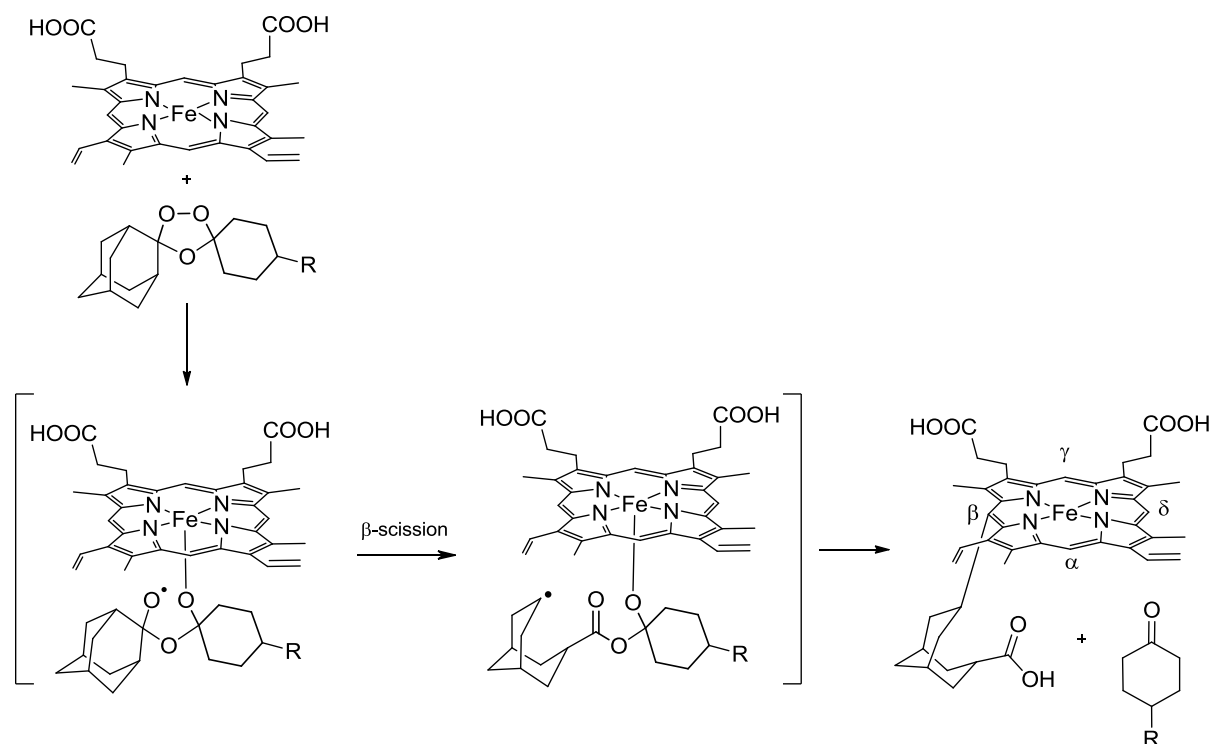
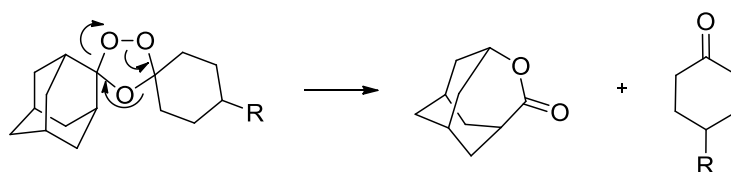


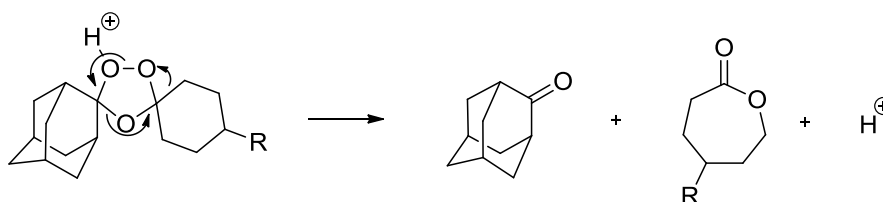
Figure 6: Proposed mechanism of action of trioxolanes in reaction with Fe(II) heme. Only alkylation of β -meso position shown for clarity but there is likely to be a mixture of isomeric adducts as with artemisinin.

2.5. Functional group transformations by post-ozonolysis reactions of 1,2,4-trioxolanes

Vennerstrom *et al.* continued to investigate a wide range of post-ozonolysis reactions at the 4'-position on the spirocyclohexane. The trioxolanes proved to be quite stable to triphenylphosphine, borohydrides, hydrazine, organolithiums, Grignard reagents and aqueous potassium hydroxide as illustrated by the synthesis of amine, alcohol, acid, ester, ether, sulfide, and heterocycle-functionalised ozonides using a number of different methods.⁶ Reaction temperatures were kept below 60°C to avoid decomposition of the ozonide heterocycle into adamantanone lactone and the starting material cyclohexanone *via* Hock-type fragmentations (**Schemes 5 and 6**).



Scheme 5: Thermal ozonide decomposition above 60°C.



Scheme 6: Acid-catalysed Hock-type fragmentation.

2.6. Ozonide drug development

2.6.1. First generation ozonides

The main problems with peroxide drug candidates are attributed to solubility and bioavailability. The first prototype trioxolanes were no exception to this; the spiroadamantane trioxolane pharmacophore is intrinsically lipophilic and therefore highly susceptible to metabolism. Excellent absorption and bioavailability of drugs following oral administration requires a fine balance between good aqueous solubility, which is improved for more polar structures, and good membrane permeability, which is favoured for less polar compounds. However, substitution at the 4'-position of the spirocyclohexane was shown to increase the polarity of the trioxolane.¹¹ Vennerstrom *et al.* described the synthesis and antimalarial properties of 43 diversely functionalised derivatives of the 1,2,4-trioxolane prototypes with a wide spectrum of polarity. They found that more lipophilic trioxolanes had improved oral activities compared to their more polar counterparts and trioxolanes with a wide range of neutral and basic, but not acidic, functional groups had good antimalarial profiles.¹¹

2.6.2. Second generation ozonides

Identification of the trioxolane OZ277 (also called *arterolane*, **Figure 7**), by Vennerstrom *et al.*¹ was a significant breakthrough in antimalarial drug development efforts during the past decade. The key pharmacophore of OZ277 is the 1,2,4-trioxolane moiety.

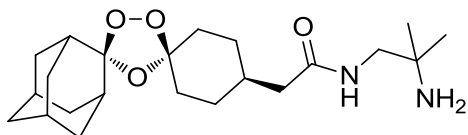


Figure 7: OZ277, arterolane.

As the trioxolane pharmacophore is inherently lipophilic, the polarity of trioxolanes was adjusted by the addition of an amine or amide side chain at the 4'-position of the cyclohexyl moiety. OZ277 was shown to have the optimum balance between lipophilicity, aqueous solubility, metabolism and potent antimalarial activity and was advanced into “first-in-man” clinical studies in 2004.¹

The clinical trials of OZ277 identified some issues with the first generation ozonides. The drugs tended to degrade rapidly in rats' blood *in vivo*; consequently a higher concentration is required to achieve the desired antimalarial effect, proving to be less cost-effective than desired. It is well known that cleavage of the peroxide bond and subsequent formation of free radicals is required for activity; therefore making structural modifications to reduce blood instability without sacrificing potency was the next challenge in developing second generation analogues. Slight structural modifications resulted in improved properties such as improved stability in blood without compromising biological activity; better oral bioavailability and excellent prophylactic activity in mice. The latest generation trioxolanes are faster acting and some are even showing signs of completely curing malaria in only one dose. These are properties that artemisinin and the first generation trioxolanes were lacking.

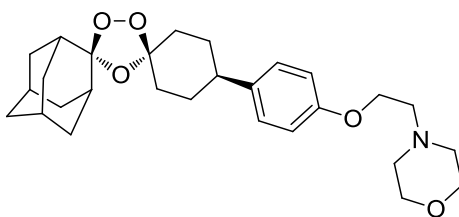


Figure 8: OZ439. This is the next ‘one-shot’ lead drug candidate to be tested and supported by MMV, it is currently in early stage clinical trials.¹² Costing less than \$1 per dose to produce, OZ439 is finally a promising, cost-effective solution to the burden of malaria.

2.6.3. Metabolites of OZ277

In 2008, Vennerstrom *et al.*¹³ showed that trioxolane OZ277 can be hydroxylated by human liver microsomes at the distal bridgehead carbon atoms of the spiroadamantane moiety to give two carbinol metabolites that were devoid of antimalarial activity (**Figure 9**).

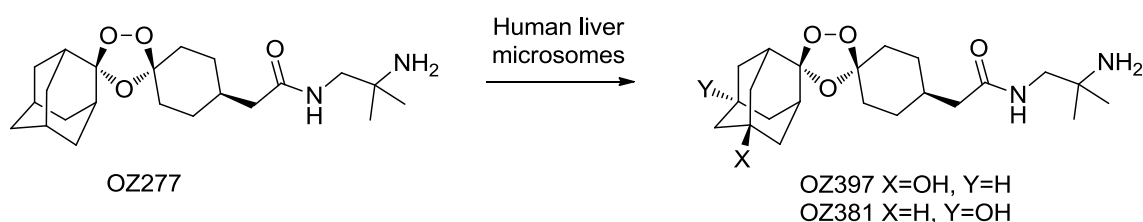


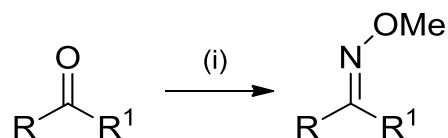
Figure 9: OZ277 and its hydroxylated metabolites, OZ397 and OZ381.

The complete lack of antimalarial activity for these metabolites may be an indication of the importance of an unsubstituted spiroadamantane ring system to the antimalarial properties of the ozonides. It may be that the steric hindrance provided by the bridgehead carbinols in these metabolites prevents efficient alkylation reactions of the spiroadamantane-derived secondary C-centered radicals from occurring when the ozonide reacts with Fe(II) in the parasite. This suggests that any substitution on the adamantane moiety would prevent efficient heme alkylation. However, the work presented in this thesis has shown that this is not always the case, as discussed in the next sections.

2.7. Results and Discussion

2.7.1. Synthesis of *O*-methyl oximes

The synthesis of 1,2,4-trioxolanes began with the optimisation of conditions for the synthesis of the precursors, *O*-methyl oximes using various ketone substrates (**Table 1**).



(i) $\text{NH}_2\text{OMe}\cdot\text{HCl}$ (1.5eq), pyridine (1.2eq), MeOH, rt, 48hrs.

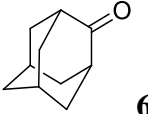
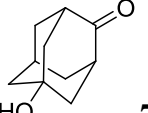
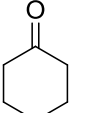
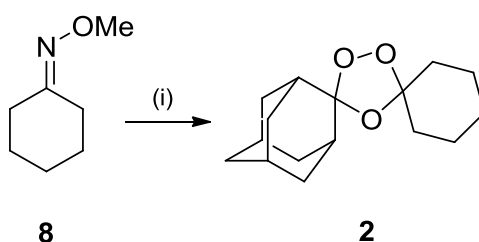
Entry	Ketone	Yield (%)
1	 6	81
2	 7	56
3	 5	70 - 80

Table 1: Synthesis of *O*-methyl oximes.

Cyclohexanone **5** was found to give consistently high yields of the corresponding *O*-methyl oxime and because it is also the cheapest commercially available ketone of the ones surveyed, this was taken forward for trioxolane synthesis.

2.7.2. Optimisation of conditions for the synthesis of 1,2,4-trioxolanes

O-Methyl 5-hydroxy-2-adamantanone oxime was used in a Griesbaum co-ozonolysis reaction with cyclohexanon. This would potentially provide a trioxolane bearing a synthetic handle on the adamantyl moiety on which further transformations could be performed. However, a very low yield was obtained so this route was abandoned because 5-hydroxy-2-adamantanone **7** is expensive. We decided to continue trioxolane synthesis using *O*-methyl cyclohexanone oxime **8** (Scheme 7). The conditions for this co-ozonolysis reaction between 2-adamantanone and *O*-methyl cyclohexanone oxime were changed slightly each time and the resulting yields of trioxolane are summarised in Table 2.



Scheme 7: (i) 2-adamantanone **6** (1.1 equiv), O₃, 4:1 pentane/DCM, 5hrs.

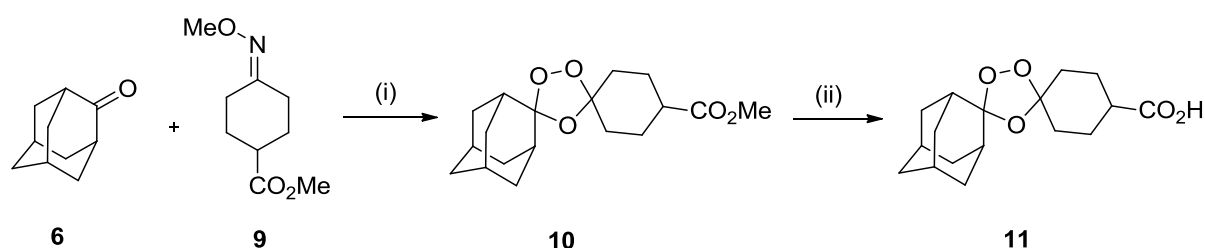
Entry	Conditions	Yield (%)
1	Bubble O ₃ into reaction at -78°C	16
2	Cool O ₃ to -78°C before bubbling into reaction	6
3	Bubble O ₃ into reaction at 0°C	6-9
4	Bubble O ₃ into reaction at 0°C, anhydrous conditions	9

Table 2: Yields of trioxolane from varying reaction conditions.

In general, the yields obtained were very poor under all of the reaction conditions used. There was also the problem of the trioxolane product being very non-polar and this made it difficult to obtain a mass spectrum because all modes of ionisation failed to ionise the molecule. However, further optimisation by a member of the O'Neil group allowed the trioxolane to be obtained in higher yields (*ca.* 40%) when 5-hydroxy-2-adamantanone **7** was used as the starting ketone. This meant that a trioxolane that was capable of undergoing further transformations had been synthesised successfully.

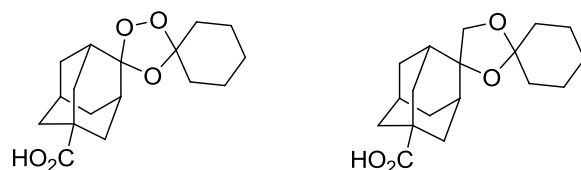
2.7.3. 1,2,4-Trioxolanes for heme alkylation experiments

The next targets were trioxolanes for heme alkylation/fluorescence experiments involving *Geobacter*. These trioxolanes had functionality on the cyclohexyl moiety (**Scheme 8**) and direct tetraoxane analogues (discussed in Chapter 3) have also been synthesised to allow comparison of results. The results from these experiments are currently pending. Incorporation of a carboxylic acid group should aid with solubility of the molecule in aqueous conditions when used in experiments with *Geobacter*.



Scheme 8: Synthesis of trioxolanes for heme alkylation experiments. (i) O_3 , pentane, rt, 5hrs, 45%. (ii) 15% NaOH, MeOH, rt, 3hrs, then H^+ , 80%.

The application of trioxolanes in heme alkylation experiments were carried out by the group of Dr. Abraham Esteve-Núñez, University of Alcalá de Henares. Fe^{2+} -heme groups are known to emit blue light under UV (254nm) light excitation. They hypothesised that the addition of trioxolanes to reduced cytochromes should allow monitoring of the auto-fluorescence that originates in the cytochromes of *Geobacter*. When the bacteria are oxidised as a result of heme alkylation, the auto-fluorescence should be lost. As the reaction between the trioxolane and heme is oxidative, auto-fluorescence should decrease as the reaction progresses. Trioxolane **12** (**Scheme 9**) and the ketal control **13** (**Scheme 9**) were used in spectrofluorimetric assays to determine if binding of the trioxolane to heme caused the loss of auto-fluorescence.



Scheme 9: Trioxolane **12** and ketal control **13** for auto-fluorescence experiments.

Anaerobic cell suspensions of *Geobacter sulfurreducens* were incubated in sealed fluorimeter cuvettes in the presence of different concentrations of the trioxolane in 10% DMSO. The results showed that there was indeed a loss of auto-fluorescence after the addition of the trioxolane (**Figure 10**). As expected, the ketal control showed no loss in auto-fluorescence, which was an indication of it not reacting with heme.

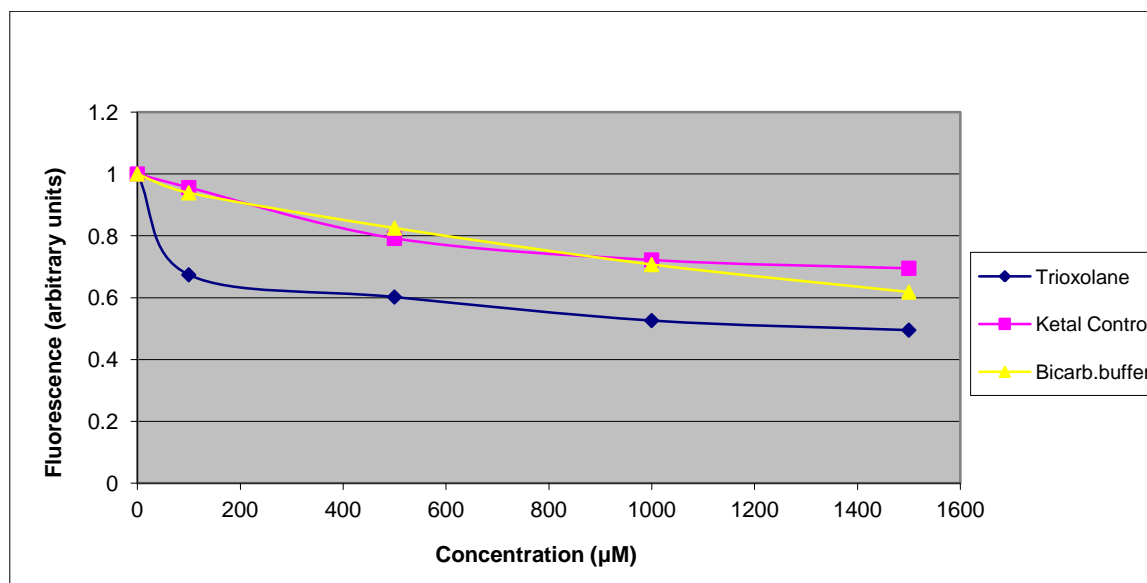


Figure 10: Results from auto-fluorescence experiments.

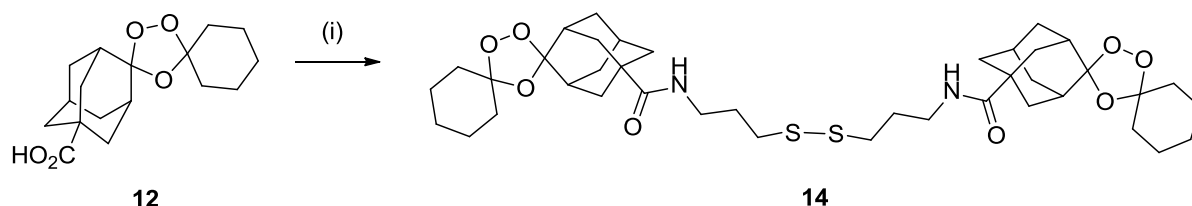
2.7.4. 1,2,4-Trioxolanes with functionality on the adamantane moiety

According to literature precedent, trioxolanes to date only have functionality at the 4'-position on the cyclohexyl moiety to tune their physicochemical and pharmacological properties. Herein, we report work by the O'Neil group involving the synthesis of novel, dispiro-trioxolane molecular wires containing functionality at the 5-position of the adamantane moiety that are capable of binding heme to carbon or gold surfaces. In the next section, we show that the presence of significant bridgehead substitution on the adamantane moiety does not hinder the trioxolane from heme alkylation as thought previously by Vennerstrom *et al.* Trioxolanes bearing functional groups that are capable of binding to gold/carbon were synthesized and heme successfully immobilised on the surface.

2.7.5. 1,2,4-Trioxolane molecular wires synthesised within the O'Neil group

1,2,4-Trioxolane molecular wire for immobilising heme on gold

We envisaged that a trioxolane bearing a thiol-based group could bind to a gold surface. The synthesis of a trioxolane dimer containing a disulfide linkage was carried out in the O'Neil group (**Scheme 10**). It was assumed that the thiol is formed initially and the disulfide linkage is thought to have formed as a result of aerobic oxidation.



Scheme 10: Synthesis of trioxolane dimer bearing disulfide linkage **14**. (i)

HCl.NH₂CH₂CH₂SH (0.5eq), EDC.HCl (1.2eq), HOBt (1.2eq), NMM (2.5eq), DMF, 0°C-rt, 12hrs, 60%.

In the presence of gold, the disulfide linkage should undergo cleavage and the resulting thiol bind to the gold surface. The peroxide bond is then available to react with reduced heme (**Figure 11**). These experiments showed that heme was successfully immobilised on the gold surface.

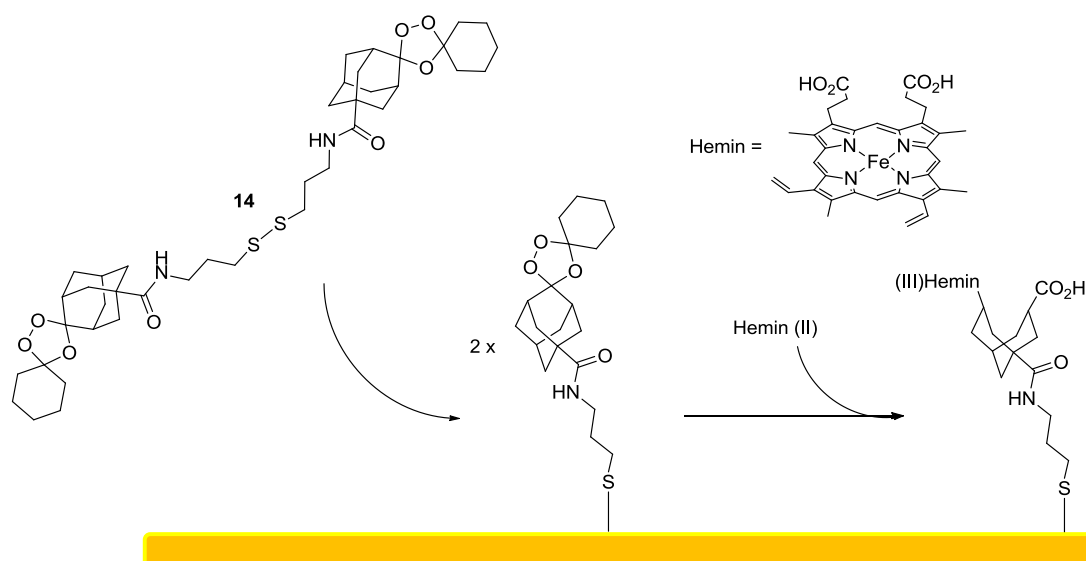


Figure 11: Immobilisation of heme on a gold surface by trioxolane dimer **14**.

1,2,4-Trioxolane molecular wire for immobilising heme on carbon

We also envisaged that a trioxolane bearing a diazonium group **15** could be selectively reductively coupled to a carbon surface. This would immobilise the trioxolane on the surface and the peroxide bond could then react with heme groups, tethering them to the surface (**Figure 12**). This trioxolane **15** was synthesised with a senior member of the O'Neil group (**Scheme 11**).

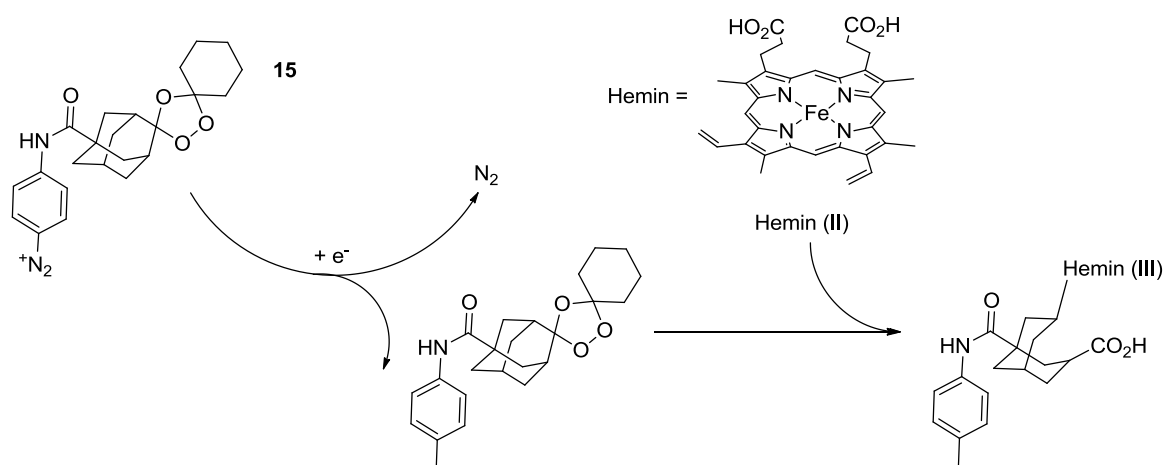
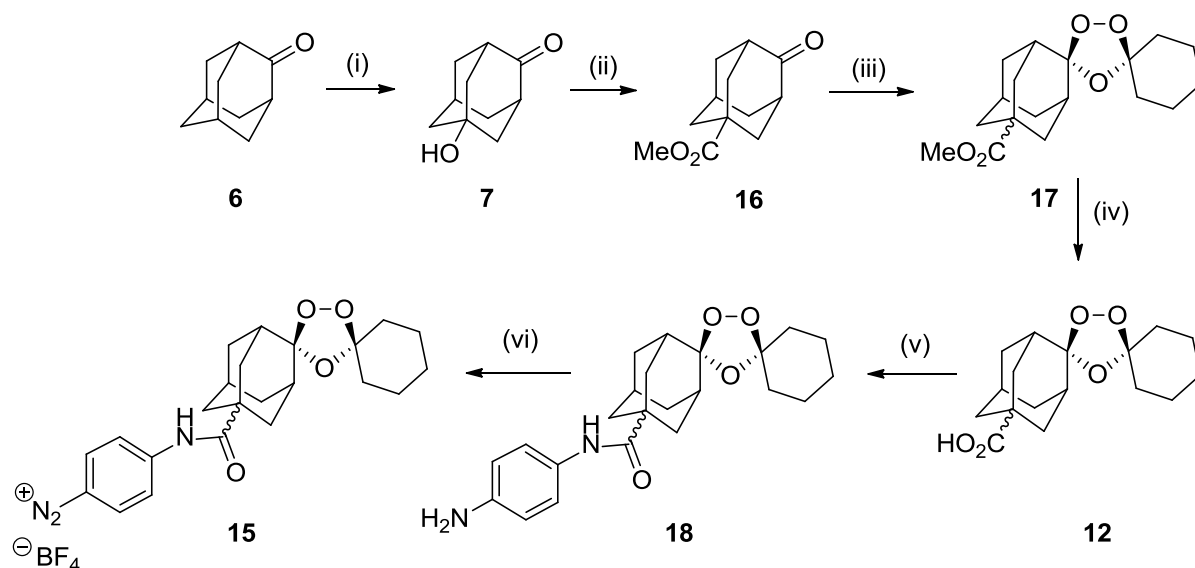


Figure 12: Trioxolane diazonium salt for functionalisation of carbon surfaces.



Scheme 11: Synthesis of trioxolane **15** for immobilising heme on carbon surfaces. (i) 100% HNO_3 , rt, 3 days, 52%. (ii) 30% SO_3 (8eq), 100% HCO_2H (0.5eq), 60°C , MeOH, 0°C , 3hrs, 65%. (iii) *O*-methyl cyclohexanone oxime (1.5eq), O_3 , pentane, rt, 5hrs, 45%. (iv) 15% NaOH, MeOH, 65°C , 3hrs, H^+ , 80%. (v) *p*-phenylenediamine (1eq), EDC.HCl (1.2eq), HOBT (1.2eq), NMM (2.5eq), DMF, 0°C -rt, 12hrs, 60%. (vi) $[\text{NO}][\text{BF}_4]$ (1eq), DCM, 0°C , 60%.

Typical conditions for diazotisation involve the use of NaNO_2 , strong acid and water. These conditions could cause decomposition of the trioxolane so an alternative milder method was sought after, involving the use of nitrosyl tetrafluoroborate. After some investigation (**Table 3**) into the optimum conditions for this reaction, it was found that one equivalent of $[\text{NO}][\text{BF}_4]$ in DCM at 0°C gave the best yield of diazonium product.

Entry	Solvent	$[\text{NO}][\text{BF}_4]$ (eq.)	Yield (%)
1	Et_2O	1	25
2	DCM	1	60
3	DCM	2	Decomposed

Table 3: Optimisation of conditions for diazonium salt formation (step (vi) **Scheme 11**).

The interesting feature of the diazonium salt formation was that the reaction was self-indicating. The amine-functionalised trioxolane **18** was a yellow/orange colour and the trioxolane diazonium product **15** was purple (**Figure 13**).

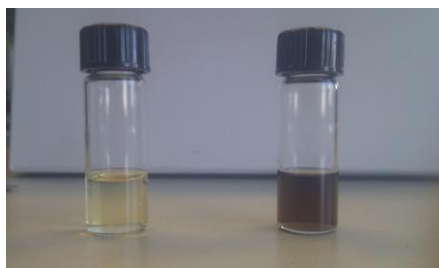
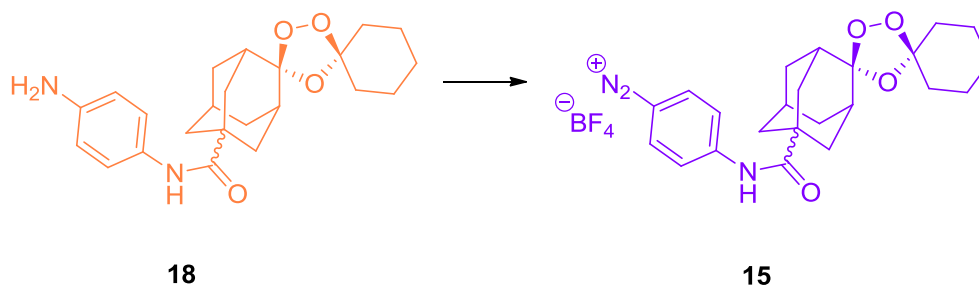
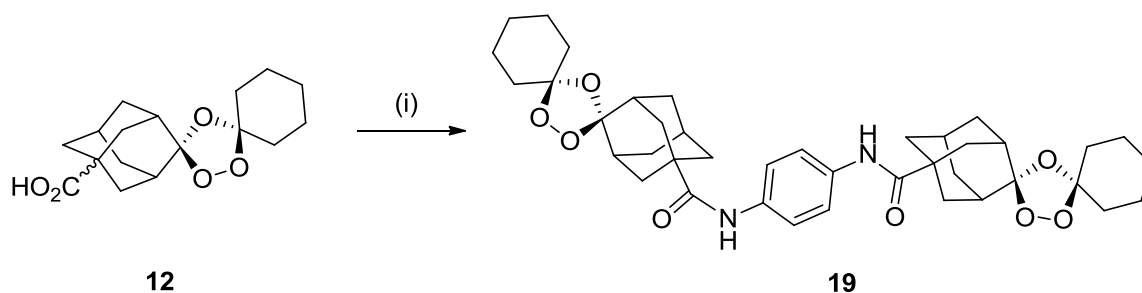


Figure 13: Diazonium salt formation shows colour change from yellow to purple.

Due to the unstable nature of the trioxolane bearing the diazonium group, it was only synthesised when needed and used immediately, as decomposition occurred when stored at room temperature. It was however, stable when stored in the fridge at 2-5°C. To avoid the risk of decomposition when the diazonium salt was used in electrochemical experiments, a trioxolane dimer **19** was synthesised as the more stable alternative (**Scheme 12**). This dimer was then used to successfully immobilise heme on a glassy carbon surface (**Figure 14**).



Scheme 12: Synthesis of trioxolane dimer **19** for immobilisation of heme on carbon surface.
 (i) *p*-phenylenediamine (0.5eq), EDC.HCl (1.2eq), HOBT (1.2eq), NMM (2.5eq), DMF, 0°C,
 3hrs, rt, 16hrs, 66%.

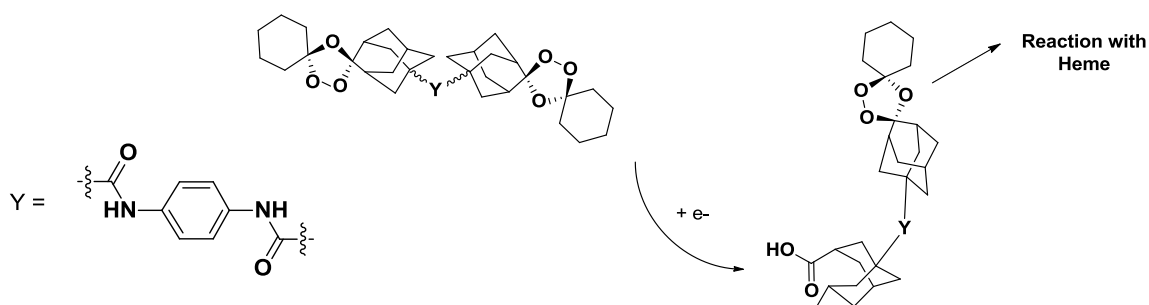


Figure 14: Immobilising heme on a glassy carbon surface by a trioxolane dimer bearing an amide linkage.

Having successfully synthesised bi-functional trioxolane-based molecular wires, the O'Neil group wanted to expand on this work by designing similar bi-functional, tetraoxane-based molecular wires. These wires should, in theory, be better heme alkylators than their trioxolane counterparts and our efforts towards them are discussed in detail in Chapter 3.

2.8. Bibliography

1. Vennerstrom, J. L.; Arbe-Barnes, S.; Brun, R.; Charman, S. A.; Chiu, F. C. K.; Chollet, J.; Dong, Y. X.; Dorn, A.; Hunziker, D.; Matile, H.; McIntosh, K.; Padmanilayam, M.; Tomas, J. S.; Scheurer, C.; Scorneaux, B.; Tang, Y. Q.; Urwyler, H.; Wittlin, S.; Charman, W. N., Identification of an antimalarial synthetic trioxolane drug development candidate. *Nature* **2004**, *430* (7002), 900-904.
2. Dong, Y. X.; Chollet, J.; Matile, H.; Charman, S. A.; Chiu, F. C. K.; Charman, W. N.; Scorneaux, B.; Urwyler, H.; Tomas, J. S.; Scheurer, C.; Snyder, C.; Dorn, A.; Wang, X. F.; Karle, J. M.; Tang, Y. Q.; Wittlin, S.; Brun, R.; Vennerstrom, J. L., Spiro and dispiro-1,2,4-trioxolanes as antimalarial peroxides: Charting a workable structure-activity relationship using simple prototypes. *J. Med. Chem.* **2005**, *48* (15), 4953-4961.
3. Creek, D. J.; Charman, W. N.; Chiu, F. C. K.; Prankerd, R. J.; McCullough, K. J.; Dong, Y. X.; Vennerstrom, J. L.; Charman, S. A., Iron-mediated degradation kinetics of substituted dispiro-1,2,4-trioxolane Antimalarials. *J. Pharm. Sci.* **2007**, *96* (11), 2945-2956.
4. Creek, D. J.; Charman, W. N.; Chiu, F. C. K.; Prankerd, R. J.; Dong, Y.; Vennerstrom, J. L.; Charman, S. A., Relationship between antimalarial activity and heme alkylation for spiro- and dispiro-1,2,4-trioxolane antimalarials. *Antimicrob. Agents Chemother.* **2008**, *52* (4), 1291-1296.
5. Griesbaum, K.; Ovez, B.; Huh, T. S.; Dong, Y. X., Ozonolyses of *O*-methyloximes in the presence of acid-derivatives - a new access to substituted ozonides. *Liebigs Ann.* **1995**, (8), 1571-1574.
6. Tang, Y. Q.; Dong, Y. X.; Karle, J. M.; DiTusa, C. A.; Vennerstrom, J. L., Synthesis of tetrasubstituted ozonides by the griesbaum coozonolysis reaction: Diastereoselectivity and functional group transformations by post-ozonolysis reactions. *J. Org. Chem.* **2004**, *69* (19), 6470-6473.
7. Vennerstrom, J. L.; Dong, Y.; Chollet, J.; Matile, H. Spiro and Dispiro 1,2,4-Trioxolane Antimalarials, US Patent 6,486,199 B1. **2002**.
8. Griesbaum, K.; Liu, X. J.; Kassiaris, A.; Scherer, M., Ozonolyses of *O*-alkylated ketoximes in the presence of carbonyl groups: A facile access to ozonides. *Liebigs Ann.-Recl.* **1997**, (7), 1381-1390.
9. Criegee, R., Mechanism of ozonolysis. *Angew. Chem.-Int. Edit. Engl.* **1975**, *14* (11), 745-752.
10. Geletneky, C.; Berger, S., The mechanism of ozonolysis revisited by O-17-NMR spectroscopy. *Eur. J. Org. Chem.* **1998**, (8), 1625-1627.
11. Dong, Y. X.; Tang, Y. Q.; Chollet, J.; Matile, H.; Wittlin, S.; Charman, S. A.; Charman, W. N.; Tomas, J. S.; Scheurer, C.; Snyder, C.; Scorneaux, B.; Bajpai, S.; Alexander, S. A.; Wang, X. F.; Padmanilayam, M.; Cheruku, S. R.; Brun, R.; Vennerstrom, J. L., Effect of functional group polarity on the antimalarial activity of spiro and dispiro-1,2,4-trioxolanes. *Bioorg. Med. Chem.* **2006**, *14* (18), 6368-6382.

12. Hartwig, C. L.; Lauterwasser, E. M. W.; Mahajan, S. S.; Hoke, J. M.; Cooper, R. A.; Renslo, A. R., Investigating the Antimalarial Action of 1,2,4-Trioxolanes with Fluorescent Chemical Probes. *J. Med. Chem.* **2011**, *54* (23), 8207-8213.
13. Zhou, L.; Alker, A.; Ruf, A.; Wang, X. F.; Chiu, F. C. K.; Morizzi, J.; Charman, S. A.; Charman, W. N.; Scheurer, C.; Wittlin, S.; Dong, Y. X.; Hunziker, D.; Vennerstrom, J. L., Characterization of the two major CYP450 metabolites of ozonide (1,2,4-trioxolane) OZ277. *Bioorg. Med. Chem. Lett.* **2008**, *18* (5), 1555-1558.

Chapter 3

Synthetic antimalarials - Dispiro-1,2,4,5-Tetraoxanes

This chapter contains a separate numbering system for all schemes, tables, figures and references. Numbering of compounds has continued from chapter 2.

3.1. Introduction to 1,2,4,5-tetraoxanes

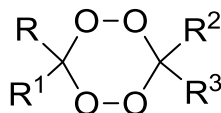


Figure 1: General structure of tetra-substituted tetraoxanes.

1,2,4,5-Tetraoxanes (**Figure 1**) are synthetic cyclic peroxides that have received significant attention in the literature. Initially, these compounds were used industrially for the production of macrocyclic hydrocarbons and lactones.¹ They are achiral compounds and can be prepared from readily available, inexpensive starting materials in only two synthetic steps. This currently represents the shortest sequence reported for the synthesis of non-symmetrical tetraoxanes with activity profiles similar to artemisinin.²

3.1.1. Stability and reactivity of synthetic endoperoxides: 1,2,4,5-tetraoxanes Vs 1,2,4-trioxolanes

While impressive antimalarial activity profiles have been observed with the 1,2,4-trioxolane class, the recent development of trioxolane OZ277 (discussed in chapter 2) has been hampered as this molecule was found to be unstable in the plasma of malaria patients during phase II dose-ranging study,³ so a more stable alternative was required. It was found that the achiral, 1,2,4,5-tetraoxane template is more stable (both thermodynamically and *in vivo*) than its 1,2,4-trioxolane counterpart (**Figure 2**). This was confirmed by the observation that 3,5-dicyclohexyl trioxolane **1** is inactive and unstable, whereas the analogous tetraoxane **20** is relatively stable and expresses good antimalarial activity. Unsymmetrical tetraoxanes containing a spiroadamantane group **21** were found to give enhanced stability and antimalarial activity.

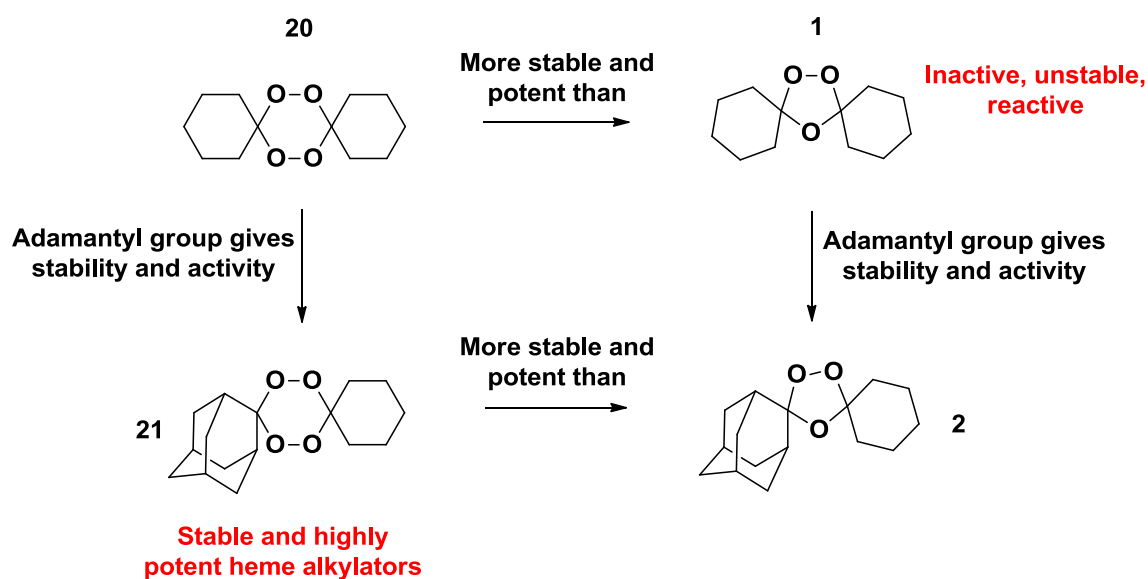


Figure 2: Rationale for dispiro-1,2,4,5-tetraoxanes.

In 1992, Vennerstrom *et al.*⁴ showed that symmetrical dispiro-1,2,4,5-tetraoxanes such as WR148999 (**Figure 3**) possessed high *in vitro* antimalarial activity. Despite being more potent than artemisinin *in vitro*, these compounds did not show good activity when tested orally as a result of extensive first-pass metabolism rather than solubility-limited dissolution.⁵

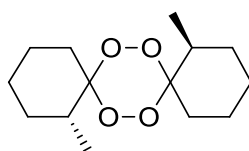


Figure 3: WR148999.

In 2008, O'Neill *et al.*² explored 1,2,4,5-tetraoxanes that incorporated a spiroadamantane group. They designed unsymmetrical dispiro-tetraoxanes, easily prepared from inexpensive materials *via* cyclocondensation of 1,1-dihydroperoxides with various ketones. Incorporation of water-soluble and polar functionalities *via* amide coupling produced several simple and achiral analogues. These analogues exhibited remarkable antimalarial activities *in vitro* and preliminary *in vivo* evaluation demonstrated that they also had promising oral activities.^{2, 6}

From a library of over 150 tetraoxanes, RKA182 (**Figure 4 and Scheme 1**) was selected as the candidate for full formal pre-clinical development.³ RKA182 has shown outstanding *in vitro* and *in vivo* activity against *Plasmodium falciparum* and improved pharmacokinetic characteristics compared to other peroxide drugs.

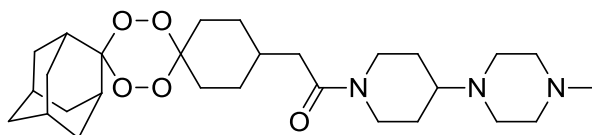
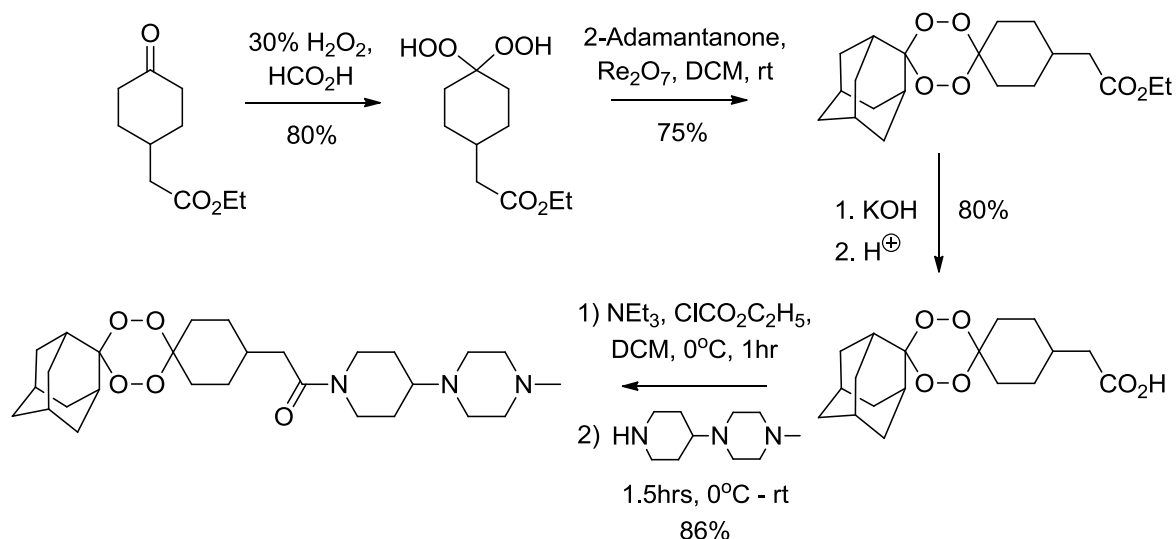
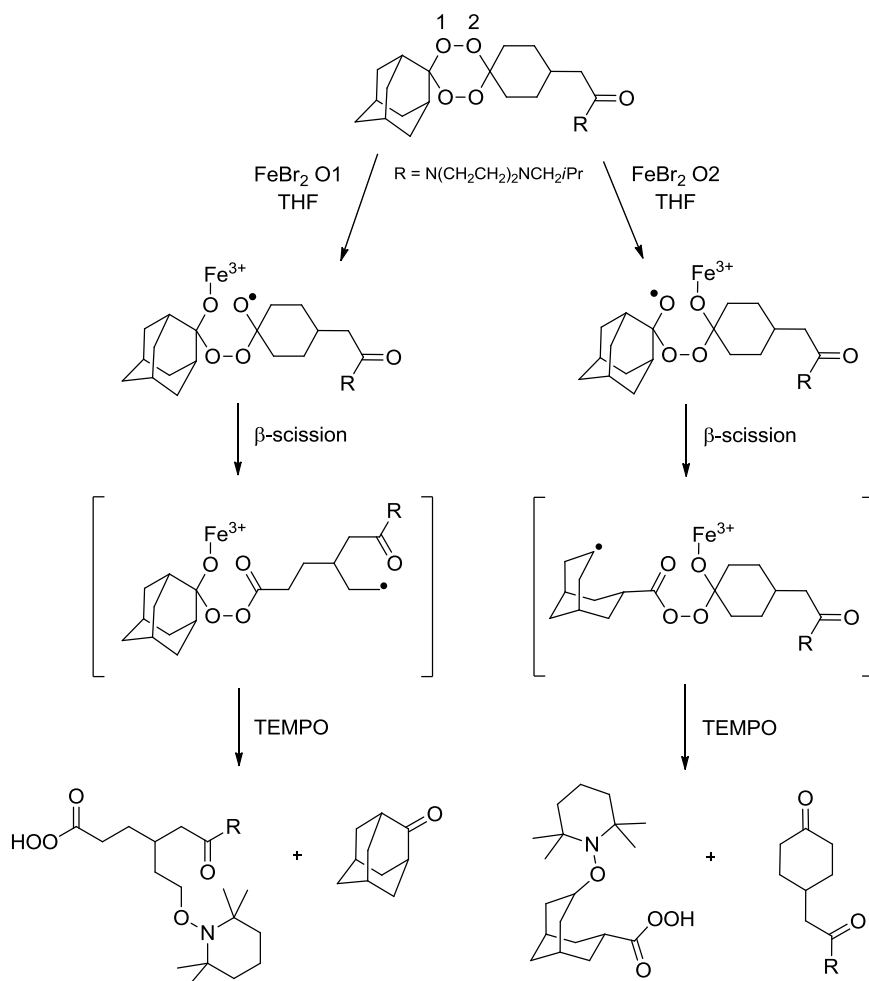


Figure 4: Structure of RKA182.

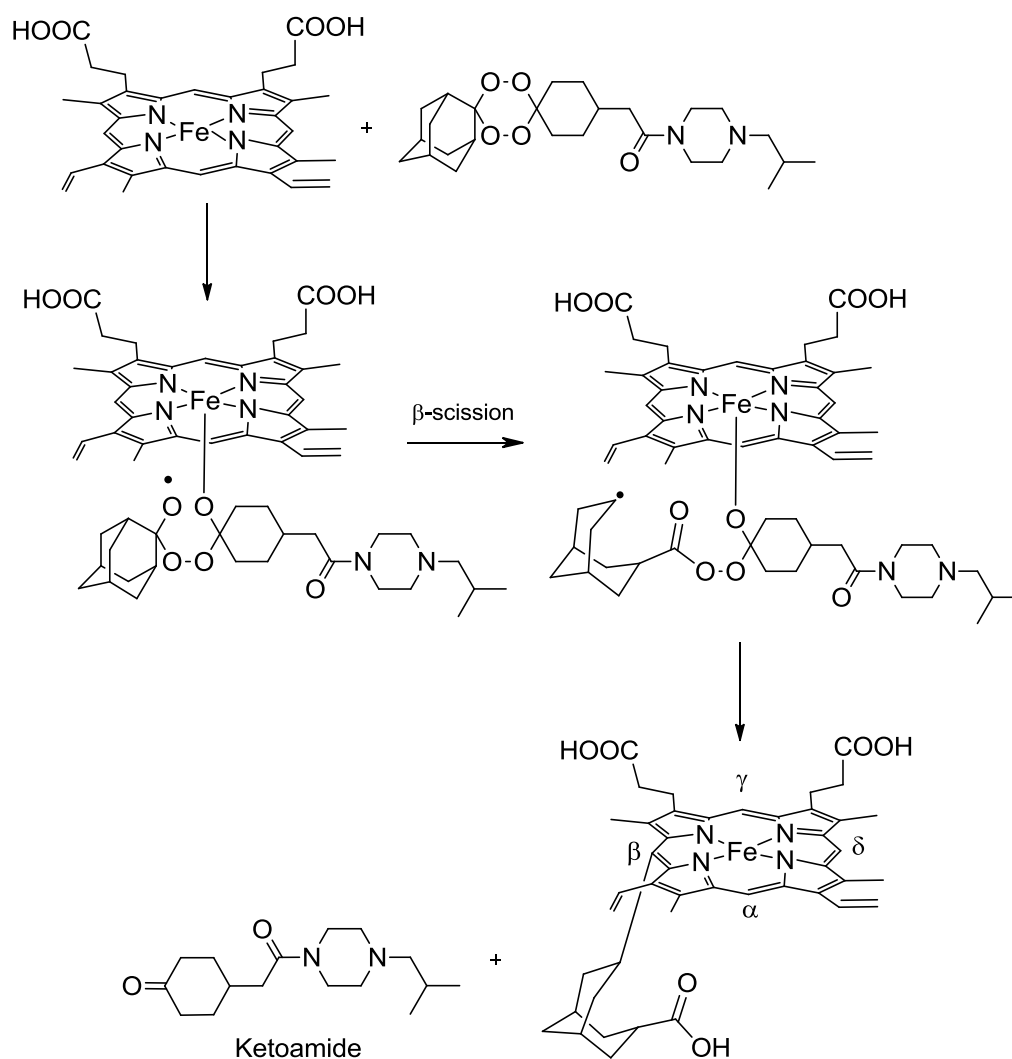
RKA182 has excellent *in vitro* activity against sensitive and resistant strains of *Plasmodium falciparum* and it retains this level of activity in South East Asia, where artemisinin combination chemotherapy has failed. The drug candidate has a fast rate of parasite kill and superior *in vivo* activity to artesunate in rodent models of malaria. It also has improved stability in the presence of infected red blood cells, when compared to synthetic ozonides or semi-synthetic artemisinins.



Scheme 1: Synthesis of RKA182.

3.1.2. Mechanistic studies of RKA182 using TEMPO³**Scheme 2:** TEMPO spin-trapping of C-centred radicals generated following Fe(II) activation.

To characterise the potential mediators of the antimalarial activity of RKA182, mechanistic studies with FeBr₂ in THF and TEMPO were performed (**Scheme 2**). From this investigation, both the primary and secondary C-centred radicals were intercepted to give two TEMPO adducts. The behaviour of the tetraoxanes reported by O'Neill *et al.* is distinct from 1,2,4-trioxolanes, as only the secondary C-centred radical species has been characterised from OZ277 and other trioxolanes. Since heme alkylation is believed to play an important role in the mechanism of action of endoperoxide antimalarials, the reactivity of tetraoxanes with ferrous heme was next investigated (**Scheme 3**). O'Neill *et al.* isolated the alkylated heme adduct, which confirmed that the mechanism is analogous to that shown by trioxolanes and that heme alkylation does indeed play an important role in their antimalarial activity.



Scheme 3: Proposed mechanism of action of 1,2,4,5-tetraoxanes. For clarity purposes, only the β -regioisomer of the alkylated heme adduct has been shown.

O'Neill *et al.* have also compared the reactivity of tetraoxanes with trioxolanes in the presence of ferrous iron salts, heme and ferrous iron salts/phosphatidylcholine.⁷ This study showed that the stability of the two classes of drugs with inorganic Fe(II) was comparable when they were substituted with identical side chains on the cyclohexyl ring. O'Neill *et al.* also carried out a modelling study between heme and RKA182 to confirm that the less hindered oxygens (O2 and O4) of the peroxide bond co-ordinate to the iron centre in heme (**Figure 5**).⁷

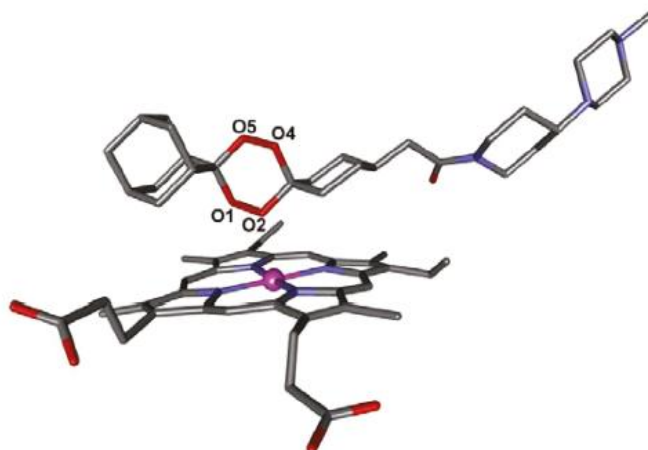


Figure 5: Docking configuration between heme and RKA182.⁷

The purpose of this was to determine if the regioselectivity of heme alkylation could be predicted by docking calculations. In all of the docking conformations studied, the shortest distance between iron-heme and RKA182 was found to be with O2 (2.4-2.8Å) for the lowest energy conformations. This suggests that there is a preferred co-ordination of iron on the sterically less hindered O2 atom of the peroxide bond, confirming regioselectivity observed in alkylation experiments and the proposed mechanism of action of tetraoxanes.

3.1.3. Second generation analogues of RKA182

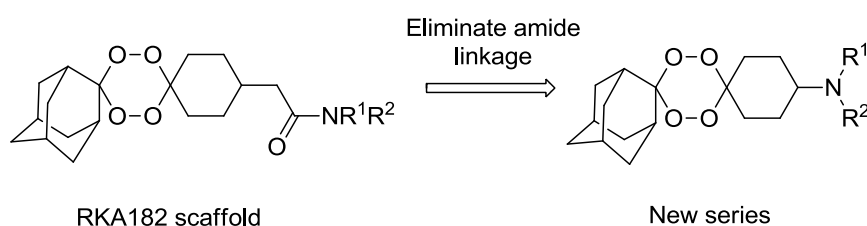


Figure 6: Elimination of the amide linkage provides second generation analogues.

A new series (**Figure 6**) of analogues was designed by O'Neill *et al.*⁸ to eliminate any potential metabolic liability due to the amide linkage present in RKA182. They hypothesised that by doing this, they would have access to compounds with increased metabolic stability and they carried out a study comparing preliminary results of metabolic stability of compounds from the new series with RKA182. They found that all of the compounds synthesised exhibited remarkable *in vitro* and *in vivo* antimalarial activity in the low nanomolar range (0.2 - 3.7nM) and several demonstrated promising oral activity. This meant that some members of this series are more metabolically stable than RKA182 and these compounds are currently under further investigation.

3.2. Molecular wire design

The main properties that our molecular wires must possess are functionality that can bind to heme centres (provided by the peroxide bond in the tetraoxanes) in the cytochromes of bacteria and allow robust attachment to either a carbon or gold surface, while simultaneously giving a high rate of electron transfer.

The synthetic peroxide antimalarials discussed so far have different functionalities incorporated at the 4'-position on the spirocyclohexyl moiety. However, according to the proposed mechanism of action of these compounds, it is the adamantane portion of the molecule that ends up alkylating the porphyrin ring in ferrous heme. This means that connective functionality must be incorporated into the spiroadamantane moiety (ideally at the 5-position for minimal steric effects) to act as a versatile synthetic handle for further transformations. This would create a bi-functional scaffold upon which a molecular wire, as shown in **Figure 7**, can be constructed.

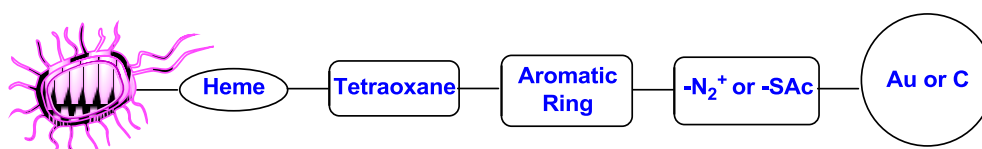


Figure 7: Diagram (not drawn to scale) showing components of tetraoxane molecular wire and its ability to tether bacteria to carbon/gold surfaces *via* appropriate functional groups.

We proposed that incorporation of an aromatic ring would increase electrical conductivity. The rationale behind using only one aromatic ring is to keep the molecular wire short so that tethering bacteria to a surface remains structured, organised and robust as a result of minimal flexibility. The design and synthesis of bi-functional tetraoxanes will be mainly focused on functional group transformations on the aromatic ring to incorporate amine and sulfur-based groups.

3.3. Methods of binding to carbon and gold surfaces

A key challenge in molecular electronics is to improve the efficiency of charge transfer through target molecules and across interfaces. This is particularly conspicuous for protein-based systems since electronic coupling between the protein and the electrode is relatively weak. Molecular wiring self-assembly has offered solutions for coupling the protein redox centre physically and electronically to the electrode surface.⁹ The O'Neil group envisaged that similar chemistry could be applied to bi-functional tetraoxane-based molecular wires as discussed in the next sections.

3.3.1. Binding to a carbon surface

One option for attachment of the molecular wire to a carbon electrode would involve diazonium chemistry as shown by Evrard *et al.*¹⁰ where carbon surfaces have been functionalised by aromatic azide molecules using “Click” chemistry (**Figure 8**).

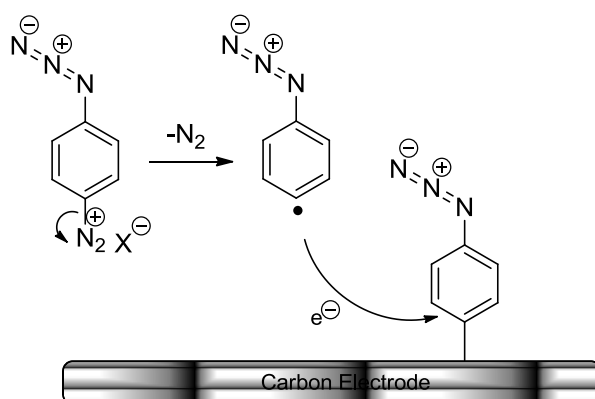


Figure 8: Electroreduction of diazonium salt for covalent immobilisation of phenylazide molecule on a carbon electrode surface.

These immobilised azides could then be functionalised with our tetraoxane molecular wires (**Figure 9**), and consequently attaching them to the carbon surface.

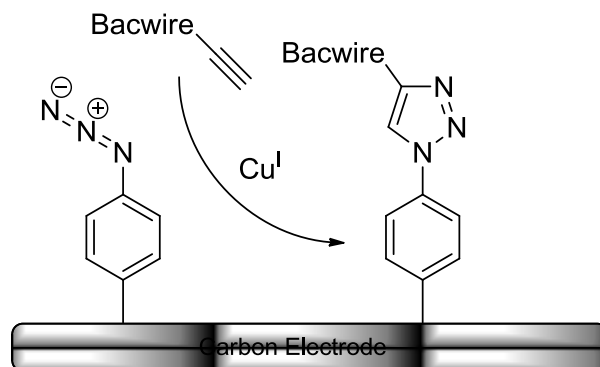
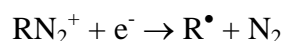


Figure 9: Cu(I)-catalysed Huisgen 1,3-dipolar cycloaddition between covalently immobilised phenylazide and our tetraoxane molecular wire (“Bacwire”) bearing the corresponding ethynyl group.

The main concern with applying “Click” chemistry to our work is that Cu(I) may reduce the peroxide bond of the tetraoxane as well as catalysing the cycloaddition with the immobilised azide. In 2009, Robert *et al.*¹¹ reported the Cu(I) activation of artemisinin and found that the reactivity of the peroxide bond was similar to that of Fe(II) analogues even though the reaction was more sluggish and product distribution slightly different.

Pinson and Podvorica¹² have shown that the electrochemical reduction of aryl diazonium salts on carbon leads to the formation of a strong C-C bond between a carbon atom from the surface of the solid and a carbon atom from the organic molecule. This technique is based on the reductive attachment of diazonium organic residues according to:



followed by attachment of the radical formed to the carbon surface, where R is a phenyl group substituted with appropriate (thiol or disulfide) functional groups that allow attachment to nanoparticles. Similar chemistry was used by Delamar *et al.*¹³ in 1992 and they found that the one-electron reduction of diazonium salts leads to a very robust covalent attachment of aryl groups onto a carbon surface. This method was also used by Toupin and Bélanger¹⁴ in 2008 where they functionalised the surface of carbon with 4-nitrophenyldiazonium cations.

3.3.2. Binding to a gold surface

In 2004, Schiffrin *et al.*¹⁵ reported the wiring of redox-active molecules to gold nanoparticles. Viologen-based dithiols (**Figure 10**) were self-assembled from solution on Au(111) for use as tethers to attach nanoparticles to a conducting substrate.

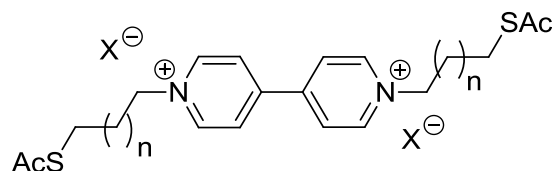


Figure 10: Viologen-based dithiols.

The topography, electrical properties and orientation of these molecules were investigated by STM, STS and FTIR. Remarkably, it was possible to isolate a single redox-active molecule in an alkanethiol matrix and by subsequent attachment of a single gold nanoparticle, the electrical properties of the conductivity of single wired molecules could be investigated. The aim of this work was to create single molecules that could perform basic electronic functions for use in molecular electronic devices and the main requirement was stable contacts at both ends of the wire. In 2007, Schiffrin *et al.*⁹ reported the gold nanoparticle-assisted assembly of a heme protein, namely a *c*-type cytochrome, for enhancement of long-range interfacial electron transfer (**Figure 11**).

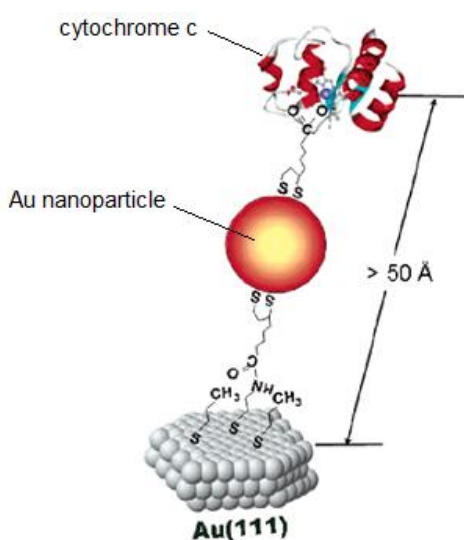


Figure 11: Molecular assembly of a *c*-type cytochrome on a Au(111) surface.

This work was towards improving long-range electronic interactions between the gold nanoparticle and the protein molecule for bio-electronics and bio-sensing devices. In addition to the thiol groups at one end of the wire, an amine or carboxylic moiety has been incorporated at the other extreme for linking to proteins through either covalent or non-covalent interactions.

3.4. Toward bi-functional 1,2,4,5-tetraoxane molecular wires

3.4.1. Introduction to 1,1,-dihydroperoxides

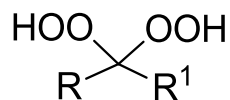


Figure 12: Structure of 1,1,-dihydroperoxides.

1,1- or *gem*-dihydroperoxides (**Figure 12**) are unstable derivatives of ketones and aldehydes and are important intermediates in the synthesis of a number of classes of peroxides, including tetraoxanes,^{6, 16, 17} bisperoxyketals¹⁸ and 1,2,4,5-tetraoxacycloalkanes.¹⁹ Dihydroperoxides have also been employed as reagents for nucleophilic epoxidations and oxidations,²⁰ sulfoxidation of sulfides²¹ and as precursors for the synthesis of dicarboxylic acid diesters.²²

3.4.2. Methods of synthesising 1,1-dihydroperoxides

The major pathways for the synthesis of 1,1-dihydroperoxides are:

1. Ozonolysis of ketone enol ethers or α -olefins in the presence of H_2O_2 ;
2. Reaction of ketals with H_2O_2 in the presence of tungstic acid or $\text{BF}_3 \cdot \text{Et}_2\text{O}$;
3. Peroxidation of ketones using an acidic solvent.

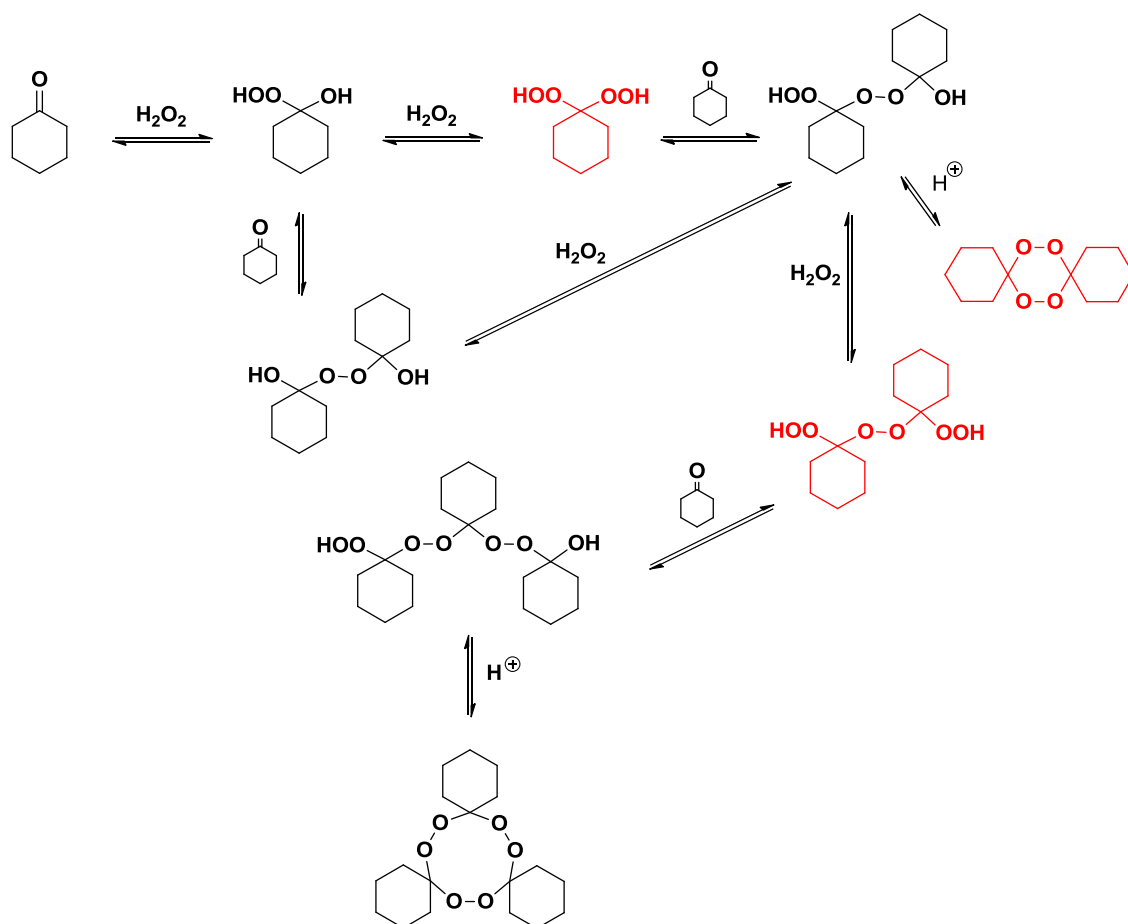
Drawbacks of these methods include the need for the prior synthesis of starting materials, use of highly concentrated H_2O_2 , the need for excess acid, moderate yields and limited scope of substrates.

In 2006, Žmitek *et al.*²³ discovered that all of these limitations could be overcome by using iodine as a catalyst to synthesise dihydroperoxides directly from the carbonyl compounds using commercially available 30% H₂O₂. As molecular iodine has already proven to be a useful Lewis acid catalyst for the activation of carbonyl compounds, they envisaged that it would benefit the peroxidation reactions of such compounds. The optimised conditions for this straightforward and efficient method for the synthesis of 1,1-dihydroperoxides gave yields in the region of 70-90%.

In 2007, Das *et al.*²⁴ reported a similar procedure that used CAN in place of iodine and they claimed that reaction times were typically reduced from 24hrs to 1hr. However, due to the big difference in cost per gram of CAN compared to iodine, we decided to not employ this method. Later in 2009, Li *et al.*²⁵ reported a different procedure that involved using PMA as the catalyst and ethereal hydrogen peroxide as the solvent for the reaction. They found that this method gave nearly quantitative yields of dihydroperoxides for most ketone substrates. However, due to the explosive nature of hydrogen peroxide, and the need to use Et₂O to “wash” it to prepare ethereal hydrogen peroxide, we decided against using this method.

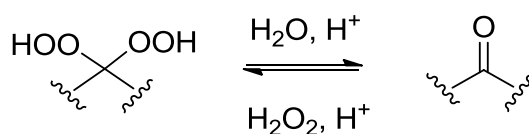
3.4.3. Stability of and side products from 1,1-dihydroperoxides

1,1-Dihydroperoxides are very thermally and chemically labile and tend to decompose readily at room temperature to give a number of dimeric and trimeric side products as shown by 1,1,-dihydroperoxycyclohexane in **Scheme 4**.



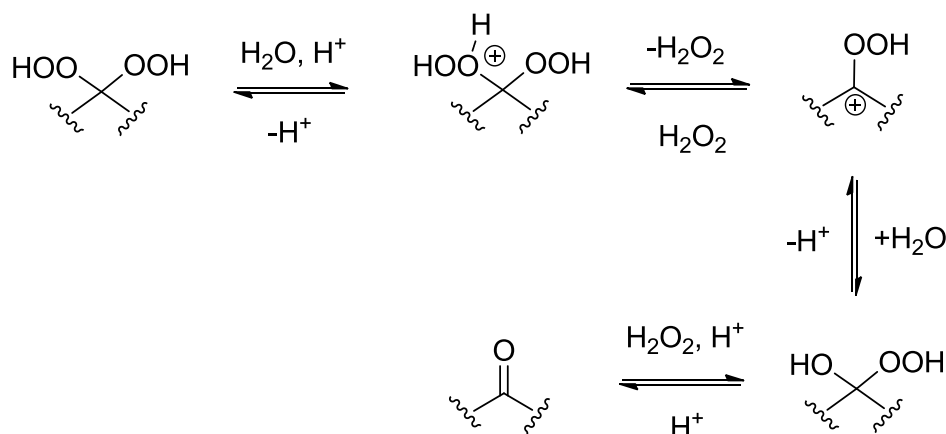
Scheme 4: Side products from the decomposition of 1,1-dihydroperoxycyclohexane.¹⁶ Structures highlighted in red are the compounds that have been isolated in our work.

In 2010, Terent'ev *et al.*²⁶ showed a new property of 1,1-dihydroperoxides; they could undergo hydrolysis in the presence of hydrogen peroxide with the removal of hydroperoxide groups in acidic media to form the corresponding ketones (**Scheme 5**). This transformation was found to exist as an equilibrium between the dihydroperoxide and the ketone.



Scheme 5: Equilibrium between dihydroperoxide and ketone.

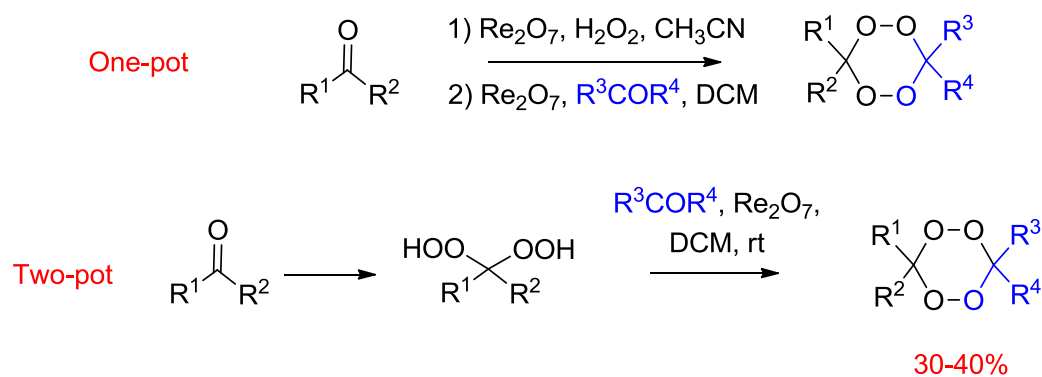
They found that the tendency of cyclic peroxides to hydrolyse increases from 6-membered to 8- and 12-membered rings. The mechanism for this transformation was proposed (**Scheme 6**).



Scheme 6: Proposed mechanism for hydrolysis of 1,1-dihydroperoxides.

3.4.4. Methods of synthesising 1,2,4,5-tetraoxanes

A number of useful procedures have been developed for the preparation of tetraoxanes. The key steps involve introduction of the peroxide group and where appropriate, transformation of hydroperoxide intermediates into cyclic peroxides. Since peroxides, especially hydroperoxide intermediates are both thermally and chemically labile, the choice of reagents and reaction conditions compatible with them is generally rather limited. This restriction poses additional challenges in stereochemical control and subsequent functionalisation. The synthesis of 1,2,4,5-tetraoxanes is dependent on several factors such as the structure of the ketone or aldehyde, temperature, solvent, pH, the choice of catalyst, concentration of the substrate and also the equilibria between the ketone and the precursors of cyclic peroxides. All of these factors result in variable yields being achieved from the carbonyl starting materials. Most of them have been investigated during our efforts toward tetraoxane molecular wires as examined in detail in the results and discussion section.



Scheme 7: Synthesis of 1,2,4,5-tetraoxanes using Re_2O_7 catalyst.

The most widely used method of tetraoxane synthesis was developed by Ghorai and Dussault in 2009,²⁷ which involves the rhenium (VII) oxide catalysed condensation of a 1,1,-dihydroperoxide with a carbonyl compound in a one- or two-pot procedure (**Scheme 7**). Due to the unstable nature of the dihydroperoxide, the one-pot method is usually preferred as this avoids its isolation and risk of decomposition. The mechanism of tetraoxane formation undoubtedly begins with the reversible addition of the dihydroperoxide to the ketone (or aldehyde). The resulting dihydroperoxide can undergo the desired cyclocondensation to give a tetraoxane or alternatively, oligomerisation to give a hexaoxonane¹⁶ (**Figure 13**).

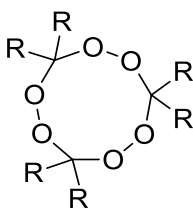
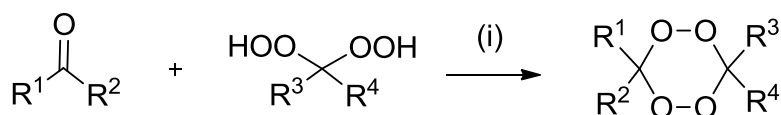


Figure 13: A hexaoxonane (trioxide).

Tetraoxanes can often be contaminated with hexaoxonanes and open-chain hydroperoxides. Purification can be achieved by using dimethyl sulphide, or the more strongly reducing agent potassium iodide, for selective removal of the more reactive hydroperoxides. Heating the mixture in acidic media can aid decomposition of the thermodynamically less stable hexaoxonanes to the more water-soluble lactones, which may also facilitate the purification process.¹⁶

In 2011, a procedure by Yan *et al.*²⁸ reported the use of PMA as the catalyst for tetraoxane synthesis with MgSO_4 as the drying agent in the reaction (**Scheme 8**). Both the rhenium (VII) oxide and PMA catalysed methods have been applied and optimised in our work towards the synthesis of adamantyl-functionalised tetraoxanes.

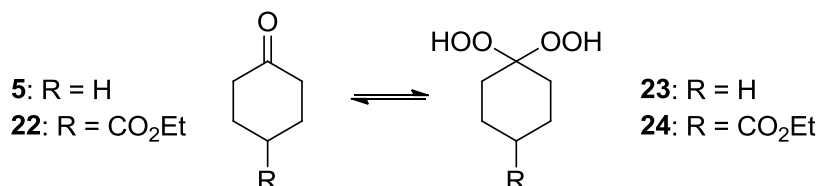


Scheme 8: Tetraoxane synthesis using phosphomolybdic acid (PMA) catalyst. (i) PMA (1mol%), MgSO_4 (1.5eq), DCM, rt, 4hrs.

3.5. Results and Discussion

3.5.1. Synthesis of 1,1-dihydroperoxides : Optimisation of 1,1-dihydroperoxide synthesis

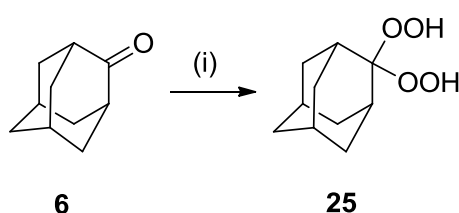
Efforts towards tetraoxane synthesis began with optimisation of the synthesis of 1,1-dihydroperoxides using literature procedures and this was necessary because of their inherently unstable and reactive nature. It was important to find a method of synthesis that gave consistently good yields.



Entry	R=	Conditions	Yield (%)
1	H	50% aq. H_2O_2 , HCO_2H , 30min, rt.	3
2	H	50% aq. H_2O_2 , Re_2O_7 (5mol%), CH_3CN , 1hr, rt.	47
3	H	50% aq. H_2O_2 , I_2 (10mol%), CH_3CN , 24hrs, rt.	75
4	CO_2Et	50% aq. H_2O_2 , I_2 (10mol%), CH_3CN , 24hrs, rt.	47
5	CO_2Et	50% aq. H_2O_2 , I_2 (10mol%), CH_3CN , 3-5 days, rt.	70-80

Table 1: Yields of dihydroperoxides obtained from following literature procedures.

The results are summarised in **Table 1**. Entry 1 was a procedure reported by Amewu *et al.*⁶ who obtained yields in the region of 70%. It was not surprising when we obtained a 3% yield because dihydroperoxides are not at all stable in the presence of acid as discussed in the previous section. Using formic acid as the solvent for the reaction would have caused the formation of dimeric/trimeric side products and decomposition of the dihydroperoxide product back to the starting ketone. Entry 2 was a procedure reported by Ghorai and Dussault²⁹ and yields obtained were typically >80%. We managed to obtain only 47% yield so it was clear that the methods attempted were unreliable and gave inconsistent yields on repetition. Entry 3 used a procedure by Žmitek *et al.*²³ and Selvam *et al.*²¹ reported a similar procedure two years later, which gave 75% yield of 1,1-dihydroperoxycyclohexane **23**. Yields were reproducible when an ester functionality was present (Entry 5), though they are still not as high as the reported 93%. We found that longer reaction times were required to achieve higher yields even though the presence of the ester group should, in theory, make the carbonyl carbon more electrophilic and hence more reactive.



Scheme 9: Synthesis of dihydroperoxide **25** from 2-adamantanone **6**. (i) 50% aq. H₂O₂, I₂ (10mol%), CH₃CN, 24hrs, rt, 57%.

The synthesis was also carried out starting with 2-adamantanone **6** (**Scheme 9**) which gave a 57% yield of the corresponding dihydroperoxide **25**. We decided against using this in tetraoxane formation with cyclohexanone as yields of tetraoxane produced were slightly lower (20%) than if the dihydroperoxide and carbonyl compounds were “reversed” (25%). Another reason is that 2-adamantanone **6** is approximately five times more expensive per gram than cyclohexanone **5** so there was no justification in using a more expensive substrate that gave lower overall yields. This investigation determined that iodine was the optimum catalyst for the synthesis of dihydroperoxides and this was the method of choice throughout this work. The authors proposed the following reaction mechanism:

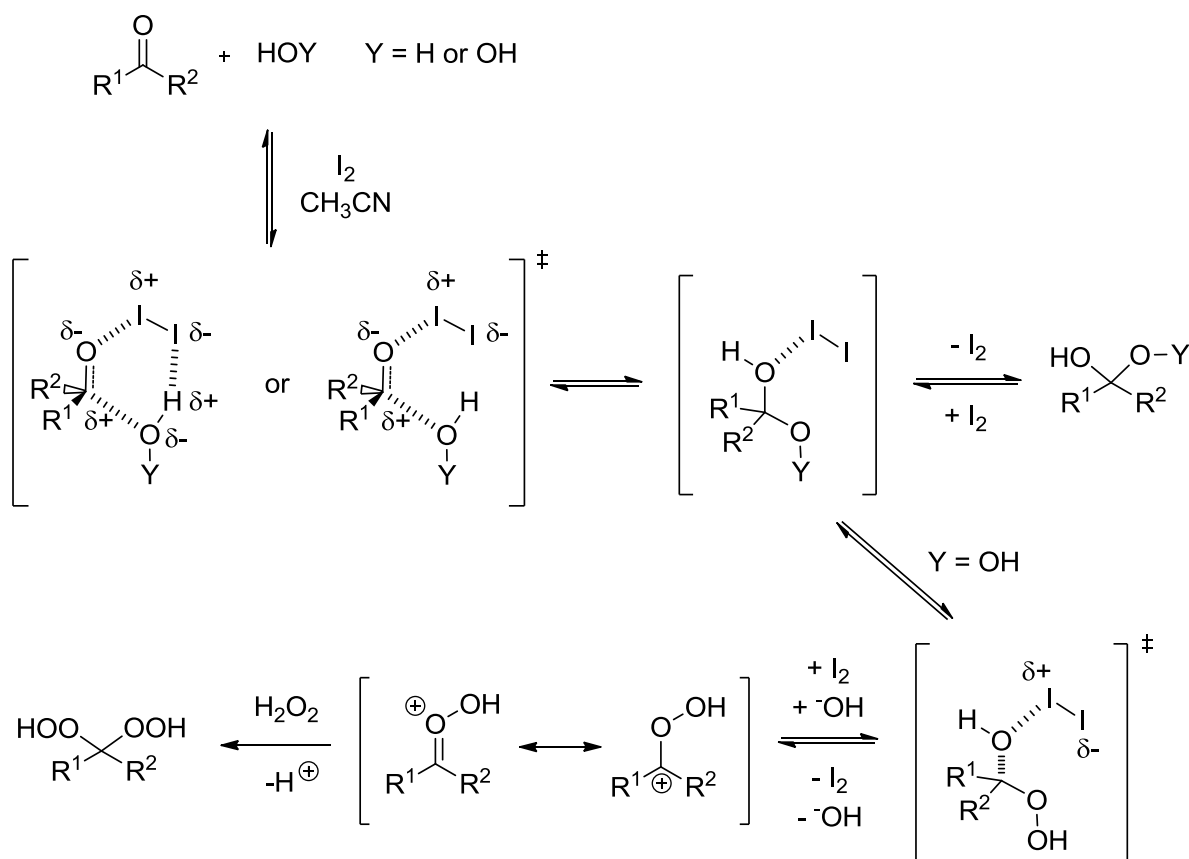


Figure 14: Iodine-catalysed synthesis of dihydroperoxides.²³

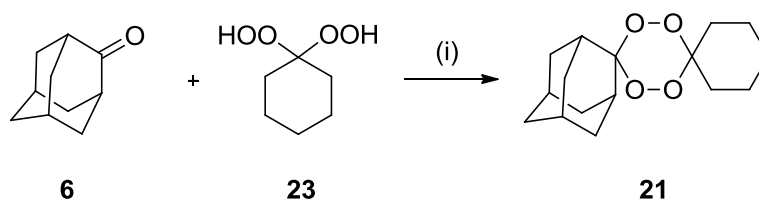
3.5.2. Problems caused by the unstable nature of 1,1-dihydroperoxides

As discussed, dihydroperoxides are both thermally and chemically labile. It was found that on isolation after chromatography, decomposition of the dihydroperoxide back to the starting ketone could be seen by TLC after only one day when left to stand at room temperature. For this reason, dihydroperoxides were, initially, only synthesised and used immediately when needed. It was later found that when stored in the freezer at -18°C , dihydroperoxides were very stable and no decomposition to the starting ketones was observed for over two years. Following this discovery, dihydroperoxides were synthesised on a gram scale in batches and stored in the freezer to be used when required. It was found that 1-2g was the maximum scale in which the synthesis could be carried out safely and efficiently with reproducible yields.

On one occasion when the synthesis of 1,1-dihydroperoxycyclohexane was carried out on a larger scale using 5g of cyclohexanone, the reaction mixture spontaneously and exothermically decomposed in the flask before it could be purified by column chromatography. Another possible explanation for not being able to obtain yields higher than 80% may be due to some decomposition occurring on silica gel. However, 2D TLCs showed that there was no decomposition on TLC plates so any decomposition that occurred on the column was assumed to be minimal.

3.6. Synthesis of 1,2,4,5-tetraoxanes: Initial work on the synthesis of unfunctionalised tetraoxanes

Having optimised the synthesis of dihydroperoxides, we proceeded to use them in tetraoxane synthesis. The investigation with repeating a literature procedure by Ghorai and Dussault that used Re_2O_7 as a catalyst, to obtain familiarity with the procedure and get an indication of what yields to expect. The first reaction involved the condensation of 2-adamantanone **6** with 1,1-dihydroperoxycyclohexane **23** (Scheme 10).

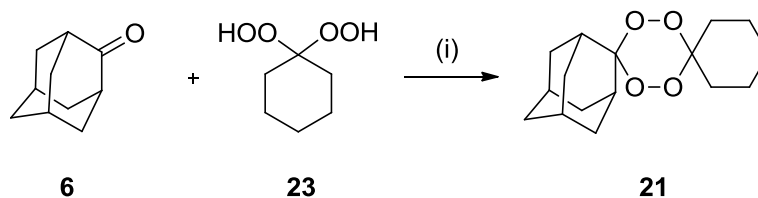


Scheme 10: Condensation of 2-adamantanone **6** with 1,1-dihydroperoxycyclohexane **23**. (i) Re_2O_7 (2mol%), DCM, rt, 1hr, 35%.

The literature yield for tetraoxane **21** was reported as 69%. We were unable to obtain yields as high as this on repetition and instead found that they were typically <35% and 25% would be a better approximation for this reaction. The yields were the same when the DCM had been freshly distilled prior to use or used as purchased. The use of molecular sieves in the reaction also had no effect on the yield obtained. The reasons for such poor yields are that although the ketone is used in slight excess (1.2-1.5eq), during the course of the reaction, some dihydroperoxide undoubtedly decomposes back to the starting ketone, some of it dimerises to form a symmetrical tetraoxane (can be seen on TLC) and the remainder reacts to give the desired tetraoxane product.

3.6.1. Tetraoxane synthesis using different samples of Re_2O_7

To confirm that the tetraoxane yields were not dependent on the batch of Re_2O_7 catalyst used, we next used two different samples of Re_2O_7 in the reaction (**Scheme 11**).



Scheme 11: Tetraoxane formation using different batches of Re_2O_7 catalyst.

Entry	Conditions (i)	Result (followed by TLC)
1	No catalyst	No reaction
2	Usual batch of Re_2O_7 (pale green)	Gone to completion after 1hr
3	Black Re_2O_7 (assumed to be inactive)	Gone to completion after 4hrs

Table 2: Results from monitoring reactions by TLC.

We concluded that the colour of the catalyst and its method of storage did not have any significant effect on the reaction (**Table 2**). The black catalyst, which had been stored at room temperature in air, was assumed to be inactive. It was in fact still active but less so than the usual batch of catalyst that had been stored under inert atmosphere in a desiccator.

3.6.2. Attempted synthesis of a tetraoxane for use as a control in heme alkylation experiments

We thought it would be beneficial to synthesise a compound analogous to tetraoxane **21** that did not have a peroxide bond. This would render it incapable of alkylating heme and is therefore able to act as a control (**Figure 15**) in heme alkylation experiments.

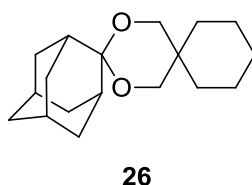
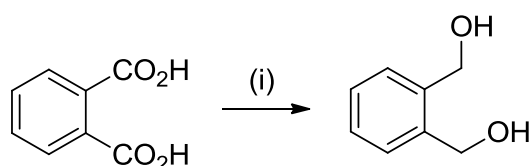


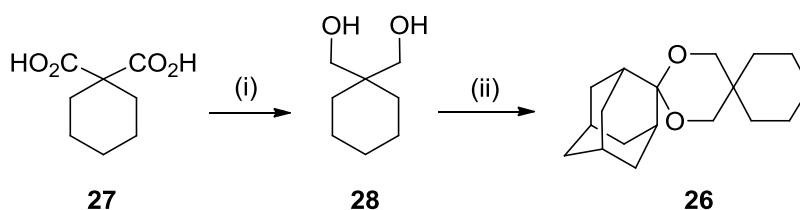
Figure 15: Target molecule **26** to be used as a control in heme alkylation experiments.

In 1973, a procedure reported by Yoon *et al.*³⁰ showed that carboxylic acids could be reduced to the corresponding alcohols using $\text{BH}_3\cdot\text{THF}$. They showed that the reduction of phthalic acid using this method gave the diol in 95% yield (**Scheme 12**).



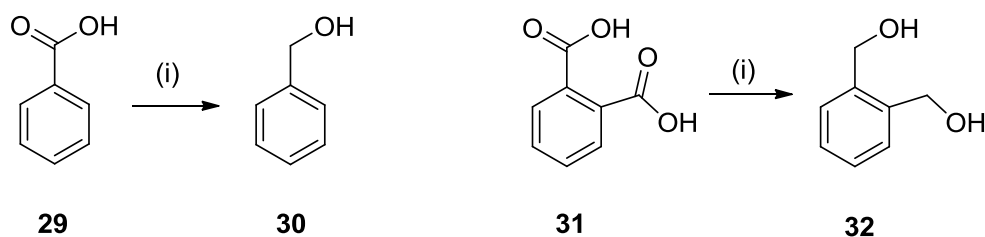
Scheme 12: Reduction of phthalic acid to 1,2-phenylenedimethanol. (i) 2.39M $\text{BH}_3\cdot\text{THF}$ (2.3eq), THF, 0°C-rt, 6hrs, 95%.

We were optimistic that this method would work with cyclohexane-1,1-dicarboxylic acid **27** and subsequent acetal formation with 2-adamantanone **6** would then yield the target control molecule **26** (**Scheme 13**).



Scheme 13: Route to target control molecule **26**. (i) 1.0M $\text{BH}_3\cdot\text{THF}$ in THF (2.3eq), THF, 0°C-rt, 6hrs (ii) 2-adamantanone **6**, $p\text{-TSA}$ (10mol%), toluene, Δ Dean Stark, 24hrs.

Initially, when 2.3 equivalents of $\text{BH}_3\cdot\text{THF}$ were used, no reaction took place so another 1 equivalent was added. However, analysis by TLC and ^1H NMR showed that no reaction had taken place. We decided to test this method on the reduction of benzoic acid and the reduction of phthalic acid (**Scheme 14**) to determine whether there was a problem with the procedure or if our starting substrate was not tolerated by these reaction conditions.



Scheme 14: Reductions of benzoic acid **29** and phthalic acid **31**. (i) 1.0M $\text{BH}_3\cdot\text{THF}$ in THF (2.3eq), THF, 0°C -rt, 6hrs.

The products for both reactions were not isolated but analysis by TLC and ^1H NMR showed that the diol product was clearly present. This result inferred that our substrate could not be reduced under these reaction conditions rather than there being an issue with the procedure itself or any differences in experimental set-up. We imagine that the most likely reason for this reaction not working is that the boron atom in $\text{BH}_3\cdot\text{THF}$ forms a complex between the two carboxylic acid groups using its empty p orbital, rendering it inactive.

3.7. Tetraoxane synthesis using camphor and norcamphor

Having obtained low yields for adamantyl-derived tetraoxanes, we questioned whether or not the same result would be obtained if another bulky/hindered ketone was used in place of 2-adamantanone. We predicted that camphor and norcamphor (**Figure 16**) would be good alternatives because in theory, the tetraoxanes from these would form tertiary and secondary C-centred radicals respectively when alkylating heme.

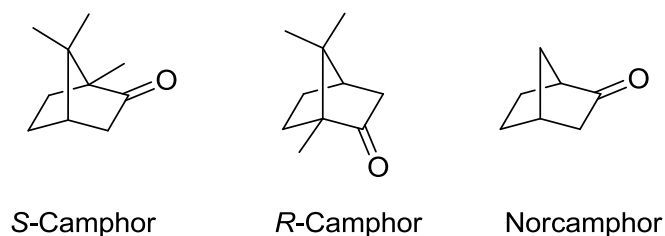
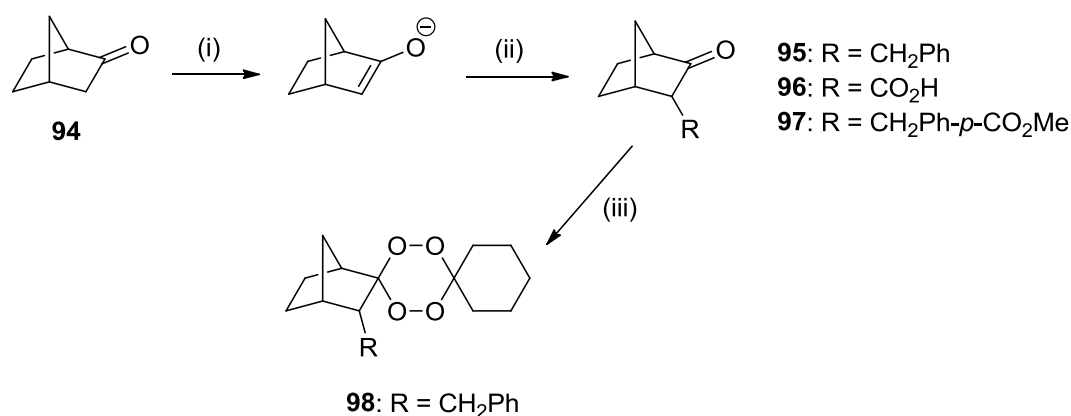


Figure 16: Structures of camphor and norcamphor.

We first attempted synthesising the dihydroperoxides from camphor and norcamphor using iodine catalyst but in both cases, no product was isolated, which is most likely a result of decomposition either during the reaction or the purification process. We next attempted tetraoxane synthesis using camphor then norcamphor with 1,1-dihydroperoxycyclohexane but found that these reactions did not work at all. We were then intrigued by the possibility of using functionalised camphor/norcamphor derivatives in tetraoxane synthesis. If successful, this would provide an easily accessible route to bi-functional tetraoxanes as camphor/norcamphor can be easily functionalised *via* their corresponding enolates.

Tetraoxane synthesis using camphor was unsuccessful so we decided to use norcamphor instead, which is less bulky, achiral and very readily functionalised using a literature procedure.³¹ Norcamphor was pre-functionalised using different electrophilic substrates before it was used in tetraoxane formation (**Scheme 15** and **Table 3**).



Scheme 15: Functionalisation of norcamphor **94** followed by tetraoxane formation.

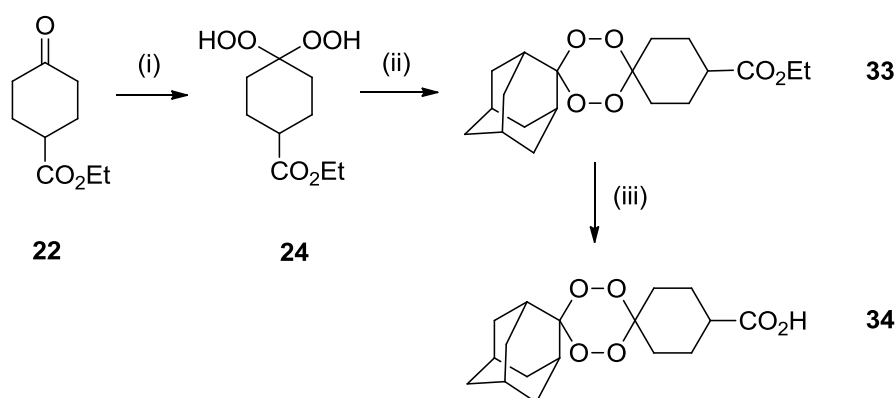
Entry	R =	Step (ii) Yield (%)	Step (iii) yield (%)
1	-CH ₂ Ph	94	22
2	-CO ₂ H	69	0
3	-CH ₂ Ph- <i>p</i> -CO ₂ Me	31	0

Table 3: Tetraoxane synthesis using functionalised norcamphor derivatives. (i) LDA (1.1eq), THF, 0°C, 30min. (ii) Benzyl bromide (1.1eq) or CO₂ (excess), THF, -78°C, 30min. (iii) 1,1-Dihydroperoxycyclohexane (1eq), Re₂O₇ (2mol%), DCM, rt, 1hr.

Norcamphor bearing a benzyl group **95** (Entry 1) gave its corresponding tetraoxane **98** in 22% yield, which is comparable to the yields obtained from adamantane-derived tetraoxanes. The norcamphor substrates bearing acid **96** or ester functionality **97** (Entries 2 and 3) failed to give any tetraoxane product. It was found that the Baeyer Villiger oxidation was also the major competing reaction pathway when norcamphor derivatives were used and dimerisation of the dihydroperoxide was taking place. The major product isolated was the lactone from oxidation of the starting ketone. For these reasons, we decided to abandon the use of norcamphor derivatives as we had encountered the same problems that were previously observed with adamantane derivatives.

3.8. Synthesis of cyclohexyl-functionalised tetraoxanes for heme alkylation experiments

The syntheses of tetraoxanes bearing functional groups on the cyclohexyl moiety were carried out (**Scheme 16**). These compounds are direct analogues of trioxolanes **10** and **11** (Chapter 2) synthesised within the O'Neil group. The application of these in heme alkylation experiments were to be carried out by the group of Dr. Abraham Esteve-Núñez, University of Alcalá de Henares. The results from these experiments are currently pending.



Scheme 16: Synthesis of tetraoxanes bearing functionality on the cyclohexyl moiety. (i) 50% aq. H_2O_2 (3eq), I_2 (10mol%), CH_3CN , rt, 3 days, 71%. (ii) 2-Adamantanone (1.5eq), Re_2O_7 (5mol%), DCM, rt, 5hrs, 43%. (iii) 15% aq. NaOH , MeOH , 65°C , 5hrs, H^+ , 97%.

3.9. Initial work on the synthesis of adamantyl-functionalised tetraoxanes

According to the mechanism of action of tetraoxanes, it is the adamantane moiety that alkylates the porphyrin ring in heme (**Figure 17**).

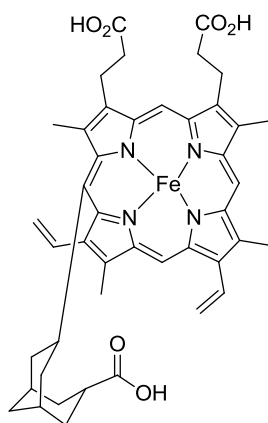
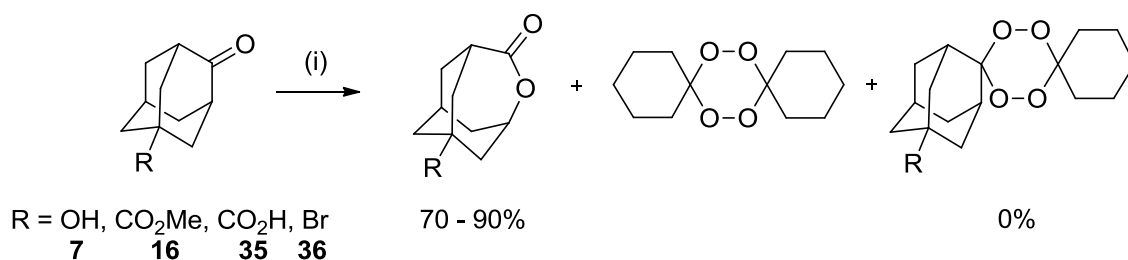


Figure 17: Alkylation of porphyrin ring in heme by adamantane moiety of tetraoxane.

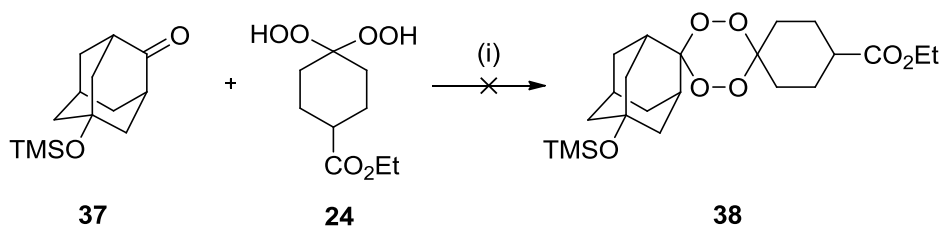
Having successfully carried out the synthesis of an unfunctionalised tetraoxane, we next applied the same procedure to several functionalised adamantanones (**Scheme 17**). They each had a functional group at the 5-position of the adamantanone to act as a synthetic handle for further transformations.



Scheme 17: Attempted syntheses of adamantyl-functionalised tetraoxanes. (i) 1,1-dihydroperoxycyclohexane **23** (1eq), Re₂O₇ (2mol%), DCM, rt, 4hrs.

The Re_2O_7 -catalysed tetraoxane synthesis was carried out using 1,1-dihydroperoxycyclohexane **23** and four different 5-functionalised adamantanones (1.2-1.5eq). All of these reactions either did not give any of the desired tetraoxane products or negligible yields. In each case, we instead isolated the tetraoxane from dimerisation of the dihydroperoxide, and the lactone from Baeyer Villiger oxidation of the starting ketone as the major products (70-90% yield). Only 0.5 equivalents of the dihydroperoxide is required to oxidise one equivalent of the ketone to the lactone while one equivalent of dihydroperoxide is required to make one equivalent of the desired tetraoxane product. These results suggested that when there is an electron-withdrawing group (EWG) bonded directly to the adamantane skeleton; the Baeyer Villiger oxidation is favoured over tetraoxane formation.

We also attempted tetraoxane formation using 5-hydroxy-2-adamantanone bearing a TMS protecting group on the adamantyl alcohol **37** (**Scheme 18**). However, it was shown by ^1H NMR and mass spectrometry that these reaction conditions caused the TMS group to fall off and no desired tetraoxane product was isolated.



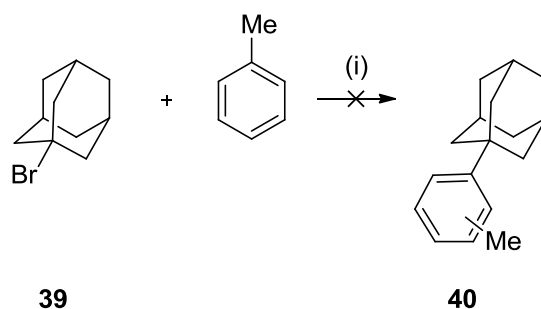
Scheme 18: Attempted tetraoxane formation using TMS-protected 5-hydroxy-2-adamantanone. (i) Re_2O_7 (2mol%), DCM, rt, 4hrs, 0%.

3.10. Initial attempts at synthesising functionalised adamantanes and adamantanones

We envisaged that the problem with the Baeyer Villiger oxidation taking place preferentially could be solved simply by replacing the electron-withdrawing group (EWG) with an electron-donating group (EDG). There is no literature precedent for the synthesis of such adamantane derivatives so our investigation began with the synthesis of functionalised 1-bromoadamantane **39** derivatives.

3.10.1. S_N1 reactions using water as a catalyst³²

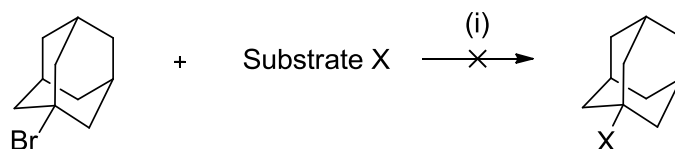
Following a literature procedure, water was used as a catalyst in an attempt to arylate 1-bromoadamantane **39** with toluene (**Scheme 19**). Unfortunately, under both sets of reaction conditions, no desired product was isolated and all starting material was recovered.



Scheme 19: Attempted arylation of 1-bromoadamantane **39** with toluene. (i) Water (24mol%), 120°C, 24hrs, 0% or dry glassware, N₂ atmosphere, 120°C, 24hrs, 0%.

3.10.2. Attempted Heck-type coupling reactions with 1-bromoadamantane^{33, 34}

We next attempted Heck-type coupling reactions on 1-bromoadamantane **39** with various substrates (**Table 4**) but no desired products were isolated under these conditions.

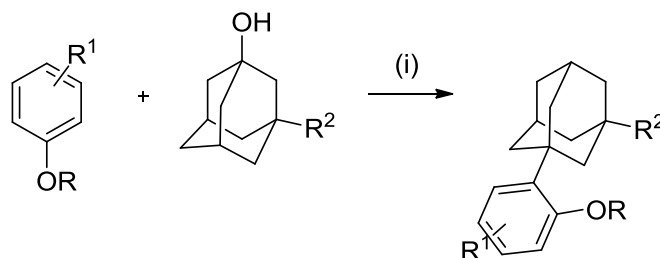


Entry	Substrate X	Conditions	Yield (%)
1	Styrene	Pd/C, DMF, K ₂ CO ₃ , 120°C, 24hrs	0
2	Toluene	Pd/C, K ₂ CO ₃ , 120°C, 24hrs	0
3	Toluene	Pd(OAc) ₂ , K ₂ CO ₃ , 120°C, 24hrs	0
4	Acrylonitrile	Pd(OAc) ₂ , DMF, K ₂ CO ₃ , 145°C, 24hrs	0

Table 4: Attempted Heck-type coupling reactions on 1-bromoadamantane **39**.

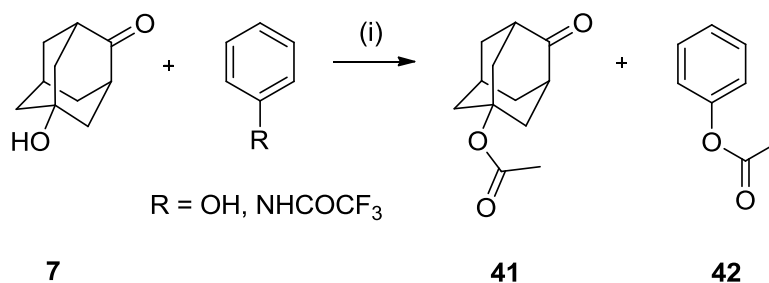
3.10.3. Attempted arylation of 5-hydroxy-2-adamantanone using Amberlite™ resin

In 2012, Wang *et al.*³⁵ reported the functionalisation of 1-adamantanol derivatives using Amberlite™ resin and different aryl substrates (**Scheme 20**). Amberlite™ is a strongly acidic cross-linked polystyrene-type sulfonic acid resin which can be recycled. The extraordinarily high yields obtained (reported as 98% after recrystallisation) for some of the reported compounds made this method appear very promising.



Scheme 20: Arylation of 1-adamantanol derivatives using Amberlite™ resin. (i) Amberlite™ 200, AcOH, 100°C, 2hrs, 66-98%.³⁵

We aimed to find a flexible route towards a range of functionalised adamantanones using *any* aryl substrate, instead of developing a new synthetic route for each target compound. The scope of the reaction appeared to be rather limited but reaction times were short and yields were high. We therefore applied the Amberlite™ chemistry in an attempt to functionalise 5-hydroxy-2-adamantanone **7**. Before the Amberlite™ could be used, it had to be dried. It was first stirred in 20% conc. H₂SO₄ overnight, washed with water then THF and dried under vacuum over P₂O₅ for 1 day. It was then used in reactions with 5-hydroxy-2-adamantanone **7** with phenol and trifluorophenylacetamide (**Scheme 21**).



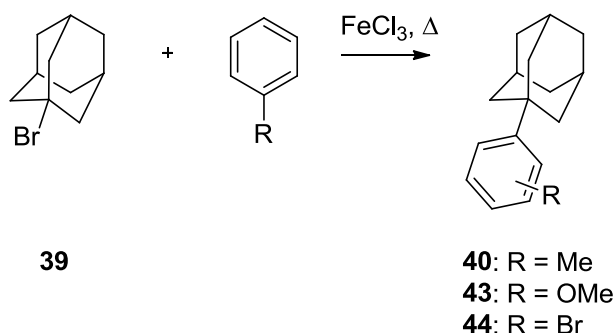
Scheme 21: Attempted Amberlite™ catalysed arylation of 5-hydroxy-2-adamantanone. (i) Amberlite™ 200, AcOH, 100°C, 24hrs, 0% desired product, 79% 4-oxoadamantan-1-yl acetate **41**, 20% phenylacetate **42**.

Unfortunately, both of these reactions failed to give any arylated product. We instead isolated the esters of both starting materials, which, in hindsight, was not surprising as acetic acid was the solvent used for both reactions.

3.11. Friedel Crafts arylations of 1-bromoadamantane and 5-bromo-2-adamantanone

3.11.1. Friedel Crafts arylation of 1-bromoadamantane

In 2004, Su *et al.*³⁶ reported the synthesis of functionalised adamantane derivatives using Friedel Crafts chemistry employing FeCl_3 . We first decided to obtain familiarity with and test the scope of this procedure by synthesising several functionalised adamantane derivatives. To do this, we carried out Friedel Crafts arylations of 1-bromoadamantane **39**, which is commercially available, inexpensive and has a similar structure to 5-bromo-2-adamantanone **36** (Table 5).



Entry	R =	FeCl_3 (eq)	Ortho : Para	Yield (%)
1	-Me	0.08	Para only	83
2	-OMe	0.08	1 : 1.5	5
3	-Br	0.08	1 : 7	25
4	-OMe	1.5	Para only	99
5	-Br	1.5	1 : 5	86

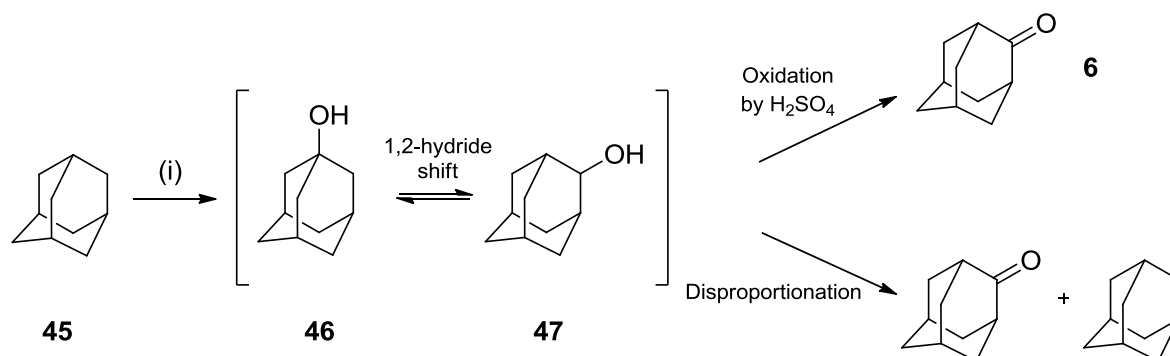
Table 5: Friedel Crafts arylations of 1-bromoadamantane **39**. Ratios of regioisomers of the product were estimated by ^1H NMR analysis.

Due to steric considerations in further transformations, we wished to obtain only the para-substituted products in these investigations. Entry 1, the Friedel Crafts arylation of 1-bromoadamantane with toluene, catalysed by FeCl_3 was taken from a procedure by Su *et al.*³⁶ and the yield of 83% was promising, which encouraged us to investigate other aryl substrates. When anisole (Entry 2) and bromobenzene (Entry 3) were used, not only did the yields drop significantly but the products were isolated as inseparable mixtures of ortho/para isomers. This may be caused by the aryl substrate co-ordinating to the catalytic amount of FeCl_3 , which in turn hinders the reaction. However, when 1.5 equivalents of FeCl_3 are used, the yields increased dramatically (Entries 4 and 5) but the selectivity of the products also changed. We currently do not have an explanation for the differences in these results. We propose that further work involving a wider range of aryl substrates should be investigated to determine the reasons behind the differences in yield and selectivity for this reaction.

3.11.2. Attempted synthesis of 5-bromo-2-adamantanone

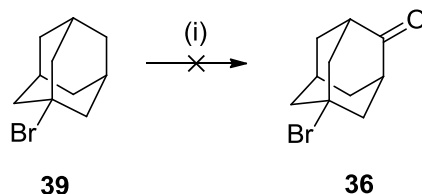
We next wanted to investigate the Friedel Crafts arylation of 5-bromo-2-adamantanone **36**. This is commercially available but also very expensive and we wanted to establish whether or not it could be synthesised from 1-bromoadamantane.

In 1968, Geluk and Schlattmann³⁷ and then in 1973, Geluk and Keizer³⁸ reported the oxidation of adamantane **45** to 2-adamantanone **6** using 98% H_2SO_4 , where the intermediate was found to be an equilibrium between 1-adamantanol **46** and 2-adamantanol **47** (Scheme 22). There were two possible reaction pathways observed; the oxidation of 2-adamantanol gave 2-adamantanone or a disproportionation reaction gave a mixture of 2-adamantanone from oxidation of 2-adamantanol, and adamantane from reduction of adamantanol.



Scheme 22: Oxidation of adamantane **45**. (i) 98% H_2SO_4 , 80°C, 4hrs, 47%.

We envisaged that the same conditions could be applied to oxidise 1-bromoadamantane **39** to 5-bromo-2-adamantanone **36** (**Scheme 23**) where the intermediates formed should be an equilibrium between 5-bromo-1-adamantanol and 5-bromo-2-adamantanol. Unfortunately, this reaction was unsuccessful and gave a black tar-like substance.

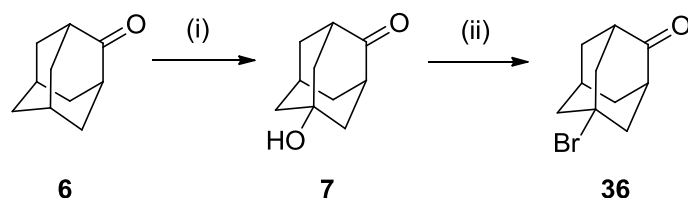


Scheme 23: Attempted oxidation of 1-bromoadamantane **39** to 5-bromo-2-adamantanone **36**.

(i) 98% H₂SO₄, 80°C, o/n, 0%.

3.11.3. Friedel Crafts arylation of 5-bromo-2-adamantanone

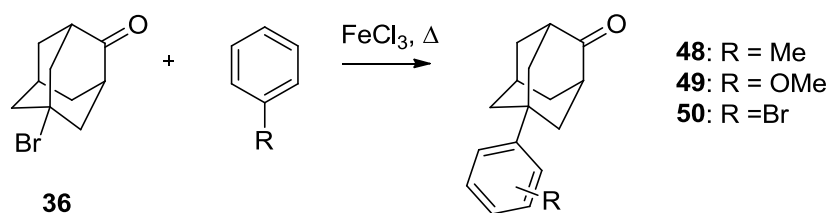
With encouraging results from the Friedel Crafts arylation of 1-bromoadamantane **39** in hand, we next investigated the Friedel Crafts arylations of 5-bromo-2-adamantanone, which is more relevant for this work (**Scheme 24**).



Scheme 24: Synthesis of 5-bromo-2-adamantanone **36**. (i) 100% HNO₃, 3 days, rt, 52%. (ii)

48% HBr, Δ, 24hrs, 60%.

2-Adamantanone **6** (commercially available) was oxidised to 5-hydroxy-2-adamantanone **7** using 100% nitric acid³⁹ by a post-doctoral researcher in the O'Neil group on a 25g scale. 5-Hydroxy-2-adamantanone **7** (1-2g was found to be the optimum scale) was then brominated by refluxing in hydrobromic acid overnight⁴⁰ to afford 5-bromo-2-adamantanone **36** in 52% yield. The Friedel Crafts arylation of 5-bromo-2-adamantanone **36** was then carried out using a variety of aryl substrates (**Table 6**).



Entry	R =	FeCl ₃ (eq.)	Ortho : Para : Meta	Yield (%)
1	-Me	0.08	-	Not isolated
2	-Me	0.22	-	Not isolated
3	-Me	1.0	-	Not isolated
4	-Me	1.5	1 : 10 : 0	93
5	-OMe	1.5	2.6 : 1 : 0	27 (p) 67 (o)
6	-Br	1.5	Para only	76

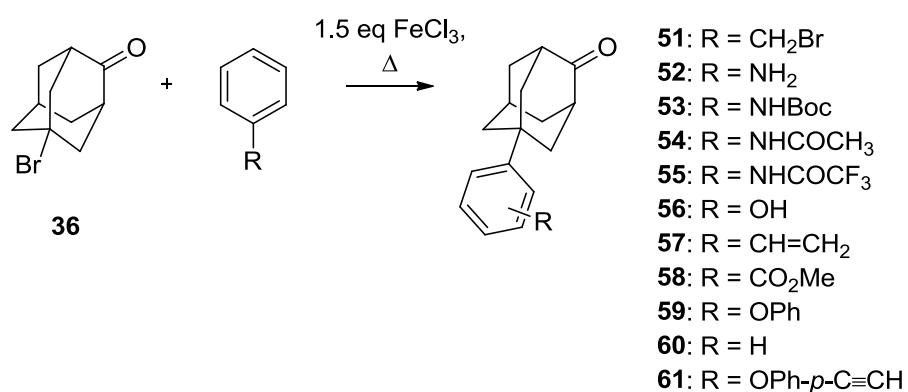
Table 6: Optimisation of conditions for Friedel Crafts arylation of 5-bromo-2-adamantanone.

We began the investigation by using literature conditions reported for the arylation of 1-bromoadamantane with 0.08 equivalents FeCl₃ (Entry 1). On monitoring by TLC, this led to incomplete conversion of starting material and the same result was observed on increasing to 0.22 equivalents and 1.0 equivalent (Entries 2 and 3). When 1.5 equivalents of FeCl₃ was used (Entry 4), the reaction went to completion but the product was formed as a mixture of ortho/para isomers that were inseparable by column chromatography. By using a more electron rich aryl substrate, anisole (Entry 5), we managed to obtain a mixture of isomers that were separable by column chromatography. However, the desired para-substituted product **49** was the minor isomer at only 27% yield. When bromobenzene was used (Entry 6), the product **50** was obtained as the para isomer only in a good yield. This was a critical result as we now had an adamantanone derivative with suitable functionality at the 5-position that could be used in tetraoxane synthesis.

Having used the same substrates for Friedel Crafts arylation of 1-bromoadamantane **39** and 5-bromo-2-adamantanone **36**, we noticed a dramatic change in selectivity that was dependent on the presence of the ketone (comparing Entries 4 and 5, **Table 5** with Entries 5 and 6, **Table 6**) having kept the reaction conditions the same. We have yet to establish a plausible explanation for this observation.

3.11.4. Testing the scope of the Friedel Crafts arylation of 5-bromo-2-adamantanone

To investigate the scope of the optimised conditions for the Friedel Crafts arylation, we carried out this reaction using a range of solid and liquid aryl substrates (**Table 7**). Having only used liquid aryl substrates as the solvent for reaction so far, we hoped that the scope would also include solid aryl substrates. We aimed to find at least one arylated adamantanone was capable of undergoing further transformations and could also be obtained in good yield.



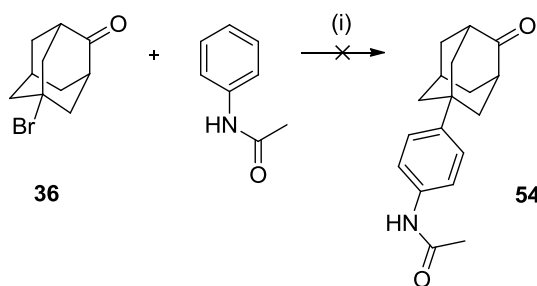
Entry	R =	Solvent	Ortho : Para : Meta	Yield (%)
1	-CH ₂ Br 51	-	-	Polymerised
2	-NH ₂ 52	-	-	No reaction
3	-NHBoc 53	CHCl ₃ /DCM	-	Decomposed
4	-NHCOCH ₃ 54	CHCl ₃ /DCM	-	No reaction
5	-NHCOCF ₃ 55	CHCl ₃ /DCM	-	No reaction
6	-OH ³⁶ 56	-	-	Decomposed
7	-CH=CH ₂ 57	-	-	Polymerised
8	-CO ₂ Me 58	-	Meta only	65
9	-OPh 59	-	Para only	30
10	-H 60	-	-	69
11	-OPh- <i>p</i> -C≡CH 61	-	-	Decomposed

Table 7: Scope of optimised Friedel Crafts arylation.

The general result was that most aryl substrates decomposed, polymerised or did not react at all under these conditions. The ones that did react (Entries 8-10) gave single isomers of the arylated products. It appears that only liquid aryl substrates that can be used as the solvent at reflux temperatures will afford arylated adamantanones (either as mixtures of isomers or single isomers) using this method. There has been great difficulty in finding a suitable solvent to use in this reaction with solid aryl substrates. Both chloroform and DCM were tried but these have boiling points that are far below the temperatures required for the Friedel Crafts arylation to take place. The choice of solvents that are high boiling but at the same time will not interfere with the Friedel Crafts reaction is very limited. 5-Phenyl-2-adamantanone **60** (Entry10) was obtained in 69% yield. Nitration of the phenyl ring was attempted using NO_2BF_4 in DCM at 0°C but no reaction occurred. Theoretically, this would have been the most direct route to an amine-functionalised adamantanone derivative, capable of further transformations. However, as benzene is required for the synthesis of 5-phenyl-2-adamantanone **60**, we did not deem this to be a long term feasible route towards large scale production of bi-functional molecular wires.

3.11.5. Solvent screen for Friedel Crafts reaction using a solid aryl substrate

We next carried out a solvent screen (**Table 8**) in an attempt to find one suitable for use with acetanilide, a solid aryl substrate, in the Friedel Crafts reaction.



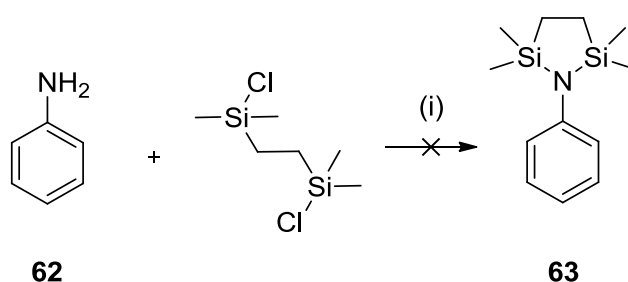
Entry	Solvent	T ($^\circ\text{C}$)
1	DCM	40
2	CHCl_3	80
3	1,2-Dichloroethane	85
4	DMF	130

Table 8: Solvent screening for Friedel Crafts reaction using acetanilide as the solid aryl substrate. (i) FeCl_3 (1.5eq), solvent, $T^\circ\text{C}$, 24hrs, 0%.

Of all the solvents that were screened (Entries 1-4), no desired product could be isolated because no reaction occurred. We therefore decided to not pursue this any further and continue by taking forward the suitable arylated products (Entry 6, **Table 5** and Entries 8-10, **Table 6**) for tetraoxane synthesis.

3.11.6. Attempted silyl protection of aniline before Friedel Crafts arylation

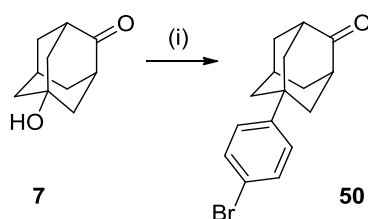
The simplest route to a suitable compound for aryl diazonium formation would be to functionalise adamantanone **6** with aniline **62** or an aniline derivative, which can then be used in tetraoxane formation. The reaction was unsuccessful when aniline was used directly in the Friedel Crafts arylation so we next decided to protect the aniline with a hindered silyl group first before attempting the arylation again (**Scheme 25**). However, crude ^1H NMR of the reaction mixture showed that only aniline was present. It is thought that the silyl protecting group was hydrolysed during the course of the reaction or when exposed to air at the end.



Scheme 25: Attempted silyl protection of aniline **62**. (i) NEt_3 (2eq), dry DCM, rt, 2hrs, 0%.⁴¹

3.12. Synthesis of 5-(4-bromophenyl)adamantan-2-one starting from 5-hydroxy-2-adamantanone

Before moving on to tetraoxane synthesis, we wanted to reduce the number of steps towards functionalised adamantanones. A route to 5-(4-bromophenyl)adamantan-2-one **50** starting from 5-hydroxy-2-adamantanone **7** was sought after. This would eliminate the need to synthesise 5-bromo-2-adamantanone **36** first and hence reduce the amount of material lost. We envisaged that an acid would protonate the alcohol in 5-hydroxy-2-adamantanone **7** to give water as a leaving group and generate a tertiary carbocation that could react with bromobenzene. Several acids were screened in the optimisation stage (**Table 9**).



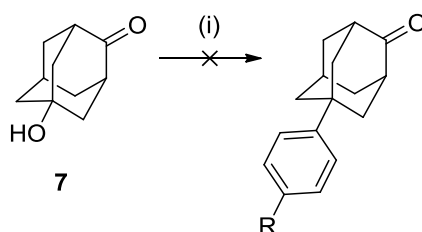
Entry	Acid (1eq)	Yield (%)
1	<i>p</i> -TSA	0
2	Conc. H ₂ SO ₄	0
3	TFA ⁴²	0
4	TfOH ⁴³	59

Table 9: Synthesis of 5-(4-bromophenyl)adamantan-2-one **50** from 5-hydroxy-2-adamantanone **7** in one step. (i) Acid (1eq), bromobenzene, Δ, 1-20hrs.

Triflic acid (Entry 4) was found to be the optimum choice, giving 5-(4-bromophenyl)adamantan-2-one **50** in 59% in one step starting from 5-hydroxy-2-adamantanone **7**. When the synthesis was carried out in two steps previously, starting with bromination of 5-hydroxy-2-adamantanone **7** and subsequent Friedel Crafts arylation of 5-bromo-2-adamantanone **36**, the yield over both steps was only 40%.

3.12.1. Testing the scope of the adamantyl arylation using triflic acid

Having had success with synthesising 5-(4-bromophenyl)adamantan-2-one **50** using triflic acid, we wanted to determine the scope of this method when carried out in a chlorinated solvent (**Scheme 26**).



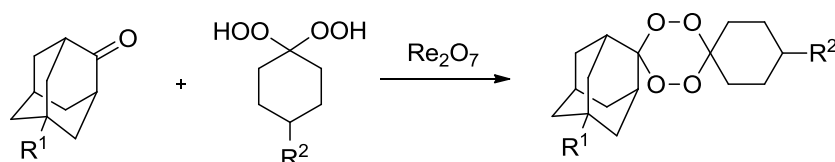
Scheme 26: Attempted triflic acid catalysed arylation of 5-hydroxy-2-adamantanone **7**. (i) TfOH (1eq), benzyl bromide/aniline/allyl bromide (1.5eq), CHCl₃, 70°C, 24hrs, 0%.

We attempted the arylation using benzyl bromide and then aniline in chloroform but unfortunately, both reactions failed to give any product. In the case of benzyl bromide, we believe that the benzylic cation may have formed in preference to the tertiary cation of 2-adamantanone, preventing the desired arylation reaction from taking place.

In the case of aniline, we assumed that the reflux temperature of the solvent was not high enough to allow the reaction to proceed, which was the same problem in the Friedel Crafts arylations. Under the strongly acidic conditions, it is very likely that aniline was simply protonated by the acid, rendering it unreactive. The reason for no reaction taking place with allyl bromide could be due to temperatures not being high enough or allyl bromide itself being rather unreactive.

3.13. Synthesis of novel adamantyl-functionalised tetraoxanes

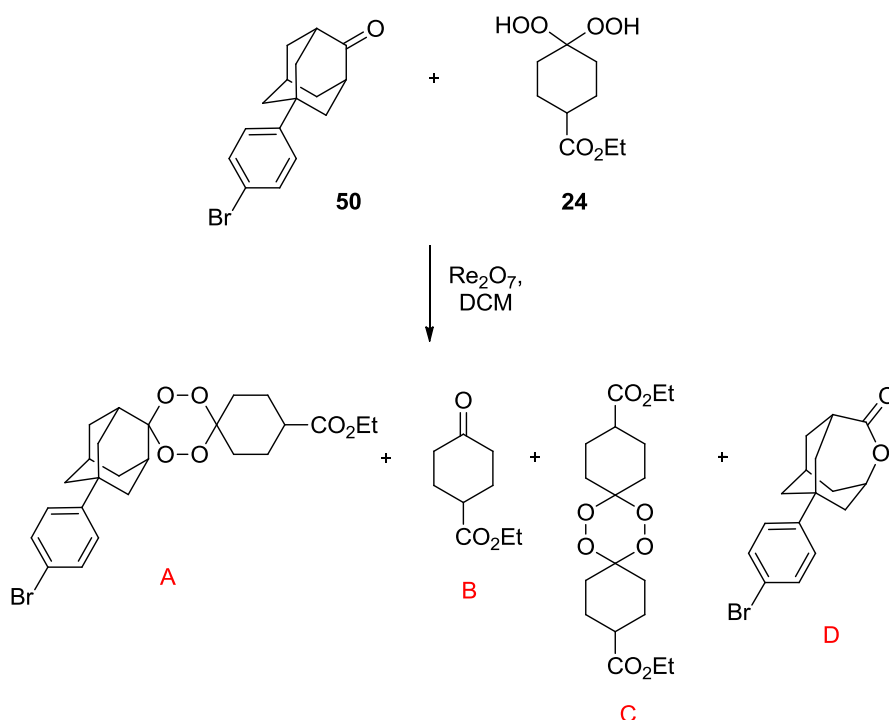
The functionalised adamantanones from the optimised Friedel Crafts arylation that gave single isomers of the products were taken forward for tetraoxane synthesis using Re_2O_7 catalyst (**Table 10**).



Entry	R ¹ =	R ² =	Yield (%)
1	-H 6	-CO ₂ Et 24	43 33
2	-H 6	-H 23	25-35 21
3	-Ph- <i>p</i> -Me 48	-CO ₂ Et 24	38 (mixture o/p isomers) 64
4	-Ph- <i>p</i> -Br 50	-CO ₂ Et 24	24 65
5	-Ph- <i>p</i> -Br 50	-H 23	9 66
6	-Ph- <i>m</i> -CO ₂ Me 58	-CO ₂ Et 24	14 67
7	-Ph- <i>m</i> -CO ₂ Me 58	-H 23	8 68
8	-Ph- <i>p</i> -OPh 59	-H 23	8 69

Table 10: Yields of adamantyl-functionalised tetraoxanes, synthesised using 1 equivalent of the dihydroperoxide and 1.2 equivalents of the adamantanone derivative.

These results suggested that tetraoxane yields are significantly higher when there was no functionality on the adamantyl skeleton (Entries 1 and 2). When there was an electron withdrawing group present with a phenyl ring acting as an electron-rich “spacer group”, tetraoxane yields decreased to as low as 8% (Entries 5-8). With entry 4 giving the highest yield for the adamantyl-functionalised tetraoxanes in this investigation, we strived to further increase the yield by slightly altering the reaction conditions used in the Re_2O_7 -catalysed reaction (**Table 11**).

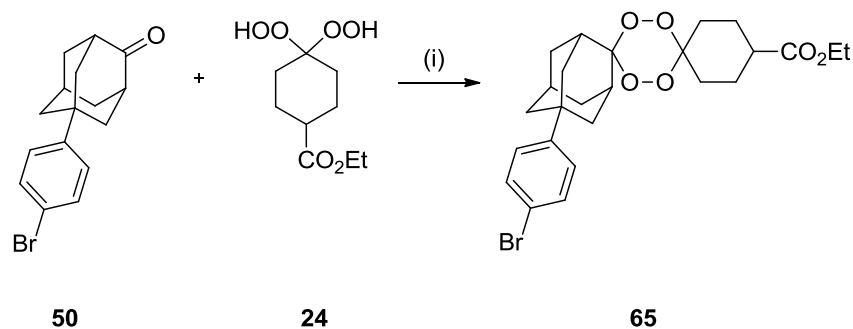


Entry	DHP (mg)	Conditions	A (%)	B (%)	C (%)	D (%)
1	25	rt, 4hrs	35	-	-	-
2	200	rt, 4hrs	24	10	3	53
3	200	0°C 2hrs, rt 2hrs	34	35	3	25

Table 11: Yields of bromophenyl-tetraoxane and side products.

3.14. Experiments to determine if concentration of dihydroperoxide affected tetraoxane yields

Having found that temperature has some effect on the yield of tetraoxane obtained, we next investigated the effect of concentration of the starting dihydroperoxide (**Table 12**).



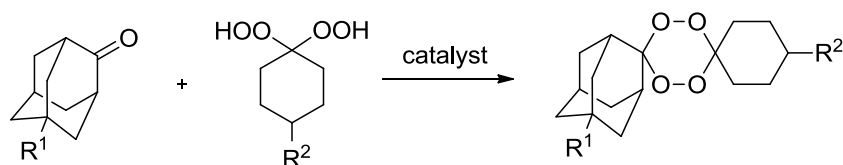
Entry	Mass of 24 (mg)	DCM (ml)	Conc ⁿ of DHP (mg/ml)	Yield of 65 (%)
1	30	15	2	42
2	40	20	2	35
3	200	25	8	24
4	200	100	2	24

Table 12: Yields of tetraoxane from varying concentrations of dihydroperoxide.

Entries 1, 2 and 4 used 2mg of dihydroperoxide per millilitre of DCM and the yields all varied due to differences in scale of the reactions carried out and errors associated with smaller scale reactions. Entry 3 used 8mg of dihydroperoxide per millilitre of DCM and the yield obtained was the same as in entry 4, on the same scale. This result confirmed that the concentration of the starting dihydroperoxide does not affect the yield of tetraoxane obtained.

3.15. PMA-catalysed tetraoxane formation

This prompted us to search for a better method of tetraoxane synthesis. A procedure from 2011 by Yan *et al.*²⁸ used PMA catalyst for tetraoxane formation in DCM with MgSO₄ as the drying agent (**Scheme 8**). We next compared yields of tetraoxanes obtained from the Re₂O₇-catalysed method with those from the PMA-catalysed method (**Table 13**).



Entry	R ¹	R ²	Catalyst	DHP (eq.)	Yield (%)
1	-H 6	-CO ₂ Et 24	Re ₂ O ₇	1	43 33
2	-H 6	-CO ₂ Et 24	PMA	1	85 (lit. 91) 33
3	-H 6	-CO ₂ Et 24	PMA	2	73 33
4	-Ph- <i>p</i> -Br 50	-CO ₂ Et 24	Re ₂ O ₇	1	24 65
5	-Ph- <i>p</i> -Br 50	-CO ₂ Et 24	PMA	1	37 65
6	-Ph- <i>p</i> -Br 50	-CO ₂ Et 24	PMA	2	42 65
7	-Ph- <i>m</i> -CO ₂ Me 58	-H 23	Re ₂ O ₇	1	8 68
8	-Ph- <i>m</i> -CO ₂ Me 58	-H 23	PMA	1	14 68
9	-Ph- <i>m</i> -CO ₂ Me 58	-H 23	PMA	2	22 68

Table 13: Comparison of tetraoxane yields obtained with Re₂O₇ and PMA catalysts.

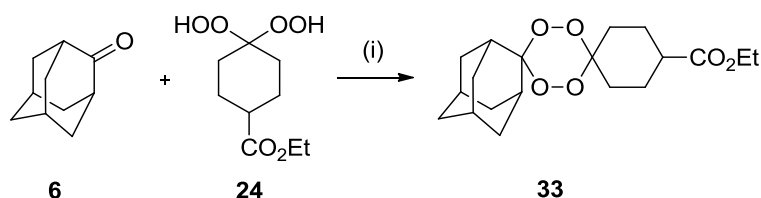
Entries 1, 4 and 7 are results from **Table 10**. Entries 2, 5 and 8 used 1 equivalent of dihydroperoxide, 1.2 equivalents of functionalised adamantanone and PMA catalyst in DCM with MgSO₄ as a drying agent. In all cases, the yields obtained from the PMA-catalysed reactions were far superior to those from the Re₂O₇-catalysed reactions and for entry 2; we managed to obtain a yield of 85%, which is very close to the literature yield of 91%.

Entries 3, 6 and 9 involved the same reaction conditions as before, but an excess of dihydroperoxide was used. When TLC analysis showed that the first equivalent had all reacted, a second equivalent was added. This was to compensate for any decomposition/dimerisation that had taken place with the first equivalent.

For entry 3, the use of excess dihydroperoxide caused a slight drop in tetraoxane yield but for entries 6 and 9, yields were increased slightly. However, the yields of the adamantyl-functionalised tetraoxanes were still not as high as desired because the Baeyer Villiger oxidation (though now somewhat suppressed compared with the Re₂O₇-catalysed reactions) was still taking place.

3.15.1. Solvent screening for PMA-catalysed tetraoxane formation

Having found that PMA was a better catalyst for tetraoxane formation than Re_2O_7 , we next decided to carry out a solvent screening with the aim of finding one that suppressed the Baeyer Villiger oxidation side reaction and produced equally high yields of the tetraoxane as when DCM is used (**Table 14**).



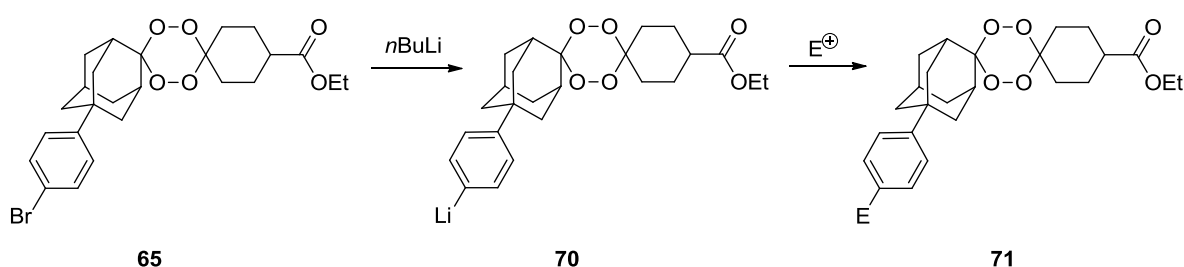
Entry	Solvent	Yield of tetraoxane 33 (%)
1	DCM	85
2	Et_2O	40
3	CHCl_3	30
4	MeOH	0
5	Toluene	40
6	DCM/Hexane (1:10)	50

Table 14: Solvent screening for PMA-catalysed tetraoxane formation. (i) PMA (2mol%), MgSO_4 (1.5eq), solvent, rt, 4hrs.

The results showed no correlation between yield and polarity of solvent. The huge difference between yields obtained in DCM and CHCl_3 (Entries 1 and 3) does not explain why one chlorinated solvent is preferred over the other. A mixture of solvent using a minimum amount of DCM in hexane (Entry 6) gave an intermediate yield, which also suggests that solvent polarity has no effect. These results are currently inconclusive and further work involving more solvents or solvent mixtures are required to determine if any trends can be seen.

3.16. Further transformations on adamantyl-functionalised tetraoxanes – organolithium chemistry

We continued our investigation by taking tetraoxane **65** and carrying out further transformations in an attempt to incorporate an amine group that could then be converted to a diazonium group for attachment to a carbon surface. We began our studies with organometallic chemistry. We envisaged that lithium-bromine exchange could be carried out on tetraoxane **65** (Scheme 27) and the resulting organolithium intermediate **70** could then be trapped out with a suitable electrophile to give the desired functionalised tetraoxane **71**.



Scheme 27: Lithium-bromine exchange with bromophenyl-functionalised tetraoxane **65**.

However, according to literature precedent, this chemistry has never been applied to tetraoxanes and there were a few issues regarding possible side reactions that needed to be addressed before continuing (**Figure 18**).

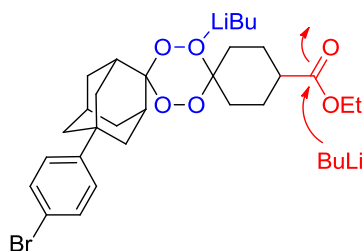
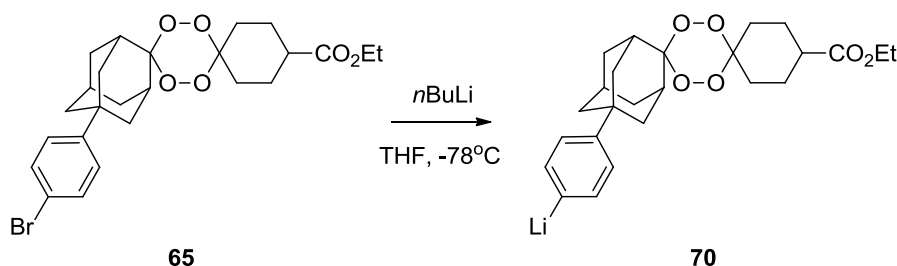


Figure 18: Possible side reactions when carrying out lithium-bromine exchange.

Firstly, it was not known whether the peroxide bond in the tetraoxane was stable to organolithiums and how likely it was for fragmentation to occur if lithium co-ordinated to the oxygen(s). Secondly, the ester group at the 4'-position of the cyclohexyl moiety could hinder lithium-bromine exchange by reacting with the organolithium reagent itself.

3.16.1. Experiments to determine stability of tetraoxane in the presence of *n*BuLi

Lithium-bromine exchange experiments were carried out on the bromophenyl-functionalised tetraoxane **65** in THF at -78°C using freshly titrated *n*BuLi and the reactions were monitored by TLC until no more starting material could be seen (**Table 15**).



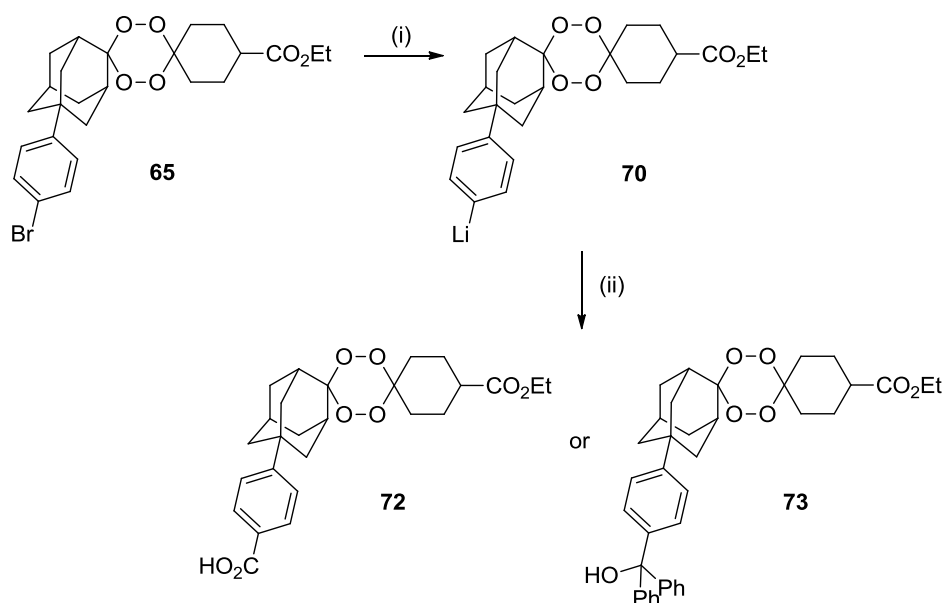
Entry	<i>n</i> BuLi (eq.)	Result of lithium-bromine exchange
1	1.0	Does not reach completion.
2	1.5	Does not reach completion.
3	2.0	Reaches completion but some fragmentation also seen.
4	3.0	Further fragmentation.

Table 15: Results from lithium-bromine exchange experiments using freshly titrated *n*BuLi.

There was great difficulty in finding the exact number of equivalents of *n*BuLi to use that would allow lithium-bromine exchange to reach completion but at the same time, would not cause any fragmentation to take place. However, it is important to note that in all cases, ^1H NMR spectra showed that the ester group on the tetraoxane remained intact, which confirmed that it does not interfere with lithium-bromine exchange and the reactivity of tetraoxanes towards organolithiums is affected by involvement of the peroxide bond.

3.16.2. Lithium-bromine exchange experiments involving electrophiles

We decided to use 2 equivalents of *n*BuLi in lithium-bromine exchange reactions that also involved electrophiles; CO_2 and benzophenone, to determine the extent to which the intermediate debrominated species **70** reacted (**Scheme 28**).



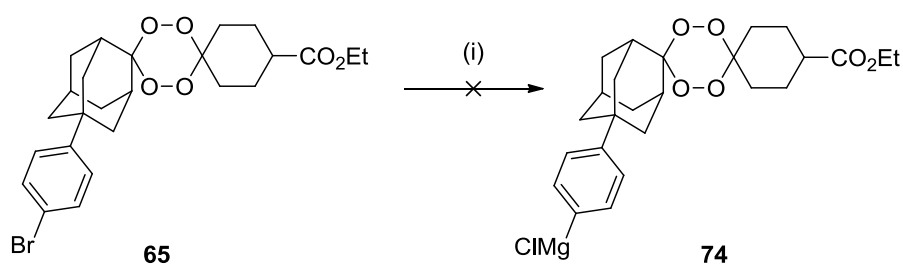
Scheme 28: Lithium-bromine exchange followed by reaction with electrophile. (i) $n\text{BuLi}$ (2eq), THF, -78°C , 20min, (ii) CO_2 (excess) or benzophenone (1 eq), -78°C , 45min, H^+ , 0%.

TLC analysis for both reactions showed that lithium-bromine exchange had gone to completion, but a lot of fragmentation had also occurred. Separation of the components by column chromatography allowed us to obtain mass spectra for each, which confirmed that no desired product was present. From these results, we concluded that:

1. The peroxide bond in the tetraoxane is (to some extent) co-ordinating to the organolithium and hindering/preventing lithium-bromine exchange from taking place.
2. $n\text{BuLi}$ is far too reactive to use in these experiments and could be forming polymeric aggregates, which would prevent lithium-bromine exchange from taking place.
3. Although $n\text{BuLi}$ was freshly titrated before use each time, the titres varied by more than 0.01M, which meant that the concentration was never known precisely. As a result of this, there was difficulty in finding the number of equivalents of $n\text{BuLi}$ required for lithium-bromine exchange without causing fragmentation of the tetraoxane, which suggests that a milder reagent should be used.
4. There was difficulty in finding a suitable electrophile to trap out the intermediate organolithium species with (if any of it had formed) under these reaction conditions.

3.16.3. Experiments using *i*PrMgCl in place of *n*BuLi

We next used chemistry developed by Knochel,⁴⁴ employing a Grignard reagent, *i*PrMgCl. This is a milder and less reactive reagent than *n*BuLi and we predicted that it would allow magnesium-bromine exchange to take place but not cause too much fragmentation of the tetraoxane. We performed two experiments, one at -78°C and another at room temperature. One equivalent of *i*PrMgCl was added to the tetraoxane and allowed to stir at the specified temperature for 2hrs with monitoring by TLC (**Scheme 29**).

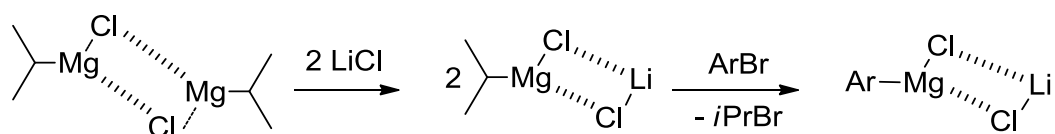


Scheme 29: Attempted magnesium-bromine exchange on tetraoxane **65**. (i) *i*PrMgCl (1eq), THF, -78°C or rt, 2hrs.⁴⁴

The results of these experiments showed that no reaction had taken place at either temperature. We assumed that *i*PrMgCl, being less reactive than *n*BuLi, may have either completely co-ordinated to the peroxide bridge of the tetraoxane or formed dimeric/polymeric aggregates and had not reacted at all.

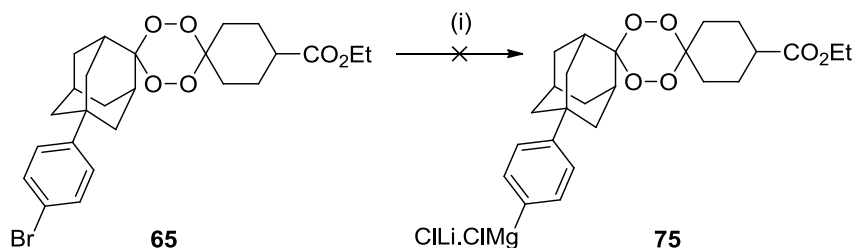
3.16.4. Experiment using a “TurboGrignard”: *i*PrMgCl.LiCl⁴⁴

Knochel had a solution to this problem of aggregation by using lithium salts. The Grignard reagent forms a complex with the lithium salt. This helps break up any aggregation and allows reaction with an electrophile to take place (**Scheme 30**). The resulting “TurboGrignard” is more reactive towards electrophiles than the standard Grignard reagent.



Scheme 30: Lithium chloride breaks up polymeric aggregates formed by Grignard reagent.

Magnesium-bromine exchange was attempted on tetraoxane **65** using the “TurboGrignard” (**Scheme 31**) but unfortunately, monitoring by TLC showed that no reaction had taken place.

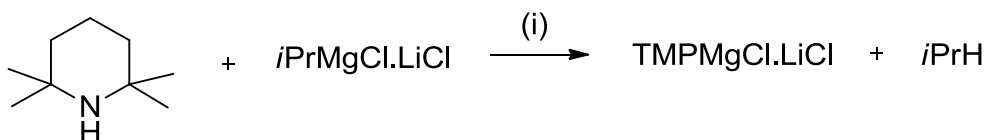


Scheme 31: Attempted magnesium-bromine exchange using the “TurboGrignard”. (i) $i\text{PrMgCl} \cdot \text{LiCl}$ (1eq), THF, -15°C , 20mins, 0%.

As it appeared that aggregation and co-ordination to the peroxide bond of the tetraoxane was the main cause of unsuccessful reactions, we predicted that a more hindered “TurboGrignard” reagent would solve both of these problems.

3.16.5. Experiment using a “TurboGrignard”: $\text{TMPMgCl} \cdot \text{LiCl}$ ⁴⁵

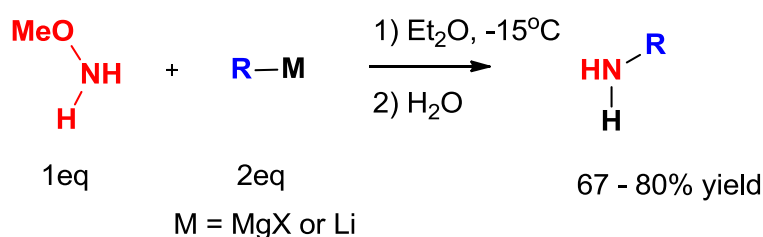
One of Knochel’s more hindered “TurboGrignard” reagents was synthesised from TMP and $i\text{PrMgCl} \cdot \text{LiCl}$ (**Scheme 32**). The “TurboGrignard” was then added to the tetraoxane **65** in THF and allowed to stir at room temperature. Once again, monitoring by TLC showed that no reaction had taken place after one day.



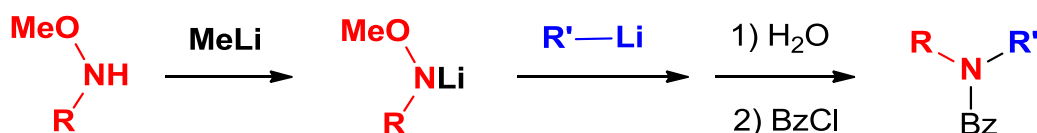
Scheme 32: Synthesis of $\text{TMPMgCl} \cdot \text{LiCl}$. (i) THF, rt, 24hrs.

3.17. Attempted electrophilic amination on bromophenyl-functionalised tetraoxane

Having had very little success in using organometallic chemistry to further functionalise our tetraoxane, we decided to try a different approach. The next method that was attempted to incorporate amine functionality in our tetraoxane was a modified electrophilic amination. This involved methoxyamine with organolithium compounds or Grignard reagents and was first developed by Schverdina and Kotscheschkow in 1938 then later modified by Beak and Kokko in the 1980s (**Schemes 33 and 34**).



Scheme 33: Electrophilic amination using methoxyamine and organometallic reagents.⁴⁶

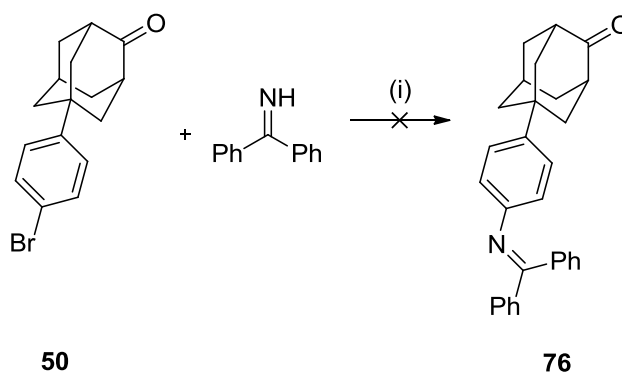


Scheme 34: Modified electrophilic amination.^{47, 48}

However, this was unsuccessful when the reaction was carried out using the bromophenyl-functionalised tetraoxane **65**. The reason for this was that only MeONH₂.HCl is commercially available and making the free-base was not achievable as the solvent required for the procedure was DCM, which has the same boiling point as MeONH₂ so separation of the two components would not have been possible. In an attempt to overcome this problem, two equivalents of *n*BuLi were added to MeONH₂.HCl in an attempt to “free-base” it to make the lithium-methoxyamine species *in situ* before addition of the tetraoxane. Regrettably, it remained insoluble in THF even after sonication so this was not investigated any further.

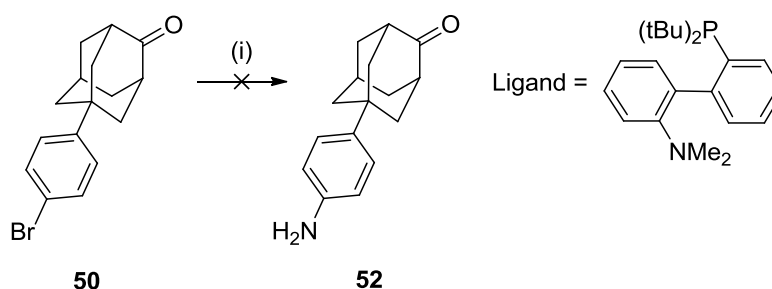
3.18. Attempted aminations using Pd chemistry

Having had no success with further transformations on the bromophenyl-tetraoxane, we decided to try and first functionalise the synthetically more accessible and higher yielding precursor, 5-(4-bromophenyl)adamantan-2-one then carry out tetraoxane formation afterwards. We began our investigation with Pd-catalysed aminations, developed by Buchwald. We first used benzophenone imine (**Scheme 35**) as a surrogate for ammonia. Benzophenone imine degraded on TLC, which initially gave the impression that the reaction had proceeded but NMR analysis confirmed that no reaction had taken place.



Scheme 35: Attempted amination of 5-(4-bromophenyl)adamantan-2-one **50** using benzophenone imine. (i) $\text{Pd}_2(\text{dba})_3$ (1mol%), NaO^tBu , BINAP, toluene, 80°C , 24hrs.⁴⁹

We next attempted an amination using ammonia (**Scheme 36**) but once again, only starting material was obtained.

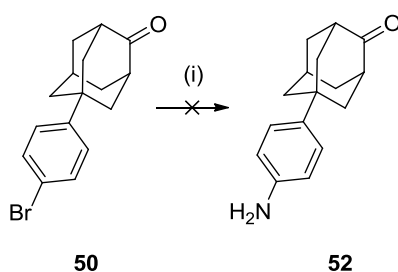


Scheme 36: Attempted amination of 5-(4-bromophenyl)adamantan-2-one **50**. (i) $\text{Pd}_2(\text{dba})_3$ (1mol%), Ligand (5mol%), 0.5M NH_3 in dioxane (5eq), NaO^tBu , 1,4-dioxane, 80°C , 24hrs.⁵⁰

Both reactions attempted used the literature conditions and they failed to work on our bulky substrate. It would have been very difficult (costly and time consuming) to find the optimal combination of Pd source, ligand, base, solvent and temperature that would allow our substrate to react in good yield so we decided not to pursue this any further.

3.19. Attempted amination using Cu₂O catalyst

We next attempted a copper-catalysed amination (**Scheme 37**) using aqueous ammonia. This did not proceed as expected because the mixture turned a blue colour, an indication that the copper catalyst had formed a tetra-amine complex, [Cu(NH₃)₄(H₂O)₂], rendering it inactive.

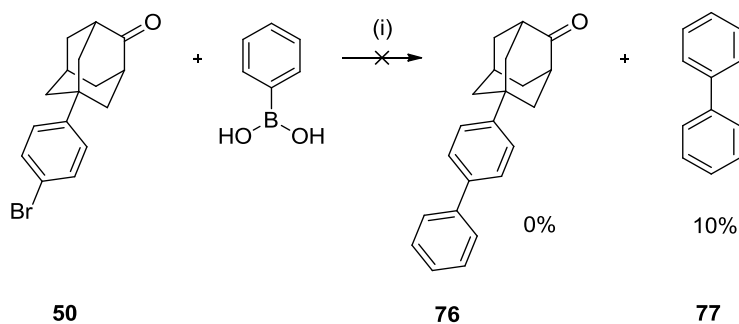


Scheme 37: Attempted Cu-catalysed amination of 5-(4-bromophenyl)adamantan-2-one **50**.

(i) aq. NH₃, Cu₂O (5mol%), 1:1 H₂O:NMP, 80°C, 24hrs.⁵¹

3.20. Attempted Suzuki cross coupling reaction

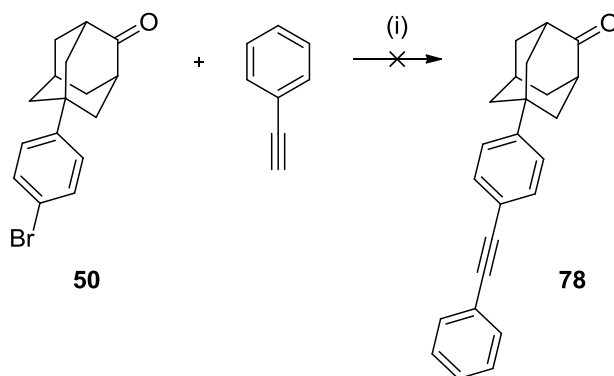
We next carried out a Suzuki cross coupling reaction on 5-(4-bromophenyl)adamantan-2-one using phenylboronic acid (**Scheme 38**). This reaction did not produce any desired product **76** and instead, 1,1'-biphenyl **77** was isolated in 10% yield with the majority of the starting ketone **50**.



Scheme 38: Attempted Suzuki cross coupling. (i) Pd(OAc)₂ (5mol%), K₂CO₃, acetone/water 10:1, 60°C, 4hrs, 0%.⁵²

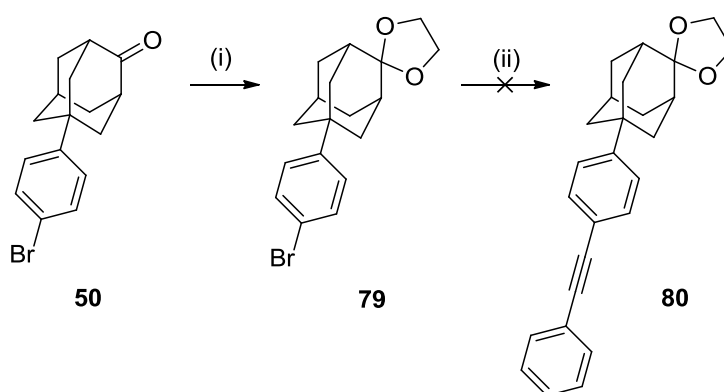
3.21. Attempted Sonogashira cross coupling reactions⁵³

We next attempted a Sonogashira cross coupling reaction on 5-(4-bromophenyl)adamantan-2-one **50** using phenylacetylene (**Scheme 39**). After leaving the reaction overnight, TLC analysis showed that only starting material was present.



Scheme 39: Attempted Sonogashira cross coupling. (i) $\text{PdCl}_2(\text{PPh}_3)_2$ (5mol%), CuI (3mol%), $i\text{Pr}_2\text{NH}$, 80°C , o/n.

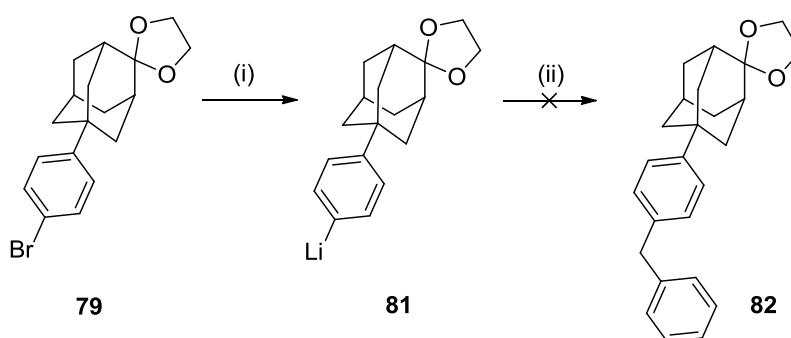
There was a possibility that the presence of the ketone was somewhat hindering the reaction. To confirm whether or not this was the case; we decided to protect the ketone to determine if the reaction gave the same result as above and indeed it did (**Scheme 40**). From this, we could conclude that it was not an electronic effect hindering the reaction and may possibly be due to steric bulk of the adamantyl skeleton.



Scheme 40: Protection of ketone followed by attempted Sonogashira coupling. (i) $p\text{-TSA}$ (10mol%), ethylene glycol, toluene, Δ Dean Stark, 24hrs, 89%. (ii) $\text{PdCl}_2(\text{PPh}_3)_2$ (5mol%), CuI (3mol%), $i\text{Pr}_2\text{NH}$, 80°C , o/n, 0%.

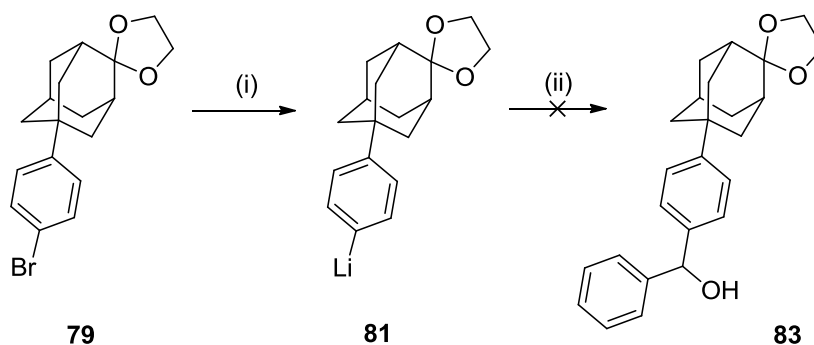
3.2.2. Attempted lithium-bromine exchange on 5-(4-bromophenyl)spiro[adamantane-2,2'-[1,3]dioxolane]

We next attempted lithium-bromine exchange on the protected ketone, 5-(4-bromophenyl)spiro[adamantane-2,2'-[1,3]dioxolane] **79** using one equivalent of *n*BuLi and trapped out the organolithium intermediate using benzyl bromide (**Scheme 41**). Mass spectrometry confirmed that this reaction was unsuccessful. It was assumed that benzyl bromide was not a good enough electrophile to use in this reaction.



Scheme 41: Attempted lithium-bromine exchange and subsequent trapping with benzyl bromide. (i) *n*BuLi (1eq), -78°C, 30mins. (ii) Benzyl bromide (1eq), -78°C, 30mins, 0%.

We carried out lithium-bromine exchange again using freshly distilled benzaldehyde (more reactive than benzyl bromide) as the electrophile (**Scheme 42**). However, mass spectrometry confirmed that this reaction had also failed to give any desired product.

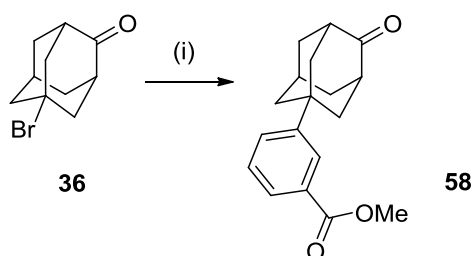


Scheme 42: Attempted lithium-bromine exchange and subsequent trapping with benzaldehyde. (i) *n*BuLi (1eq), -78°C, 30mins. (ii) Benzaldehyde (1eq), -78°C, 30mins, 0%.

3.23. Synthesis of tetraoxanes with meta-substituted aromatic rings

Having had no success in carrying out further transformations on the bromophenyl-tetraoxane **65** and 5-(4-bromophenyl)adamantan-2-one **50**, we decided to not continue with these substrates and use a different functionalised adamantanone from our Friedel Crafts optimisation reactions.

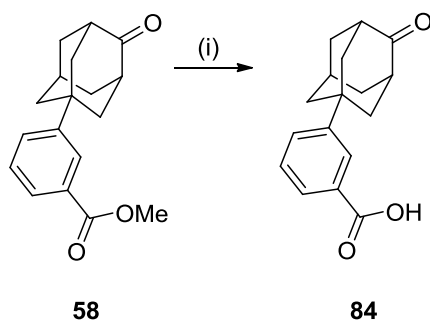
We envisaged that the optimal choice was methyl 3-(4-oxoadamantan-1-yl)benzoate **58**. As this possessed an ester group on the meta-position of the aromatic ring, we predicted that there would not be a great deal of difference in terms of steric crowding compared with having functionality at the para-position. This would also solve the problem of obtaining functionalised adamantanones as inseparable mixtures of ortho/para isomers and avoid the use of organometallic or palladium chemistry for further functionalisation. As ester groups are strongly deactivating, the Friedel Crafts arylation of 5-bromo-2-adamantanone **36** with methyl benzoate required longer reaction times and higher temperatures than its electron rich counterparts. The yields also tended to vary on repetition (**Scheme 43**).



Scheme 43: Friedel Crafts arylation of 5-bromo-2-adamantan-2-one **36** using methyl benzoate.

(i) FeCl₃ (1.5eq), PhCO₂Me, 170°C, 3 days, 45-65%.

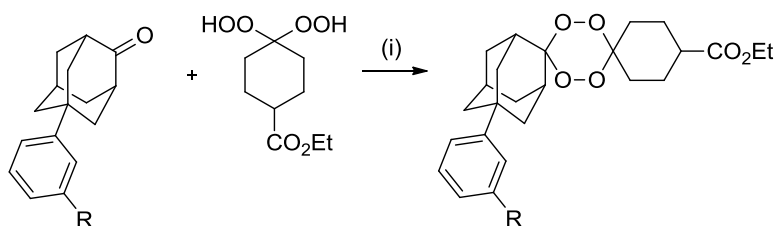
We next carried out base hydrolysis of the ester to give the corresponding carboxylic acid **84** (**Scheme 44**). This opened up the possibility of an amide coupling reaction with phenylenediamine. The product from this could then be used in tetraoxane formation and subsequent synthesis of the aryl diazonium (or vice versa) would generate a suitable compound for binding to a carbon surface.



Scheme 44: Base hydrolysis of methyl 3-(4-oxoadamantan-1-yl)benzoate. (i) 15% aq. NaOH, MeOH, 65°C, 6hrs, H⁺, 66%.

3.23.1. Tetraoxane formation using adamantanones bearing meta-substituted aromatic rings

Tetraoxane formation using adamantanone derivatives **58** and **84** was carried out (Table 16).



Entry	R =	Yield (%)
1	-CO ₂ Me 58	14 67
2	-CO ₂ H 84	73 (inseparable mixture with SM) 85

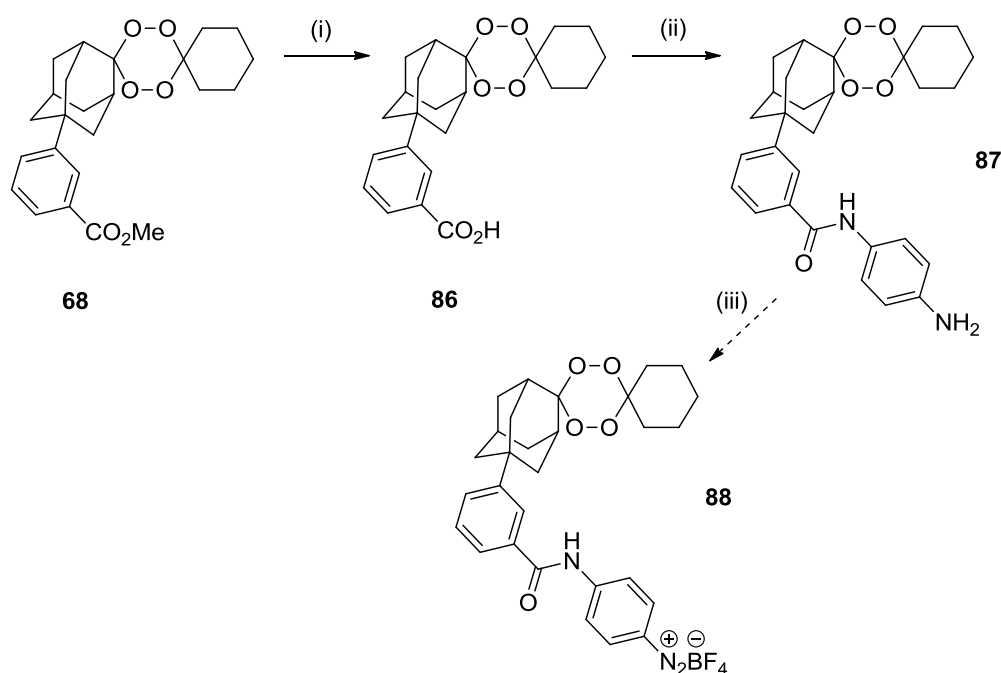
Table 16: Synthesis of functionalised tetraoxanes. (i) Re₂O₇ (6mol%), DCM, rt, 4hrs.

We used the dihydroperoxide bearing an ethyl ester as we anticipated that it could be later hydrolysed to a carboxylic acid, making the tetraoxane more soluble in aqueous conditions when used in experiments with *Geobacter*. Entry 1 showed that tetraoxane formation took place but only in 14% yield. When the functional group was a carboxylic acid (Entry 2), tetraoxane formation took place (confirmed by mass spectrometry) but it could only be isolated as an inseparable mixture with the carboxylic acid starting material **84**. The ratio of these could not be determined by ¹H NMR.

As we were unable to selectively hydrolyse the methyl ester in the presence of the ethyl ester in the tetraoxane formed in entry 1, we decided to continue our investigation with the tetraoxane that had no functionality on the cyclohexyl moiety **68** (Entry 7, **Table 10** earlier). This meant that we could not incorporate a carboxylic acid group for solubility purposes but we first wanted to establish whether or not further transformations could be carried out on tetraoxanes without fragmentation taking place. As the trioxolanes synthesised by the O'Neil group (chapter 2) did not have any functionality on the cyclohexyl moiety and were used successfully in heme alkylation experiments, we were positive that this would also be the case for tetraoxanes.

3.23.2. Ester hydrolysis and subsequent amide coupling to incorporate a NH₂ group

With the intention of making a tetraoxane functionalised with a diazonium, ester hydrolysis and subsequent amide coupling was carried out on tetraoxane **68** (**Scheme 45**).

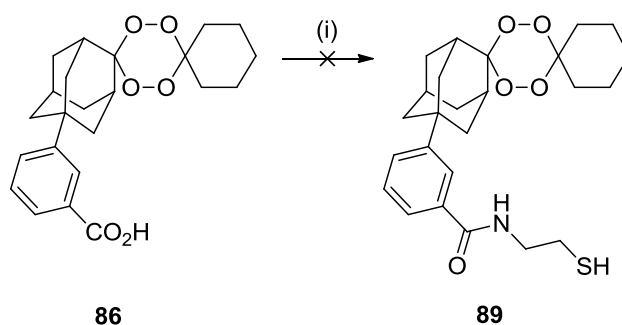


Scheme 45: Further functionalisation on tetraoxane **68**. (i) aq. NaOH, MeOH, 65°C, 4hrs, H₃O⁺, 100%. (ii) EDC.HCl (1.2eq), NMM (2.5eq), HOBT (1.2eq), DMF, 0°C, 24hrs, *p*-phenylenediamine (1eq), rt, 24hrs, 12%. (iii) [NO][BF₄] (1eq), DCM, 0°C, o/n.

The amide coupling (step (ii)) did not give a very good yield. These were conditions that had previously been used for amide coupling with a trioxolane functionalised with a carboxylic acid group at the 5-position of the adamantane moiety.⁵⁴ The tetraoxane bearing the carboxylic acid on an aromatic ring may have hindered this reaction to some degree. Only 4mg of the coupled tetraoxane product was isolated, which made it difficult to characterise by NMR as the sample was very dilute and hence gave very weak signals in the spectrum. However, mass spectrometry confirmed that it had been synthesised successfully with a molecular ion peak at 513.2 $[M+Na]^+$.

3.23.3. Attempted amide coupling to incorporate a thiol group

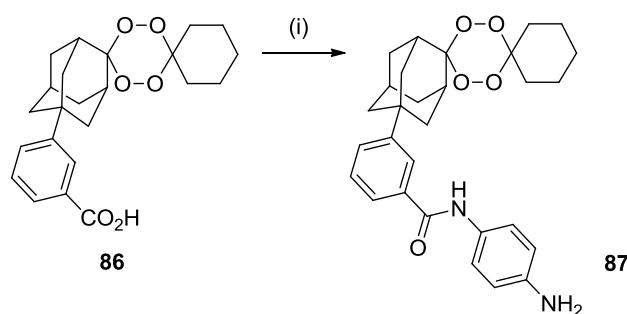
We also attempted amide coupling with the acid-functionalised tetraoxane **86** using cysteamine hydrochloride, which would incorporate a thiol group that is capable of binding to a gold surface (**Scheme 46**). However, this reaction failed to give any desired product. We concluded that the conditions used for the amide coupling required further optimisation.



Scheme 46: Attempted amide coupling with cysteamine hydrochloride. (i) EDC.HCl (1.2eq), NMM (2.5eq), HOBt (1.2eq), DMF, 0°C-rt, o/n, HSCH₂CH₂NH₃Cl (1eq), rt, o/n, 0%.

3.23.4. Solvent screening for amide coupling on tetraoxane

We next carried out a solvent screen (**Scheme 47** and **Table 17**) in an attempt to find a better solvent for the amide coupling reaction.

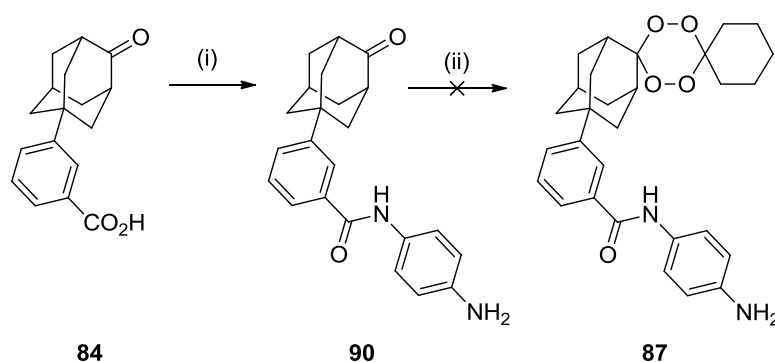


Scheme 47: Amide coupling on tetraoxane. (i) EDC.HCl (1.2eq), NMM (2.5eq), HOBT (1.2eq), DMF, 0°C, 24hrs, *p*-phenylenediamine (1eq), rt, 24hrs.

Entry	Solvent	Yield (%)
1	DCM	12
2	DMF	0
3	Water	0

Table 17: Solvent screen for amide coupling.

As the reaction was unsuccessful in both DMF and water, we decided to “reverse” the steps by carrying out amide coupling with the acid-functionalised adamantanone **84** first followed by tetraoxane formation with the product **90** (**Scheme 48**).



Scheme 48: Amide coupling on carboxylic acid-functionalised adamantanone **84** and subsequent tetraoxane formation. (i) EDC.HCl (1.2eq), NMM (2.5eq), HOBT (1.2eq), DMF, 0°C, 24hrs, *p*-phenylenediamine (1eq), rt, 24hrs, 34%. (ii) PMA (18mol%), 1,1-dihydroperoxycyclohexane (2eq), MgSO₄ (2eq), DCM, rt, 4hrs, 0%.

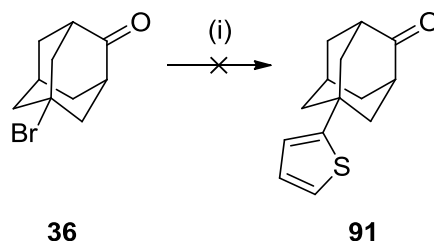
The amide coupling step gave a higher yield of 34% when performed on the acid-functionalised adamantanone **84** compared with the acid-functionalised tetraoxane **86**. Unfortunately, the amide coupled product **90** failed to react in the tetraoxane formation step and we believe the reason for this was its steric bulk.

3.24. Synthesis of adamantanones functionalised with thiophene and thiophene derivatives

Having had little success with synthesising tetraoxanes functionalised with benzene derivatives, we then explored other aromatic compounds that could replace benzene but were still electrically conductive. We next turned our attention to thiophene because it is less aromatic and in theory, should be more reactive than benzene.

3.24.1. Attempted synthesis of adamantanone functionalised with thiophene

Our investigation began with using thiophene in the optimised Friedel Crafts arylation (**Scheme 49**). We envisaged that the thiophene ring could be functionalised by selective deprotonation at the 5-position using *n*BuLi, followed by addition of a suitable electrophile.

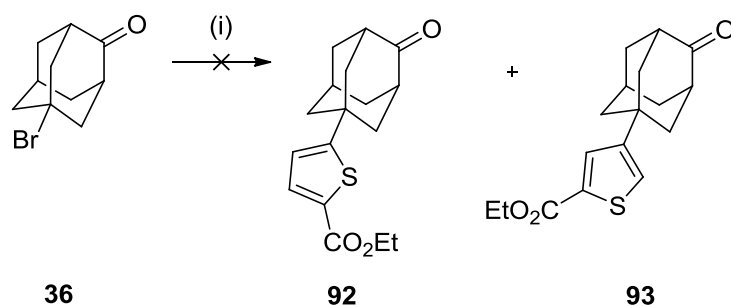


Scheme 49: Attempted Friedel Crafts arylation of 5-bromo-2-adamantanone **36** using thiophene. (i) FeCl₃ (1.5eq), thiophene, 75°C, 20hrs, 0%.

Mass spectrometry for the compound isolated from this reaction showed a molecular ion peak that was 50 mass units higher than the expected mass. This did not agree with the expected mass for when the adamantanone is functionalised with a thiophene dimer. We do not yet have an explanation for this result.

3.24.2. Attempted synthesis of adamantanone functionalised with ethyl 2-thiophenecarboxylate

We next attempted Friedel Crafts arylation using ethyl 2-thiophenecarboxylate (Scheme 50). We anticipated that a pre-functionalised thiophene would give a product that was more readily ionised and hence easier to characterise by mass spectrometry.



Scheme 50: Attempted Friedel Crafts arylation of 5-bromo-2-adamantanone **36** using ethyl 2-thiophenecarboxylate as the solvent for reaction. (i) FeCl_3 (1.5eq), ethyl 2-thiophenecarboxylate, 80°C , 20hrs, 0%.

^1H NMR for the compound isolated from this reaction showed that there was a mixture of isomers and TLC showed that they both had the same R_f . However, mass spectrometry showed a molecular ion peak that was 30 mass units higher than the expected mass. We do not yet have an explanation for this result.

3.25. Conclusions and Further Work

In summary, the synthesis and optimisation of many novel 5-functionalised 2-adamantanones has been achieved using liquid aryl substrates possessing high boiling points. Further study in finding a suitable solvent for this reaction to allow the use of solid aryl substrates is still required.

The Baeyer Villiger oxidation side reaction in the tetraoxane formation step has been somewhat suppressed after optimisation of the conditions (PMA Vs. Re_2O_7) used for tetraoxane formation. However, tetraoxane yields are still not satisfactory so an extensive solvent screen for this reaction is required to find a suitable solvent/mixture of solvents that would, ideally, prevent the Baeyer Villiger oxidation from taking place. Many novel tetraoxanes bearing different functional groups on the adamantyl moiety have been successfully synthesised. The antimalarial activity of these could also be tested because to date; no adamantyl-functionalised tetraoxanes have been reported in the literature. It would be interesting to determine whether or not they have superior activity to those synthesised by the O'Neill group, where they only have functionality on the cyclohexyl moiety.

The synthesis of a tetraoxane with suitable functionality for aryl diazonium formation has been achieved but only in 12% yield and this provided enough material for characterisation only. Optimisation of the conditions for the amide coupling step is required as it appears that these conditions only work well for aliphatic carboxylic acids (trioxolane **12**) but not aromatic carboxylic acids (tetraoxane **86**). An alternative method would be to use the corresponding acid chloride (more reactive) instead of the carboxylic acid in the amide coupling step but the stability of the tetraoxane in the presence of reagents such as SOCl_2 needs to be determined.

Once a robust synthetic route has been found, these bi-functional tetraoxane molecular wires can be used in heme alkylation experiments involving *Geobacter* and the results from these can be compared with the trioxolane molecular wires.

3.26. Bibliography

1. Harding, M. J. C.; Whalen, D. M., Synthesis of hexadecanolide. *Industrial & Engineering Chemistry Product Research and Development* **1975**, *14* (4), 232-239.
2. Ellis, G. L.; Amewu, R.; Sabbani, S.; Stocks, P. A.; Shone, A.; Stanford, D.; Gibbons, P.; Davies, J.; Vivas, L.; Charnaud, S.; Bongard, E.; Hall, C.; Rimmer, K.; Lozanom, S.; Jesus, M.; Gargallo, D.; Ward, S. A.; O'Neill, P. M., Two-step synthesis of achiral dispiro-1,2,4,5-tetraoxanes with outstanding antimalarial activity, low toxicity, and high-stability profiles. *J. Med. Chem.* **2008**, *51* (7), 2170-2177.
3. O'Neill, P. M.; Amewu, R. K.; Nixon, G. L.; ElGarah, F. B.; Mungthin, M.; Chadwick, J.; Shone, A. E.; Vivas, L.; Lander, H.; Barton, V.; Muangnoicharoen, S.; Bray, P. G.; Davies, J.; Park, B. K.; Wittlin, S.; Brun, R.; Preschel, M.; Zhang, K. S.; Ward, S. A., Identification of a 1,2,4,5-Tetraoxane Antimalarial Drug-Development Candidate (RKA 182) with Superior Properties to the Semisynthetic Artemisinins. *Angew. Chem.-Int. Edit.* **2010**, *49* (33), 5693-5697.
4. Vennerstrom, J. L.; Fu, H. N.; Ellis, W. Y.; Ager, A. L.; Wood, J. K.; Andersen, S. L.; Gerena, L.; Milhous, W. K., Dispiro-1,2,4,5-tetraoxanes - a new class of antimalarial peroxides. *J. Med. Chem.* **1992**, *35* (16), 3023-3027.
5. Vennerstrom, J. L.; Ager, A. L.; Andersen, S. L.; Grace, J. M.; Wongpanich, V.; Angerhofer, C. K.; Hu, J. K.; Wesche, D. L., Assessment of the antimalarial potential of tetraoxane WR 148999. *Am. J. Trop. Med. Hyg.* **2000**, *62* (5), 573-578.
6. Amewu, R.; Stachulski, A. V.; Ward, S. A.; Berry, N. G.; Bray, P. G.; Davies, J.; Labat, G.; Vivas, L.; O'Neill, P. M., Design and synthesis of orally active dispiro 1,2,4,5-tetraoxanes; synthetic antimalarials with superior activity to artemisinin. *Org. Biomol. Chem.* **2006**, *4* (24), 4431-4436.
7. Bousejra-El Garah, F.; Wong, M. H. L.; Amewu, R. K.; Muangnoicharoen, S.; Maggs, J. L.; Stigliani, J. L.; Park, B. K.; Chadwick, J.; Ward, S. A.; O'Neill, P. M., Comparison of the Reactivity of Antimalarial 1,2,4,5-Tetraoxanes with 1,2,4-Trioxolanes in the Presence of Ferrous Iron Salts, Heme, and Ferrous Iron Salts/Phosphatidylcholine. *J. Med. Chem.* **2011**, *54* (19), 6443-6455.
8. Marti, F.; Chadwick, J.; Amewu, R. K.; Burrell-Saward, H.; Srivastava, A.; Ward, S. A.; Sharma, R.; Berry, N.; O'Neill, P. M., Second generation analogues of RKA182: synthetic tetraoxanes with outstanding in vitro and in vivo antimalarial activities. *MedChemComm* **2011**, *2* (7), 661-665.
9. Jensen, P. S.; Chi, Q.; Grumsen, F. B.; Abad, J. M.; Horsewell, A.; Schiffrin, D. J.; Ulstrup, J., Gold nanoparticle assisted assembly of a heme protein for enhancement of long-range interfacial electron transfer. *J. Phys. Chem. C* **2007**, *111* (16), 6124-6132.
10. Evrard, D.; Lambert, F.; Policar, C.; Balland, V.; Limoges, B., Electrochemical Functionalization of Carbon Surfaces by Aromatic Azide or Alkyne Molecules: A Versatile Platform for Click Chemistry. *Chem.-Eur. J.* **2008**, *14* (30), 9286-9291.
11. Bousejra-El Garah, F.; Pitie, M.; Vendier, L.; Meunier, B.; Robert, A., Alkylating ability of artemisinin after Cu(I)-induced activation. *J. Biol. Inorg. Chem.* **2009**, *14* (4), 601-610.

12. Pinson, J.; Podvorica, F., Attachment of organic layers to conductive or semiconductive surfaces by reduction of diazonium salts. *Chem. Soc. Rev.* **2005**, *34* (5), 429-439.
13. Delamar, M.; Hitmi, R.; Pinson, J.; Saveant, J. M., Covalent modification of carbon surfaces by grafting functionalized aryl radicals produced from electrochemical reduction of diazonium salts. *J. Am. Chem. Soc.* **1992**, *114* (14), 5883-5884.
14. Toupin, M.; Belanger, D., Spontaneous functionalization of carbon black by reaction with 4-nitrophenyldiazonium cations. *Langmuir* **2008**, *24* (5), 1910-1917.
15. Haiss, W.; Nichols, R. J.; Higgins, S. J.; Bethell, D.; Hobenreich, H.; Schiffrin, D. J., Wiring nanoparticles with redox molecules. *Faraday Discuss.* **2004**, *125*, 179-194.
16. Dong, Y., Synthesis and Antimalarial Activity of 1,2,4,5-Tetraoxanes. *Mini Reviews in Medicinal Chemistry* **2002**, *2*, 113-123.
17. Terent'ev, A. O.; Kutkin, A. V.; Starikova, Z. A.; Antipin, M. Y.; Ogibin, Y. N.; Nikishina, G. I., New preparation of 1,2,4,5-tetraoxanes. *Synthesis* **2004**, (14), 2356-2366.
18. Hamada, Y.; Tokuhara, H.; Masuyama, A.; Nojima, M.; Kim, H. S.; Ono, K.; Ogura, N.; Wataya, Y., Synthesis and notable antimalarial activity of acyclic peroxides, 1-(alkyldioxy)-1-(methyldioxy)cyclododecanes. *J. Med. Chem.* **2002**, *45* (6), 1374-1378.
19. Kim, H. S.; Nagai, Y.; Ono, K.; Begum, K.; Wataya, Y.; Hamada, Y.; Tsuchiya, K.; Masuyama, A.; Nojima, M.; McCullough, K. J., Synthesis and antimalarial activity of novel medium-sized 1,2,4,5-tetraoxacycloalkanes. *J. Med. Chem.* **2001**, *44* (14), 2357-2361.
20. Jakka, K.; Liu, J. Y.; Zhao, C. G., Facile epoxidation of alpha,beta-unsaturated ketones with cyclohexylidenebishydroperoxide. *Tetrahedron Lett.* **2007**, *48* (8), 1395-1398.
21. Selvam, J. J. P.; Suresh, V.; Rajesh, K.; Babu, D. C.; Suryakiran, N.; Venkateswarlu, Y., A novel rapid sulfoxidation of sulfides with cyclohexylidenebishydroperoxide. *Tetrahedron Lett.* **2008**, *49* (21), 3463-3465.
22. Terent'ev, A. O.; Platonov, M. M.; Kutkin, A. V., A new oxidation process. Transformation of gem-bishydroperoxides into esters. *Cent. Eur. J. Chem* **2006**, *4* (2), 207-215.
23. Zmitek, K.; Zupan, M.; Stavber, S.; Iskra, J., Iodine as a catalyst for efficient conversion of ketones to gem-dihydroperoxides by aqueous hydrogen peroxide. *Org. Lett.* **2006**, *8* (12), 2491-2494.
24. Das, B.; Krishnaiah, M.; Veeranjanyulu, B.; Ravikanth, B., A simple and efficient synthesis of gem-dihydroperoxides from ketones using aqueous hydrogen peroxide and catalytic ceric ammonium nitrate. *Tetrahedron Lett.* **2007**, *48* (36), 6286-6289.
25. Li, Y.; Hao, H. D.; Zhang, Q.; Wu, Y. K., A Broadly Applicable Mild Method for the Synthesis of gem-Diperoxides from Corresponding Ketones or 1,3-Dioxolanes. *Org. Lett.* **2009**, *11* (7), 1615-1618.
26. Terent'ev, A. O.; Krivykh, O. B.; Krylov, I. B.; Ogibin, Y. N.; Nikishin, G. I., A new property of geminal bishydroperoxides: Hydrolysis with the removal of hydroperoxide groups to form a ketone. *Russ. J. Gen. Chem.* **2010**, *80* (8), 1667-1671.

27. Ghorai, P.; Dussault, P. H., Broadly Applicable Synthesis of-1,2,4,5-Tetraoxanes. *Org. Lett.* **2009**, *11* (1), 213-216.
28. Yan, X.; Chen, J. L.; Zhu, Y. T.; Qiao, C. H., Phosphomolybdic Acid Catalyzed Synthesis of 1,2,4,5-Tetraoxanes. *Synlett* **2011**, (19), 2827-2830.
29. Ghorai, P.; Dussault, P. H., Mild and Efficient Re(VII)-Catalyzed Synthesis of 1,1-Dihydroperoxides. *Org. Lett.* **2008**, *10* (20), 4577-4579.
30. Yoon, N. M.; Pak, C. S.; Brown, H. C.; Krishnam.S; Stocky, T. P., Selective reductions. 19. Rapid reaction of carboxylic acids with borane-tetrahydrofuran - remarkably convenient procedure for selective conversion of carboxylic acids to corresponding alcohols in presence of other functional groups. *J. Org. Chem.* **1973**, *38* (16), 2786-2792.
31. Hutchinson, J. H.; Li, D. L. F.; Money, T.; Palme, M.; Agharahimi, M. R.; Albizati, K. F., Stereoselectivity of C(3) methylation and aldol condensation of camphor and derivatives. *Can. J. Chem.-Rev. Can. Chim.* **1991**, *69* (3), 558-566.
32. Stetter, H.; Wulff, C.; Weber, J., Uber verbindungen mit urotropin-struktur 31. Herstellung von derivaten des 1-phenyl-adamantans. *Chem. Ber.-Recl.* **1964**, *97* (12), 3488-3492.
33. Kantam, M. L.; Srinivas, P.; Yadav, J.; Likhar, P. R.; Bhargava, S., Trifunctional N,N,O-Terdentate Amido/Pyridyl Carboxylate Ligated Pd(II) Complexes for Heck and Suzuki Reactions. *J. Org. Chem.* **2009**, *74* (13), 4882-4885.
34. Brase, S.; Waegell, B.; de Meijere, A., Palladium-catalyzed coupling reactions of 1-bromoadamantane with styrenes and arenes. *Synthesis* **1998**, (2), 148-152.
35. Wang, N.; Wang, R. H.; Shi, X.; Zou, G., Ion-exchange-resin-catalyzed adamantylation of phenol derivatives with adamantanol: Developing a clean process for synthesis of 2-(1-adamantyl)-4-bromophenol, a key intermediate of adapalene. *Beilstein J. Org. Chem.* **2012**, *8*, 227-233.
36. Su, Y. C.; Chen, W. C.; Chang, F. C., Investigation of the thermal properties of novel adamantane-modified polybenzoxazine. *J. Appl. Polym. Sci.* **2004**, *94* (3), 932-940.
37. Geluk, H. W.; Schlatma, J. I., Hydride transfer reactions of adamantyl cation. I. A new and convenient synthesis of adamantanone. *Tetrahedron* **1968**, *24* (15), 5361-5368.
38. Geluk, H. W.; Keizer, V. G., Adamantanone. *Organic Syntheses* **1973**, *53*, 8.
39. Geluk, H. W., Improved synthesis of 1,4-disubstituted adamantanes. *Synthesis-International Journal of Methods in Synthetic Organic Chemistry* **1972**, (7), 374-375.
40. Wagner, G.; Knoll, W.; Bobek, M. M.; Brecker, L.; van Herwijnen, H. W. G.; Brinker, U. H., Structure-Reactivity Relationships: Reactions of a 5-Substituted Aziadamantane in a Resorcin[4]arene-based Cavitand. *Org. Lett.* **2010**, *12* (2), 332-335.
41. Guggenheim, T. L., Protection of substituted anilines with 1,1,4,4-tetramethyl-1,4-bis(N,N-dimethylamino)disilethylene. *Tetrahedron Lett.* **1984**, *25* (12), 1253-1254.
42. Stepakov, A. V.; Molchanov, A. P.; Kostikov, R. R., Alkylation of aromatic compounds with adamantan-1-ol. *Russ. J. Organ. Chem.* **2007**, *43* (4), 538-543.
43. Merck Patent, WO 2007/113634, PCT/IB2007/000830. 2007.

44. Krasovskiy, A.; Knochel, P., A LiCl-mediated Br/Mg exchange reaction for the preparation of functionalized aryl- and heteroarylmagnesium compounds from organic bromides. *Angew. Chem.-Int. Edit.* **2004**, 43 (25), 3333-3336.
45. Krasovskiy, A.; Krasovskaya, V.; Knochel, P., Mixed Mg/Li amides of the type R₂NMgCl center dot LiCl as highly efficient bases for the regioselective generation of functionalized aryl and heteroaryl magnesium compounds. *Angew. Chem.-Int. Edit.* **2006**, 45 (18), 2958-2961.
46. Schverdina, N. I.; Kotscheschkow, Z. J., *Journal of General Chemistry USSR* **1938**, 8, 1825.
47. Beak, P.; Kokko, B. J., A modification of the Sheverdina-Kocheshkov amination - the use of methoxyamine-methylolithium as a convenient synthetic equivalent for NH₂⁺. *J. Org. Chem.* **1982**, 47 (14), 2822-2823.
48. Kokko, B. J.; Beak, P., The electrophilic amination of organolithiums with methylolithium complexes of N-substituted methoxyamines. *Tetrahedron Lett.* **1983**, 24 (6), 561-564.
49. Wolfe, J. P.; Ahman, J.; Sadighi, J. P.; Singer, R. A.; Buchwald, S. L., An ammonia equivalent for the palladium-catalyzed amination of aryl halides and triflates. *Tetrahedron Lett.* **1997**, 38 (36), 6367-6370.
50. Surry, D. S.; Buchwald, S. L., Selective palladium-catalyzed arylation of ammonia: Synthesis of anilines as well as symmetrical and unsymmetrical Di- and triarylamines. *J. Am. Chem. Soc.* **2007**, 129 (34), 10354.
51. Xu, H. H.; Wolf, C., Efficient copper-catalyzed coupling of aryl chlorides, bromides and iodides with aqueous ammonia. *Chem. Commun.* **2009**, (21), 3035-3037.
52. Miyaura, N.; Suzuki, A., Palladium-catalyzed cross-coupling reactions of organoboron compounds. *Chem. Rev.* **1995**, 95 (7), 2457-2483.
53. Sonogashira Coupling.
<http://www.organic-chemistry.org/namedreactions/sonogashira-coupling.shtm>.
54. Barton, V. PhD Thesis "Design and synthesis of activity based probes to investigate the biological target(s) of the endoperoxide antimalarials". University of Liverpool, **2009**.

Chapter 4

Synthesis of β -turn mimetics and chiral enamine N-oxides

This chapter contains a separate numbering system for all schemes, figures and references. Numbering of compounds has continued from chapter 3.

4.1. Introduction to amino acids and proteins

Amino acids play central roles both as building blocks of proteins and as intermediates in metabolism. They have a unique chemical structure with a backbone consisting of $\text{H}_2\text{N}-\text{CRH}-\text{CO}_2\text{H}$ where R is a side group. There are 20 genetically coded amino acids in nature i.e. 20 R groups and they can exist as two enantiomers at the α -centre, *D* and *L*; all conveying a vast array of chemical versatility. The *L* enantiomer appears in nature and is easily distinguished from the *D* enantiomer as it possesses an up-facing R group.

4.1.1. Primary structure of proteins

The precise amino acid content, and the sequence of those amino acids, of a specific protein, is determined by the sequence of the bases in the gene that encodes that protein to give the primary structure. The chemical properties of the amino acids of proteins determine the biological activity of the protein. In addition, proteins contain within their amino acid sequences the necessary information to determine how that protein will fold into a 3D structure, and the stability of the resulting structure. The field of protein folding and stability has been a critically important area of research for years, and remains today one of the great unsolved mysteries.¹

4.1.2. Secondary structure of proteins: α -helix and β -sheet

The secondary structure is the specific geometric shape caused by intramolecular and intermolecular hydrogen bonding of primarily amide groups.² There are two main secondary structures of proteins in nature; α -helices and β -sheets.

In the α -helix, the polypeptide chain is coiled tightly like a spring. The backbone of the peptide forms the inner part of the coil while the side chains (R groups) extend outward from the coil. The helix is stabilized by hydrogen bonding between the N-H of one amino acid and the C=O on the 4th amino acid away from it. One "turn" of the coil requires 3.6 amino acid units.² The helix can be either right-handed or left-handed in the sense of threads on a screw. The naturally occurring α -helices found in proteins are all right-handed.

In the β -pleated sheet, individual protein chains are aligned side-by-side with every other protein chain aligned in an opposite direction. The protein chains are held together by intermolecular hydrogen bonding between amide groups of two separate chains. The hydrogen on the amide of one protein chain is hydrogen bonded to the amide oxygen of the neighbouring protein chain. The pleated sheet effect arises from the fact that the amide structure is planar while the "bends" occur at the carbon containing the side chain.

β -sheets come in two forms as the chains can run anti-parallel or parallel to one another (**Figure 1**). In both of these, there is an average of one hydrogen bond for each pair of amino acid residues and both require a "turn". The parallel turn is much longer than the anti-parallel turn and the anti-parallel turns are known as β -turns or "reverse" turns.

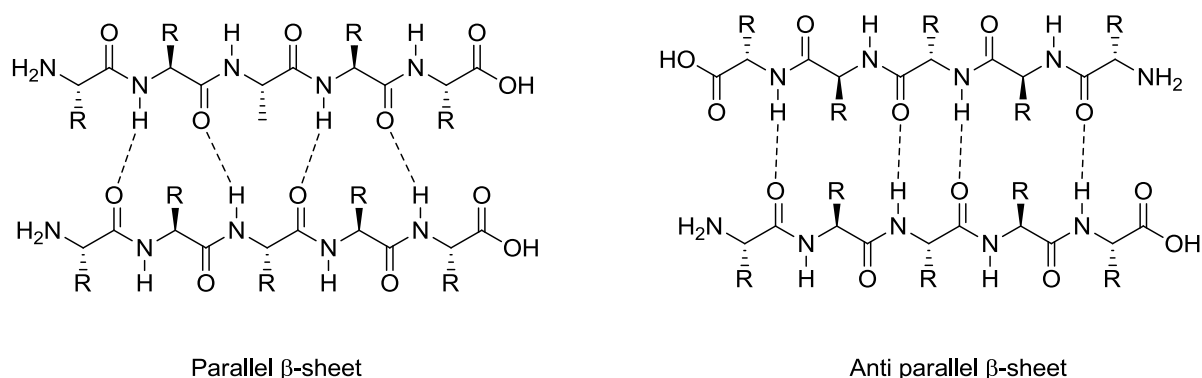


Figure 1: Parallel and anti-parallel β -sheets.

4.2. Introduction to β -turns

A turn is defined as a site where the polypeptide chain reverses its overall direction. The term β has a more restricted definition and describes a turn of four residues and γ describes a turn of three residues.^{3, 4} The β -turn is one of the three major motifs of peptide and protein secondary structure.⁵ β -Turns play a key role in many biological molecular recognition events including interactions between antigens and antibodies, peptide hormones and their receptors and regulatory enzymes and their corresponding substrates. The idea that turns have functions related to their structural characteristics appears throughout the literature.⁴ Turns are intrinsically polar structures with backbone groups that pack closely together and side chains that project outward. Such an array of atoms may constitute a site for molecular recognition e.g. antibody recognition. In peptides, turns are the conformations of choice for simultaneously optimising both backbone-chain compactness (intramolecular non-bonded contacts) and side chain clustering (to facilitate intermolecular recognition).

The formation of a β -turn requires four consecutive amino acids with a hydrogen bond joining the C=O of the first residue (i) with the N-H of the last residue (i+3) to give a 10 atom loop (**Figure 2**). This steric arrangement requires that any hydrogen bond involving the remaining two residues (i+2, i+3) be formed with partners outside the turn.

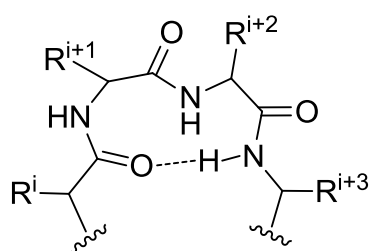


Figure 2: The β -turn motif.⁶

An isolated β -turn is already highly polar due to these unpaired N-H and C=O groups. In the context of a protein, polarity is further enhanced because turn formation is promoted at chain sites where the average linear hydrophobicity is locally minimal. Hence, turns are almost always situated at the molecular surface in contact with solvent water.

4.3. Introduction to protein β -turn mimetics

A β -turn mimetic is a synthetic variant of a β -turn that has a non-peptidic backbone but retains the functional groups of the peptide in their correct active conformations to act on a receptor. An important structural feature of many peptides and proteins is the β -turn motif and it may well be crucial in receptor interactions that ultimately lead to biological activity.⁷ Peptides and proteins play a vital role in the control and modulation of virtually all biological processes regulating biological functions by acting as hormones, enzymes, receptors and inhibitors.⁷

The understanding of the relationship between protein and peptide structure and their biological function has dramatically increased as a result of the growth in the fields of molecular biology, peptide synthesis, structure elucidation and molecular modelling. This recent progress in the synthesis and screening of huge peptide libraries has focused attention on small peptides as important lead structures for the development of potential therapeutic agents. Peptides themselves cannot be used as therapeutic candidates due to poor receptor selectivity, unfavourable absorption properties, metabolic instability and lack of oral bioavailability.⁶ Hence there has been much interest in establishing general synthetic strategies for converting these potent peptides into peptidomimetics that may overcome the pharmacokinetic limitations of the peptides themselves.

In order to attain high affinity and selective binding to a targeted receptor, a β -turn mimetic must reproduce both the functionality and orientation of the side chains of the receptor-bound peptide ligand. The inherent diversity in β -turn structure and difficulties in identifying the key residues responsible for binding has made the design of β -turn mimetics quite challenging.

4.3.1. Design of peptidomimetics

The design of peptidomimetics may be based on a particular protein structural motif and the β -turn offers the significant advantage that it is compact and of such a size that it can be readily mimicked by a small organic molecule. To successfully mimic even a small helix would require molecules significantly larger than steroids.⁷

It would be advantageous to have a rigid molecule that could mimic any β -turn structure and position the four side chains (i, i+1, i+2, i+3 residues) in their proper orientation as determined by x-ray crystallography of β -turn sequences in known proteins.⁷ A great deal of effort has therefore been focused on the design of small constrained mimetics of turn structure in order to provide a better understanding of the molecular basis of peptide and protein interactions in addition to providing potent and specific therapeutic agents.⁸ These efforts have met with only limited success due to difficulties in identifying the key turn residues and the relative orientations of those residues in the receptor-bound conformation. To date, peptide mimetics have already been reported to show biological activity although they were found by serendipity. Examples include opiate analgesics and antagonists for β -endorphins,⁹ benzodiazepines as cholecystokinin (CCK) antagonists¹⁰ and substituted imidazoles as angiotensin II receptor antagonists.¹¹ These all involved synthetic modifications to the peptides to produce suitable drug targets.

The difficulties in identifying the optimal structure for a given turn mimetic could be circumvented by the synthesis and screening of a combinatorial library of β -turn mimetics which include all possible side-chain combinations as well as multiple relative orientations of the side chains. In 1994, Virgilio and Ellman⁸ reported a general method for the solid-phase synthesis of β -turn mimetics that incorporated a variety of side-chain functionality and demonstrated the simultaneous synthesis of multiple turn derivatives (**Figure 3**).

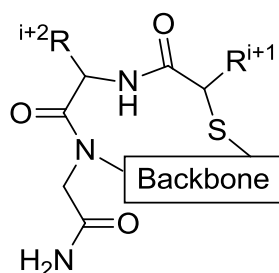


Figure 3: A β -turn mimetic with different backbone linkages.

The different backbone linkages determine the flexibility of the mimetic and the relative orientations of the side chains e.g. to provide 9- or 10-membered rings, as well as by preparing different combinations of the absolute configurations at each of the stereocentres introduced by the i+1 and i+2 side chains.

4.3.2. β -Turn mimetic classification

Turn mimetics can be classified into two distinct groups; internal and external.⁶ Internal mimetics are constructed upon skeletons that lie within the pseudo 10-membered ring framework of the turn motif, and place an emphasis on side chain presentation as displayed by the structure reported by Kahn¹² (**Figure 4**).

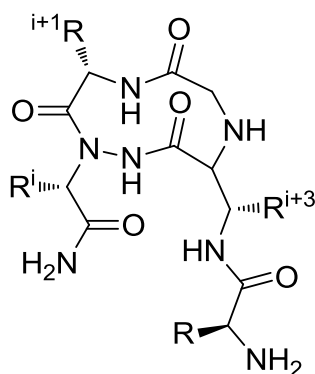


Figure 4: An example of internal turn mimetics.

The external mimetics are often constructed on dipeptide isostere skeletons that do not display side chain functionality at the central $i+1$ and $i+2$ positions. These structures reduce the conformational flexibility of a peptide with a rigidified skeleton that lies outside of the turn's general framework, and are primarily employed to orient the surrounding peptide chain into a turn conformation. **Figure 5** developed by Freidinger¹³ is a notable example.



Figure 5: An example of external turn mimetics.

One problem with the synthesis of β -turn mimetics is steric crowding around side chains $i+2$ and $i+3$. Some methods have been developed to overcome this issue; including the addition of smaller R groups such as glycine, inverting the stereochemistry from *L* to *D*, or cyclising R^2 onto the next amino group. This can be done using proline efficiently; hence β -turn mimetics from proline derivatives are the main focus of the work in this chapter. Molecular modelling has strongly suggested that two novel morpholine templates (**Figure 6**) will behave as β -turn mimetics so we intended to base our β -turn mimetics on this structure.

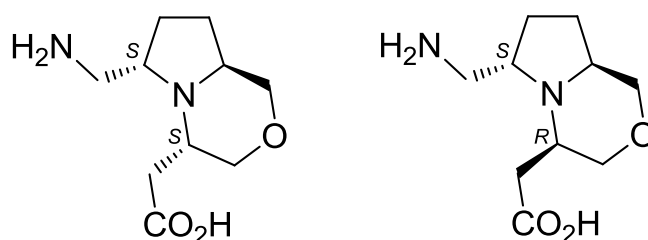
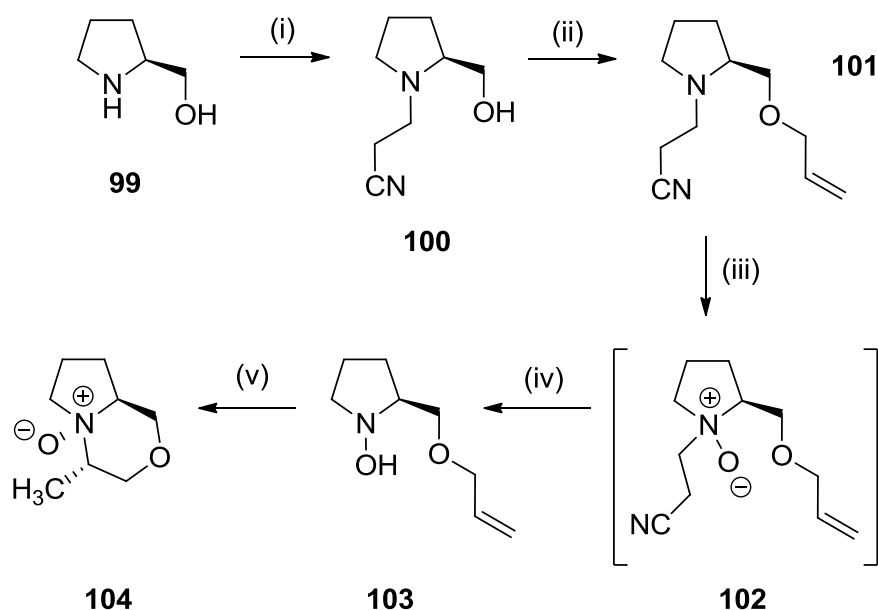


Figure 6: β -Turn mimetics with a fused morpholine template.

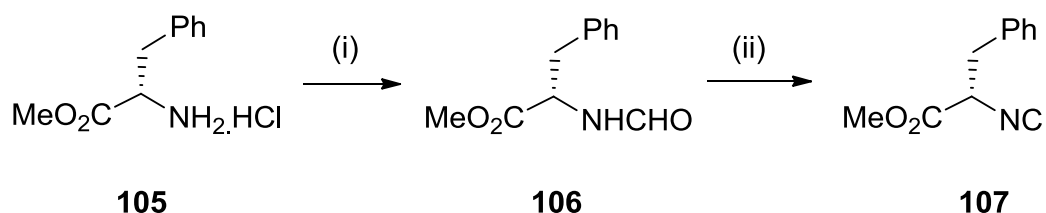
4.4. Proposed route to β -turn mimetics based on a fused morpholine skeleton

The O'Neil group proposed a route for the synthesis of a fused morpholine template (**Scheme 1**). The reaction of *S*-prolinol **99** with acrylonitrile followed by *O*-allylation gives the tertiary amine **101**. Selective oxidation of this tertiary amine gives the *N*-oxide **102** which undergoes Cope elimination to give the hydroxylamine **103**. Stirring the hydroxylamine **103** under a nitrogen atmosphere in $CDCl_3$ should give the fused morpholine *N*-oxide **104** as a single diastereoisomer.

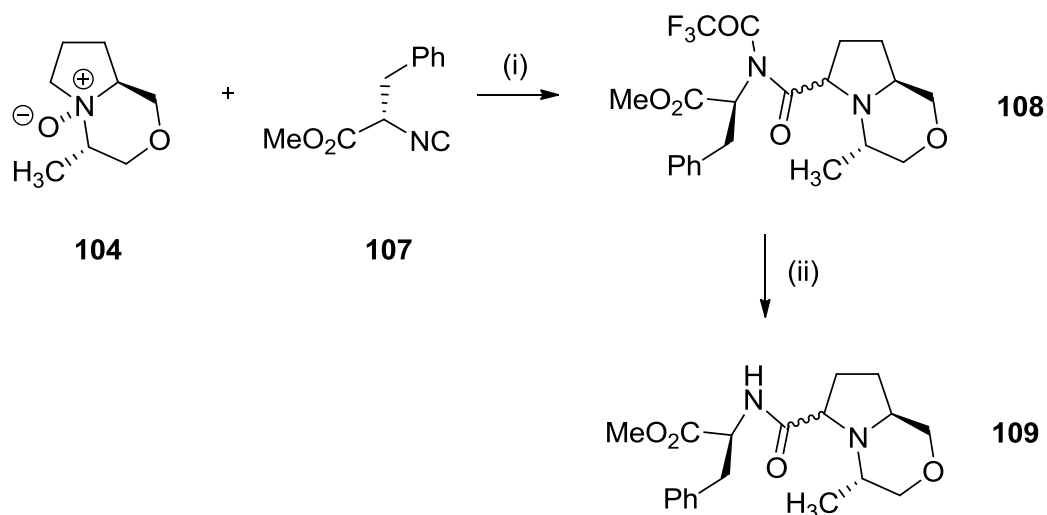


Scheme 1: Route to β -turn mimetics. (i) Acrylonitrile, MeOH (ii) Allyl bromide, NaH, THF (iii) *m*-CPBA, DCM (iv) Cope elimination (v) Reverse-Cope cyclisation.¹⁴

We then aspired to couple the final *N*-oxide **104** with an isocyanide **107** derived from an amino acid (**Schemes 2 and 3**).



Scheme 2: Synthesis of isocyanide **107** from *L*-phenylalanine methyl ester hydrochloride **105**. (i) Acetic formic anhydride (ii) Triphosgene, NEt₃, DCM.



Scheme 3: Coupling of *N*-oxide **104** with isocyanide **107**, a new variant of the Ugi/Polonovski reaction. (i) TFAA, DCM (ii) NaOMe, THF.

4.5. Introduction to chiral enamine *N*-oxides

A large number of chiral ligands based on amines have been reported over the years but there have been virtually no examples of asymmetric synthesis using homochiral tertiary amine *N*-oxides, despite the excellent metal-binding properties of this functional group.

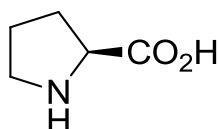
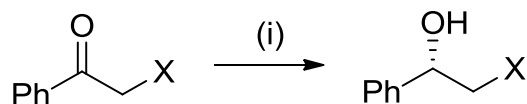


Figure 7: Structure of *S*-Proline.

Proline derived amine oxides have been extensively studied by the O'Neil group. A variety of chiral *N*-oxide derivatives of proline are capable of catalysing a wide range synthetically useful transformations such as the borane reduction of ketones (**Scheme 4**), giving products with high e.e.¹⁵ The e.e. of the products were determined by converting them to their trifluoroacetates and analysing by chiral GC. The amine oxides were found to be stable and simple to prepare and could be recovered from the reaction mixture in >90% yield.



Scheme 4: Borane reduction of ketones catalysed by amine *N*-oxides. (i) BH_3SMe_2 , Ligand, Solvent, 5mins.¹⁶

On the other hand, enamine *N*-oxides are virtually unknown and there are only a limited number of literature examples describing their synthesis. So far, there have been two methods described; the first is the elimination of HX from a suitably β -functionalised tertiary amine *N*-oxide e.g. quinuclidine enamine *N*-oxide (**Figure 8**).¹⁷

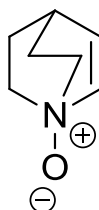
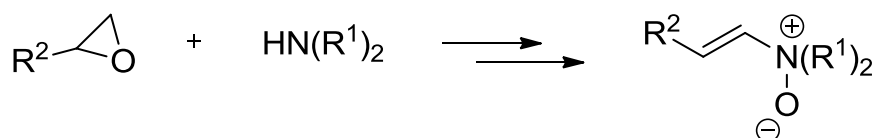


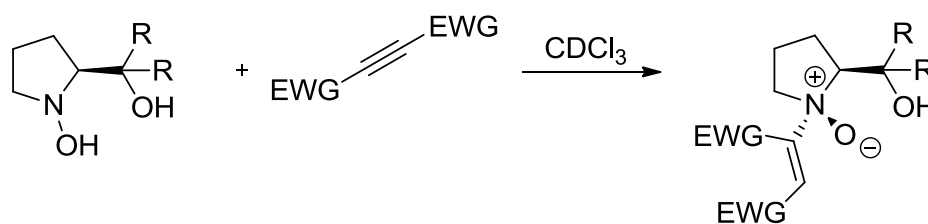
Figure 8: Quinuclidine enamine *N*-oxide.

The second method developed by Woodward involves the aminolysis of epoxides followed by chlorination, *N*-oxidation and dehydrochlorination (**Scheme 5**).¹⁸



Scheme 5: Preparation of enamine *N*-oxides by Woodward.¹⁸

The O'Neil group have since developed a short and highly efficient route to chiral enamine *N*-oxides. The reverse-Cope cycloaddition of chiral prolinol derived hydroxylamines to activated acetylenes gave single diastereomeric enamine *N*-oxides where the *N*-oxide was hydrogen-bonded to the side chain hydroxyl group (**Scheme 6**).

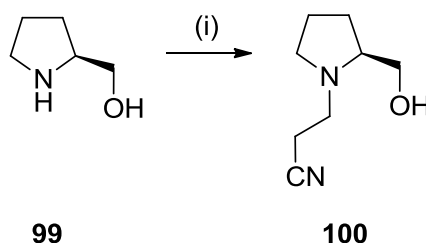


Scheme 6: Addition of prolinol-derived hydroxylamines to activated acetylenes.

4.6. Results and Discussion

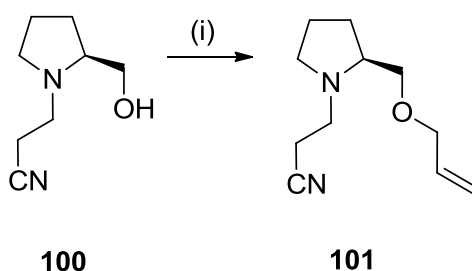
4.6.1. Route to β -turn mimetics using a modified Ugi/Polonovski reaction

The synthesis began with the straightforward cyanoethylation of *S*-prolinol **99** (Scheme 7). *S*-Prolinol **99** and excess acrylonitrile were stirred in methanol at room temperature overnight to give the cyanoethyl-protected product **100** in high yield. On repetition, it was found that reaction times did not need to be as long as 16hrs (1-4hrs was sufficient for the reaction to reach completion) and in some cases, the crude product was pure enough to use without purification by column chromatography.



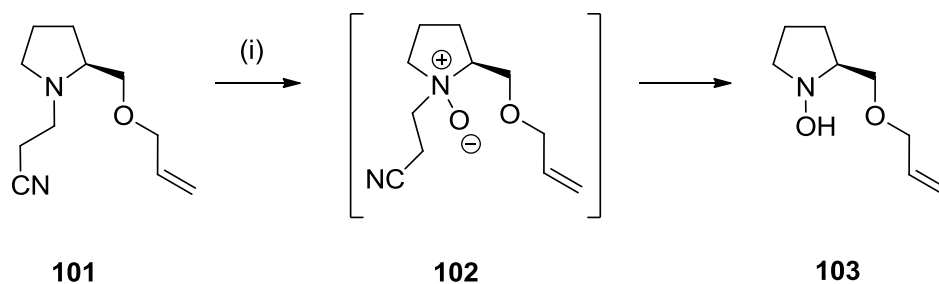
Scheme 7: Cyanoethylation of *S*-prolinol **99**. (i) Acrylonitrile (1.2eq), MeOH, rt, o/n, 87%.

The next step involved the *O*-allylation of the cyanoethyl-protected prolinol **100** (Scheme 8). This reaction did not proceed to give as high a yield as expected. We presumed that this was because the sodium hydride, a very fine solid dispersed in mineral oil, was used without pre-washing with hexanes. On repetition, yields obtained were in the region of 75% when the sodium hydride was washed immediately before use in the reaction.



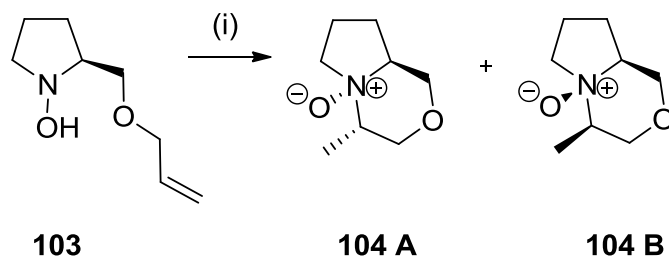
Scheme 8: *O*-Allylation of cyanoethyl-protected prolinol **100**. (i) NaH (1.1eq), THF, 0°C, 40mins, allyl bromide (1.5eq), TBAI (cat.), rt, o/n, 56%.

The *O*-allylated product **101** was then oxidised to the corresponding hydroxylamine using *m*-CPBA (**Scheme 9**).



Scheme 9: Oxidation of prolinol derivative **101** using *m*-CPBA followed by Cope elimination to give hydroxylamine **103**. (i) *m*-CPBA (1.1eq), K₂CO₃ (1.5eq), DCM, -78°C, 3hrs, rt, o/n.

The hydroxylamine could not be isolated in pure form as it underwent reverse Cope cyclisation slowly at room temperature (**Scheme 10**). Subsequent refluxing in methanol gave the cyclised product as a mixture of diastereoisomers in 13% yield. It was later found that simply stirring in CDCl₃ under a N₂ atmosphere at room temperature gave the cyclised product as a single diastereoisomer **104A** in 25% yield over 2 steps starting from **101**.



Scheme 10: Reverse-Cope cyclisation. (i) MeOH, N₂, Δ , 3 days, 13%, 4:3 (A:B) or CDCl₃, N₂, rt, 4 days, 25% over 2 steps, 1:0 (A:B).

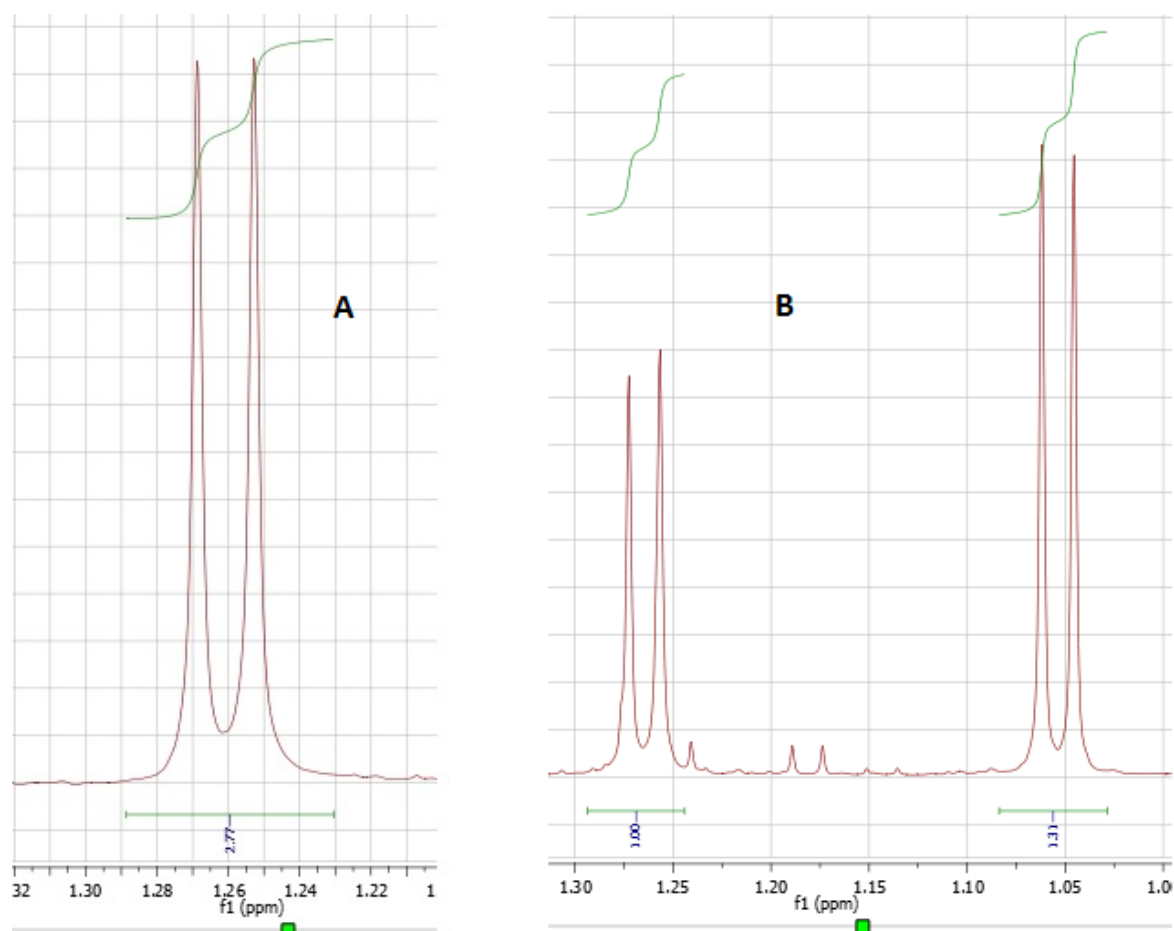
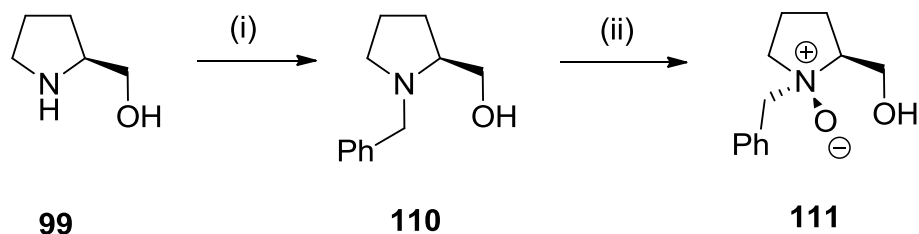


Figure 9: ¹H NMR showing characteristic doublet peak(s) corresponding to -CH₃ on morpholine ring. Single diastereoisomer formed in CDCl₃ (A) and a mixture of diastereoisomers formed in MeOH (B).

A prolinol-derived *N*-oxide with a simpler structure **111** was synthesised (**Scheme 11**) with the intention of coupling this with an isocyanide to test the feasibility of the reaction. *N*-oxide **111** exhibited long term stability when stored at room temperature.

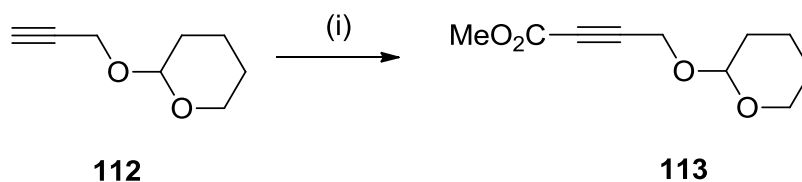


Scheme 11: Synthesis of (1*R*, 2*S*)-1-benzyl-2-(hydroxymethyl)pyrrolidine-1-oxide **111**. (i) Benzyl bromide (1.4eq), K₂CO₃ (1.03eq), N₂, toluene, 110°C, 21hrs, 56%. (ii) *m*-CPBA 1.1eq), K₂CO₃ (1.5eq), DCM, N₂, -78°C, 2hrs, rt, o/n, 70%.

4.6.2. Synthesis of β -turn mimetics using a reverse-Cope cyclisation

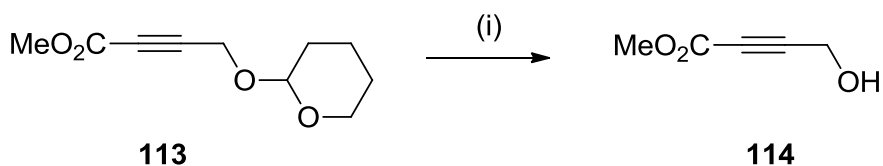
Having successfully synthesised a fused morpholine template (**104A**, **Scheme 10**), we were encouraged to investigate similar analogues possessing a side chain on the morpholine ring that was capable of undergoing further transformations, with the intention of incorporating an alkyne ester substrate at this position.

The tetrahydropyranyl derivative of propargyl alcohol **112** was deprotonated using ethylmagnesium bromide and the resulting acetylenic anion trapped out with freshly distilled methyl chloroformate (**Scheme 12**).



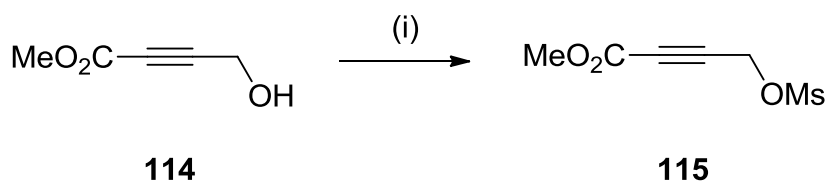
Scheme 12: (i) EtMgBr (1.0M in THF, 1.1eq), THF, -78°C, 30mins, ClCO₂Me (1.1eq), THF, -78°C-rt, o/n, 25%.

On repetition, this afforded the alkyne ester product in only 25% yield. Having separated all the components in the crude reaction mixture by column chromatography, it was found that half of the starting tetrahydropyranyl derivative was left unreacted. It was suspected that the cause of this was the concentration of the ethylmagnesium bromide solution, as supplied by Sigma Aldrich was not 1.0M as labelled. For this reason, freshly titrated *n*BuLi was used in place of ethylmagnesium bromide but this gave only 14% yield of product. It was assumed that the intermediate alkoxide formed from methyl chloroformate is better stabilised by a magnesium bromide cation than it is by a lithium cation. Without further optimisation of the conditions for deprotonation, the alkyne ester was deprotected under mildly acidic conditions (**Scheme 13**).



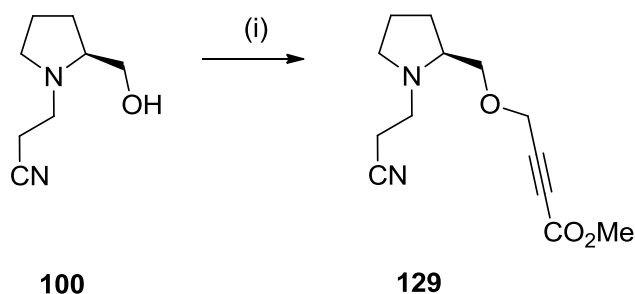
Scheme 13: Deprotection of alkyne ester derivative **113**. (i) *p*-TSA (10mol%), MeOH, rt, 4hrs, 100%.

Due to concerns about its stability on silica gel, the crude alcohol **114** was then used immediately to make the corresponding mesylate (**Scheme 14**).



Scheme 14: Mesyl chloride (1.1eq), NEt₃ (1.5eq), dry DCM, N₂ atmosphere, -40°C-rt, 2hrs, 73%.

Due to the unstable nature of the mesylate **115** at room temperature, it was used immediately in separate coupling reactions with cyanoethylprolinol **100** at 0°C and -40°C to yield the resulting coupled product in 5% and 7% isolated yields respectively (**Scheme 15**).



Scheme 15: Coupling mesylate with cyanoethylprolinol. (i) NaH (1.1eq), THF, 0°C or -40°C, 30mins, mesylate **115** (1.5eq), TBAI (cat.), 0°C or -40°C - rt, o/n.

Mass spectrometry confirmed the presence of the desired product with a molecular ion peak at 252.2 $[M+H]^+$ but ^1H NMR showed that the prolinol ring protons were not present. It was concluded that the desired product had been formed but only as a very minor product in the reaction (not detectable by NMR) and this could not be determined quantitatively by mass spectrometry. We proposed that the major possible product from this coupling reaction could be addition of the prolinol alkoxide derivative into the triple bond instead of displacing the mesylate group (**Figure 9**) but mass spectrometry did not show a peak for this product.

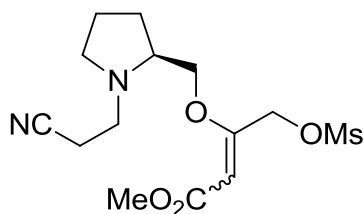
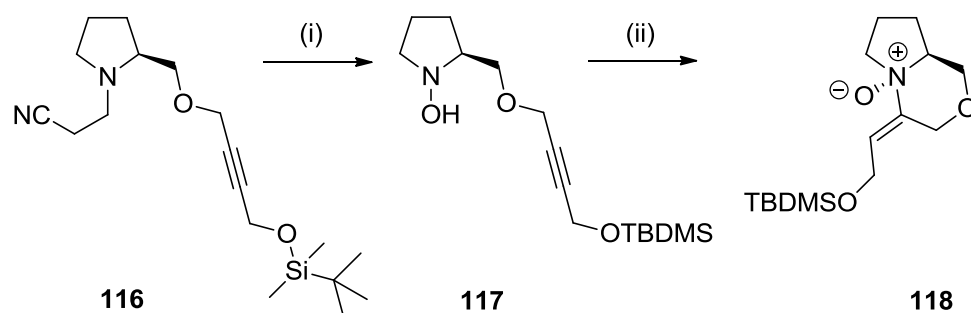


Figure 10: Possible side product resulting from alkoxide attacking alkyne.

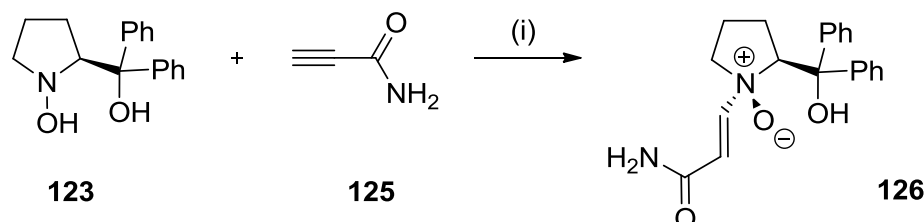
Another prolinol derivative synthesised by a member of the O'Neil group was successfully used in the reverse-Cope cyclisation (**Scheme 16**). The *N*-oxide was rigorously dried in a vacuum desiccator over P_2O_5 where it changed from a yellow to dark green and eventually a black, viscous oil, an indication that decomposition had occurred.



Scheme 16: Oxidation of the TBDMS prolinol derivative to corresponding hydroxylamine followed by reverse-Cope cyclisation. (i) *m*-CPBA (1.1eq), K₂CO₃ (1.5eq), DCM, N₂, -78°C, 18hrs (ii) CDCl₃ (10ml), N₂, rt, 5 days, 31% over 2 steps.

4.6.3. Synthesis of chiral enamine *N*-oxides

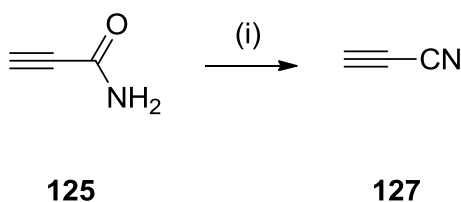
We next focused on the synthesis of chiral enamine *N*-oxides using diphenylprolinol hydroxylamine **123** in reactions with activated alkynes. We began with the commercially available propiolamide **125** as the alkyne substrate (**Scheme 17**).



Scheme 17: Synthesis of a chiral enamine *N*-oxide. (i) CDCl₃, N₂, rt, 3 days, 83%.

The yield of 83% encouraged us to use other alkyne substrates bearing electron withdrawing groups. We envisaged that cyanoacetylene **127** and propiolaldehyde **129** would furnish similar yields. Both of these alkyne substrates were synthesised and used immediately in the coupling reactions with diphenylprolinol hydroxylamine.

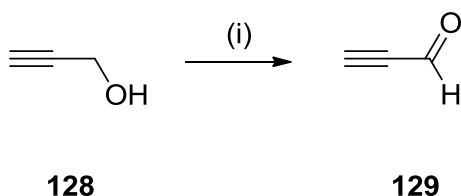
The synthesis of cyanoacetylene **127** involved the dry distillation of propiolamide **125** under reduced pressure (**Scheme 18**). However, the reaction of cyanoacetylene **127** with diphenylprolinol hydroxylamine **123** was unsuccessful at -78°C (no reaction or very slow at low temperature) but due to the volatile nature of cyanoacetylene, this reaction was not feasible at room temperature.



Scheme 18: Synthesis of cyanoacetylene **127** *via* dry distillation of propiolamide **125**.

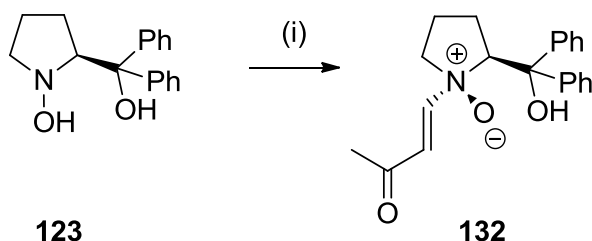
Cyanoacetylene collected at -78°C . (i) Sand, P_2O_5 (1.5eq), 140°C , 20mmHg.

Propiolaldehyde **129** was synthesised *via* the Jones oxidation of propargyl alcohol in moderate yield (67%) after a short path distillation (**Scheme 19**). The reaction of propiolaldehyde **129** with diphenylprolinol hydroxylamine **123** was attempted but we encountered the same problem of volatility as previously observed with cyanoacetylene.



Scheme 19: Synthesis of propiolaldehyde. (i) Jones' reagent, butanone, 0°C , 30mins, 67%.

The reaction was also attempted using 3-butyne-2-one as the alkyne substrate. This was carried out twice, using one and then three equivalents of 3-butyne-2-one (**Scheme 20**). However, on both occasions, there was no product seen by ^1H NMR after purification by column chromatography or mass spectrometry. It appeared that decomposition had taken place as the ring protons were not present in the ^1H NMR and TLC showed multiple components.



Scheme 20: Coupling diphenylprolinol hydroxylamine with 3-butyne-2-one. (i) CDCl_3 , N_2 , rt, 7 days, 0%.

4.7. Conclusions and Further Work

The yield and ratio of diastereoisomers for the product from reverse-Cope cyclisation was found to be inconsistent with the literature when MeOH was the solvent for the reaction.¹⁴ This needs to be repeated to determine reproducibility of the yields. The coupling of isocyanide **107** with *N*-oxide **104A** from reverse-Cope cyclisation (attempted once within the O'Neil group but unsuccessful) and benzyl-protected prolinol *N*-oxide **111** is still required to determine the feasibility of the modified Ugi/Polonovski reaction. Once an efficient and reliable synthesis has been established, the resulting β -turn mimetics can be screened for biological activity.

The synthesis of an alkyne bearing ester and mesylate functionality **115** for use in the synthesis of a β -turn mimetic using a reverse-Cope cyclisation was found to be unsuccessful due to its tendency to decompose at room temperature. Alternative syntheses of this alkyne are required.

The synthesis of a novel, chiral enamine *N*-oxide **126** has been successfully carried out by coupling diphenylprolinol hydroxylamine **123** with propiolamide **125**. Similar coupling reactions using activated alkyne substrates, cyanoacetylene **127** and propiolaldehyde **130** were attempted but were found to be unsuccessful due to their volatile nature. The chiral enamine *N*-oxides synthesised within the O'Neil group can, in future, be screened as ligands for catalysis.

4.8. Bibliography

1. The Chemistry of Amino Acids.
http://www.biology.arizona.edu/biochemistry/problem_sets/aa/aa.html.
2. Secondary Protein Structure.
<http://www.elmhurst.edu/~chm/vchembook/566secprotein.html>.
3. Rose, G. D.; Young, W. B.; Gierasch, L. M., Interior turns in globular proteins. *Nature* **1983**, 304 (5927), 654-657.
4. Rose, G. D.; Gierasch, L. M.; Smith, J. A., Turns in peptides and proteins. *Adv. Protein Chem.* **1985**, 37, 1-109.
5. Virgilio, A. A.; Bray, A. A.; Zhang, W.; Trinh, L.; Snyder, M.; Morrissey, M. M.; Ellman, J. A., Synthesis and evaluation of a library of peptidomimetics based upon the beta-turn. *Tetrahedron* **1997**, 53 (19), 6635-6644.
6. Souers, A. J.; Ellman, J. A., beta-turn mimetic library synthesis: scaffolds and applications. *Tetrahedron* **2001**, 57 (35), 7431-7448.
7. Ripka, W. C.; Delucca, G. V.; Bach, A. C.; Pottorf, R. S.; Blaney, J. M., Protein beta-turn mimetics. 1. Design, synthesis and evaluation in model cyclic-peptides. *Tetrahedron* **1993**, 49 (17), 3593-3608.
8. Virgilio, A. A.; Ellman, J. A., Simultaneous solid-phase synthesis of beta-turn mimetics incorporating side-chain functionality. *J. Am. Chem. Soc.* **1994**, 116 (25), 11580-11581.
9. Johnson, M. R.; Milne, G. M., Recent discoveries in the search for non-opiate analgesics. *J. Heterocycl. Chem.* **1980**, 17 (8), 1817-1820.
10. Bock, M. G.; Dipardo, R. M.; Evans, B. E.; Rittle, K. E.; Veber, D. F.; Freidinger, R. M.; Chang, R. S. L.; Lotti, V. J., Cholecystokinin antagonists - synthesis and biological evaluation of S-triazolo(4,3-A)-3-substituted-1,4-benzodiazepines. *Abstr. Pap. Am. Chem. Soc.* **1987**, 193, 13-MEDI.
11. Carini, D. J.; Duncia, J. V.; Aldrich, P. E.; Chiu, A. T.; Johnson, A. L.; Pierce, M. E.; Price, W. A.; Santella, J. B.; Wells, G. J.; Wexler, R. R.; Wong, P. C.; Yoo, S. E.; Timmermans, P., Non-peptide angiotensin II receptor antagonists - the discovery of a series of N-(biphenylmethyl)imidazoles as otent, orally active antihypertensives. *J. Med. Chem.* **1991**, 34 (8), 2525-2547.
12. Gardner, B.; Nakanishi, H.; Kahn, M., Conformationally constrained non-peptide beta-turn mimetics of enkephalin. *Tetrahedron* **1993**, 49 (17), 3433-3448.
13. Freidinger, R. M.; Veber, D. F.; Perlow, D. S.; Brooks, J. R.; Saperstein, R., Bioactive conformation of luteinizing hormone-releasing hormone - evidence from a conformationally constrained analog. *Science* **1980**, 210 (4470), 656-658.
14. O'Neil, I. A.; Cleator, E.; Ramos, V. E.; Chorlton, A. P.; Tapolczay, D. J., The synthesis of chiral functionalised morpholine N-oxides using a tandem Cope elimination/reverse-Cope elimination protocol. *Tetrahedron Lett.* **2004**, 45 (18), 3655-3658.
15. O'Neil, I.; Turner, C. D.; Kalindjian, S. B., Homochiral Amine Oxides in the Enantioselective Reduction of Ketones. *Synlett* **1997**, 777-780.

16. Gamble, M. P.; Studley, J. R.; Wills, M., New Chiral Phosphinamide Catalysts for Highly Enantioselective Reduction of Ketones. *Tetrahedron Lett.* **1996**, 37, 2853.
17. O'Neil, I. A.; Wynn, D.; Lai, J. Y. Q., The synthesis and functionalisation of quinuclidine enamine N-oxide and borane complex. *Tetrahedron Lett.* **2000**, 41, 271-274.
18. Bernier, D.; Blake, A. J.; Woodward, S., Improved Procedure for the Synthesis of Enamine N-Oxides. *J. Org. Chem.* **2008**, 73, 4229-4232.

Chapter 5

Experimental Details

5.1. General Information

5.1.1. Purification of chemicals

All chemicals and solvents were used as purchased without further purification unless otherwise stated. Re_2O_7 was stored under N_2 in a desiccator containing self indicating silica gel. Diisopropylamine was freshly distilled over CaH_2 and stored under N_2 prior to use.

5.1.2. Purification of solvents

THF was freshly distilled from Na/benzophenone under an inert atmosphere of N_2 prior to use. DCM was freshly distilled from CaH_2 under an inert atmosphere of N_2 prior to use. All other solvents were purified by standard methods. See W. L. F. Armarego and C. L. L. Chai, "Purification of Laboratory Chemicals", 5th Edition, Butterworth-Heinemann Publications, 2003. DMF and 1,4,-dioxane were purchased from Sigma Aldrich in 100ml bottles and used without further purification. Petroleum ether (40-60°C) was used for flash column chromatography.

5.1.3. Titration of *n*BuLi

*n*BuLi was purchased from Sigma Aldrich in 100ml bottles as a 1.6M solution in hexanes. The precise molarity was determined by titration against a solution of *N*-benzylbenzamide in THF at -45°C to a blue endpoint.¹

5.1.4. Purification of *m*-CPBA

m-CPBA (*ca.* 50% pure as supplied by Sigma Aldrich) was purified prior to use. Di-sodium hydrogen phosphate dihydrate (2.66g, 15mmol), and sodium di-hydrogen phosphate (0.52g, 4.33mmol) were dissolved in distilled water (500ml). *m*-CPBA (13g) was added to DCM (150ml), the insoluble white solid was filtered off and the filtrate washed with the buffer (3 x 150ml). The organic extracts were dried (MgSO_4) and the solvent removed under reduced pressure, furnishing *m*-CPBA (*ca.* 90-100% pure), which was dried in a vacuum desiccator over P_2O_5 for 1 day. The product was obtained as a white flocculent solid (*ca.* 7g).²

5.1.5. Preparation of glassware

For anhydrous reactions, all syringes, needles, flasks, condensers and stirrer bars were flame dried prior to use. All were cooled in a desiccator containing self indicating silica gel, fitted with a septum and flushed with N₂ prior to use. All anhydrous reactions were performed under a small positive pressure of nitrogen.

5.1.6. Other apparatus

Ozone (3-4% in a stream of O₂) was generated *via* a Wallace and Tiernan B. A. 023012 ozonizer. Sonication of reaction flasks were performed with a Camlab Transsonic T 460/H sonic bath.

5.1.7. Chromatography

Thin layer chromatography was carried out on Merck silica gel 60 F-254 aluminium-backed plates. Compounds were visualised by exposure to iodine mixed with silica gel, treatment with potassium permanganate (1% w/v in water) or an acidic, ethanolic solution of *p*-anisaldehyde. Flash column chromatography was performed using silica gel, pore size 60Å from Sigma Aldrich, using a compressed air line to apply a positive pressure to the column.

5.1.8. Characterisation of compounds

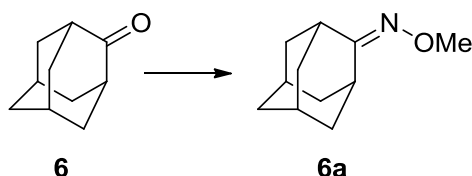
¹H (400MHz) and ¹³C (100MHz) NMR spectra were recorded on a Bruker AMX400 machine. Chemical shifts (δ) are recorded in ppm downfield from an internal standard of TMS, using CDCl₃ as solvent. Multiplicities are quoted as: singlet (s), doublet (d), triplet (t), doublet of doublets (dd), doublet of triplets (dt), multiplet (m). Coupling constants are in Hz.

Mass spectra were recorded on TRIO-1000 and Micromass LCT mass spectrometers using chemical ionisation (CI) in ammonia as the reagent gas or electrospray ionisation (ESI) in MeOH. Elemental analyses were carried out in the University of Liverpool Chemistry Department microanalysis laboratory. IR spectra were recorded in the range 4000-600 cm⁻¹ using a JASCO FT/IR 4200 spectrometer. Melting points were performed on a Gallenkamp melting point apparatus in degrees Celsius and are uncorrected.

5.2. Individual Experimental Procedures

Synthesis of 1,2,4-trioxolanes and 1,2,4,5-tetraoxanes

Synthesis of *O*-methyl 2-adamantanone oxime **6a**³



To a stirred solution of 2-adamantanone **6** (1.00g, 6.66mmol) in MeOH (20ml), was added pyridine (1ml, 12.40mmol) and methoxyamine hydrochloride (0.84g, 10.00mmol). The reaction was stirred at room temperature under a N₂ atmosphere for 48hrs, concentrated under reduced pressure to yield a yellow residue, and diluted with DCM (20ml) and water (20ml). The organic layer was separated and the crude product extracted with DCM (2 x 20ml). The combined organic extracts were washed with 1M HCl (2 x 20ml), brine (20ml) and dried (MgSO₄). The solvent was removed under reduced pressure to afford *O*-methyl 2-adamantanone oxime **6a** (0.96g, 81%) as a colourless solid.

¹H NMR (400MHz, CDCl₃) δ 3.85-3.81 (3H, s, CH₃), 2.57-2.52 (2H, s, 2 x CHC=N), 2.10-1.78 (12H, m, adamantyl H).

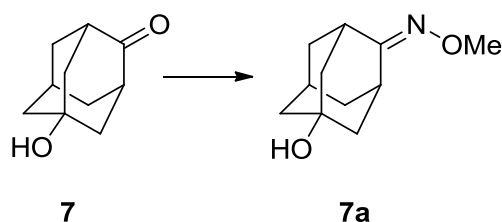
¹³C NMR (100MHz, CDCl₃) δ 167.2 (C=N), 61.4 (CH₃), 38.0, 36.9, 29.9, 28.2.

m.p 112-114°C

IR (neat)/cm⁻¹: 2915 (C-H alkyl), 2852, 1718 (C=N), 1452, 1049, 892.

LRMS (CI); 180.2 [M+H]⁺, 150.2 [M-OMe]⁺.

Synthesis of *O*-methyl 5-hydroxy-2-adamantanone oxime **7a**



To a stirred solution of 5-hydroxy-2-adamantanone **7** (1.00g, 6.02mmol) in MeOH (20ml), was added pyridine (1ml, 12.40mmol) and methoxyamine hydrochloride (0.75g, 8.98mmol). The reaction was stirred at room temperature under a N₂ atmosphere for 48hrs, concentrated under reduced pressure to yield a cloudy residue, and diluted with DCM (40ml) and water (30ml). The organic layer was separated and the crude product extracted with DCM (30ml). The combined organic extracts were washed with 1M HCl (2 x 20ml), brine (20ml) and dried (MgSO₄). The solvent was removed under reduced pressure to afford *O*-methyl 5-hydroxy-2-adamantanone oxime **7a** (0.66g, 56%) as a colourless solid.

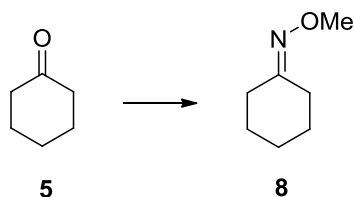
¹H NMR (400MHz, CDCl₃) δ 3.85-3.80 (3H, s, CH₃), 3.65-3.60 (1H, br s, OH), 2.73-2.69 (1H, s, CHC=N), 2.31-2.25 (1H, s, CHC=N), 1.90-1.72 (11H, m, adamantyl H).

¹³C NMR (100MHz, CDCl₃) δ 164.5 (C=N), 68.2 (C-OH), 61.5 (CH₃), 45.9, 44.6, 37.9, 36.7, 30.9.

C₁₁H₁₇NO₂ requires C 67.66 %, H 8.78 %, N 7.17 % found C 67.77 %, H 8.85 %, N 7.07 %.

IR (neat)/cm⁻¹: 3149 (br, OH), 2965 (C-H), 1606 (C=N), 1056 (C-O).

LRMS (CI); 196.1 [M+H]⁺.

Synthesis of *O*-methyl cyclohexanone oxime **8³**

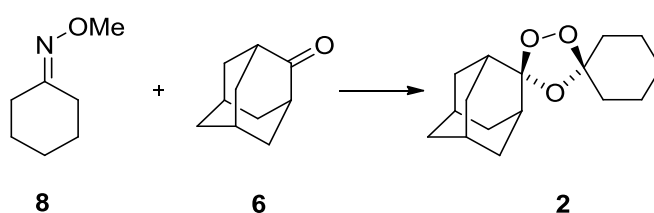
To a stirred solution of cyclohexanone **5** (2.2ml, 21.2mmol) in MeOH (20ml), was added pyridine (2ml, 24.8mmol, 1.2eq) and $\text{NH}_2\text{OMe}\cdot\text{HCl}$ (2.56g, 30.6mmol, 1.4eq). The reaction was stirred at room temperature under a N_2 atmosphere for 48hrs, concentrated under reduced pressure and diluted with DCM (50ml) and water (50ml). The product was extracted with DCM (2 x 50ml). The combined organic extracts were washed with 1M HCl (2 x 50ml) and brine (30ml), and dried (MgSO_4). The solvent was removed under reduced pressure to afford *O*-methyl cyclohexanone oxime **8** (2.17g, 80%) as a colourless oil.

^1H NMR (400MHz, CDCl_3) δ 3.82-3.80 (3H, s, CH_3), 2.46-2.42 (2H, m, CH_2), 2.21-2.17 (2H, m, CH_2), 1.68-1.56 (6H, m, 3 x CH_2).

^{13}C NMR (100MHz, CDCl_3) δ 160.7 (C=N), 61.4 (CH_3), 32.6, 27.4, 26.2, 26.1, 25.6.

IR (neat)/ cm^{-1} : 2935 (C-H alkyl), 1733 (C=N), 1448 (C-O), 1051 (C-O)

LRMS (CI); 144.2 $[\text{M}+\text{NH}_4]^+$.

Synthesis of adamantane-2-spiro-3'-1',2',4'-trioxaspiro[4.5]decane **2³**

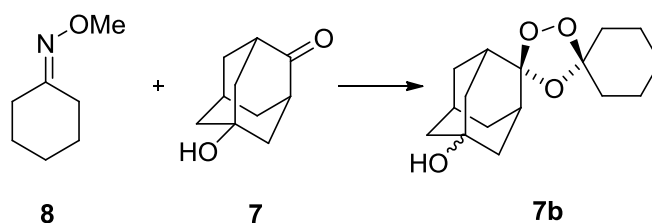
Ozone (3-4% in a stream of O_2) was bubbled into a solution of *O*-methyl cyclohexanone oxime **8** (0.20g, 1.56mmol) and 2-adamantanone **6** (0.26g, 1.74mmol, 1.1eq) in *n*-pentane (60ml) and DCM (15ml) at -78°C . The reaction was stirred for 5hrs and quenched by flushing with N_2 for 5mins until the blue colour disappeared to leave behind a colourless solution. The solvent was removed under reduced pressure and the residue purified by flash column chromatography using EtOAc/*n*-Hex (eluting with 10:90) to afford the product **2** (0.67g, 16%) as a colourless solid.

^1H NMR (400MHz, CDCl_3) δ 2.11-1.32 (24H, m, adamantyl/cyclohexyl H)

^{13}C NMR (100MHz, CDCl_3) δ 110.2 (quaternary C), 110.1 (quaternary C), 39.7, 31.2, 30.4, 30.2, 25.8, 23.0, 22.9.

IR (neat)/ cm^{-1} : 2942 (C-H alkyl), 1060 (C-O), 914 (O-O).

Synthesis of 5-hydroxy-adamantane-2-spiro-3'-1',2',4'-trioxaspiro[4.5]decane **7b**



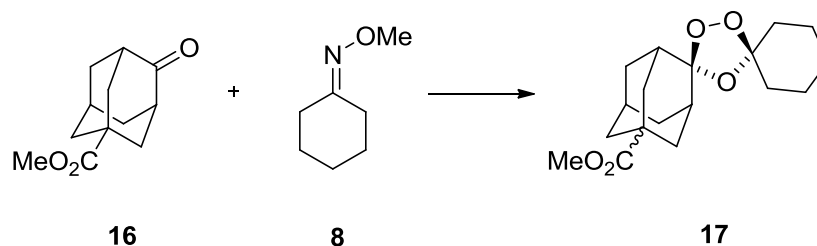
Ozone (3-4% in a stream of O_2) was bubbled into a solution of *O*-methylcyclohexanone oxime **8** (0.21g, 1.61mmol) and 5-hydroxy-2-adamantanone **7** (0.29g, 1.72mmol, 1.1eq) in *n*-pentane (60ml) and DCM (15ml) at -78°C . The reaction was left for 5hrs and quenched by flushing with N_2 for 5mins until the blue colour disappeared to leave behind a colourless solution. The solvent was removed under reduced pressure and the residue purified by flash column chromatography using EtOAc/*n*-Hex (eluting with 10:90) to afford the product **7b** (47mg, 10%) as a colourless solid.

^1H NMR (400MHz, CDCl_3) δ 1.91-1.80 (10H, m), 1.61-1.40 (9H, m), 1.5-1.20 (4H, m).

^{13}C NMR (100MHz, CDCl_3) δ 111.7 (quaternary C), 111.5 (quaternary C), 32.1, 30.2, 25.7, 23.1, 21.4.

IR (neat)/ cm^{-1} : 3405 (OH), 2942 (C-H), 1060 (C-O), 914 (O-O).

Synthesis of 5-adamantane-2-spiro-1' 2' 4'-trioxaspiro[4.5]decane methyl ester **17**



Ozone (3-4% in a stream of O₂) was bubbled through DCM at -78°C then into a solution of *O*-methyl cyclohexanone oxime **8** (0.55g, 4.34mmol, 1.25eq) and 5-carbomethoxy-2-adamantanone **16** (0.72g, 3.46mmol, 1eq) in *n*-pentane (60ml) at room temperature. After 3hrs, excess ozone in the reaction mixture was quenched by flushing with N₂ for 5mins. Ozone was bubbled through a second batch of *O*-methyl cyclohexanone oxime (0.14g, 1.11mmol, 1.29eq) and 5-carbomethoxy-2-adamantanone (0.18g, 0.86mmol, 1eq) in *n*-pentane (60ml) at room temperature. After 3hrs, excess ozone was quenched by flushing with N₂ for 5mins. The flask containing DCM was saturated with ozone and had turned blue. This was quenched by flushing with N₂ for 35mins to leave behind a colourless solution. Both reaction mixtures were combined and the crude product adsorbed onto silica and purified by flash column chromatography using EtOAc/petroleum ether (eluting with 2:98) to afford the product **17** (0.69g, 50%) as a colourless oil. Ratio of diastereoisomers 1:1.3.

¹H NMR (400MHz, CDCl₃) δ 3.67-3.66 (3H, s, OCH₃), 3.65-3.64 (3H, s, OCH₃), 2.25-1.35 (46H, m, adamantyl/cyclohexyl H).

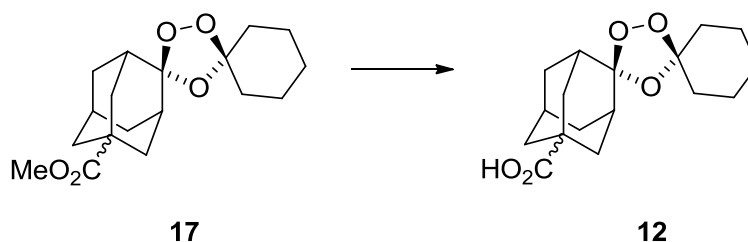
¹³C NMR (100MHz, CDCl₃) δ 177.7(3) (C=O), 177.6(3) (C=O), 110.5(1) (quaternary C), 110.4(8) (quaternary C), 109.7(0) (quaternary C), 109.6(6) (quaternary C), 52.1 (OCH₃), 40.3, 39.9, 38.6, 36.7, 36.5, 36.4, 36.2, 35.1, 34.1, 34.0, 29.5, 28.1, 27.0, 26.6, 25.3, 24.2.

C₁₈H₂₆O₅ requires C 67.06 %, H 8.13 % found C 67.15 %, H 8.13 %.

IR (neat)/cm⁻¹: 2935 (C-H alkyl), 1727 (C=O), 1241 (C-O), 1091 (O-O).

HRMS (ESI); 345.1679 [M+Na]⁺, C₁₈H₂₆O₅Na requires 345.1678.

Synthesis of 5-adamantane-2-spiro-1' 2' 4'-trioxaspiro[4.5]decane carboxylic acid **12**



To a solution of 5-adamantane-2-spiro-1' 2' 4'-trioxaspiro[4.5]decane methyl ester **17** (0.41g, 1.28mmol) in MeOH (5ml) was added 15% aq. NaOH (5ml). The mixture was stirred at 65°C for 2hrs and acidified to pH 2 using 2M HCl (10ml). The product was extracted with DCM (3 x 30ml), the combined organic extracts were dried (MgSO₄) and the solvent removed under reduced pressure to afford the product **12** (0.31g, 79%) as a colourless solid.

¹H NMR (400MHz, CDCl₃) δ 2.36-1.32 (48H, m, adamantyl/cyclohexyl H).

¹³C NMR (100MHz, CDCl₃) δ 183.4(2) (C=O), 183.2(8) (C=O), 110.3(8) (quaternary C), 110.3(6) (quaternary C), 109.7(8) (quaternary C), 109.7(4) (quaternary C), 42.4, 40.0, 39.7, 38.4, 38.3, 36.4, 36.3(2), 36.2(6), 36.1(7) 35.1, 34.0, 33.9, 27.4, 26.9, 26.5, 25.3, 24.3.

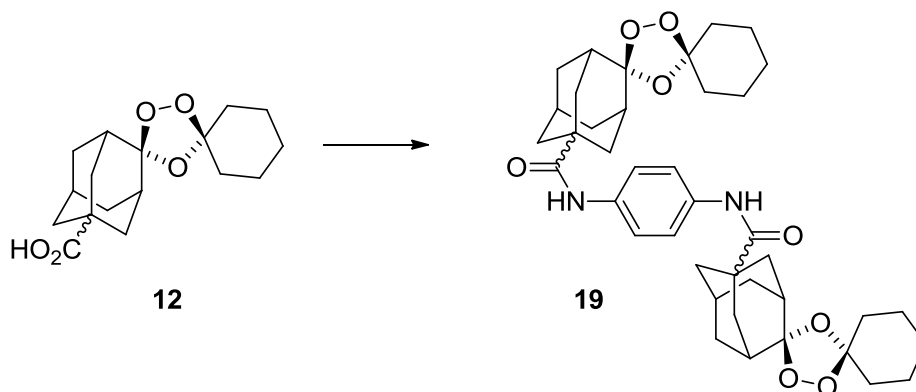
m.p 130-132°C

C₁₇H₂₄O₅ requires C 66.21 %, H 7.84 % found C 66.28 %, H 7.93 %.

IR (neat)/cm⁻¹: 2935 (C-H), 1689, (C=O), 1114 (C-O), 941 (O-O).

HRMS (ESI); 331.1520 [M+Na]⁺, C₁₇H₂₄O₅Na requires 331.1521.

Synthesis of trioxolane dimer **19**



To a stirred solution of 5-adamantane-2-spiro-1' 2' 4'-trioxaspiro[4.5]decane carboxylic acid **12** (95mg, 0.31mmol) in DMF (2.5ml) was added EDC.HCl (95mg, 0.50mmol, 1.6eq), HOBt (50mg, 0.37mmol, 1.2eq), and NMM (0.07ml, 0.064g, 0.64mmol, 2.06eq) at 0°C. The mixture was allowed to activate for 3hrs under a N₂ atmosphere. *p*-Phenylenediamine (17.5mg, 0.16mmol, 0.52eq) and NMM (0.03ml, 0.028g, 0.27mmol, 0.87eq) were added and the mixture was allowed to warm to room temperature overnight before being diluted with Et₂O (30ml) and washed with water (2 x 30ml). The combined aqueous phases were extracted with Et₂O (2 x 30ml). The combined organic extracts were washed with water (2 x 40ml), dried (MgSO₄) and the solvent removed under reduced pressure. The crude product was adsorbed onto silica gel and purified by flash column chromatography using EtOAc/petroleum ether (eluting with 20:80) to afford the product **19** (26mg, 12%) as a pale, straw coloured solid. The mono-coupled trioxolane (65mg, 32%) was also isolated as an orange oil.

¹H NMR (400MHz, CDCl₃) δ 7.72-7.69 (1H, m, NH), 7.55-7.52 (1H, m, NH), 7.48-7.44 (2H, d, CH aromatic), 7.25-7.21 (2H, d, CH aromatic), 2.30-0.85 (46H, m, adamantyl/cyclohexyl H).

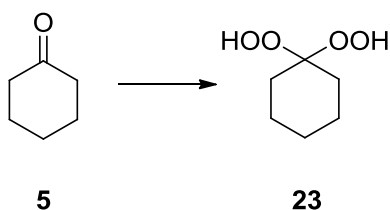
¹³C NMR (100MHz, CDCl₃) δ 174.8 (C=O), 134.1 (aromatic C), 128.8 (aromatic C), 120.5 (quaternary C), 109.9 (quaternary C), 40.2, 38.3, 34.7, 33.6, 29.7, 28.9, 26.3, 24.9, 23.7.

C₄₀H₅₂N₂O₈ requires C 69.74 %, H 7.61 %, N 4.07 found C 70.55 %, H 8.33 %, N 3.05 %.

IR (neat)/cm⁻¹: 3328 (N-H), 2933 (C-H), 1644 (C=O amide), 1536 (C=C aromatic), 1240 (C-O), 941 (O-O).

HRMS (ESI); 711.3600 [M+Na]⁺, C₄₀H₅₂N₂O₈Na requires 711.3621.

Synthesis of 1,1-dihydroperoxycyclohexane **23**⁴



To a stirred solution of I₂ (0.25g, 0.97mmol, 10mol%) in CH₃CN (20ml) was added cyclohexanone **5** (1.0ml, 9.66mmol) and 50% aq. H₂O₂ (1.7ml, 29.9mmol, 3.1eq) in CH₃CN (10ml). The reaction mixture was stirred at room temperature for 24hrs. The solvent was removed under reduced pressure, water (30ml) was added and the product extracted with Et₂O (5 x 30ml). The combined organic extracts were dried (Na₂SO₄), and the solvent removed under reduced pressure. The crude product was adsorbed onto silica gel and purified by flash column chromatography using EtOAc/*n*-Hex (eluting with 10:90) to afford pure 1,1-dihydroperoxycyclohexane **23** (1.10g, 77%) as a colourless oil.

¹H NMR (400MHz, CDCl₃) δ 8.80-8.72 (2H, s, 2 x OOH), 1.87-1.81 (4H, t, *J* = 5.9 Hz, 2 x CH₂), 1.62-1.55 (4H, m, 2 x CH₂), 1.50-1.42 (2H, m, CH₂).

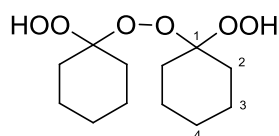
¹³C NMR (100MHz, CDCl₃) δ 111.3 (quaternary C), 29.9, 25.7, 22.8.

C₆H₁₂O₄ requires C 48.64 %, H 8.16 % found C 48.43 %, H 8.41 %.

IR (neat)/cm⁻¹: 3448 (OOH), 3181 (OH), 2937 (C-H alkyl), 1741, 1349 (C-O), 927 (O-O).

LRMS (CI); 132.1 [M-OH]⁺, 116.1 [M-2OH]⁺.

Side product: 1,1'-peroxybis(1-hydroperoxycyclohexane) **23a**



23a

¹H NMR (400MHz, CDCl₃) δ 9.55 (2H, s, 2 x OOH), 1.93-1.80 (8H, m, 8 x H-3), 1.64-1.55 (8H, m, 8 x H-2), 1.51-1.40 (4H, m, 4 x H-4).

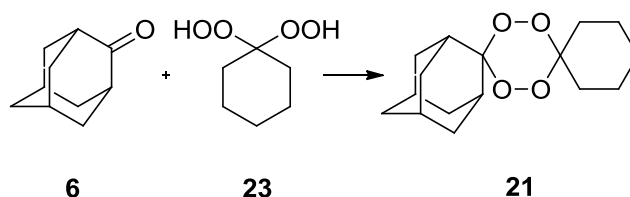
¹³C NMR (100MHz, CDCl₃) δ 111.2 (2 x C-1), 29.8 (4 x C-2), 25.3 (4 x C-3), 22.5 (2 x C-4).

C₁₂H₂₂O₆ requires C 54.94 %, H 8.45 % found C 54.92 %, H 8.41 %.

IR (neat)/cm⁻¹: 3438 (OOH), 2937 (C-H alkyl), 1060 (C-O), 936 (O-O).

HRMS (ESI); 285.1315 [M+Na]⁺, C₁₂H₂₂O₆Na requires 285.1314.

Synthesis of adamantane-2-spiro-3'-1',2',4',5'-tetraoxane-6'-spiro-1''-cyclohexane **21**⁵



To a stirred solution of 1,1-dihydroperoxycyclohexane **23** (0.30mg, 2.00mmol) and Re_2O_7 (24.3mg, 0.05mmol, 2.5mol%) in DCM (20ml) was added 2-adamantanone **6** (0.46g, 3.03mmol, 1.5eq) in DCM (20ml). The reaction mixture was stirred at room temperature for 4hrs. The crude product was adsorbed onto silica gel and purified by flash column chromatography using EtOAc/*n*-Hex (eluting with 2:98) to afford the product **21** (0.20g, 35%) as a colourless solid.

^1H NMR (400MHz, CDCl_3) δ 2.30-1.25 (m, adamantyl/cyclohexyl H)

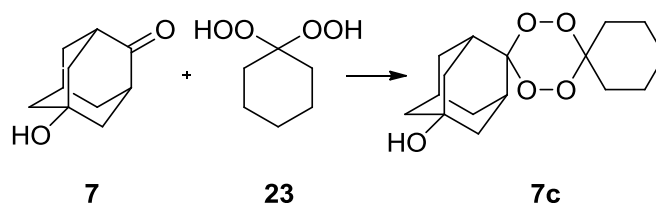
^{13}C NMR (100MHz, CDCl_3) δ 110.7 (quaternary C), 108.4 (quaternary C), 37.4, 33.6, 27.5, 25.8.

m.p 78-80°C

$\text{C}_{16}\text{H}_{24}\text{O}_4$ requires C 68.54 %, H 8.63 % found C 68.63 %, H 8.68 %.

IR (neat)/ cm^{-1} : 2933 (C-H), 1448 (C-O), 1060 (C-O), 923 (O-O).

Synthesis of 5-hydroxy-adamantane-2-spiro-3'-1',2',4',5'-tetraoxane-6'-spiro-1''-cyclohexane **7c**



To a solution of 1,1-dihydroperoxycyclohexane **23** (160mg, 1.09mmol) and Re_2O_7 (15.8mg, 0.03mmol, 3.0mol%) in DCM (20ml) was added 5-hydroxy-2-adamantanone **7** (270mg, 1.62mmol, 1.5eq) in DCM (20ml). The reaction mixture was stirred at room temperature overnight. The crude product was adsorbed onto silica gel and purified by flash column chromatography using EtOAc/*n*-Hex (eluting with 2:98) to afford the product **7c** (52mg, 16%) as a colourless solid.

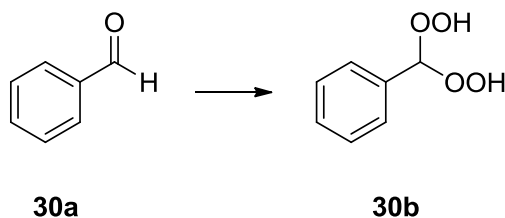
^1H NMR (400MHz, CDCl_3) δ 2.29-1.25 (m, adamantyl/cyclohexyl H).

^{13}C NMR (100MHz, CDCl_3) δ 110.7 (quaternary C), 108.5 (quaternary C), 108.4 (C-OH), 37.4, 33.7, 32.2, 30.1, 27.5, 25.8, 22.6.

IR (neat)/ cm^{-1} : 2919 (OH), 2854 (C-H alkyl), 1060 (C-O), 995 (O-O).

HRMS (ESI): 351.1796 $[(\text{M}+\text{CH}_3\text{OH})+\text{Na}]^+$, $\text{C}_{17}\text{H}_{28}\text{O}_6\text{Na}$ requires 351.1784.

Synthesis of (dihydroperoxymethyl)benzene **30b**



To a stirred solution of I_2 (1.25g, 4.93mmol, 10mol%) in CH_3CN (30ml) was added freshly distilled benzaldehyde **30a** (5.0ml, 49.1mmol) and 50% aq. H_2O_2 (8.50ml, 149.6mmol, 3.1eq) followed by CH_3CN (20ml). The reaction mixture was stirred at room temperature for 20hrs. The solvent was removed under reduced pressure, water (50ml) was added and the product extracted with Et_2O (6 x 50ml). The combined organic extracts were dried (Na_2SO_4) and evaporated under reduced pressure. The crude product was adsorbed onto silica gel and purified by flash column chromatography using EtOAc/*n*-Hex (eluting with 10:90) to afford the product **30b** (1.86g, 24%) as a yellow oil.

^1H NMR (400MHz, CDCl_3) δ 9.60-9.30 (2H, br s, 2 x OOH), 7.50-7.30 (5H, m, aromatic H), 6.40-6.30 (1H, br s, CH).

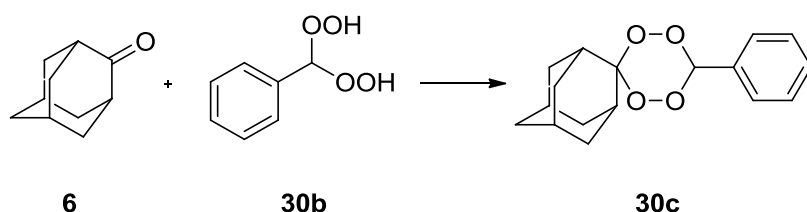
^{13}C NMR (100MHz, CDCl_3) δ 130.2 (quaternary C), 129.3, 128.9, 127.4, 110.5 (CH).

$\text{C}_7\text{H}_8\text{O}_4$ requires C 53.84 %, H 5.16 % found C 54.70 %, H 5.34 %.

IR (neat)/ cm^{-1} : 3134 (OOH), 2843 (C-H aryl), 1683 (C=C), 1454, 1187 (C-O), 935 (O-O).

LRMS (CI); 124.1 $[\text{M}-\text{OOH}]^+$.

Synthesis of 5-adamantane-2-spiro-3'-1',2',4',5'-tetraoxane-6'-spiro-1"-methylbenzene **30c**⁵



To a stirred solution of 2-adamantanone **6** (0.44g, 2.90mmol, 1.5eq) and Re_2O_7 (60mg, 0.12mmol, 6mol%) in DCM (20ml) was added (dihydroperoxymethyl)benzene **30b** (0.30g, 1.92mmol) in DCM (10ml). After stirring at room temperature for 1.5hrs, the crude product was adsorbed onto silica gel and purified by flash column chromatography using EtOAc/*n*-Hex (eluting with 2:98) to afford the product **30c** (0.23g, 41%) as a colourless solid.

^1H NMR (400MHz, CDCl_3) δ 7.42 (5H, m, Ar H), 6.68 (1H, s, benzylic CH), 2.18-1.63 (14H, m, adamantyl H).

^{13}C NMR (100MHz, CDCl_3) δ 132.1, 131.4, 129.0, 127.9, 111.2 (quaternary C), 108.1 (quaternary C), 37.4, 34.9, 31.3, 27.5.

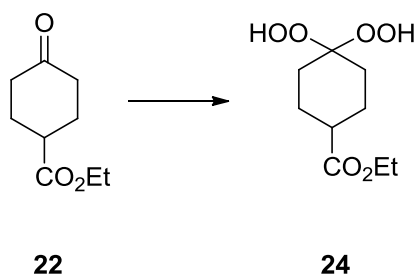
m.p 63-65°C

$\text{C}_{17}\text{H}_{20}\text{O}_4$ requires C 70.81 %, H 6.99 % found C 71.05 %, H 6.99 %.

IR (neat)/ cm^{-1} : 2978 (C-H aryl), 2929 (C-H alkyl), 1687 (C=C), 1454 (C-O), 1294 (C-O), 707 (O-O).

HRMS (ESI); 311.1262 $[\text{M}+\text{Na}]^+$, $\text{C}_{17}\text{H}_{20}\text{O}_4\text{Na}$ requires 311.1259.

Synthesis of ethyl 4,4-dihydroperoxycyclohexanecarboxylate **24**



To a solution of I_2 (47mg, 0.19mmol, 9mol%) in CH_3CN (10ml) was added ethyl 4-oxocyclohexanecarboxylate **22** (0.28ml, 300mg, 1.76mmol) in CH_3CN (10ml) and 50% aq. H_2O_2 (0.30ml, 5.27mmol, 3eq). The mixture was stirred at room temperature for 4 days. Most of the solvent was removed under reduced pressure, water (30ml) was added and the product extracted with DCM (6 x 30ml). The combined organic extracts were dried (Na_2SO_4) and the solvent removed under reduced pressure. The crude product was adsorbed onto silica gel and purified by flash column chromatography using EtOAc/petroleum ether (eluting with 20:80) to afford the product **24** (344mg, 88%) as a colourless oil.

1H NMR (400MHz, $CDCl_3$) δ 9.10-8.95 (2H, br s, 2 x OOH), 4.20-4.10 (2H, q, $J=7.1$ Hz, CH_2CH_3), 2.45-2.36 (1H, m, $J=3.7, 8.0$ Hz, $CHCO_2Et$), 2.27-2.19 (2H, dt, $J=3.7, 13.9$ Hz, 2 x CH), 1.96-1.88 (2H, dt, $J=3.7, 13.9$ Hz, 2 x CH), 1.82-1.71 (2H, m, 2 x CH), 1.65-1.56 (2H, m, 2 x CH), 1.26 (3H, t, $J=7.1$ Hz, CH_3).

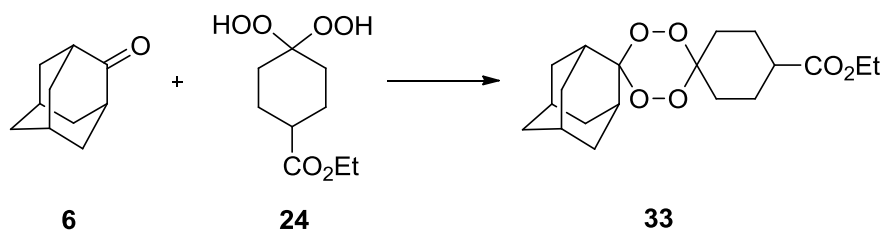
^{13}C NMR (100MHz, $CDCl_3$) δ 176.3 ($C=O$), 110.0 ($C-(OOH)_2$), 61.2 (CH_2CH_3), 42.2 (CH), 28.6 (2 x CH_2), 25.1 (2 x CH_2), 14.6 (CH_3).

$C_9H_{16}O_6$ requires C 49.08 %, H 7.32 % found C 48.33 %, H 7.65 %.

IR (neat)/ cm^{-1} : 3421 (O-H), 2942 (C-H), 1708 (C=O), 1446 (O-O), 1060 (C-O).

LRMS (CI); 188.2 $[(M-OOH)+H]^+$.

Synthesis of adamantane-2-spiro-3'-1',2',4',5'-tetraoxane-6'-spiro-1''-cyclohexane-4''-ethyl carboxylate **33**



Method 1

To a solution of 2-adamantanone **6** (110mg, 0.73mmol, 1.6eq) and Re₂O₇ (5mg, 0.01mmol, 2mol%) in DCM (15ml) was added ethyl 4,4-dihydroperoxycyclohexanecarboxylate **24** (105mg, 0.47mmol, 1eq) in DCM (15ml). The mixture was stirred at room temperature for 16hrs. The crude product was adsorbed onto silica gel and purified by flash column chromatography using EtOAc/petroleum ether (eluting with 5:95) to afford the product **33** (122mg, 50%) as a colourless solid.

Method 2

To a solution of 2-adamantanone **6** (105mg, 0.70mmol, 1.5eq) in DCM (10ml) was added MgSO₄ (99mg, 0.82mmol, 1.7eq) and PMA (16mg, 9.1μmol, 2mol%). The mixture was stirred at room temperature for 20mins. Ethyl 4,4-dihydroperoxycyclohexanecarboxylate **24** (104mg, 0.47mmol, 1eq) in DCM (10ml) was added drop-wise over 10mins and the mixture was stirred at room temperature for 3hrs. The crude product was adsorbed onto silica gel and purified by flash column chromatography using EtOAc/petroleum ether (eluting with 5:95) to afford the product **33** (142mg, 85%) as a colourless solid. In CHCl₃, 40% yield was obtained and in Et₂O, 30% yield was obtained.

Method 3

To a solution of 2-adamantanone **6** (111mg, 0.74mmol, 1.6eq) was added MgSO_4 (99mg, 0.82mmol, 1.9eq) and PMA (14mg, 8 μmol , 2mol%). The mixture was stirred at room temperature for 20mins. A solution of ethyl 4,4-dihydroperoxycyclohexanecarboxylate **24** (96mg, 0.44mmol, 1eq) in DCM (5ml) was added drop-wise over 5mins and the mixture was stirred at room temperature until TLC showed that the dihydroperoxide had all reacted (2hrs). Ethyl 4,4-dihydroperoxycyclohexanecarboxylate **24** (112mg, 0.51mmol, 1.2eq) in DCM (5ml) was added and the mixture left to stir at room temperature for 4hrs. The crude product was adsorbed onto silica gel and purified by flash column chromatography using EtOAc/petroleum ether (eluting with 5:95) to afford the product **33** (190mg, 73%) as a colourless solid.

^1H NMR (400MHz, CDCl_3) δ 4.13 (2H, q, $J=7.1$ Hz, CH_2CH_3), 2.10-1.55 (23H, m, adamantyl/cyclohexyl H), 1.25 (3H, t, $J=7.1$ Hz, CH_2CH_3).

^{13}C NMR (100MHz, CDCl_3) δ 175.0 ($\text{C}=\text{O}$), 110.9 (quaternary C), 107.6 (quaternary C), 60.8 (CH_2CH_3), 47.4 (CHCO_2Et), 42.0 (CH_2 bridgehead), 39.6 (2 x CH), 37.3 (2 x CH), 33.5 (4 x CH_2), 27.8 (2 x CH_2 cyclohexyl), 27.4 (2 x CH_2 cyclohexyl), 14.1 (CH_3).

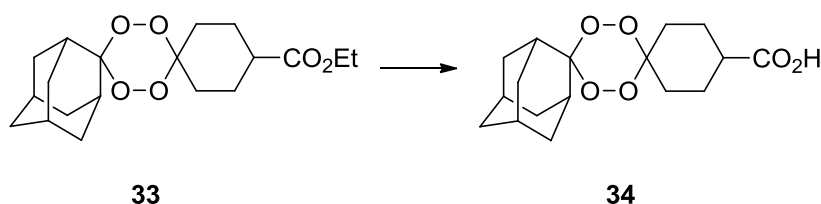
m.p 78-80°C

$\text{C}_{19}\text{H}_{28}\text{O}_6$ requires C 64.75 %, H 8.01 % found C 64.72 %, H 8.22 %.

IR (neat)/ cm^{-1} : 2935 (C-H), 1732 (C=O), 1442 (O-O), 1060 (C-O).

HRMS (ESI); 375.1783 $[\text{M}+\text{Na}]^+$, $\text{C}_{19}\text{H}_{28}\text{O}_6\text{Na}$ requires 375.1784.

Synthesis of adamantane-2-spiro-3'-1',2',4',5'-tetraoxane-6'-spiro-1''-cyclohexane-4''-carboxylic acid **34**



To a solution of adamantane-2-spiro-3'-1',2',4',5'-tetraoxane-6'-spiro-1''-cyclohexane-4''-ethyl carboxylate **33** (70mg, 0.20mmol) in MeOH (10ml) was added 15% aq. NaOH (10ml). The mixture was stirred at room temperature overnight and then acidified to pH 2 using 30% aq. HCl (10ml). The product was extracted with DCM (3 x 40ml). The combined organic extracts were dried (MgSO₄) and the solvent evaporated under reduced pressure to afford the product **34** (63mg, 97%) as a colourless solid.

¹H NMR (400MHz, CDCl₃) δ 3.20-1.25 (24H, m, adamantyl/cyclohexyl H).

¹³C NMR (100MHz, CDCl₃) δ 189.9 (C=O), 111.0 (quaternary C), 107.4 (quaternary C), 41.5, 39.7, 37.3, 33.5, 27.4.

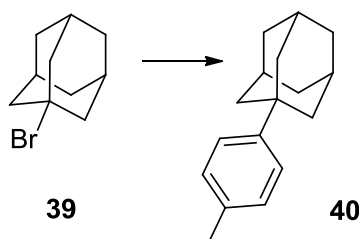
m.p 156-158°C

C₁₇H₂₄O₆ requires C 62.95 %, H 7.46 % found C 63.47 %, H 7.58 %.

IR (neat)/cm⁻¹: 2931 (C-H), 1685 (C=O), 1446 (O-O), 1060 (C-O).

HRMS (ESI); 347.1473 [M+Na]⁺, C₁₇H₂₄O₆Na requires 347.1471.

Synthesis of 1-(4-tolyl)adamantane **40**⁶



1-Bromoadamantane **39** (103mg, 0.48mmol) and FeCl₃ (9mg, 0.06mmol, 12mol%) was added to toluene (5ml). The reaction mixture turned a red/brown colour and was stirred at 140°C under a N₂ atmosphere for 23hrs. After cooling to room temperature, the reaction mixture was washed with 2M HCl (50ml) and the product extracted with DCM (3 x 40ml). The combined organic extracts were dried (MgSO₄) and the crude product adsorbed onto silica gel and purified by flash column chromatography using petroleum ether (100%) to afford the product **40** (90mg, 83%) as a colourless solid.

^1H NMR (400MHz, CDCl_3) δ 7.28-7.25 (2H, d, $J=8.1$ Hz, 2 x aromatic $\underline{\text{H}}$), 7.14-7.12 (2H, d, $J=8.1$ Hz, 2 x aromatic $\underline{\text{H}}$), 2.32 (3H, s, $\underline{\text{CH}_3}$), 2.09 (3H, br s, 3 x $\underline{\text{CH}}$), 1.90 (6H, s, 3 x $\underline{\text{CH}_2}$), 1.80-1.73 (6H, m, 3 x $\underline{\text{CH}_2}$).

^{13}C NMR (100MHz, CDCl_3) δ 148.9 (quaternary aromatic $\underline{\text{C}}$), 135.3 (quaternary aromatic $\underline{\text{C}}$), 129.2 (2 x aromatic $\underline{\text{C}}$), 125.1 (2 x aromatic $\underline{\text{C}}$), 43.7, 37.2, 36.2 (quaternary adamantyl $\underline{\text{C}}$), 29.4, 21.3 ($\underline{\text{CH}_3}$).

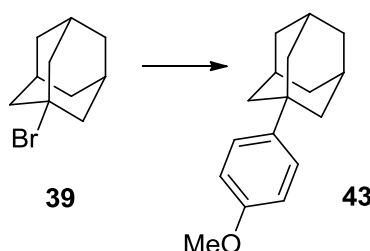
m.p 83-85°C

$\text{C}_{17}\text{H}_{22}$ requires C 90.20 %, H 9.80 % found C 89.73 %, H 10.08 %.

IR (neat)/ cm^{-1} : 2908 (C-H aryl), 2850 (C-H alkyl), 1511 (C=C).

LRMS (CI): 226.2 $[\text{M}+\text{H}]^+$.

Synthesis of 1-(4-methoxyphenyl)adamantane **43**



1-Bromoadamantane **39** (108mg, 0.50mmol) and FeCl_3 (111mg, 0.68mmol) were added to anisole (5ml). The reaction mixture turned a red/brown colour and was stirred at 155°C under a N_2 atmosphere for 21hrs. After cooling to room temperature, the reaction mixture was washed with 2M HCl (50ml) and the product extracted with DCM (3 x 40ml). The combined organic extracts were dried (MgSO_4) and the crude product adsorbed onto silica gel and purified by flash column chromatography using EtOAc/petroleum ether (eluting with 4:96) to afford the product **43** (120mg, 99%) as a colourless solid.

^1H NMR (400MHz, CDCl_3) δ 7.30-7.27 (2H, d, $J=8.9$ Hz, 2 x aromatic $\underline{\text{CH}}$), 6.88-6.83 (2H, d, $J=8.9$ Hz, 2 x aromatic $\underline{\text{CH}}$), 3.79 (3H, s, OCH_3), 2.10-2.05 (3H, br s, 3 x adamantyl $\underline{\text{CH}}$), 1.90-1.87 (6H, br d, 3 x adamantyl $\underline{\text{CH}_2}$), 1.81-1.69 (6H, br m, 3 x adamantyl $\underline{\text{CH}_2}$).

^{13}C NMR (100MHz, CDCl_3) δ 157.7 ($\text{C}-\text{OCH}_3$), 144.1 (quaternary aromatic C), 126.2 (2 x aromatic C), 113.8 (2 x aromatic C), 55.6 (OCH_3), 43.8 (quaternary adamantyl C), 37.2, 35.9, 29.4.

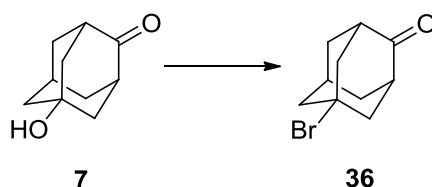
m.p 70-72°C

$\text{C}_{17}\text{H}_{22}\text{O}$ requires C 84.25 %, H 9.15 % found C 84.07 %, H 9.37 %.

IR (neat)/ cm^{-1} : 2912 (C-H aryl), 2850 (C-H alkyl), 1511 (C=C), 1180 (C-O).

LRMS (CI): 242.0 $[\text{M}+\text{H}]^+$.

Synthesis of 5-bromo-2-adamantanone **36**⁷



5-Hydroxy-2-adamantanone **7** (0.80g, 4.83mmol) was added to 48% aq. HBr (50ml) and stirred at 124°C for 24hrs. After cooling to room temperature, the reaction mixture was added to water (125ml) and the product extracted with Et_2O (4 x 40ml). The combined organic extracts were washed with brine (40ml), dried (MgSO_4) and the solvent evaporated under reduced pressure to afford the product **36** (0.62g, 56%) as a pale orange solid.

^1H NMR (400MHz, CDCl_3) δ 2.67-2.50 (8H, m, 4 x CH_2), 2.26 (1H, br s, CH), 2.13-1.94 (4H, m).

^{13}C NMR (100MHz, CDCl_3) δ 215.0 ($\text{C}=\text{O}$), 60.3 ($\text{C}-\text{Br}$), 49.5 (2 x CH_2 next to C-Br), 49.4 (2 x CH next to $\text{C}=\text{O}$), 48.2 (CH_2CBr), 37.9 (2 x CH_2), 31.7 (CH).

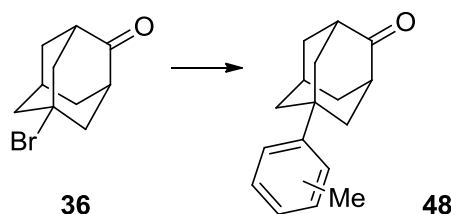
m.p 143-146°C

$\text{C}_{10}\text{H}_{13}\text{BrO}$ requires C 52.42 %, H 5.72 % found C 53.07 %, H 5.84 %.

IR (neat)/ cm^{-1} : 2927 (C-H), 1724 ($\text{C}=\text{O}$), 651 (C-Br).

HRMS (ESI); 229.0218 $[M+H]^+$, $C_{10}H_{13}O^{79}Br$ requires 229.0223 and 231.0196 $[M+H]^+$, $C_{10}H_{13}O^{81}Br$ requires 231.0203.

Synthesis of 5-(*o/p*-tolyl)adamantan-2-one **48**



5-Bromo-2-adamantanone **36** (110mg, 0.48mmol) and $FeCl_3$ (116mg, 0.72mmol) were added to toluene (5ml) and stirred at 125°C under a N_2 atmosphere for 24hrs. After cooling to room temperature, the reaction mixture was washed with 2M HCl (40ml) and the product extracted with DCM (3 x 40ml). The combined organic extracts were dried ($MgSO_4$) and the crude product adsorbed onto silica gel and purified by flash column chromatography using EtOAc/petroleum ether (eluting with 10:90) to afford the product **48** (103mg, 89%, ratio of regioisomers 1:10, ortho:para) as a colourless solid.

1H NMR (400MHz, $CDCl_3$) δ 7.25-7.23 (2H, d, $J=8.20$ Hz, 2 x aromatic H), 7.16-7.13 (2H, d, $J=8.20$ Hz, 2 x aromatic H), 2.69-2.64 (2H, br s, 2 x $\underline{CHC=O}$), 2.43-2.02 (14H, m, adamantyl H).

^{13}C NMR (100MHz, $CDCl_3$) δ 200.6 ($\underline{C=O}$), 145.5 (quaternary aromatic \underline{C}), 136.2 (quaternary aromatic \underline{C}), 129.5 (2 x aromatic \underline{C}), 126.0 (2 x aromatic \underline{C}), 47.1 ($\underline{CH_2}$), 44.9 (2 x $\underline{CHC=O}$), 43.1 (2 x $\underline{CH_2}$), 38.9 (2 x $\underline{CH_2}$ bridgehead), 36.2 (quaternary \underline{C}), 28.6 (\underline{CH}), 21.2 ($\underline{CH_3}$).

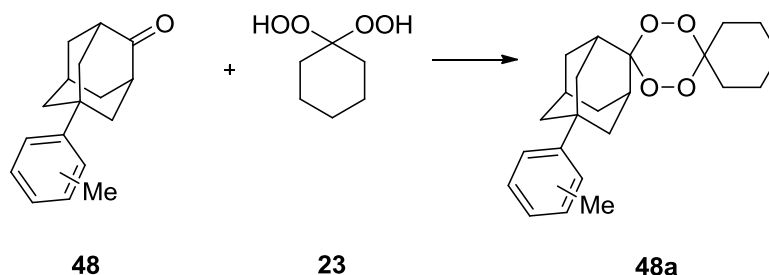
m.p 52-54°C

$C_{17}H_{20}O$ requires C 84.96 %, H 8.39 % found C 84.67 %, H 8.23 %.

IR (neat)/ cm^{-1} : 2927 (C-H aryl), 2824 (C-H alkyl), 1720 (C=O), 1454 (C=C).

LRMS (CI): 241.3 $[M+H]^+$, 258.3 $[M+NH_4]^+$.

Synthesis of 5-(*o/p*-tolyl)adamantane-2-spiro-3'-1',2',4',5'-tetraoxane-6'-spiro-1''-cyclohexane **48a**



To a solution of 5-(*o/p*-tolyl)adamantan-2-one **48** (71mg, 0.30mmol, 1.1eq) and Re_2O_7 (12mg, 0.02mmol, 6mol%) in DCM (10ml) was added 1,1-dihydroperoxycyclohexane **23** (44mg, 0.29mmol) in DCM (10ml). The mixture was stirred at room temperature for 4hrs. The crude product was adsorbed onto silica gel and purified by flash column chromatography using EtOAc/petroleum ether (eluting with 10:90) to afford the product **48a** (13mg, 12%) as a colourless solid.

^1H NMR (400MHz, CDCl_3) δ 7.25-7.22 (2H, d, $J=8.09$ Hz, 2 x aromatic H), 7.14-7.10 (2H, d, $J=8.09$ Hz, 2 x aromatic H), 2.35-1.40 (26H, m, adamantyl/cyclohexyl H).

^{13}C NMR (100MHz, CDCl_3) δ 146.9 (quaternary aromatic C), 135.7 (CCH₃), 129.3 (2 x aromatic C), 125.2 (2 x aromatic C), 110.2 (quaternary C), 108.6 (quaternary C), 42.7 (CH₂), 39.3 (quaternary C), 35.8 (2 x CH₂), 32.9 (2 x CH₂ bridgehead), 32.7 (2 x CH), 30.1 (CH), 28.2 (2 x CH₂), 25.8 (CH₂), 22.4 (2 x CH₂), 21.3 (CH₃).

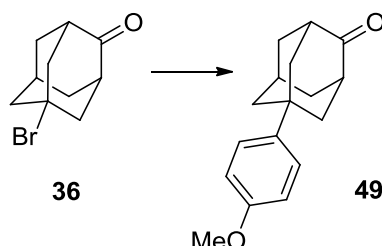
m.p 67-70°C

$\text{C}_{23}\text{H}_{30}\text{O}_4$ requires C 74.56 %, H 8.16 % found C 70.57 %, H 8.45 %.

IR (neat)/ cm^{-1} : 2935 (C-H), 2881 (C-H), 1446 (C=C), 1068 (C-O), 921 (O-O).

HRMS (ESI): 393.2038 $[\text{M}+\text{Na}]^+$, $\text{C}_{23}\text{H}_{30}\text{O}_4\text{Na}$ requires 393.2042.

Synthesis of 5-(4-methoxyphenyl)adamantan-2-one **49**



5-Bromo-2-adamantanone **36** (102mg, 0.45mmol) and FeCl_3 (106mg, 0.65mmol) were added to anisole (5ml). The red/brown reaction mixture was stirred at 155°C under N_2 for 23hrs. After cooling to room temperature, the reaction mixture was washed with 2M HCl (40ml) and the product extracted with DCM (3 x 30ml). The combined organic extracts were dried (MgSO_4) and the crude product adsorbed onto silica gel and purified by flash column chromatography using EtOAc/petroleum ether (eluting with 10:90) to afford the product **49** (30mg, 27%, para and 74mg, 65%, ortho) as a colourless solid.

^1H NMR (400MHz, CDCl_3) δ 7.28-7.25 (2H, d, $J=8.9$ Hz, 2 x aromatic H), 6.89-6.86 (2H, d, $J=8.9$ Hz, 2 x aromatic H), 3.80 (3H, s, OCH_3), 2.67-2.63 (br s, 2 x CH next to $\text{C}=\text{O}$), 2.30-2.03 (11H, m, adamantyl H).

^{13}C NMR (100MHz, CDCl_3) δ 218.5 (C=O), 158.3 (C-OMe), 140.6 (quaternary aromatic C), 126.2 (2 x aromatic C), 114.1 (2 x aromatic C), 55.7 (OCH_3), 47.1 (quaternary adamantyl C), 45.0 (2 x CH next to $\text{C}=\text{O}$), 42.6 (2 x CH}_2), 38.9 (2 x CH}_2), 35.9 (CH}_2), 28.6 (CH).

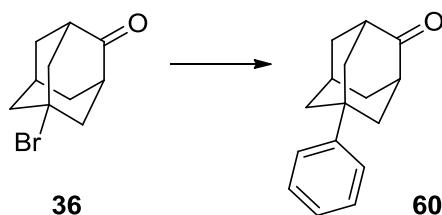
m.p $60\text{-}64^\circ\text{C}$

$\text{C}_{17}\text{H}_{20}\text{O}_2$ requires C 79.65 %, H 7.86 % found C 78.83 %, H 7.78 %.

IR (neat)/ cm^{-1} : 2927 (C-H), 1720 ($\text{C}=\text{O}$), 1515 ($\text{C}=\text{C}$), 1060 (C-O).

HRMS (ESI): 279.1362 $[\text{M}+\text{Na}]^+$, $\text{C}_{17}\text{H}_{20}\text{O}_2\text{Na}$ requires 279.1361.

Synthesis of 5-phenyladamantan-2-one **60**



Benzene (2ml) was added to 5-bromo-2-adamantanone **36** (32mg, 0.14mmol) and FeCl₃ (38mg, 0.23mmol, 1.6eq) and stirred at 70°C under N₂ for 30hrs. After cooling to room temperature, the reaction mixture was washed with 2M HCl (30ml), the product extracted with DCM (2 x 20ml), dried (MgSO₄) and the solvent removed under reduced pressure to afford the product **60** (22mg, 69%) as a brown, sticky solid.

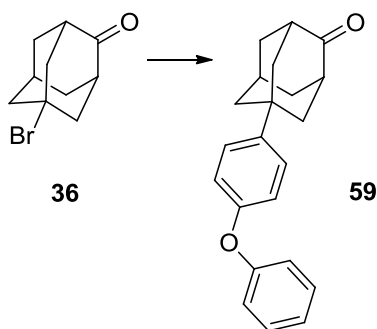
¹H NMR (400MHz, CDCl₃) δ 7.37-7.33 (4H, m, 4 x aromatic H), 7.24-7.20 (1H, m, aromatic H), 2.70-2.65 (2H, br s, 2 x CH=CO), 2.46-1.95 (11H, m, adamantyl H).

¹³C NMR (100MHz, CDCl₃) δ 200.8 (C=O), 137.8 (quaternary aromatic C), 128.8 (2 x aromatic C), 126.6. (2 x aromatic C), 125.2 (aromatic C), 48.4 (CH₂), 47.1 (2 x CHC=O), 42.4 (2 x CH₂), 38.9 (2 x CH₂ bridgehead), 36.5 (quaternary C), 28.6 (CH).

IR (neat)/cm⁻¹: 2919 (C-H), 2854 (C-H), 1716 (C=O).

LRMS (CI); 244.1 [M+NH₄]⁺.

Synthesis of 5-(4-phenoxyphenyl)adamantan-2-one **59**



5-Bromo-2-adamantanone **36** (50mg, 0.22mmol) and FeCl_3 (60mg, 0.37mmol, 1.7eq) was added to diphenylether (2ml) and stirred at 155°C under N_2 for 24hrs. After cooling to room temperature, the reaction mixture was washed with 2M HCl (40ml) and the product extracted with DCM (3 x 40ml). The combined organic extracts were dried (MgSO_4) and the crude product adsorbed onto silica gel and purified by flash column chromatography using EtOAc/petroleum ether (eluting with 10:90) to afford the product **59** (20mg, 29%) as a sticky, orange solid.

^1H NMR (400MHz, CDCl_3) δ 7.36-7.28 (4H, m, aromatic H), 7.12-7.07 (1H, m, aromatic H), 7.02-6.94 (4H, m, aromatic H), 2.70-2.65 (2H, br s, 2 x CH next to $\text{C}=\text{O}$), 2.30-2.02 (11H, m, adamantyl H).

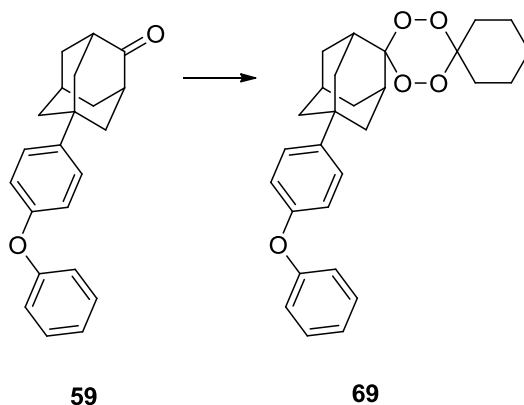
^{13}C NMR (100MHz, CDCl_3) δ 218.3 ($\text{C}=\text{O}$), 157.7 (quaternary aromatic C), 155.9 (quaternary aromatic C), 143.3 (quaternary aromatic C), 130.1 (2 x aromatic C), 126.5 (2 x aromatic C), 123.6 (aromatic C), 119.3 (2 x aromatic C), 119.0 (2 x aromatic C), 47.1 (CH₂ adamantyl), 45.0 (2 x CH next to $\text{C}=\text{O}$), 42.6 (2 x CH₂ adamantyl), 38.9 (2 x CH₂ adamantyl), 36.1 (quaternary adamantyl C), 28.6 (adamantyl CH).

$\text{C}_{22}\text{H}_{22}\text{O}_2$ requires C 82.99 %, H 6.96 % found C 80.12 %, H 6.61 %.

IR (neat)/ cm^{-1} : 2927 (C-H), 1720 ($\text{C}=\text{O}$), 1589 ($\text{C}=\text{C}$), 1234 (C-O).

HRMS (ESI): 341.1505 $[\text{M}+\text{Na}]^+$, $\text{C}_{22}\text{H}_{22}\text{O}_2\text{Na}$ requires 341.1517.

Synthesis of 5-(4-phenoxyphenyl)adamantyl-2-spiro-3'-1',2',4',5'-tetraoxane-6'-spiro-1''-cyclohexane **69**



To a solution of 5-(4-phenoxyphenyl)adamantan-2-one **59** (41mg, 0.13mmol, 1.0eq) and Re_2O_7 (23mg, 0.05mmol, 38mol%) in DCM (10ml) was added 1,1-dihydroperoxycyclohexane (21mg, 0.14mmol) in DCM (10ml). The mixture was stirred at room temperature for 3hrs. The crude product was adsorbed onto silica gel and purified by flash column chromatography using EtOAc/petroleum ether (eluting with 8:92) to afford the product **69** (5mg, 8%) as a colourless semi-solid.

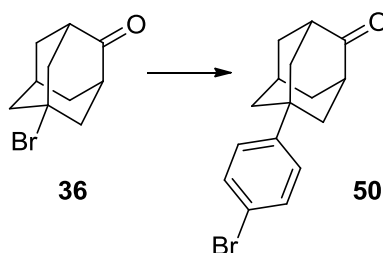
^1H NMR (400MHz, CDCl_3) δ 7.35-7.28 (4H, m, aromatic H), 7.11-7.06 (1H, m, aromatic H), 7.02-6.93 (4H, m, aromatic H), 2.35-1.41 (23H, m, adamantyl/cyclohexyl H).

^{13}C NMR (100MHz, CDCl_3) δ 167.1 (aromatic C-O), 155.3 (aromatic C-O), 140.4 (quaternary aromatic C), 130.1 (2 x aromatic C), 126.6 (2 x aromatic C), 123.4 (2 x aromatic C), 119.1 (aromatic C), 118.9 (2 x aromatic C), 110.1 (quaternary C), 108.6 (quaternary C), 42.9 (CH₂), 39.3 (quaternary C), 35.8 (2 x CH₂), 32.7 (2 x CH₂ bridgehead), 32.2 (2 x CH), 30.0 (CH), 28.2 (2 x CH₂), 25.8 (CH₂), 22.5 (2 x CH₂).

IR (neat)/ cm^{-1} : 2957 (C-H), 1604 (C=C aromatic), 1241 (C-O), 904 (O-O).

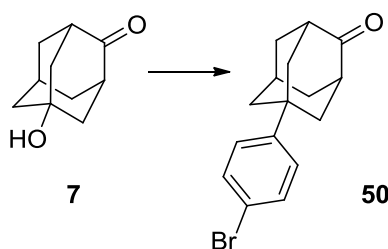
HRMS (ESI): 471.2139 $[\text{M}+\text{Na}]^+$, $\text{C}_{28}\text{H}_{32}\text{O}_5\text{Na}$ requires 471.2147.

Synthesis of 5-(4-bromophenyl)adamantan-2-one **50**



Method 1 – starting from 5-bromo-2-adamantanone

5-Bromo-2-adamantanone **36** (78mg, 0.34mmol) and FeCl_3 (92mg, 0.57mmol, 1.7eq) were added to bromobenzene (5ml) and stirred at 130°C under N_2 for 24hrs. The reaction mixture was washed with 2M HCl (50ml) and the product extracted with DCM (3 x 40ml). The combined organic extracts were dried (MgSO_4) and the crude product adsorbed onto silica gel and purified by flash column chromatography using EtOAc/petroleum ether (eluting with 10:90) to afford the product **50** (79mg, 76%) as a pale orange solid.



Method 2 – starting from 5-hydroxy-2-adamantanone

To a stirred solution of 5-hydroxy-2-adamantanone **7** (48mg, 0.29mmol) in bromobenzene (10ml) was added TfOH (0.03ml, 0.34mmol, 1.2eq) *slowly drop-wise* (**caution: fumes on addition**). The yellow-ish reaction mixture was left to stir at room temperature for 5mins. The reaction was then heated at 130°C for 1hr and a colour change from yellow to orange to brown was observed. After cooling to room temperature, the reaction mixture was quenched (*slow addition*) with aq. NaHCO₃ (10ml) at 0°C and the product extracted with Et₂O (2 x 30ml). The combined organic extracts were dried (Na₂SO₄) and the crude product adsorbed onto silica gel and purified by flash column chromatography using EtOAc/petroleum ether (eluting with 10:90) to afford the product **50** (52mg, 59%) as a pale orange solid.

¹H NMR (400MHz, CDCl₃) δ 7.46-7.43 (2H, d, *J*=8.8 Hz, 2 x aromatic H), 7.23-7.20 (2H, d, *J*=8.8 Hz, 2 x aromatic H), 2.67 (2H, br s, 2 x CH next to C=O), 2.31-2.02 (11H, m, adamantyl H).

¹³C NMR (100MHz, CDCl₃) δ 217.9 (C=O), 147.4 (quaternary aromatic C), 131.9 (2 x aromatic C), 127.1 (2 x aromatic C), 120.5 (C-Br), 46.9 (2 x CH next to C=O), 44.6, 42.3, 38.8, 36.3, 28.5.

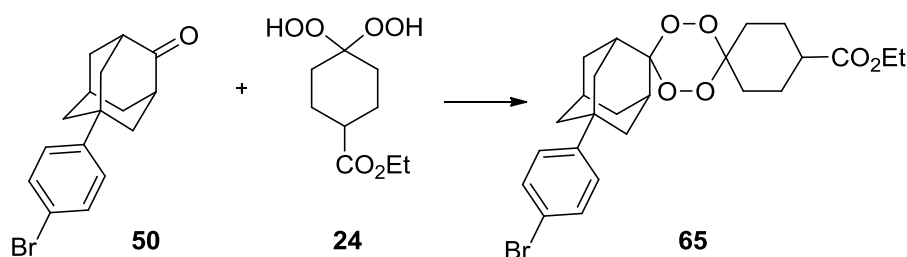
m.p 120-122°C

C₁₆H₁₇BrO requires C 62.96 %, H 5.61 % found C 62.74 %, H 5.44 %.

IR (neat)/cm⁻¹: 2927 (C-H aryl), 2857 (C-H alkyl), 1716 (C=O), 1492 (C=C), 628 (C-Br).

HRMS (ESI); 327.0366 [M+Na]⁺, C₁₆H₁₇ONa⁷⁹Br requires 327.0360 and 329.0355 [M+Na]⁺, C₁₆H₁₇ONa⁸¹Br requires 329.0340.

Synthesis of 5-(4-bromophenyl)adamantane-2-spiro-3'-1',2',4',5'-tetraoxane-6'-spiro-1''-cyclohexane-4''-ethyl carboxylate **65**



Method 1

To a solution of 5-(4-bromophenyl)adamantan-2-one **50** (320mg, 1.05mmol, 1.1eq) and Re₂O₇ (26mg, 0.05mmol, 6mol%) in DCM (15ml) was added ethyl 4,4-dihydroperoxycyclohexanecarboxylate **24** (210mg, 0.96mmol, 1eq) in DCM (15ml). The mixture was stirred at room temperature for 4hrs. The crude product was adsorbed onto silica gel and purified by flash column chromatography using EtOAc/petroleum ether (eluting with 8:92) to afford the product **65** (120g, 24%) as a colourless solid.

Method 2

To a solution of 5-(4-bromophenyl)adamantan-2-one **50** (83mg, 0.27mmol, 1.1eq) was added MgSO₄ (59mg, 0.50mmol 2eq) and PMA (9mg, 5μmol, 2mol%) and stirred at room temperature for 20mins. Ethyl 4,4-dihydroperoxycyclohexanecarboxylate **24** (54mg, 0.25mmol, 1eq) in DCM (5ml) was added drop-wise over 10mins and the mixture stirred at room temperature for 4hrs. The crude product was adsorbed onto silica gel and purified by flash column chromatography using EtOAc/petroleum ether (eluting with 8:92) to afford the product **65** (46mg, 37%) as a colourless solid.

Method 3

To a solution of 5-(4-bromophenyl)adamantan-2-one **50** (77mg, 0.25mmol, 1.07eq) was added MgSO_4 (53mg, 0.44mmol, 1.8eq) and PMA (18mg, 10 μmol , 4mol%) and stirred at room temperature for 20mins. Ethyl 4,4-dihydroperoxycyclohexanecarboxylate **24** (52mg, 0.24mmol, 1eq) in DCM (5ml) was added drop-wise over 5mins and the mixture stirred at room temperature until TLC showed that all of the dihydroperoxide had reacted (2hrs). Ethyl 4,4-dihydroperoxycyclohexanecarboxylate **24** (54mg, 0.25mmol, 1eq) in DCM (5ml) was added and the mixture was left to stir at room temperature for 4hrs. The crude product was adsorbed onto silica gel and purified by flash column chromatography using EtOAc/petroleum ether (eluting with 8:92) to afford the product **65** (54mg, 42%) as a colourless solid.

^1H NMR (400MHz, CDCl_3) δ 7.43-7.40 (2H, d, $J=8.6$ Hz, 2 x aromatic H), 7.23-7.19 (2H, d, $J=8.6$ Hz, 2 x aromatic H), 4.17-4.11 (2H, q, $J=7.1$ Hz, CH_2CH_3), 2.45-1.50 (22H, m, adamantyl/cyclohexyl H), 1.27-1.23 (3H, t, $J=7.1$ Hz, CH_2CH_3).

^{13}C NMR (100MHz, CDCl_3) δ 175.0 ($\text{C}=\text{O}$), 148.7 (quaternary aromatic C), 131.6 (2 x aromatic C), 127.2 (2 x aromatic C), 120.1 ($\text{C}-\text{Br}$), 110.2 (quaternary C), 107.8 (quaternary C), 60.9 ($\text{O}-\text{CH}_2\text{CH}_3$), 42.5 ($\text{C}-\text{CO}_2\text{Et}$), 42.0, 41.9, 39.0, 36.0, 32.5, 28.0, 14.6 ($\text{O}-\text{CH}_2\text{CH}_3$).

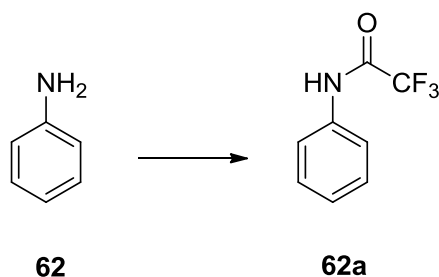
m.p 102-105°C

$\text{C}_{25}\text{H}_{31}\text{BrO}_6$ requires C 59.18 %, H 6.16 % found C 59.05 %, H 6.05 %.

IR (neat)/ cm^{-1} : 2938 (C-H aryl), 2861 (C-H alkyl), 1724 (C=O), 1450 (O-O), 1056 (C-O).

HRMS (ESI); 529.1185 $[\text{M}+\text{Na}]^+$, $\text{C}_{25}\text{H}_{31}\text{O}_6\text{Na}^{79}\text{Br}$ requires 529.1202 and 531.1159 $[\text{M}+\text{Na}]^+$, $\text{C}_{25}\text{H}_{31}\text{O}_6\text{Na}^{81}\text{Br}$ requires 531.1181.

Synthesis of 2,2,2-trifluoro-*N*-phenylacetamide **62a**⁸



To a stirred solution of aniline **62** (0.35ml, 3.83mmol) in dry DCM (15ml) was added TFAA (1.50ml, 10.60mmol, 2.8eq) and the reaction mixture changed from colourless to pink. NEt₃ (3.50ml, 25.00mmol, 6.5eq) was added *slowly drop-wise* over 10mins (**caution: fumes on addition**) and the reaction mixture changed from pink to yellow. After stirring at room temperature for 4hrs, water (30ml) was added and the product extracted with DCM (3 x 30ml). The combined organic extracts were dried (MgSO₄) and the crude product adsorbed onto silica gel and purified by flash column chromatography using EtOAc/petroleum ether (eluting with 8:92) to afford the product **62a** (0.53g, 73%) as a colourless solid.

¹H NMR (400MHz, CDCl₃) δ 7.59-7.55 (2H, d, *J*=7.9 Hz, 2 x aromatic H), 7.43-7.38 (2H, t, *J*=15.9, 7.9 Hz, 2 x aromatic H), 7.27-7.25 (1H, m, aromatic H).

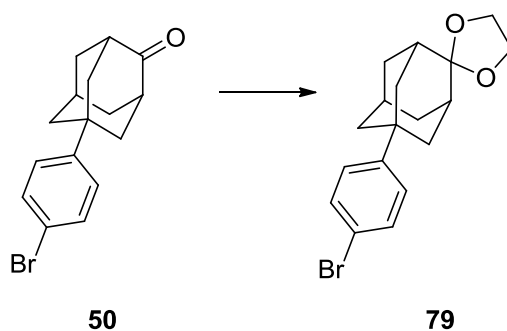
¹³C NMR (100MHz, CDCl₃) δ 155.0 (C=O), 135.4 (C-NH), 129.8 (2 x aromatic C), 126.8 (aromatic C), 120.9 (2 x aromatic C), 117.5 (CF₃).

m.p 78-80°C

IR (neat)/cm⁻¹: 3320 (N-H), 2972 (C-H aryl), 1700 (C=O), 1546 (C=C).

LRMS (CI); 189.2 [M+H]⁺, 207.2 [M+NH₄]⁺.

Synthesis of 5-(4-bromophenyl)spiro[adamantane-2,2'-[1,3]dioxolane] **79**



To a stirred solution of 5-(4-bromophenyl)adamantan-2-one **50** (254mg, 0.83mmol) and *p*-toluenesulfonic acid (62mg, 0.36mmol) in toluene (30ml) was added ethylene glycol (0.1ml, 1.8mmol, 2.2eq) and the resulting mixture was refluxed in a Dean Stark apparatus for 24hrs. The reaction mixture was allowed to cool to room temperature, 20% aq. K₂CO₃ (50ml) was added and the product extracted with toluene (2 x 40ml). The combined organic extracts were dried (Na₂SO₄) and the crude product adsorbed onto silica gel and purified by flash column chromatography using EtOAc/petroleum ether (eluting with 8:92) to afford the product **79** (260mg, 89%) as a colourless solid.

¹H NMR (400MHz, CDCl₃) δ 7.25-7.22 (2H, d, *J*=8.7 Hz, 2 x aromatic H), 7.07-7.04 (2H, d, *J*=8.7 Hz, 2 x aromatic H), 3.80 (4H, s, 2 x CH₂), 2.05-2.00 (2H, d, 2 x CH next to C-O), 1.87-1.45 (11H, m, adamantyl H).

¹³C NMR (100MHz, CDCl₃) δ 149.5 (quaternary aromatic C), 131.5 (2 x aromatic C), 127.3 (quaternary C), 119.8 (2 x aromatic C), 111.1 (C-Br), 64.8 (2 x CH₂), 42.7 (CH₂), 40.9 (2 x CH next to C-O), 37.2 (quaternary aliphatic C), 36.0 (2 x CH₂), 34.3 (2 x CH₂), 27.8 (CH).

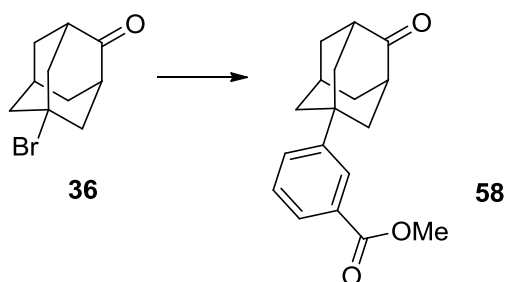
m.p 63-65°C

C₁₈H₂₁BrO₂ requires C 61.90 %, H 6.06 % found C 61.77 %, H 5.98 %.

IR (neat)/cm⁻¹: 2911 (C-H alkyl), 1621 (C=C aromatic), 1126 (C=O), 674 (C-Br).

HRMS (ESI); 349.0798 [M+H]⁺, C₁₈H₂₂O₂⁷⁹Br requires 349.0803 and 351.0784 [M+H]⁺, C₁₈H₂₂O₂⁸¹Br requires 351.0783.

Synthesis of methyl 3-(4-oxoadamantan-1-yl)benzoate **58**



Methyl benzoate (2ml, 2.20mmol) was added to 5-bromo-2-adamantanone **36** (50mg, 0.22mmol) and FeCl_3 (54mg, 0.32mmol, 1.5eq) and stirred at 170°C under N_2 for 3 days. After cooling to room temperature, the reaction mixture was washed with 2M HCl (40ml) and the product extracted with DCM (3 x 40ml). The combined organic extracts were dried (MgSO_4) and the crude product adsorbed onto silica gel and purified by flash column chromatography using EtOAc/petroleum ether (eluting with 10:90) to afford the product **58** (28mg, 45%) as a colourless, sticky semi-solid.

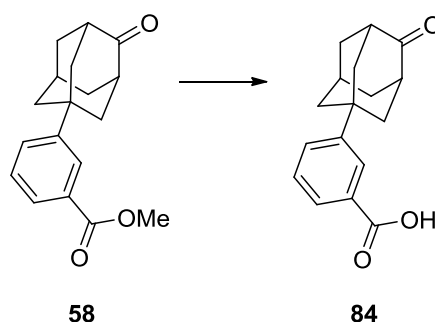
^1H NMR (400MHz, CDCl_3) δ 8.07-8.04 (1H, br m, aromatic H), 7.93-7.88 (1H, br m, aromatic H), 7.65-7.60 (1H, m, aromatic H), 7.56-7.53 (1H, m, aromatic H), 3.94 (3H, s, OCH_3), 2.71-2.69 (2H, br s, 2 x CH next to $\text{C}=\text{O}$), 2.30-2.05 (11H, m, adamantyl H).

^{13}C NMR (100MHz, CDCl_3) δ 218.1 ($\text{C}=\text{O}$ ketone), 167.6 ($\text{C}=\text{O}$ ester), 148.7 (quaternary aromatic C), 134.1 (aromatic C), 130.7 (aromatic C), 128.9 (aromatic C), 127.9 (aromatic C), 126.6 (aromatic C), 52.6 (OCH_3), 47.0, 44.6, 42.4, 38.8, 36.6 (quaternary adamantyl C), 28.5.

$\text{C}_{18}\text{H}_{20}\text{O}_3$ requires C 76.03 %, H 7.09 % found C 76.11 %, H 6.97 %.

HRMS (ESI); 307.1318 $[\text{M}+\text{Na}]^+$, $\text{C}_{18}\text{H}_{21}\text{O}_3\text{Na}$ requires 307.1310 and 285.1487 $[\text{M}+\text{H}]^+$, $\text{C}_{18}\text{H}_{21}\text{O}_3$ requires 285.1491.

Synthesis of 3-(4-oxoadamantan-1-yl)benzoic acid **84**



To a solution of methyl 3-(4-oxoadamantan-1-yl)benzoate **58** (125mg, 0.44mmol) in MeOH (5ml) was added 15% aq. NaOH (5ml). The mixture was stirred at 65°C for 6hrs and then acidified to pH 2 using 2M HCl (15ml). The product was extracted with DCM (3 x 20ml). The combined organic extracts were dried (MgSO_4) and the solvent evaporated under reduced pressure to afford the product **84** (80mg, 66%) as a colourless solid.

^1H NMR (400MHz, CDCl_3) δ 8.15-8.07 (1H, m, aromatic H), 8.01-7.97 (1H, m, aromatic H), 7.65-7.60 (1H, m, aromatic H), 7.51-7.44 (1H, m, aromatic H), 2.73-2.68 (2H, br s, 2 x CH next to $\text{C}=\text{O}$), 2.35-2.05 (12H, m, adamantyl H).

^{13}C NMR (100MHz, CDCl_3) δ 218.2 ($\text{C}=\text{O}$ ketone), 172.2 ($\text{C}=\text{O}$ acid), 148.9 (quaternary aromatic C), 134.2 (aromatic C), 130.6 (quaternary aromatic C), 128.9 (aromatic C), 128.6 (aromatic C), 127.2 (aromatic C), 47.0, 44.6, 42.4, 38.8, 36.6 (quaternary adamantyl C), 28.5.

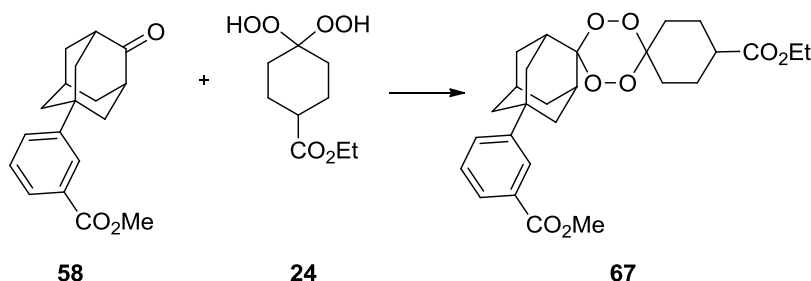
m.p 204-206°C

$\text{C}_{17}\text{H}_{18}\text{O}_3$ requires C 75.53 %, H 6.71 % found C 73.07 %, H 6.41 %.

IR (neat)/ cm^{-1} : 3000 (OH), 2927 (C-H), 1715, ($\text{C}=\text{O}$), 1735 ($\text{C}=\text{O}$), 1650 (C=C).

LRMS (CI); 288.3 $[\text{M}+\text{NH}_4]^+$.

Synthesis of methyl 3-(4-oxoadamantan-1-yl)benzoate-2-spiro-3'-1',2',4',5'-tetraoxane-6'-spiro-1''-cyclohexane-4''-ethyl carboxylate **67**



To a solution of methyl 3-(4-oxoadamantan-1-yl)benzoate **58** (83mg, 0.29mmol, 1.04eq) and Re_2O_7 (44mg, 0.09mmol, 32mol%) in DCM (10ml) was added ethyl 4,4-dihydroperoxycyclohexanecarboxylate **24** (63mg, 0.28mmol) in DCM (10ml). The mixture was stirred at room temperature for 4hrs. The crude product was adsorbed onto silica gel and purified by flash column chromatography using EtOAc/petroleum ether (eluting with 8:92) to afford the product **67** (19mg, 14%) as a colourless, sticky semi-solid.

^1H NMR (400MHz, CDCl_3) δ 8.03-8.01 (1H, br m, aromatic H), 7.89-7.85 (1H, br m, aromatic H), 7.57-7.53 (1H, br m, aromatic H), 7.41-7.36 (1H, br m, aromatic H), 4.18-4.10 (2H, q, $J=7.1$ Hz, CH_2CH_3), 3.92 (3H, s, OCH_3), 1.60-1.45 (22H, m, adamantyl/cyclohexyl H), 1.28-1.23 (3H, t, CH_2CH_3).

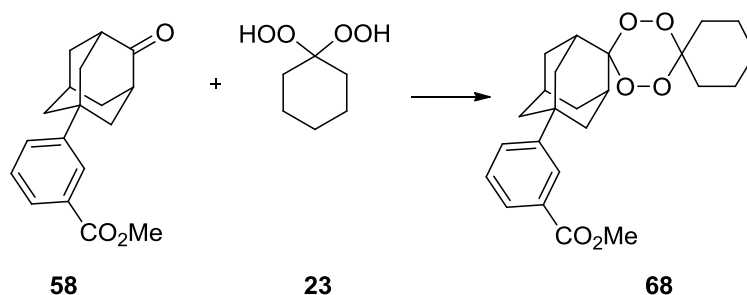
^{13}C NMR (100MHz, CDCl_3) δ 175.0 ($\text{C}=\text{O}$ ester), 167.8 ($\text{C}=\text{O}$ ester), 148.7 (quaternary aromatic C), 130.5 (aromatic C), 130.0 (aromatic C), 128.7 (aromatic C), 127.7 (aromatic C), 126.6 (aromatic C), 110.2 (quaternary C), 107.9 (quaternary C), 60.9 ($\text{O}-\text{CH}_2\text{CH}_3$), 52.5 (OCH_3), 42.7, 42.0, 41.9, 39.0, 36.3, 32.6, 28.1, 14.6 ($\text{O}-\text{CH}_2\text{CH}_3$).

m.p 52-54°C

IR (neat)/ cm^{-1} : 2935 (C-H), 1720 (C=O ester), 1184 (C-O), 937 (O-O).

HRMS (ESI); 509.2160 $[\text{M}+\text{Na}]^+$, $\text{C}_{27}\text{H}_{34}\text{O}_8\text{Na}$ requires 509.2151.

Synthesis of methyl 3-(4-oxoadamantan-1-yl)benzoate-2-spiro-3'-1',2',4',5'-tetraoxane-6'-spiro-1''-cyclohexane **68**



Method 1

To a solution of methyl 3-(4-oxoadamantan-1-yl)benzoate **58** (180mg, 0.63mmol, 1.01eq) and Re_2O_7 (60mg, 0.12mmol, 20mol%) in DCM (10ml) was added 1,1-dihydroperoxycyclohexane **23** (93mg, 0.62mmol, 1eq) in DCM (10ml). The mixture was stirred at room temperature for 4hrs. The crude product was adsorbed onto silica gel and purified by flash column chromatography using EtOAc/petroleum ether (eluting with 5:95) to afford the product **68** (20mg, 8%) as a colourless, sticky semi-solid.

Method 2

To a solution of methyl 3-(4-oxadamantan-1-yl)benzoate **58** (101mg, 0.36mmol, 1.1eq) was added MgSO_4 (75mg, 0.62mmol, 1.8eq) and PMA (11mg, 6 μmol , 2mol%). The mixture was stirred at room temperature for 20mins. 1,1-dihydroperoxycyclohexane **23** (50mg, 0.34mmol, 1eq) in DCM (10ml) was added drop-wise over 10mins and the mixture was stirred at room temperature for 3hrs. The crude product was adsorbed onto silica gel and purified by flash column chromatography using EtOAc/petroleum ether (eluting with 5:95) to afford the product **68** (20mg, 14%) as a colourless solid.

Method 3

To a solution of methyl 3-(4-oxadamantan-1-yl)benzoate **58** (60mg, 0.21mmol, 1.04eq) was added MgSO_4 (45mg, 0.37mmol, 1.8eq) and PMA (23mg, 12 μmol , 6mol%). The mixture was stirred at room temperature for 20mins. A solution of 1,1-dihydroperoxycyclohexane **23** (30mg, 0.20mmol, 1eq) in DCM (5ml) was added drop-wise over 5mins and the mixture was stirred at room temperature until TLC showed that all of the dihydroperoxide had reacted (1hr). 1,1-dihydroperoxycyclohexane **23** (30mg, 0.20mmol, 1eq) in DCM (5ml) was added and the reaction mixture left to stir at room temperature for 2hrs. The crude product was adsorbed onto silica gel and purified by flash column chromatography using EtOAc/petroleum ether (eluting with 5:95) to afford the product **68** (20mg, 22%) as a colourless solid.

^1H NMR (400MHz, CDCl_3) δ 8.04-8.02 (1H, br m, aromatic H), 7.89-7.85 (1H, br dt, aromatic H), 7.57-7.54 (1H, br m, aromatic H), 7.40-7.36 (1H, br m, aromatic H), 3.91 (3H, s, OCH_3), 2.40-1.60 (23H, m, adamantly/cyclohexyl H).

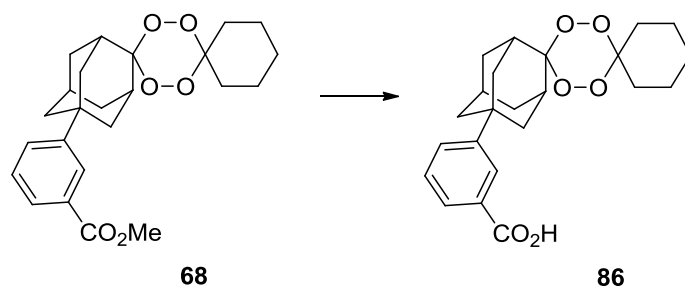
^{13}C NMR (100MHz, CDCl_3) δ 167.1 ($\text{C}=\text{O}$), 150.2 (quaternary aromatic C), 130.5 (quaternary aromatic C), 130.1 (aromatic C), 128.7 (aromatic C), 127.6 (aromatic C), 126.6 (aromatic C), 110.0 (quaternary C), 108.7 (quaternary C), 52.5 ($\text{O}-\text{CH}_3$), 44.6, 42.7, 39.0, 37.2, 36.3, 32.6, 28.1, 25.8.

$\text{C}_{24}\text{H}_{30}\text{O}_6$ requires C 69.54 %, H 7.30 % found C 69.24 %, H 7.19 %.

IR (neat)/ cm^{-1} : 2978 (C-H aryl), 2928 (C-H alkyl), 1749 (C=O), 1430 (O-O), 1046 (C-O).

HRMS (ESI); 437.1938 $[\text{M}+\text{Na}]^+$, $\text{C}_{24}\text{H}_{30}\text{O}_6\text{Na}$ requires 437.1940.

Synthesis of 3-(4-oxadamantan-1-yl)benzoic acid-2-spiro-3'-1',2',4',5'-tetraoxane-6'-spiro-1''-cyclohexane **86**



To a solution of methyl 3-(4-oxadamantan-1-yl)benzoate-2-spiro-3'-1',2',4',5'-tetraoxane-6'-spiro-1''-cyclohexane **68** (20mg, 0.05mmol) in MeOH (5ml) was added 15% aq. NaOH (5ml). The mixture was stirred at 65°C for 5hrs and then acidified to pH 2 using 2M HCl (10ml). The product was extracted with DCM (3 x 10ml). The combined organic extracts were dried (MgSO₄) and the solvent evaporated under reduced pressure to afford the product **86** (19mg, 100%) as a colourless solid.

¹H NMR (400MHz, CDCl₃) δ 8.10-8.07 (1H, br s, aromatic H), 7.95-7.91 (1H, m, aromatic H), 7.61-7.59 (1H, m, aromatic H), 7.45-7.39 (1H, m, aromatic H), 2.40-1.20 (24H, m, adamantyl/cyclohexyl H).

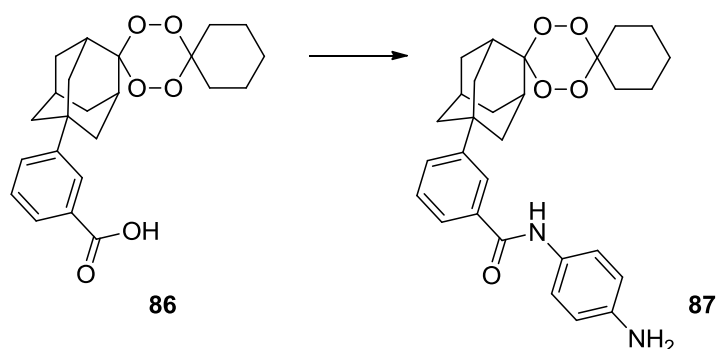
¹³C NMR (100MHz, CDCl₃) δ 160.1 (C=O), 145.1 (quaternary aromatic C), 131.4 (quaternary aromatic C), 130.5 (aromatic C), 128.2 (aromatic C), 127.3 (aromatic C), 126.6 (aromatic C), 110.2 (quaternary C), 108.5 (quaternary C), 43.7, 41.2, 40.4, 38.0, 35.3, 33.5, 27.1, 24.9.

C₂₃H₂₈O₆ requires C 68.98 %, H 7.05 % found C 68.89 %, H 7.06 %.

IR (neat)/cm⁻¹: 3049 (OH), 2978 (C-H alkyl), 1724 (C=O), 1280 (C-O).

HRMS (ESI); 399.1804 [M-H]⁻, C₂₃H₂₇O₆ requires 399.1808.

Synthesis of *N*-(4-aminophenyl)-3-(4-oxoadamantan-1-yl)benzamide-2-spiro-3'-1',2',4',5'-tetraoxane-6'-spiro-1''-cyclohexane **87**

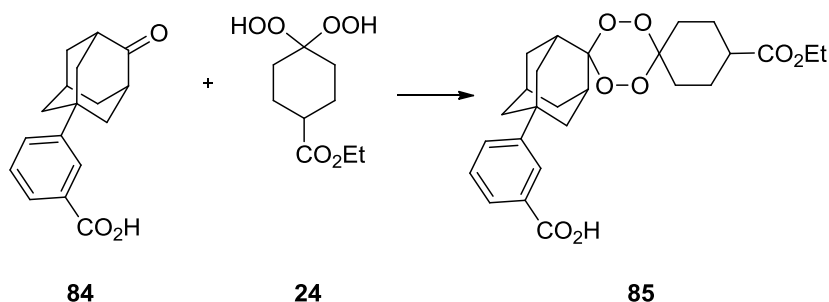


EDC.HCl (20mg, 0.1mmol, 1.6eq), HOBT (10mg, 0.07mmol, 1.2eq) and NMM (0.02ml, 0.18mmol, 3eq) were added to a stirred solution of 3-(4-oxoadamantan-1-yl)benzoic acid-2-spiro-3'-1',2',4',5'-tetraoxane-6'-spiro-1''-cyclohexane **86** (25mg, 0.06mmol, 1eq) in DMF (5ml) at 0°C. The mixture was stirred at room temperature for 3hrs under a N₂ atmosphere. *p*-Phenylenediamine (13mg, 0.12mmol, 2eq) in DMF (5ml) was added and the mixture was stirred at room temperature overnight before quenching with water (30ml), the product was extracted with Et₂O (3 x 20ml) and dried (MgSO₄). The crude product adsorbed onto silica gel and purified by flash column chromatography using EtOAc/petroleum ether (eluting with 70:30) to afford the product **87** (4mg, 12%) as a sticky yellow oil.

IR (neat)/cm⁻¹: 3343 (N-H), 2919 (C-H), 1596 (C=O), 1060 (C-O), 933 (O-O).

LRMS (ESI): 513.2 [M+Na]⁺.

Synthesis of 3-(4-oxoadamantan-1-yl)benzoic acid-2-spiro-3'-1',2',4',5'-tetraoxane-6'-spiro-1''-cyclohexane-4''-ethyl carboxylate **85**

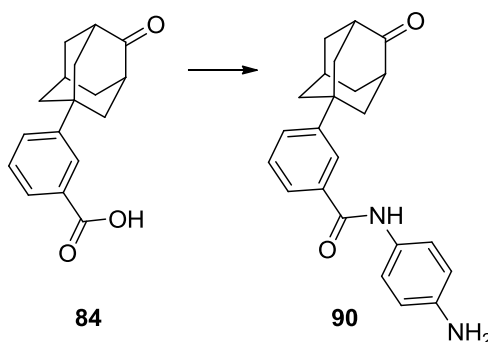


To a solution of 3-(4-oxoadamantan-1-yl)benzoic acid **84** (13mg, 0.05mmol, 1eq) and Re_2O_7 (16mg, 0.03mmol, 33mol%) in DCM (5ml) was added ethyl 4,4-dihydroperoxycyclohexanecarboxylate **24** (21mg, 0.10mmol, 2eq) in DCM (5ml). The mixture was stirred at room temperature for 4hrs. The crude product was adsorbed onto silica gel and purified by flash column chromatography using EtOAc/petroleum ether (eluting with 10:90) to afford the product **85** (32mg, 73%) as a colourless solid. This was an inseparable mixture with the starting material, 3-(4-oxoadamantan-1-yl)benzoic acid.

IR (neat)/ cm^{-1} : 3048 (OH), 2938 (C-H), 1744 (C=O acid), 1730 (C=O ester), 1037 (C-O).

HRMS (ESI); 495.1999 $[\text{M}+\text{Na}]^+$, $\text{C}_{26}\text{H}_{32}\text{O}_8\text{Na}$ requires 495.1995.

Synthesis of *N*-(4-aminophenyl)-3-(4-oxoadamantan-1-yl)benzamide **90**

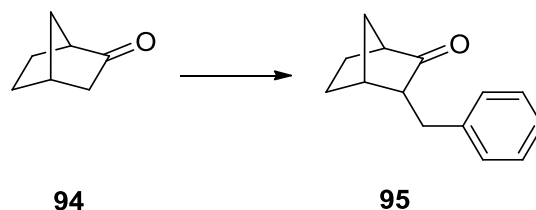


EDC.HCl (67mg, 0.35mmol, 1.2eq), HOBT (46mg, 0.34mmol, 1.2eq) and NMM (0.07ml, 0.64mmol, 2.1eq) were added to 3-(4-oxoadamantan-1-yl)benzoic acid **84** (83mg, 0.31mmol, 1eq) in DMF (5ml) at 0°C . The solution was stirred at room temperature for 3hrs under N_2 before *p*-phenylenediamine (71mg, 0.66mmol, 2.1eq) was added. After stirring at room temperature overnight, water (50ml) was added and the product extracted with Et_2O (3 x 30ml). The combined organic extracts were dried (MgSO_4) and the crude product adsorbed onto silica gel and purified by flash column chromatography using EtOAc/petroleum ether (eluting with 60:40) to afford the product **90** (37mg, 34%) as a brown oil.

^1H NMR (400MHz, CDCl_3) δ 8.04-8.01 (1H, br s, aromatic H), 7.91-7.88 (1H, br s, aromatic H), 7.66-7.62 (1H, d, $J=7.74$ Hz, aromatic H), 7.49-7.46 (1H, d, $J=7.47$ Hz, aromatic H), 7.43-7.36 (5H, m, aromatic H), 6.69-6.65 (2H, d, $J=8.72$ Hz, NH_2), 2.68-2.61 (2H, br s, 2 x CHC=O), 2.30-1.99 (11H, m, adamantyl H).

HRMS (ESI): 361.1928 $[M+H]^+$, $C_{23}H_{25}N_2O_2$ requires 361.1916.

Synthesis of 3-benzylbicycloheptan-2-one **95**⁹



LDA was prepared by reaction of $i\text{Pr}_2\text{NH}$ (0.31ml, 2.21mmol, 1.19eq) with $^n\text{BuLi}$ (1.40ml of a 1.5M solution in hexane, 2.1mmol) in dry THF (20ml) at 0°C for 15mins. Norcamphor **94** (0.20g, 1.86mmol, 1eq) in dry THF (4ml) was added and the reaction mixture was stirred at 0°C for 30mins. The flask was cooled to -78°C and benzyl bromide (0.24ml, 2.01mmol, 1.08eq) was added. The reaction mixture was stirred at -78°C for 30mins before warming to room temperature overnight. The reaction was quenched with MeOH (10ml) and the crude product adsorbed onto silica gel and purified by flash column chromatography using EtOAc/*n*-Hex (eluting with 5:95) to afford the product **95** (0.35g, 94%) as a colourless oil.

^1H NMR (400MHz, CDCl_3) δ 7.25 (5H, m, aromatic H), 2.99 (2H, dd, $J = 4.2, 14.0$ Hz, benzylic CH₂), 2.42 (1H, m, CHCH₂), 2.04 (1H, dt, $J = 3.7, 11.5$ Hz, CHC=O), 1.92 (1H, dt, $J = 1.7, 10.7$ Hz, CH), 1.79 (2H, m, bridgehead CH₂), 1.51 (2H, m), 1.34 (2H, m).

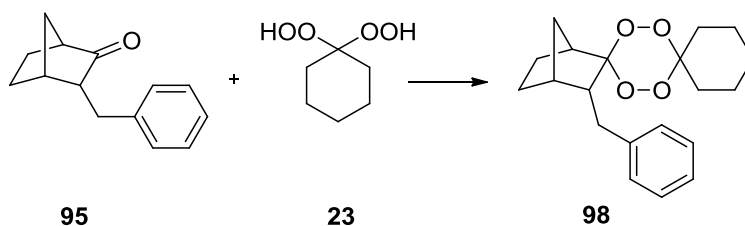
^{13}C NMR (100MHz, CDCl_3) δ 219.56 (C=O), 140.4 (quaternary C-CH₂), 129.3 (aromatic C), 128.9 (aromatic C), 126.7 (aromatic C), 55.9, 50.3, 38.4, 35.2, 34.9, 28.4, 24.4.

$\text{C}_{14}\text{H}_{16}\text{O}$ requires C 83.95 %, H 8.05 % found C 84.25 %, H 8.15 %.

IR (neat)/ cm^{-1} : 2960 (C-H aryl), 2875 (C-H alkyl), 1743 (C=O), 1498 (C=C)

HRMS (ESI); 223.1099 $[M+\text{Na}]^+$ $\text{C}_{14}\text{H}_{16}\text{O}$ requires 223.1094.

Synthesis of 3-benzylbicycloheptan-2-spiro-3'-1',2',4',5'-tetraoxane-6'-spiro-1"-cyclohexane **98**



To a stirred solution of 1,1-dihydroperoxycyclohexane **23** (130mg, 0.89mmol) and Re_2O_7 (38.6mg, 0.08mmol, 9mol%) in DCM (20ml) was added 3-benzylbicycloheptan-2-one **95** (260mg, 1.30mmol, 1.5eq) in DCM (20ml). The reaction mixture was stirred at room temperature for 1hr. The crude product was adsorbed onto silica gel and purified by flash column chromatography using EtOAc/*n*-Hex (eluting with 2:98) to afford the product **98** (65mg, 22%) as a colourless solid.

^1H NMR (400MHz, CDCl_3) δ 7.19-7.09 (5H, m, aromatic H), 2.30-1.30 (21H, m, aliphatic H)

^{13}C NMR (100MHz, CDCl_3) δ 129.4, 128.6, 126.2, 108.6 (quaternary C), 108.1 (quaternary C), 35.6, 32.7, 31.1, 29.9, 25.9, 25.7, 25.6, 23.1, 22.6, 22.3.

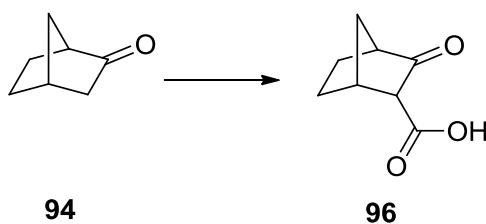
m.p 122-124°C

$\text{C}_{20}\text{H}_{26}\text{O}_4$ requires C 72.70 %, H 7.93 % found C 72.83 %, H 8.53 %.

IR (neat)/ cm^{-1} : 2938 (C-H aryl), 2861 (C-H alkyl), 1446 (C=C aromatic), 1270 (C-O), 1162 (C-O), 923 (O-O).

LRMS (ESI); 353.2 $[\text{M}+\text{Na}]^+$.

Synthesis of 3-oxobicycloheptane-2-carboxylic acid **96⁹**



LDA was prepared by reaction of $i\text{Pr}_2\text{NH}$ (0.31ml, 2.21mmol, 1.21eq) with $^n\text{BuLi}$ (1.30ml of a 1.5M solution in hexane, 1.95mmol) in dry THF (25ml) at 0°C for 15mins. Norcamphor **94** (0.20g, 1.83mmol, 1eq) in dry THF (7ml) was added and the reaction mixture was left to stir at 0°C for 30mins. A 100ml, 2-necked round bottomed flask was filled with dry ice and equipped with a septum and a CaCl_2 drying tube. CO_2 was bubbled into the reaction mixture at 0°C for 1hr *via* a cannula before it was allowed to warm to room temperature. The reaction was quenched with 1M HCl (25ml) and the product extracted with Et_2O (3 x 25ml). The combined organic extracts were dried (MgSO_4) and evaporated under reduced pressure to afford the product **96** (0.19g, 69%) as a colourless solid.

^1H NMR (400MHz, CDCl_3) δ 9.70-9.30 (1H, br s, COOH), 3.15-2.60 (3H, m), 1.95-1.40 (6H, m).

^{13}C NMR (100MHz, CDCl_3) δ 211.9 ($\text{C}=\text{O}$ ketone), 172.9 ($\text{C}=\text{O}$ acid), 59.4, 49.2, 39.6, 35.7, 27.5, 24.6.

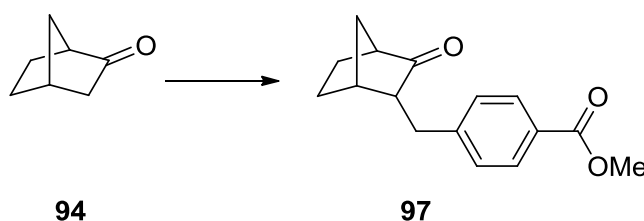
m.p $109\text{-}111^\circ\text{C}$

$\text{C}_8\text{H}_{10}\text{O}_3$ requires C 62.32 %, H 6.54 % found C 62.34 %, H 6.71 %.

IR (neat)/ cm^{-1} : 2969 (C-H alkyl), 1749 (C=O acid), 1716 (C=O ketone), 1417, 1203, 946.

LRMS (CI); 172.2 $[\text{M}+\text{NH}_4]^+$.

Synthesis of methyl 4-(3-oxobicycloheptan-2-yl)methylbenzoate **97**



LDA was prepared by reaction of $i\text{Pr}_2\text{NH}$ (0.31ml, 2.21mmol, 1.21eq) with $^n\text{BuLi}$ (1.40ml of a 1.45M solution in hexane, 2.03mmol) in dry THF (25ml) at 0°C for 15mins. Norcamphor **94** (0.20g, 1.83mmol, 1eq) in dry THF (3ml) was added and the reaction mixture was left to stir at 0°C for 30mins. The flask was cooled to -78°C and methyl 4-(bromomethyl)benzoate (0.46g, 2.01mmol, 1.10eq) in dry THF (5ml) was added. The reaction mixture changed from colourless to yellow then orange-red on addition. The reaction mixture was left to stir at -78°C for 40mins before warming to room temperature and quenching with MeOH (10ml). The crude product was adsorbed onto silica gel and purified by flash column chromatography using EtOAc/*n*-Hex (eluting with 2:98) to afford the product **97** (0.15g, 31%) as a colourless semi-solid.

^1H NMR (400MHz, CDCl_3) δ 7.98 (2H, d, $J=8.2$ Hz, aromatic $\underline{\text{H}}$), 7.26 (2H, d, $J=8.2$ Hz, aromatic $\underline{\text{H}}$), 3.93 (3H, s, $\underline{\text{CH}}_3$), 3.05 (2H, dd, $J=4.3, 14.1$ Hz, benzylic $\underline{\text{CH}}_2$), 2.51 (1H, m, $\underline{\text{CHCH}}_2$), 2.04 (1H, m), 1.91 (1H, m), 1.77 (2H, m, bridgehead $\underline{\text{CH}}_2$), 1.58 (2H, m), 1.35 (2H, m).

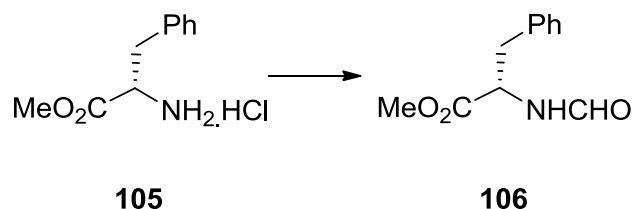
^{13}C NMR (100MHz, CDCl_3) δ 218.9 (C=O ketone), 167.4 (C=O ester), 145.9 (quaternary aromatic $\underline{\text{C-CH}}_2$), 130.3 (quaternary aromatic $\underline{\text{C-CO}}_2\text{Me}$), 129.4 (2 x aromatic $\underline{\text{C}}$), 128.7 (2 x aromatic $\underline{\text{C}}$), 55.5 (OCH_3), 52.5, 50.1, 38.5, 35.2, 34.9, 28.4, 24.2.

IR (neat)/ cm^{-1} : 2954 (C-H aryl), 2925 (C-H alkyl) 1743 (C=O ester), 1712 (C=O ketone), 1610 (C=C aromatic), 1279 (C-O).

HRMS (ESI); 281.1154 $[\text{M}+\text{Na}]^+$ $\text{C}_{16}\text{H}_{18}\text{O}_3\text{Na}$ requires 281.1148.

Synthesis of β -turn mimetics using a modified Ugi/Polonovski reaction

Synthesis of *N*-formyl *L*-phenylalanine methyl ester **106**



Method 1

L-Phenylalanine methyl ester hydrochloride **105** (0.91g, 4.22mmol, 1eq) was added to methyl formate (25ml), followed by potassium carbonate (1.18g, 8.53mmol, 2eq). The reaction mixture was stirred at 45°C for 45hrs. After cooling to room temperature, water (40ml) was added and the crude product extracted with DCM (3 x 30ml). The combined organic extracts were dried (MgSO_4) and the residue adsorbed onto silica gel and purified by flash column chromatography using EtOAc/petroleum ether (eluting with 30:70) to afford the product **106** (0.56g, 65%) as a colourless oil.

Method 2¹⁰

Acetic formic anhydride was made by stirring acetic anhydride (20ml) and formic acid (9ml) under a N_2 atmosphere at 50°C for 2hrs. *L*-Phenylalanine methyl ester hydrochloride **105** (1.04g, 4.83mmol, 1eq) was added and the reaction stirred under a N_2 atmosphere for 3 days at 50°C. After cooling to room temperature, the reaction mixture was added to water (50ml) and the crude product extracted with DCM (3 x 30ml). The combined organic extracts were dried (MgSO_4) and the residue adsorbed onto silica gel and purified by flash column chromatography using EtOAc/petroleum ether (eluting with 30:70) to afford the product **106** (0.87g, 88%) as a colourless oil.

^1H NMR (400MHz, CDCl_3) δ 8.16-8.14 (1H, br s, NHCHO), 7.32-7.24 (3H, m, 3 x aromatic H), 7.12-7.09 (2H, m, 2 x aromatic H), 6.16-6.13 (1H, br s, NHCHO), 4.99-4.94 (1H, m, CH), 3.74 (3H, s, OCH_3), 3.21-3.09 (2H, m, 2 x CH).

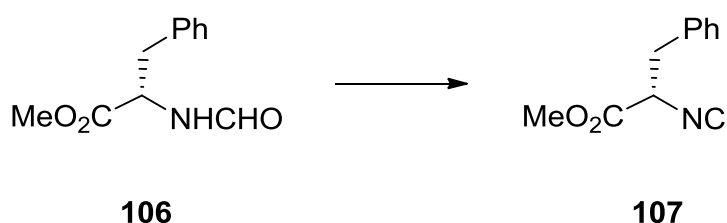
^{13}C NMR (100MHz, CDCl_3) δ 172.0 (C=O ester), 160.9 ($\underline{\text{C}}\text{HO}$), 135.9 (aromatic $\underline{\text{C}}$), 129.8 (aromatic $\underline{\text{C}}$), 129.4 (aromatic $\underline{\text{C}}$), 127.7 (aromatic $\underline{\text{C}}$), 56.6 ($\underline{\text{C}}\text{HCH}_2\text{Ph}$), 52.2 ($\text{O}\underline{\text{C}}\text{H}_3$), 38.2 ($\underline{\text{C}}\text{H}_2\text{Ph}$).

$\text{C}_{11}\text{H}_{13}\text{NO}_3$ requires C 63.76 %, H 6.32 %, N 6.76 % found C 63.72 %, H 6.42 %, N 6.71 %.

IR (neat)/ cm^{-1} : 3459 (NH), 2964 (C-H alkyl), 1743 (C=O aldehyde), 1712 (C=O ester), 1666 (C=C aromatic), 1211 (C-O), 1130 (C-N).

HRMS (ESI); 225.1237 $[\text{M}+\text{NH}_4]^+$, $\text{C}_{11}\text{H}_{17}\text{N}_2\text{O}_3$ requires 225.1234.

Synthesis of (S)-methyl 2-isocyano-3-phenylpropanoate **107**

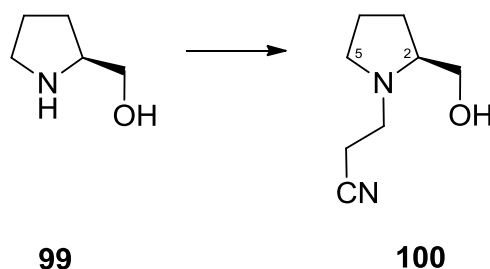


To a stirred solution of *N*-formyl phenylalanine methyl ester **106** (605mg, 2.90mmol, 1eq) in DCM (30ml) was added NEt_3 (0.80ml, 5.74mmol, 2eq). The resultant mixture was cooled to -78°C under a N_2 atmosphere. Triphosgene (303mg, 1.02mmol, 0.35eq) was quickly added in one portion (**Caution: triphosgene is highly toxic!**) and the reaction mixture was stirred at -78°C for 5mins. The reaction mixture was then stirred at -30°C for 3.5hrs before being quenched by slow addition of water (50ml). The crude product was quickly extracted using DCM (3 x 30ml). The combined organic extracts were dried (Na_2SO_4) and the crude product purified by flash column chromatography using EtOAc/petroleum ether (eluting with 20:80) to afford the product **107** (0.47g, 85%) as a pale yellow oil.

^1H NMR (400MHz, CDCl_3) δ 7.37-7.23 (5H, m, aromatic $\underline{\text{H}}$), 4.46-4.45 (1H, m, $\underline{\text{C}}\text{H}$), 3.79-3.78 (3H, br s, $\underline{\text{C}}\text{H}_3$), 3.28-3.22 (1H, dd, $J=13.9$, 4.8 Hz, $\underline{\text{C}}\text{HPh}$), 3.16-3.10 (1H, dd, $J=13.9$, 8.4 Hz, $\underline{\text{C}}\text{HPh}$).

^{13}C NMR (100MHz, CDCl_3) δ 171.5 ($\text{C}=\text{O}$), 161.4 (NC), 134.8 (quaternary aromatic C), 129.7 (2 x aromatic C), 129.2 (2 x aromatic C), 128.2 (aromatic C), 60.8 (CHNC), 53.8 (OCH_3), 39.3 (CH_2Ph).

Synthesis of (*S*)-3-(2-(hydroxymethyl)pyrrolidin-1-yl)propanenitrile **100**



Acrylonitrile (1.67g, 31.60mmol, 1.2eq) was added to a stirred solution of (*S*)-(+)-2-pyrrolidinemethanol **99** (2.59g, 25.65mmol, 1eq) in MeOH (50ml). The resulting solution was stirred at room temperature overnight. The crude product was adsorbed onto silica gel and purified by flash column chromatography using MeOH/EtOAc (eluting with 15:85) to afford the product **100** (3.75g, 87%) as a yellow oil.

^1H NMR (400MHz, CDCl_3) δ 3.65-3.40 (2H, dd, CH_2OH), 3.25-3.15 (1H, m, H2), 3.11-3.03 (1H, dt, $J=12.4, 7.7$ Hz, H5b), 2.74-2.62 (2H, m, CH_2CN), 2.56-2.50 (2H, t, $J=7.7$ Hz, $\text{CH}_2\text{CH}_2\text{CN}$), 2.37-2.30 (1H, m, H5a), 1.95-1.83 (2H, m, 2 x H3), 1.82-1.73 (2H, m, 2 x H4).

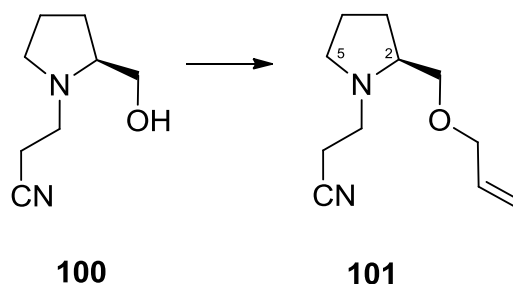
^{13}C NMR (100MHz, CDCl_3) δ 119.2 (CN), 65.1 (C-2), 63.0 (CH_2OH), 54.4 (C-5), 50.3 ($\text{CH}_2\text{CH}_2\text{CN}$), 27.8 (C-3), 24.1 (C-4), 18.6 (CH_2CN).

$\text{C}_8\text{H}_{14}\text{N}_2\text{O}$ requires C 62.31 %, H 9.15 %, N 18.17 % found C 61.60 %, H 9.35 %, N 18.19%.

IR (neat)/ cm^{-1} : 3350 (OH), 2958 (C-H alkyl), 2239 ($\text{C}\equiv\text{N}$), 1037 (C-N).

HRMS (ESI); 155.1179 $[\text{M}+\text{H}]^+$, $\text{C}_8\text{H}_{15}\text{N}_2\text{ONa}$ requires 155.1179.

Synthesis of (S)-3-(2-((allyloxy)methyl)pyrrolidin-1-yl)propanenitrile **101**



(S)-3-(2-(Hydroxymethyl)pyrrolidin-1-yl)propanenitrile **100** (2.96g, 19.22mmol, 1eq) was added to a stirring solution of sodium hydride (0.84g of a 60% dispersion in mineral oil, 21.00mmol, 1.1eq) in THF (40ml) at 0°C. The reaction mixture was stirred at 0°C under a N₂ atmosphere for 40mins. Allyl bromide (2.50ml, 28.89mmol, 1.5eq) was added followed by a trace of TBAI. Stirring was continued overnight at ambient temperature under a N₂ atmosphere. MeOH (40ml) was added, the crude product adsorbed onto silica gel and purified by flash column chromatography using EtOAc/petroleum ether (eluting with 40:60) to afford the product **101** (2.07g, 56%) as yellow oil.

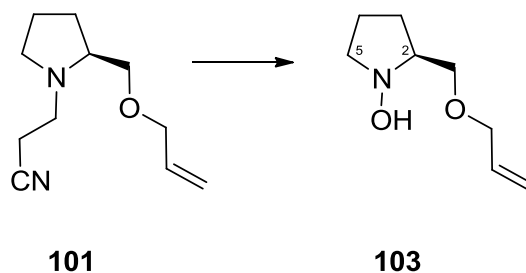
¹H NMR (400MHz, CDCl₃) δ 5.95-5.85 (1H, m, CH=CH₂), 5.30-5.15 (1H, m, CH=CH₂), 4.01-3.97 (2H, d, *J*=4.9 Hz, OCH₂CH=CH₂), 3.42-3.34 (2H, m, CHCH₂O), 3.26-3.18 (1H, dt, *J*=12.5, 7.5 Hz, H-5b), 3.17-3.11 (1H, m, H-2), 2.74-2.68 (2H, m, CH₂CN), 2.54-2.49 (2H, t, *J*=7.5 Hz), 2.36-2.28 (1H, m, H-5a), 1.95-1.85 (1H, m, H-3b), 1.82-1.70 (2H, m, 2 x H-4), 1.60-1.50 (1H, m, H-3a).

¹³C NMR (100MHz, CDCl₃) δ 135.1 (CH=CH₂), 119.5 (CN), 117.3 (CH=CH₂), 74.6 (CH₂OCH₂CH=CH₂), 72.7 (OCH₂CH=CH₂), 63.5 (C-2), 54.8 (C-5), 51.1 (CH₂CH₂CN), 28.7 (C-3), 23.6 (C-4), 18.1 (CH₂CN).

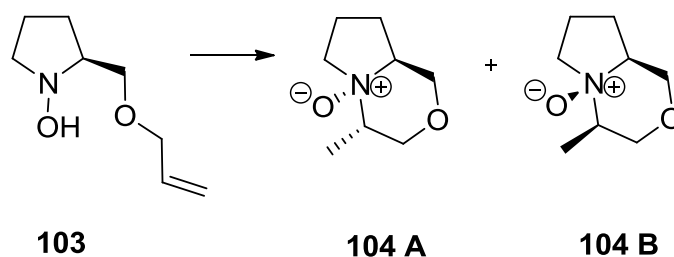
C₁₁H₁₈N₂O requires C 68.01 %, H 9.34 %, N 14.42% found C 68.36 %, H 9.66 %, N 14.41%.

IR (neat)/cm⁻¹: 2954 (C-H alkyl), 2219 (C≡N), 1621 (C=C), 1095 (C-O).

LRMS (CI); 195.3 [M+H]⁺.

Synthesis of (S)-2-((allyloxy)methyl)pyrrolidin-1-ol **103**

A stirred solution of (S)-3-(2-((allyloxy)methyl)pyrrolidin-1-yl)propanenitrile **101** (1.01g, 5.21mmol, 1eq) in DCM (50ml), was cooled to -78°C and *m*-CPBA (1.00g, 5.80mmol, 1.1eq) and potassium carbonate (1.07g, 7.53mmol, 1.45eq) were added. The solution was stirred for 1hr at -78°C then allowed to warm to room temperature and stirred for an additional hour. The resulting suspension was washed with aq. NaHCO_3 (50ml), water (50ml) and brine (50ml). The organic extracts were dried (MgSO_4) and solvent removed under reduced pressure to afford the product **103** (0.41g, 50%) as a yellow oil. The product could not be isolated in pure form as it underwent reverse Cope cyclisation slowly at room temperature.

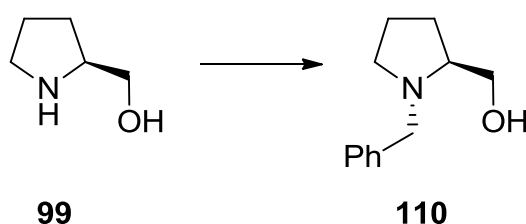
Synthesis of fused morpholine N-oxide template **104**

(S)-2-((allyloxy)methyl)pyrrolidin-1-ol **103** (0.40g, 2.54mmol, 1eq) was stirred in CDCl_3 (10ml) under a N_2 atmosphere for 4 days. The solvent was removed under reduced pressure and the resulting residue purified by flash column chromatography (gradient elution 100% EtOAc to 1:1 EtOAc/MeOH) to afford the product **104** as a yellow/orange oil (98mg, 25% over 2 steps, ratio of diastereoisomers 1:0, **104 A**:**104 B**).

^1H NMR (400MHz, CDCl_3) δ 4.31-4.26 (1H, m, CHCH_3), 3.90-3.83 (1H, m, CH), 3.81-3.75 (1H, m, CH), 3.73-3.66 (1H, m, CH), 3.60-3.55 (1H, m, CH), 3.42-3.40 (1H, m, CH), 3.39-3.33 (1H, m, CH), 3.31-3.22 (1H, m, CH), 2.30-2.22 (1H, m, CH), 2.21-2.12 (2H, m, CH_2), 1.97-1.85 (1H, m, CH), 1.27-1.25 (3H, d, $J=6.4$ Hz, CH_3).

LRMS (CI); 142.1 $[(\text{M}-\text{O})+\text{H}]^+$.

Synthesis of (S)-(1-benzylpyrrolidin-2-yl)methanol **110**¹¹



To a stirred solution of (S)-(+)-2-pyrrolidinemethanol **99** (0.97ml, 9.97mmol, 1eq) in toluene (20ml) was added benzyl bromide (1.70ml, 14.3mmol, 1.4eq) and potassium carbonate (1.42g, 10.3mmol, 1.03eq). The reaction mixture was stirred under a N_2 atmosphere at 110°C for 21hrs. After cooling to room temperature, water (30ml) was added and the crude product extracted with DCM (3 x 30ml). The combined organic extracts were dried (MgSO_4), the residue adsorbed onto silica gel and purified by flash column chromatography using EtOAc (eluting with 100%) to afford the product **110** (1.08g, 56%) as a pale yellow oil.

^1H NMR (400MHz, CDCl_3) δ 7.35-7.23 (5H, m, aromatic H), 3.95-3.60 (2H, m, CH_2Ph), 3.45-3.40 (1H, m, CHCH_2OH), 3.38-3.34 (1H, d, $J=13.0$ Hz, NCH_2), 3.00-2.95 (1H, m, CH_2OH), 2.77-2.70 (1H, m, CH_2OH), 2.31-2.25 (1H, m, NCH_2), 1.96-1.79 (2H, m, NCHCH_2), 1.73-1.64 (2H, m, NCH_2CH_2).

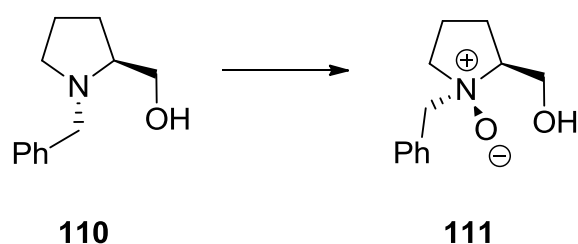
^{13}C NMR (100MHz, CDCl_3) δ 139.7 (quaternary aromatic C), 129.4 (2 x aromatic C), 128.7 (2 x aromatic C), 127.5 (aromatic C), 64.6 (NCHCH_2), 62.1 (CH_2OH), 60.6 (CH_2Ph), 54.8 (NCH_2CH_2), 28.2 (CH_2CH), 23.9 ($\text{CH}_2\text{CH}_2\text{CH}_2$).

$\text{C}_{12}\text{H}_{17}\text{NO}$ requires C 75.35 %, H 8.96 % N 7.32 % found C 75.38 %, H 8.98 % N 7.32 %.

IR (neat)/cm⁻¹: 3346 (OH), 2937 (C-H alkyl), 1609 (C=C aromatic), 1029 (C-N).

LRMS (CI); 192.29 [M+H]⁺.

Synthesis of (1*R*, 2*S*)-1-benzyl-2-(hydroxymethyl)pyrrolidine-1-oxide **111**



To a stirred solution of (*S*)-(1-benzylpyrrolidin-2-yl)methanol **110** (0.80g, 4.21mmol, 1eq) in DCM (20ml) at -78°C was added *m*-CPBA (0.80g, 4.64mmol, 1.1eq) and potassium carbonate (0.89g, 6.44mmol, 1.5eq). The reaction mixture was stirred under a N₂ atmosphere at -78°C for 2hrs and then allowed to warm to room temperature overnight. The resulting suspension was filtered through MgSO₄. The crude product was adsorbed onto silica gel and purified by flash column chromatography using MeOH/EtOAc (eluting with 1:1) to afford the product **111** (0.61g, 70%) as a pale yellow solid.

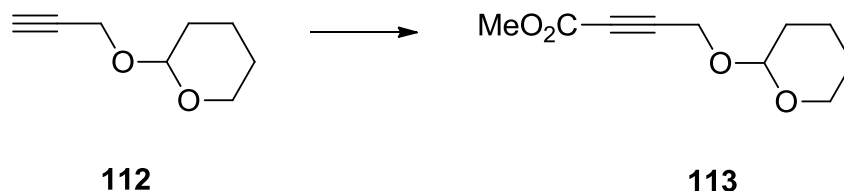
¹H NMR (400MHz, CDCl₃) δ 7.51-7.40 (5H, m, aromatic H), 4.63-4.45 (2H, m, CH₂Ph), 4.40-4.35 (1H, m, CHCH₂OH), 3.87-3.80 (1H, d, *J*=13.0 Hz, NCH₂), 3.48-3.46 (2H, m, NCHCH₂), 3.37-3.27 (1H, m, CH₂OH), 3.17-3.11 (1H, m, CH₂OH), 2.73-2.63 (1H, m, NCH₂), 2.43-2.30 (1H, m, NCH₂CH₂), 1.97-1.80 (1H, m, NCH₂CH₂).

¹³C NMR (100MHz, CDCl₃) δ 132.6 (quaternary aromatic C), 131.0 (2 x aromatic C), 130.0 (2 x aromatic C), 129.1 (aromatic C), 71.1 (NCHCH₂), 70.7 (CH₂OH), 66.8 (CH₂Ph), 59.9 (NCH₂CH₂), 23.5 (CH₂CH), 20.5 (CH₂CH₂CH₂).

C₁₂H₁₇NO₂ requires C 69.54 %, H 8.27 % N 6.76 % found C 66.47 %, H 8.36 % N 6.45 %.

IR (neat)/cm⁻¹: 3147 (OH), 2947 (C-H alkyl), 1743 (C=C aromatic), 1068 (C-N).

LRMS (CI); 208.1 [M+H]⁺, 190.1 [(M-O)+H]⁺.

Synthesis of β -turn mimetics using a reverse-Cope cyclisationSynthesis of methyl 4-((tetrahydro-2H-pyran-2-yl)oxy)but-2-ynoate **113**

2-(prop-2-yn-1-yloxy)tetrahydro-2H-pyran **112** (2.14g, 15.27mmol, 1eq) in THF (25ml) was stirred under a N₂ atmosphere at -78°C. EtMgBr (17ml, 1.0M, 17.00mmol, 1.1eq) was added slowly drop-wise. The reaction mixture was stirred for 30mins. Methyl chloroformate (1.22ml, 15.69mmol, 1.1eq) in THF (10ml) was added drop-wise. The reaction mixture turned a cloudy straw colour and was left to stir for 30mins before warming to room temperature for 5hrs (colour change to orange). The reaction was quenched with MeOH (30ml) and the crude product adsorbed onto silica gel and purified by flash column chromatography using EtOAc/petroleum ether (gradient elution 2:98 to 5:95) to afford the product **113** (0.71g, 25%) as a pale, straw coloured oil.

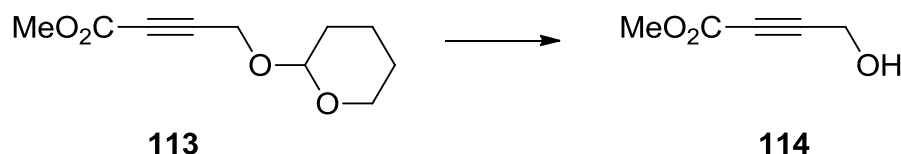
¹H NMR (400MHz, CDCl₃) δ 4.82-4.80 (1H, t, $J=3.3$ Hz, OCH), 4.40-4.38 (2H, s, CH₂O), 3.80-3.78 (3H, s, CH₃), 1.85-1.70 (2H, m, OCH₂), 1.67-1.50 (2H, m, CH₂), 1.27-1.16 (2H, m, CH₂), 1.01-0.85 (2H, m, CH₂).

¹³C NMR (100MHz, CDCl₃) δ 154.0 (C=O), 97.5 (OCHO), 96.8 (OCH₂C \equiv C), 84.4 (C-CO₂Me), 62.4 (CH₂O), 54.0 (OCH₃), 53.2 (C \equiv C-CH₂O), 30.4 (CH₂), 25.6 (CH₂), 19.2 (CH₂).

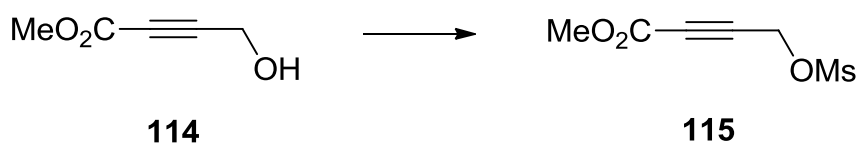
C₁₀H₁₄O₄ requires C 60.59 %, H 7.12 % found C 61.37 %, H 7.90 %.

IR (neat)/cm⁻¹: 2946 (C-H alkyl), 2241 (C \equiv C), 1716 (C=O), 1249 (C-O).

LRMS (CI); 216.1 [M+NH₄]⁺.

Synthesis of methyl 4-hydroxy-2-butynoate **114**

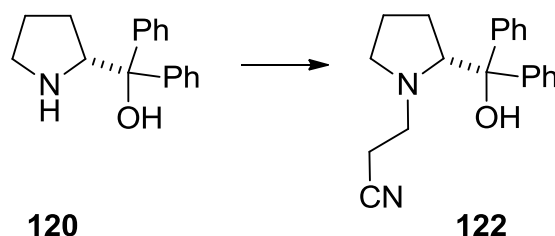
To a solution of methyl 4-((tetrahydro-2*H*-pyran-2-yl)oxy)but-2-ynoate **113** (557mg, 2.81mmol, 1eq) in MeOH (10ml) was added *p*-TSA (54mg, 0.31mmol, 0.11eq). The reaction mixture was stirred at room temperature for 3.5hrs before washing with aq. NaHCO₃ (30ml) and the product extracted with DCM (4 x 30ml). The combined organic extracts were dried (MgSO₄) and the solvent removed under reduced pressure to afford the crude product **114** (432mg) as a yellow liquid, which was used in the next step without further purification.

Synthesis of methyl 4-((methylsulfonyl)oxy)but-2-ynoate **115**

Methyl 4-hydroxy-2-butynoate **114** (306mg, 2.68mmol, 1eq) in dry DCM (20ml) was cooled to -40°C under a positive pressure of N₂. NEt₃ (0.55ml, 3.94mmol, 1.5eq) was added drop-wise with vigorous stirring, followed by the slow addition of mesyl chloride (0.22ml, 2.89mmol, 1.1eq). The reaction mixture was allowed to warm to room temperature for 2hrs and there was a colour change to yellow. Water (30ml) was added and the product extracted with DCM (3 x 30ml). The combined organic extracts were washed with water (30ml), brine (30ml) and dried (MgSO₄). The solvent was removed under reduced pressure to afford the crude product **115** (377mg, 73%) as a yellow/orange oil, which was used immediately in the next step without further purification.

Synthesis of chiral enamine N-oxides

Synthesis of (*R*)-3-(2-(hydroxydiphenylmethyl)pyrrolidin-1-yl)propanenitrile **122**



Acrylonitrile (0.70g, 13.20mmol, 1.36eq) was added to a stirred solution of (*R*)-2-diphenylpyrrolidinemethanol **120** (2.46g, 9.73mmol, 1eq) in MeOH (40ml). The resulting solution was stirred at room temperature under a N₂ atmosphere overnight. The solvent was removed under reduced pressure to afford the product **122** (2.89g, 97%) as a colourless solid.

¹H NMR (400MHz, CDCl₃) δ 7.63-7.50 (4H, m, 4 x aromatic H), 7.32-7.24 (4H, m, 4 x aromatic H), 7.19-7.14 (2H, m, 2 x aromatic H), 4.32-4.28 (1H, br s, OH), 3.91-3.86 (1H, m, N-CH), 3.31-3.26 (1H, m, CH), 2.45-2.31 (2H, m, CH₂), 2.19-2.11 (1H, m, CH), 2.10-2.02 (2H, m, CH₂), 2.00-1.88 (1H, m, CH), 1.80-1.68 (3H, m, 3 x CH).

¹³C NMR (100MHz, CDCl₃) δ 147.8 (2 x quaternary aromatic C), 128.7 (4 x aromatic C), 126.8 (4 x aromatic C), 125.9 (2 x aromatic C), 118.7 (C≡N), 78.5 (C-OH), 71.9 (C-COH), 56.0 (C-5), 51.9 (CH₂CH₂CN), 29.8 (C-3), 25.1 (C-4), 18.1 (CH₂CN).

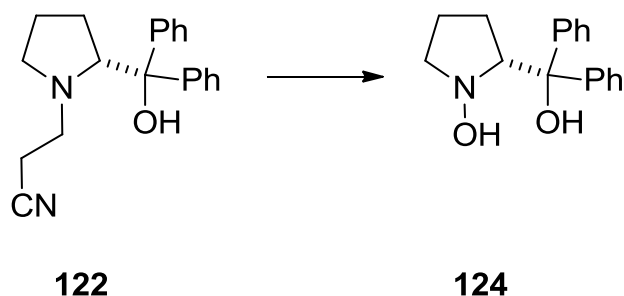
m.p. 130-132°C

C₂₀H₂₂N₂O requires C 78.40 %, H 7.24 % N 9.14 % found C 78.86 %, H 7.13 % N 8.96 %.

IR (neat)/cm⁻¹: 3363 (OH), 2938 (C-H alkyl), 2244 (CN), 1492 (C=C aromatic).

HRMS (ESI); 329.1623 [M+Na]⁺, C₂₀H₂₂N₂ONa requires 329.1630.

Synthesis of (*R*)-2-(hydroxydiphenylmethyl)pyrrolidin-1-ol **124**



A stirred solution of (*R*)-3-(2-(hydroxydiphenylmethyl)pyrrolidin-1-yl)propanenitrile **122** (1.01g, 3.29mmol, 1eq) in DCM (20ml), was cooled to -78°C and *m*-CPBA (0.63g, 3.65mmol, 1.1eq) and potassium carbonate (0.73g, 5.26mmol, 1.60eq) were added. The solution was stirred at -78°C and allowed to warm to room temperature overnight. The reaction mixture was filtered and the crude product adsorbed onto silica gel and purified by flash column chromatography using EtOAc/petroleum ether (eluting with 20:80) to afford the product **124** (0.51g, 57%) as a colourless solid.

^1H NMR (400MHz, CDCl_3) δ 7.65-7.44 (4H, m, 4 x aromatic H), 7.33-7.25 (4H, m, 4 x aromatic H), 7.20-7.13 (2H, m, 2 x aromatic H), 4.20-4.10 (1H, m, CH), 3.25-3.18 (1H, m, CH), 2.98-2.90 (1H, m, CH), 2.45-2.02 (1H, m, CH), 1.99-1.85 (1H, m, CH), 1.80-1.70 (2H, m, CH₂).

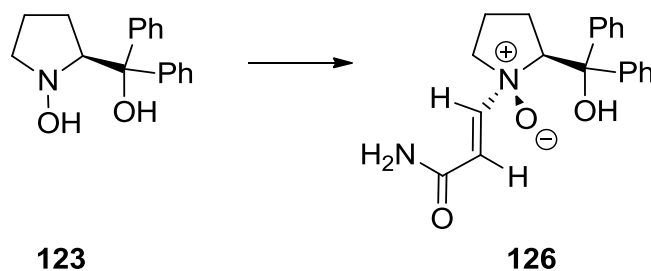
^{13}C NMR (100MHz, CDCl_3) δ 147.7 (2 x quaternary aromatic C), 128.7 (4 x aromatic C), 127.1 (4 x aromatic C), 126.1 (2 x aromatic C), 78.5 (C-OH), 71.9 (C-COH), 56.0 (C-5), 29.8 (C-3), 18.1 (C-4).

m.p. $84-86^{\circ}\text{C}$

$\text{C}_{17}\text{H}_{19}\text{NO}_2$ requires C 75.81 %, H 7.11 % N 5.20 % found C 75.94 %, H 7.09 % N 5.64 %.

IR (neat)/ cm^{-1} : 3336 (O-H), 2969 (C-H), 1446 (C=C aromatic).

HRMS (ESI); 270.1484 $[\text{M}+\text{H}]^+$, $\text{C}_{17}\text{H}_{20}\text{NO}_2$ requires 270.1494.

Synthesis of (S)-2-(hydroxydiphenylmethyl)pyrrolidin-1-acrylamide-N-oxide **126**

To a stirred solution of (S)-2-(hydroxydiphenylmethyl)pyrrolidin-1-ol **123** (202mg, 0.75mmol, 1eq) in CDCl_3 (5ml) was added propiolamide (54mg, 0.74mmol, 1eq) in CDCl_3 (5ml). The reaction mixture was stirred at room temperature under N_2 for 3 days with monitoring by TLC analysis and ^1H NMR. The solvent was evaporated under reduced pressure to afford the crude product as a yellow solid. Purification by crystallisation from CHCl_3 /hexanes gave the product **126** (207mg, 83%) as colourless crystals.

^1H NMR (400MHz, CDCl_3) δ 7.71-7.65 (2H, m, 2 x aromatic H), 7.60-7.55 (2H, m, 2 x aromatic H), 7.35-7.29 (4H, m, 4 x aromatic H), 7.23-7.17 (1H, m, aromatic H), 7.14-7.08 (1H, m, aromatic H), 6.67-6.64 (1H, d, $J=12.4$ Hz, CH alkene), 6.44-6.41 (1H, d, $J=12.4$ Hz, CH alkene), 5.30-5.20 (2H, br s, NH₂), 4.66-4.60 (1H, m, NCHCH₂OH), 3.56-3.49 (1H, m, NCHCH₂), 3.14-3.07 (1H, m, NCHCH₂), 2.74-2.63 (1H, m, NCH₂), 2.50-2.38 (1H, m, NCH₂), 2.21-2.10 (1H, m, NCH₂CH₂), 2.08-1.97 (1H, m, NCH₂CH₂).

^{13}C NMR (100MHz, CDCl_3) δ 165.4 (CONH₂), 150.2 (NCH=CHCONH₂), 128.8 (CHCONH₂), 127.4 (2 x quaternary aromatic C), 126.7 (4 x aromatic C), 125.0 (4 x aromatic C), 119.8 (2 x aromatic C), 80.4 (NCHCH₂OH), 73.7 (COH), 54.2 (NCH₂), 25.3 (NCHCH₂), 21.7 (NCH₂CH₂).

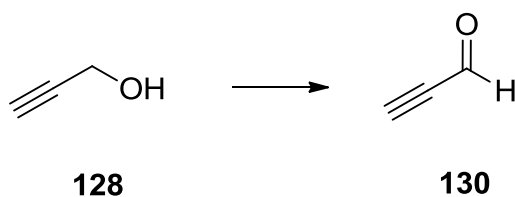
m.p. 128-130°C

$\text{C}_{20}\text{H}_{22}\text{N}_2\text{O}_3$ requires C 70.99 %, H 6.55 % N 8.28 % found C 65.11 %, H 6.12 % N 7.41 %.

IR (neat)/ cm^{-1} : 3312 (N-H), 3170 (OH), 2943 (C-H), 1689 (C=O), 1515 (C=C aromatic), 1392 (C=C).

HRMS (ESI); 339.1706 $[\text{M}+\text{H}]^+$, $\text{C}_{20}\text{H}_{23}\text{N}_2\text{O}_3$ requires 339.1709.

Synthesis of propiolaldehyde **130**¹²



Jones' reagent was made as follows: CrO₃ (1.70g) was dissolved in distilled water (7.8ml) to give an orange solution. Conc. H₂SO₄ (2.4ml) was added dropwise at 0°C.

Jones' reagent was added dropwise to propargyl alcohol **128** (1.0ml) in butanone (15ml) at 0°C over 10mins. There was a colour change to blue-green during the addition. TLC analysis showed that the reaction had reached completion after 30mins. Water (30ml) was added and the organic layer separated. The aqueous layer was extracted with Et₂O (2 x 40ml), dried (MgSO₄). Distillation gave the product **130** (b.p. 55-57°C, 0.62g, 67%) as a colourless, volatile liquid.

¹H NMR (400MHz, CDCl₃) δ 9.23 (1H, s, CHO), 2.17 (1H, s, C≡C-H).

¹³C NMR (100MHz, CDCl₃) δ 176.8 (CHO), 83.1 (C≡CH), 81.9 (C≡CH).

5.3. Bibliography

1. Burchat, A. F.; Chong, J. M.; Nielsen, N., Titration of alkyllithiums with a simple reagent to a blue endpoint. *J. Organomet. Chem.* **1997**, 542 (2), 281-283.
2. Armarego, W. L. F.; Perrin, D. D., *Purification of Laboratory Chemicals*. 4th ed.; Oxford : Butterworth Heinemann: 1996.
3. Vennerstrom, J. L.; Dong, Y.; Chollet, J.; Matile, H. Spiro and Dispiro 1,2,4-Trioxolane Antimalarials, US Patent 6,486,199 B1. **2002**.
4. Selvam, J. J. P.; Suresh, V.; Rajesh, K.; Babu, D. C.; Suryakiran, N.; Venkateswarlu, Y., A novel rapid sulfoxidation of sulfides with cyclohexylidenebishydroperoxide. *Tetrahedron Lett.* **2008**, 49 (21), 3463-3465.
5. Ghorai, P.; Dussault, P. H., Broadly Applicable Synthesis of-1,2,4,5-Tetraoxanes. *Org. Lett.* **2009**, 11 (1), 213-216.
6. Su, Y. C.; Chen, W. C.; Chang, F. C., Investigation of the thermal properties of novel adamantane-modified polybenzoxazine. *J. Appl. Polym. Sci.* **2004**, 94 (3), 932-940.
7. Wagner, G.; Knoll, W.; Bobek, M. M.; Brecker, L.; van Herwijnen, H. W. G.; Brinker, U. H., Structure-Reactivity Relationships: Reactions of a 5-Substituted Aziadamantane in a Resorcin[4]arene-based Cavitand. *Org. Lett.* **2010**, 12 (2), 332-335.
8. Pyne, S. G., Intramolecular addition of amines to chiral vinyl sulfoxides, total synthesis of (R)-(+)-canadine. *Tetrahedron Lett.* **1987**, 28 (40), 4737-4740.
9. Hutchinson, J. H.; Li, D. L. F.; Money, T.; Palme, M.; Agharahimi, M. R.; Albizati, K. F., Stereoselectivity of C(3) methylation and aldol condensation of camphor and derivatives. *Can. J. Chem.-Rev. Can. Chim.* **1991**, 69 (3), 558-566.
10. Huffman, C. W., Formylation of Amines. *J. Org. Chem.* **1958**, 23 (5), 727-729.
11. Zhu, L. B.; Cheng, L.; Zhang, Y. X.; Xie, R. G.; You, J. S., Highly efficient copper-catalyzed N-arylation of nitrogen-containing heterocycles with aryl and heteroaryl halides. *J. Org. Chem.* **2007**, 72 (8), 2737-2743.
12. Veliev, M. G.; Guseinov, M. M., An improved synthesis of propynal. *Synthesis* **1980**, (6), 461-461.